Technical Note on:

ORM Cal Val Analysis
Part 2: detailed results

Draft

28 April 2003

Delivery of WPs 9130 & 9500 of the CCN#5 of the study:

"Development of an Optimised Algorithm for Routine p, T and VMR Retrieval from MIPAS Limb Emission Spectra"

Contract No: **11717/95/NL/CN**

Prepared by:

Name	Institute
S. Ceccherini	IFAC-CNR
B.M. Dinelli	ISAC-CNR
V. Payne	Oxford University
M. Prosperi	FMA
P. Raspollini	IFAC-CNR
M. Ridolfi	DCFI-UNIBO

Approved by:

Name	Institute
B. Carli	IFAC-CNR

CONTENTS Part 2

1 REFERENCE DOCUMENTS 3

2 INTRODUCTION 4

3 TUNING OF INPUT PARAMETERS 4

3.1 Tuning of atmospheric continuum related parameters 4
3.2 Tuning of parameters linked to Levenberg-Marquardt algorithm 8
3.3 Tuning of convergence criteria 14
3.4 Retrieval grid 27
3.5 Tuning of the layering used in the forward model (linear-in-tau approximation) 29
3.6 Tuning of FOV convolution 34
3.7 Tuning of the error associated with engineering LOS information 39
3.8 VCM of a-priori profiles for the computation of the IG profiles 43
3.9 Verification of frequency calibration & determination of coefficients for second order polynomial frequency correction 48

4 VERIFICATION OF CRITICAL BASELINES 57

4.1 Verification of extrapolation rules 57
4.2 Measurement altitude range 66
4.3 Local thermodynamic equilibrium (LTE) 75
4.4 Verification of horizontal homogeneity assumption 78
4.5 Verification of hydrostatic equilibrium (assumption of vertical profiles) 83
4.6 Verification of error in the VMR profiles of interfering speciess 84
4.7 Verification of the assumptions related to the line-mixing for CO_2 Q-branches 88
4.8 Verification of Instrument Line Shape (ILS) 111
4.9 Verification of intensity calibration. 113
4.10 Zero-level calibration 115

5 OTHER TESTS: NON-LINEARITY CORRECTION FOR FORWARD AND REVERSE SWEEPS 134

1 Reference documents

[RD1] TN-IROE-RSA9603**,** Issue: 3A
Title: Software Architecture and Algorithm Definition

[RD2] TN-IROE-GS0102**,** Issue: 1 - Revision: 1
Title: Pre-flight modifications to the ORM_ABC code

[RD3] Draft:
Title: 'New functionalities implemented in ORM_ABC_1.2.3' ,
M. Ridolfi (16 November 2001)

[RD4] PO-MA-DOG-GS-0001, Issue: 2 - Revision: A
Title: ML2PP Software User Manual

[RD5] TN-IROE-GS0101, Issue: 1 - Revision: A
Title: Level 2 Algorithm Characterization & Validation Plan

[RD6] TN-IROE-GS0103, Draft Revision A
Title: ORM for Commissioning Phase (18 April 2002)

[RD7] TN-IROE-GS0104, Draft
Title: Description of Statistical Tool

[RD8] PO-PL-ESA-GS-1124, Issue 1B, Title: Implementation pf MIPAS post-launch calibration and validation tasks, (March 2002)

[RD9] Title: 'MIPAS-B Retrieval residuals analysis', V. Jay and A. Dudhia (23 Jan. 01)

[RD10] M. Carlotti, B.M. Dinelli, P. Raspollini, M. Ridolfi, 'Geo-fit approach to the analysis of satellite limb scanning measurements', *Appl. Optics*, **Vol. 40**, 1872-1875 (2001)

[RD11] Title: 'REC Analysis of MIPAS data', Draft, A. Dudhia (22 April 2003)

2 Introduction

In the frame of ESA contract 11717/95/NL/CN an Optimized forward /retrieval Model (ORM) has been developed, suitable for implementation in MIPAS near real-time Level 2 Processor. In particular, version 1.2.3 of the ORM_ABC code (described in [RD1], [RD2] and [RD3]) is the scientific reference for the Retrieval Component Library of MIPAS Level 2 NRT processor [RD4]. Before the ENVISAT launch, the most critical input parameters and the most critical baselines used in the ORM were identified and a list of tests to be performed during the Commissioning Phase for both optimising the input parameters and verifying the impact of the code approximations were described in [RD5]. In order to perform these tests a modified ORM with added functionalities [RD6] and a dedicated software tool for the analysis of ORM products (Statistical Tool) [RD7] were developed.
The tests described in [RD5] have been included in the overall calibration and validation activities of the early in-flight operation of MIPAS, described in [RD8].
These tests have been performed using first one of the first orbit detected by MIPAS, i.e. orbit #504 (acquired on the 5th April 2002) with unconsolidated Level1 data and then using orbit #2081 (acquired on the 24th July 2002) with improved Level1 data.
This TN reports the results of the tests performed on orbit #2081 following the order of presentation used in [RD5]. It is divided in two parts. The first part is a collection of the summary sheets of all performed tests according to the template provided by ESA and provides the summary of the results and the recommendations for ESA.
The second part contains, for each test, the rationale, the used procedure (if different to the one described in [RD5]), the results and the conclusions. It is meant to collect details that justify the recommendations to ESA given in the first part.
The results of the tests described in [RD5] and performed with the REC analysis are reported in [RD11].
This introduction is repeated in both parts of the report in order to make possible to consult them as independent documents.

3 Tuning of input parameters

This section includes the description of all the tests dealing with the tuning of critical processing set-up parameters. The outputs of these tests consist in modified Level2 auxiliary data (PS_FRAME.DAT, PS_PT.DAT, PS_H2O.DAT, PS_O3.DAT, PS_HNO3.DAT, PS_CH4.DAT, PS_N2O.DAT, PS_NO2.DAT and Level2 MIP_PS2_AX file).
All these modified files were delivered to ESA on 31st October 2002 and were implemented in the Payload data Segment (PDS) on the 13th of November.

3.1 Tuning of atmospheric continuum related parameters

Ref. [RD5]: Sect. 4.1.1; Ref. [RD9]: Sheet MIP_PS_2_5 - MIP_PS_2_6 /1

Introduction

One of the quantities fitted by ORM is an altitude and microwindow dependent absorption cross-section of atmospheric continuum.

The number of fitted continuum parameters is determined by the input parameter *rucl* , that indicates the maximum altitude below which continuum cross-sections are fitted.
Furthermore, it is possible to set continuum profiles equal to 0 above a given altitude, *rzc0.*
If a big number of continuum parameters are fitted (i.e. if *rucl* and *rzc0* are big), the retrieval is weakly constrained and final χ^2 values are expected to be small. On the other hand, in case that spectra do not contain enough information to retrieve them, retrieval stability decreases. Instability can induce oscillations in the retrieved profiles and can increase the number of iterations needed to reach convergence.
Rucl and *rzc0* are the continuum-related parameters that have been tuned.
Furthermore, since the continuum cross-sections are order of magnitudes smaller than the other parameters in the state vector, in order to reduce the dynamics of the parameters in the state vector and hence to avoid numerical problems, the continuum parameters are multiplied by a scaling factor named *fact_cont*. This factor is hardwired in ORM_ABC, as equal to 10^{30}, while is an input parameter in ORM_ORB. A check has been done in order to understand if a customised factor is needed for each retrieval (according to the different ranges of VMR values).

Procedure and results
The three different parameters (*rucl, rzc0* and *dfact_cont*) were tuned individually, starting from *rucl*, that is the most critical one. Dedicated parameters are possible for each speciess.
The selection of the optimal parameter is performed looking for the parameter that represents the best compromise between minimum constrain (and hence lower χ^2) and fast convergence of the retrieval. The speed of the convergence is determined by the number of Gauss and Marquardt iterations needed to reach convergence (version 3 of convergence criteria / Marquardt parameters were used for this test). The Profile Oscillation Quantifier (POQ), as well as the number of scans of the orbit reaching convergence, provides an additional indication on the 'stability' of the retrieval. The criteria originally proposed in [RD5] to quantify the retrieval 'stability' have not been used, since they were proved not to be adequate.
Complete runs of the orbit #2081 were repeated for different values of *rucl* (varying between 20 and 50 km). For all the cases the number of scans reaching convergence was reported, as well as the mean number of Gauss/Marquardt iterations per scan (averaged on the whole orbit), the mean χ^2 and the mean POQ. While tuning the *rucl* parameter, *rzc0* was set to 100 km, while customised values for each speciess (pt:10^{27}, h2o:10^{28}, o3: 10^{28}, hno3: 10^{26}, ch4: 10^{30}, n2o: 10^{27}, no2: 10^{25}) were used for *dfact_cont*. Table 1 collects the results of *rucl* tuning obtained for the different retrievals: the chosen parameters at the end of the tuning test are highlighted in blue.
Table 1 indicates that the average χ^2 is weakly dependent on the number of continuum fitted parameters, while fast convergence of the retrieval, expecially pT retrieval, is strongly dependent on that.
Therefore, the choice of *rucl* is driven by 'fast convergence' considerations.
Considering that *rucl* indicates the altitude below which atmospheric continuum is significant, from the physical point of view the same value should be selected for the different retrievals. On the other hand, considering that microwindows are localized in different spectral regions, where continuum has a different behaviour, and that fitted continuum can compensate for systematic errors having a continuum-like impact on the spectra, it was decided to choice customized values of *rucl* for the different speciess, as reported in Table 2.

Tabel 1: results of *rucl* tuning: blue lines correspond to the chosen values for *rucl*

Highest fitted continuum altitude, rucl [km]	# scans reaching convergence	# scans used for the mean	Mean # of Gauss + Marquardt iterations /scan	Mean # of Marquardt iterations /scan	Mean χ^2	POQ
PT						
50	66 2 crashes	66	6.28	1.43	1.90	2.18
36	68 1 crash	68	5.53	1.10	1.94	2.25
30	66 3 crashes	66	3.86	0.59	1.97	2.01
25	68 1 crash	68	3.85	0.59	2.03	2.07
20	69	69	2.67	0.22	2.11	2.00
H2O						
50	64	69	3.41	.88	1.4	31.03
36	67	69	2.32	.38	1.39	30.71
30	68	69	2.03	.23	1.39	30.19
25	69	69	2.04	.23	1.39	31.29
20	69	69	2.16	.33	1.40	30.04
O3						
50	68	69	3.55	1.26	2.82	34.41
36	68	69	3.35	1.16	2.82	34.71
30	69	69	3.26	1.07	2.68	35.01
25	69	69	3.49	1.25	2.92	35.36
20	69	69	3.41	1.20	2.87	36.02
HNO3						
50	59	69	5.28	1.36	1.32	70.99
36	65	69	3.93	0.87	1.33	70.99
30	66	69	3.68	.77	1.30	70.56
25	65	69	3.96	0.96	1.49	72.17
20	66	69	4.19	1.1	1.53	72.52
CH4						
50	66	69	3.39	1.09	1.93	30.23
36	66	69	3.22	1.00	1.86	30.57
30	66	69	3.00	0.90	1.84	30.83
25	67	69	2.87	0.81	1.98	32.02
20	67	69	2.75	0.68	2.10	32.36
N2O						
50	68	69	2.96	0.70	1.77	43.52
36	69	69	2.97	0.70	1.78	44.14
30	68	69	2.78	0.62	1.78	44.40
25	69	69	2.74	0.59	1.93	44.21
20	69	69	2.62	0.58	2.03	43.48
NO2						
50	68	69	3.12	0.65	1.26	34.17
36	69	69	1.87	0.06	1.24	32.68
30	69	69	1.84	0.06	1.24	32.70
25	69	69	1.72	0.00	1.25	33.45
20	69	69	2.06	0.16	1.25	32.54

Table 2 - Values of *rucl* selected for the different retrievals:

PT	H_2O	O_3	HNO_3	CH_4	N_2O	NO_2
20 km	25 km	30 km	30 km	30 km	30 km	30 km

These results are adequate for normal atmospheric continuum conditions. In case of volcanic eruptions the level of atmospheric continuum in the stratosphere can increase significantly. In that case a re-tuning of this parameter is needed, but for short term implementation the value *rucl* = 36 km can be used, since good performances are obtained also for this value.

After the tuning of the *rucl* parameter, the tuning of *rzc0* was performed.Runs of the complete orbit were repeated for *rzc0*=80 and *rzc0*=50 km.
No modifications in the results were found in terms of both stability and final χ^2 for both these values. Since stability is not affected by this parameter, it was decided to use a conservative value, i.e. *rzc0*=80 km.All runs described before were performed using a customized *dfact_cont* for each speciess, selected to minimise the dynamic of the eigenvalues of VCM of the retrieved quantities, i.e. pt: 10^{27}, h2o: 10^{28}, o3: 10^{28}, hno3: 10^{26}, ch4:10^{30}, n2o: 10^{27}, no2: 10^{25}. Runs were repeated using the value that is hardwired in the ORM_ABC code, i.e. *fact_cont*=10^{30} for all the speciess.
Also in this case, no modifications were obtained in terms of both stability and final χ^2.As a consequence, the final choice for *fact_cont* was to take the hardwired value, i.e. *fact_cont*=10^{30}

Conclusions

A customized value of *rucl* for each speciess was selected. The recommendation is to use these values in case of normal atmospheric conditions. The tuning has to be repeated in case of volcanic eruptions, but a short term solution in this case is *rucl*= 36 km.
Both the parameters *rzc0* and *dfact_cont* are not critical for retrieval, in term of both stability and final χ^2. The results reported below are very similar to the ones obtained performing the tuning on orbit #504: this indicates that the results of the tuning are stable for different orbits.

3.2 Tuning of parameters linked to Levenberg-Marquardt algorithm

Ref. [RD5]: Sect. 4.1.2; Ref. [RD9]: Sheet MIP_PS_2_5 - MIP_PS_2_6 /2

Introduction

The Levenberg - Marquardt (LM) method involves the introduction of a damping factor that reduces the amplitude of the parameter correction vector. This method is intended to induce smoother convergence especially in case of non-linear problems. The damping factor is initialized to a user-defined value and during the retrieval iterations it is increased or decreased depending on whether the chi-square cost function increases or decreases. The initial value of this damping factor and the factors used to increase and decrease it during the iterations are subject to tuning. Furthermore, the use of LM algorithm requires that also the maximum allowed number of micro-iterations must be established by the user.
The strategy for the choice of the parameters that control the behavior of the damping factor is based on the minimization of the number of iterations needed to reach the convergence. Furthermore we must consider that the forward model internal to the ORM calculates also the Jacobian at each run, therefore a micro-iteration costs as much as a macro-iteration in terms of computing time. For this reason the LM-related parameters should be optimized trying to avoid the occurrence of micro-iterations.
The trade-off between the LM-related parameters and the parameters driving the regularization is of course very strong. The adopted approach is therefore first to optimize the LM-related parameters without any regularization and subsequently optimize the strength of the regularization if profiles oscillations are evident.

Procedure

LM parameters to be tuned are: the initial value of the damping factor (λ_{in}), the number that multiplies the damping factor at each micro-iteration (λ_X) and the number that divides the damping factor at each macro-iteration ($\lambda_/$).
We started from a "reference" set (Version 3, obtained from tuning on the basis of orbit 504 data with cloud filtering) of settings and we checked the variation of the performance of the ORM for various (8) combinations of the values of the three LM parameters. The performance of the ORM was evaluated in terms of: N. of iterations, final chi-square test and, with lowest priority, profile oscillations (Profile Oscillation Quantifier = POQ, defined in TN-IROE-GS0101 Issue 1A, Sect. 4.1.3).
The ORM performances obtained in the considered test cases are summarized in Tables 1 - 7 for the various retrievals. ORM inputs were obtained from orbit 2081 data processed by ML2PP without cloud filtering and with quadratic frequency correction applied to the AILS. The 'X' reported on the left side of tables 1 - 7 denote the best set of LM parameters identified on the basis of the above mentioned criteria.

Table 1: Performance of PT retrieval in the considered test cases

ORBIT # 2081- NO CD - SUMMARY PT

	PT									
	TEST ID	Li	L/	Lx	CNVCRIT	Niter/retr	Nlm/retr	AVG(chi2)	POQ(*)	
"REF"	27	0.05	2	16	0.144	2.67	0.22	2.11	2.00	
x	30	0.02	2	16	0.144	2.56	0.19	1.99	2.11	
	31	0.05	1.1	16	0.144	2.58	0.36	55.46	1.78	(**)
	32	0.05	2	8	0.144	2.74	0.28	2.11	1.99	
	33	0.1	2	16	0.144	2.41	0.10	2.20	1.82	
	34	0.05	4	16	0.144	2.79	0.32	2.08	2.05	
	35	0.05	2	32	0.144	2.71	0.30	2.12	1.99	
	36	0.05	4	32	0.144	2.72	0.29	2.08	2.04	(+)
	37	0.05	1.1	8	0.144	2.48	0.25	35000.00	1.78	
	AVERAGES					2.63	0.26	3896.68	1.95	

(+) Scan # 39 all retrievals lost
(*) POQ = Profile Oscillation Quantifier
(**) Chi2 exploded for pT @ scan # 54

Table 2: Performance of H2O retrieval in the considered test cases

ORBIT # 2081- NO CD - SUMMARY H2O

	H2O									
	TEST ID	Li	L/	Lx	CNVCRIT	Niter/retr	Nlm/retr	AVG(chi2)	POQ(*)	
"REF"	27	0.1	4	8	0.055	2.04	0.23	1.39	31.29	
x	30	0.05	4	8	0.055	2.12	0.22	1.24	31.06	
	31	0.1	2	8	0.055	1.84	0.12	1.39	31.10	
	32	0.1	4	4	0.055	2.13	0.32	1.39	31.43	
	33	0.2	4	8	0.055	2.01	0.20	1.40	29.30	
	34	0.1	8	8	0.055	2.22	0.34	1.25	29.66	
	35	0.1	4	16	0.055	1.88	0.13	1.39	31.65	
	36	0.1	8	16	0.055	2.15	0.26	1.25	29.65	(+)
	37	0.1	2	4	0.055	1.99	0.20	1.39	31.06	
	AVERAGES					2.04	0.22	1.34	30.69	

(*) POQ = Profile Oscillation Quantifier
(+) Scan # 39 all retrievals lost

Table 3: Performance of O3 retrieval in the considered test cases

ORBIT # 2081- NO CD - SUMMARY O3

	O3									
	TEST ID	Li	L/	Lx	CNVCRIT	Niter/retr	NIm/retr	AVG(chi2)	POQ(*)	
"REF"	27	0.1	4	8	0.070	3.49	1.25	2.86	35.37	
x	30	0.05	4	8	0.070	3.37	1.19	2.71	36.02	
	31	0.1	2	8	0.070	2.97	0.84	2.87	36.08	
	32	0.1	4	4	0.070	4.54	2.03	2.87	35.36	
	33	0.2	4	8	0.070	3.65	1.29	2.80	33.54	
	34	0.1	8	8	0.070	4.44	1.87	2.55	34.12	
	35	0.1	4	16	0.070	3.12	0.93	2.93	35.35	
	36	0.1	8	16	0.070	3.59	1.25	2.69	33.98	(+)
	37	0.1	2	4	0.070	3.52	1.26	2.87	36.14	
	AVERAGES					3.63	1.32	2.79	35.11	

(*) POQ = Profile Oscillation Quantifier
(+) Scan # 39 all retrievals lost

Table 4: Performance of HNO3 retrieval in the considered test cases

ORBIT # 2081- NO CD - SUMMARY HNO3

	HNO3									
	TEST ID	Li	L/	Lx	CNVCRIT	Niter/retr	NIm/retr	AVG(chi2)	POQ(*)	
"REF"	27	0.05	2	8	0.025	3.96	0.96	1.49	72.17	
x	30	0.02	2	8	0.025	4.06	1.04	1.42	71.84	
	31	0.05	1.1	8	0.025	3.36	0.45	1.50	72.21	
	32	0.05	2	4	0.025	4.41	1.39	1.50	71.90	
	33	0.1	2	8	0.025	3.90	0.86	1.55	69.82	
	34	0.05	4	8	0.025	4.54	1.49	1.44	70.52	
	35	0.05	2	16	0.025	3.74	0.75	1.49	71.96	
	36	0.05	4	16	0.025	3.99	1.06	1.43	70.47	(+)
	37	0.05	1.1	4	0.025	3.91	0.80	1.50	71.78	
	AVERAGES					3.99	0.98	1.48	71.41	

(*) POQ = Profile Oscillation Quantifier
(+) Scan # 39 all retrievals lost

Table 5: Performance of CH4 retrieval in the considered test cases

ORBIT # 2081- NO CD - SUMMARY CH4

	CH4									
	TEST ID	Li	L/	Lx	CNVCRIT	Niter/retr	Nlm/retr	AVG(chi2)	POQ(*)	
"REF"	27	0.1	4	8	0.050	2.87	0.81	1.98	31.95	
x	30	0.05	4	8	0.050	2.66	0.74	1.90	33.06	
	31	0.1	2	8	0.050	2.30	0.33	1.99	32.34	
	32	0.1	4	4	0.050	3.19	1.13	1.99	32.13	
	33	0.2	4	8	0.050	2.38	0.47	1.94	28.07	(**)
	34	0.1	8	8	0.050	2.93	0.99	1.90	30.85	
	35	0.1	4	16	0.050	2.58	0.59	1.99	32.10	
	36	0.1	8	16	0.050	2.54	0.63	1.90	30.95	(+)
	37	0.1	2	4	0.050	2.61	0.59	1.98	32.30	
	AVERAGES					2.67	0.70	1.95	31.53	

(+) Scan # 39 all retrievals lost
(*) POQ = Profile Oscillation Quantifier
(**) Scan # 38 lost for CH4, N2O and NO2

Table 6: Performance of N2O retrieval in the considered test cases

ORBIT # 2081- NO CD - SUMMARY N2O

	N2O									
	TEST ID	Li	L/	Lx	CNVCRIT	Niter/retr	Nlm/retr	AVG(chi2)	POQ(*)	
"REF"	27	0.2	2	8	0.064	2.74	0.59	1.93	44.21	
x	30	0.1	2	8	0.064	2.44	0.53	1.82	45.51	
	31	0.2	1.1	8	0.064	2.19	0.26	1.94	42.64	
	32	0.2	2	4	0.064	2.90	0.81	1.91	43.86	
	33	0.4	2	8	0.064	2.49	0.51	1.91	39.89	(**)
	34	0.2	4	8	0.064	3.06	0.87	1.82	44.32	
	35	0.2	2	16	0.064	2.54	0.45	1.94	44.17	
	36	0.2	4	16	0.064	2.74	0.69	1.85	43.99	(+)
	37	0.2	1.1	4	0.064	2.58	0.59	1.93	43.26	
	AVERAGES					2.63	0.59	1.89	43.54	

(+) Scan # 39 all retrievals lost
(*) POQ = Profile Oscillation Quantifier
(**) Scan # 38 lost for CH4, N2O and NO2

Table 7: Performance of NO2 retrieval in the considered test cases

ORBIT # 2081- NO CD - SUMMARY NO2

	NO2									
	TEST ID	Li	L/	Lx	CNVCRIT	Niter/retr	Nlm/retr	AVG(chi2)	POQ(*)	
"REF"	27	0.1	4	8	0.040	2.25	0.25	1.25	32.60	
x	30	0.05	4	8	0.040	2.74	0.46	1.18	31.85	
	31	0.1	2	8	0.040	1.96	0.10	1.25	31.61	
	32	0.1	4	4	0.040	2.70	0.54	1.25	32.55	
	33	0.2	4	8	0.040	1.72	0.10	1.18	33.80	(**)
	34	0.1	8	8	0.040	3.00	0.68	1.18	31.88	
	35	0.1	4	16	0.040	2.09	0.16	1.25	32.42	
	36	0.1	8	16	0.040	2.44	0.32	1.18	31.90	(+)
	37	0.1	2	4	0.040	2.13	0.19	1.25	31.74	
	AVERAGES					2.34	0.31	1.22	32.26	

(*) POQ = Profile Oscillation Quantifier
(**) Scan # 38 lost for CH4, N2O and NO2
(+) Scan # 39 all retrievals lost

Results

As a result of this optimization procedure we have obtained a set of values for the LM parameters that produce performance as highlighted in table 8 reported below.

Table 8: Selected optimal set of LM parameters and related ORM performance corresponding to this set of parameters.

ORBIT # 2081- NO CD - SUMMARY LEVENBERG-MARQUARDT

All PS2 Vers. 3 but LM Vers.4								
TARGET	Li	L/	Lx	CNVCRIT	Niter/retr	Nlm/retr	AVG(chi2)	POQ(*)
PT	0.02	2	16	0.144	2.56	0.19	1.99	2.11
H2O	0.05	4	8	0.055	2.12	0.22	1.24	31.06
O3	0.05	4	8	0.070	3.37	1.19	2.71	36.02
HNO3	0.02	2	8	0.025	4.06	1.04	1.42	71.84
CH4	0.05	4	8	0.050	2.66	0.74	1.90	33.06
N2O	0.1	2	8	0.064	2.44	0.53	1.82	45.51
NO2	0.05	4	8	0.040	2.74	0.46	1.18	31.85
AVERAGES					2.85	0.62	1.75	35.92

(*) POQ = Profile Oscillation Quantifier

Conclusions / recommendations

- Optimal LM parameters Vers.3 (optimized on the basis of orbit 504 data with cloud filtering) produce stable results also on orbit 2081.
- LM parameters Vers. 4 differ from Vers.3 only for the initial value assigned to λ: Vers4 = Vers3 / 2
- It would be desirable (but not necessary) to re-tune LM parameters when cloud filter will be activated in the PDS.
- It is recommended to check / re-optimize LM parameters once per year.

3.3 Tuning of convergence criteria

Ref. [RD5]: Sect. 4.1.5; Ref. [RD9]: Sheet MIP_PS_2_5 - MIP_PS_2_6 /4

Introduction

The convergence criteria adopted in the MIPAS Level 2 processor are based on three conditions:

1. Linearity of the inversion problem. The maximum relative difference (in two subsequent iterations) between linear and real chi-square must be less than a pre-defined threshold T1.
2. Attained accuracy. The maximum relative variation (in two subsequent iterations) of the fitted parameters must be less than a pre-defined threshold T2.
3. Computing time. Due to general computing time constraints in MIPAS Level 2 processor, there is a max. number of iterations beyond which the retrieval must be stopped. However, the present runtime requirements of the Level 2 processor are not very stringent and therefore the max. number of allowed iterations can be set on the basis of the ORM team experience based on both simulated and MIPAS-B2 retrievals. From the experience we learned that if a retrieval is not converging after 10 iterations then also after 30 iterations it will not converge because of some contingent problem. Therefore we set the max. number of both micro- and macro- iterations equal to 10 for all retrieval types.

The retrieval is stopped if one of the above 3 conditions is fulfilled, the convergence is reached if one of the first two conditions is fulfilled. The task is therefore to tune the thresholds T1 and T2 related to conditions 1. and 2.

Procedure

The threshold T2 is not subject to tuning because from the physical point of view it is directly connected with the accuracy of the retrieved parameters. Therefore T2 is set equal to a fraction ($1/10^{th}$) of the expected total error affecting the target parameter to which it refers.
The threshold T1 was tuned using this approach: T1 and T2 were initially set to an arbitrarily small value (= 0) and all the retrievals relating to the selected orbit (#2081) were run with 10 iterations. Both the χ^2 and the χ^2_{lin} (χ^2 calculated in the linear approximation) were annotated into a file.
Subsequently, using the annotated data, different values of T1 were tested and for each value of T1 the following quantities were plotted:

- percentage P1 of retrievals for which $\frac{\chi^2-\chi^2(\infty)}{\chi^2(\infty)} < 0.10$ (key in Figs 1-7: "% IN ROUGH BOX")
- percentage P2 of retrievals for which $\frac{\chi^2-\chi^2(\infty)}{\chi^2(\infty)} < 0.05$ (key in Figs 1-7: "% IN MEDIUM BOX")
- percentage P3 of retrievals for which $\frac{\chi^2-\chi^2(\infty)}{\chi^2(\infty)} < 0.02$ (key in Figs 1-7: "% IN PRECISE BOX")
- percentage P4 of converging retrievals (key in Figs 1-7: "% CONVERGED")
- number of iterations normalized to the total number of micro- plus macro- iterations after 10 macro- iterations and multiplied by 100 (key in Figs 1-7: "% CPU COST")

Starting from an arbitrarily high value of T1, T1 is decreased at discrete steps (step = 0.001) and the optimal value of T1 is chosen either as:

1. the greatest value of T1 for which P1 > 99%, P2 > 95% and P3 > 85% **OR**
2. the greatest value of T1 for which P4 < 100% increased by an offset of 0.01

depending on which of the two above conditions occurs earlier. The selected value for the threshold T1 is indicated in Figs 1-7 with a vertical arrow.

In order to further characterize the precision of the selected convergence criterion (T1) the following plots were also built:

- Figures 8-14 report, for a given percentage *x* (on the horizontal axis), the percentage of retrievals for which, at convergence we have:

$$\left[\frac{\chi^2-\chi^2(\infty)}{\chi^2(\infty)}\right]\cdot 100 < x$$

- Figures 15-21 report the differences between profiles retrieved at convergence and profiles retrieved after 10 iterations, normalized to their ESD.
- Figures 22-28 report the differences between profiles retrieved after 9 iterations and profiles retrieved after 10 iterations, normalized to their ESD. These figures characterize the retrieval stability, i.e. highlight the profile fluctuations in subsequent iterations after the real convergence has been reached (we assume the convergence to be reached before the 9th iteration).

Results

In this section we include the figures resulting from the analysis described above. The analysis was carried-out on the basis of orbit #2081 measurements, with no cloud filtering applied. Cloudy scans were included in the analysis.

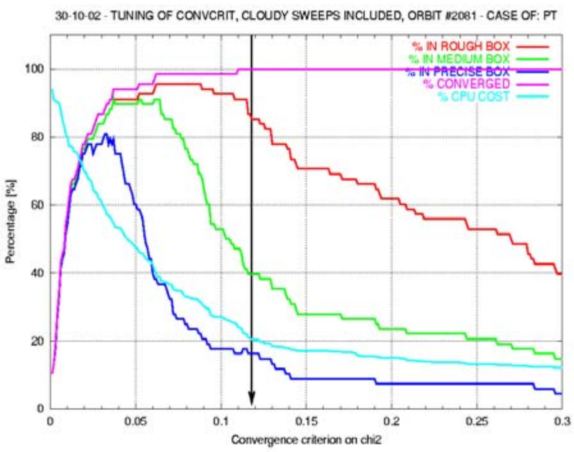

Fig. 1: Convergence characterization in case of pT

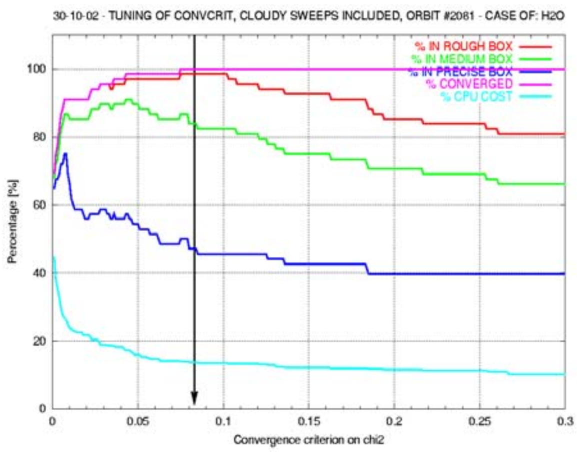

Fig. 2: Convergence characterization in case of H2O

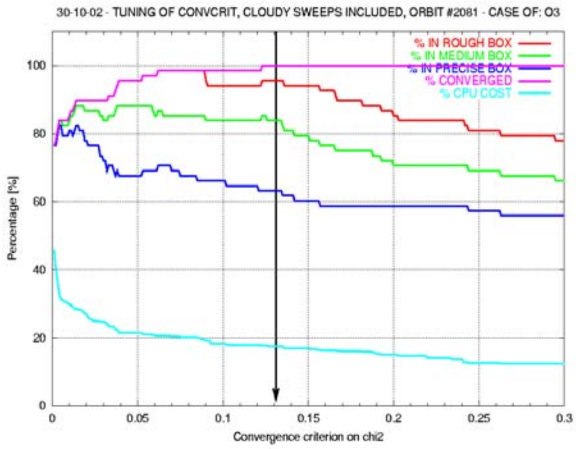

Fig. 3: Convergence characterization in case of O3

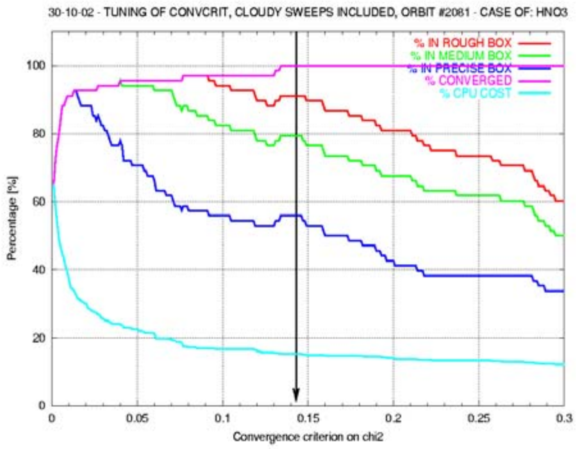

Fig. 4: Convergence characterization in case of HNO3

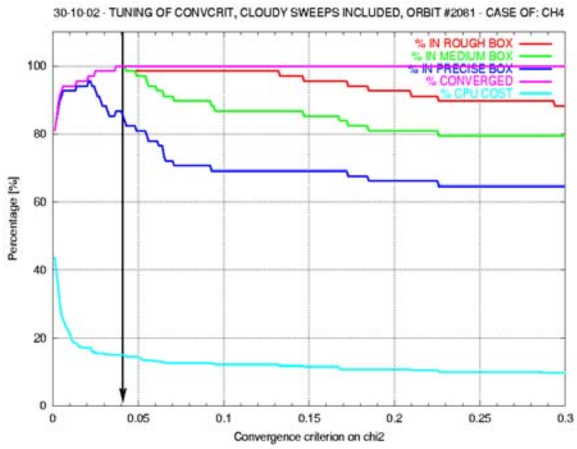

Fig.5: Convergence characterization in case of CH4

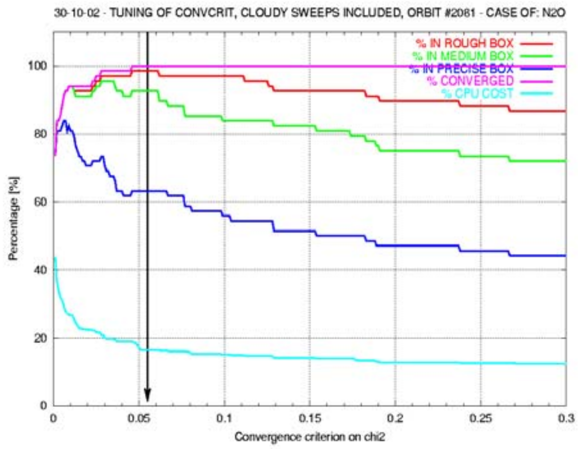

Fig. 6: Convergence characterization in case of N2O

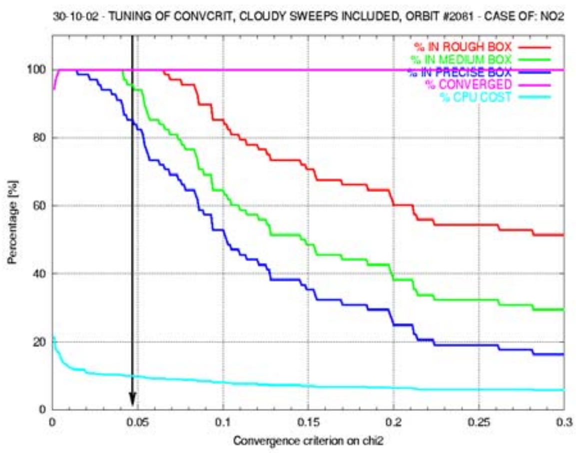

Fig.7: Convergence characterization in case of NO2

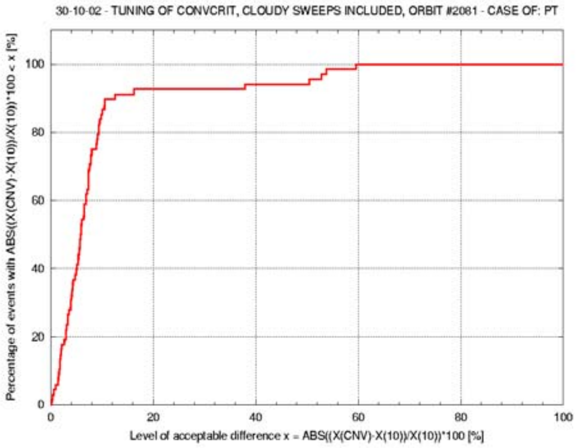

Fig.8: Convergence precision in case of pT

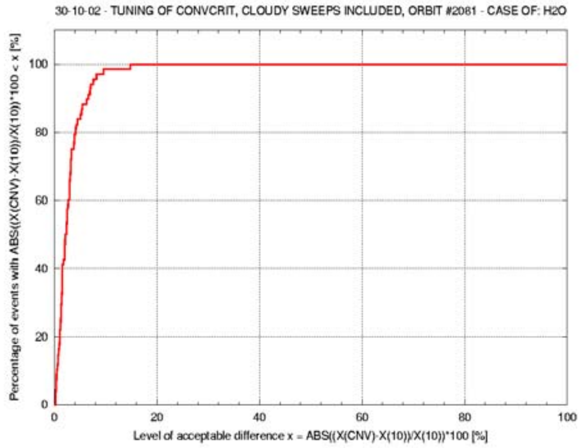

Fig.9: Convergence precision in case of H2O

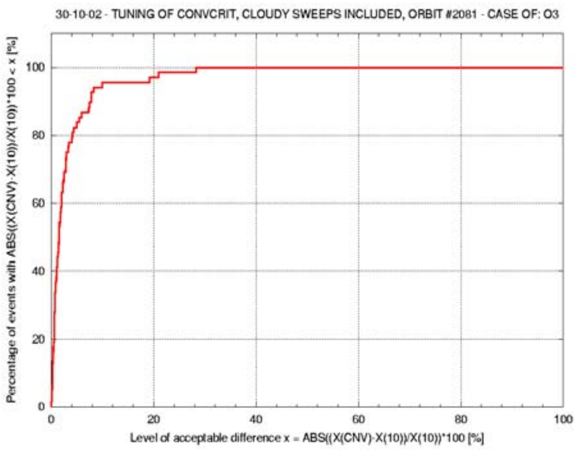

Fig.10: Convergence precision in case of O3

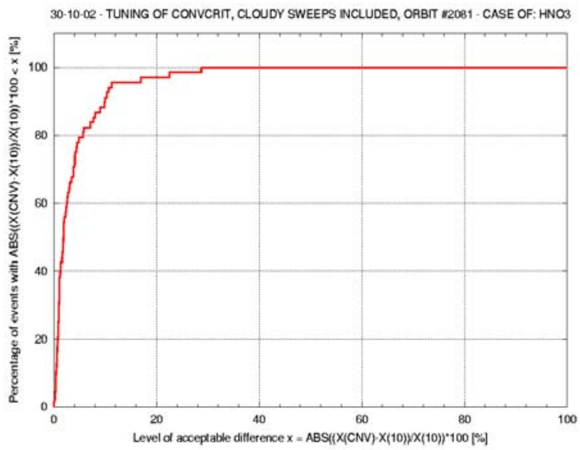

Fig.11: Convergence precision in case of HNO3

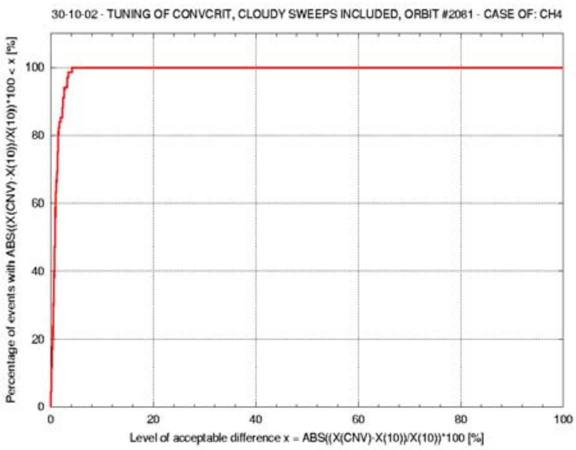

Fig.12: Convergence precision in case of CH4

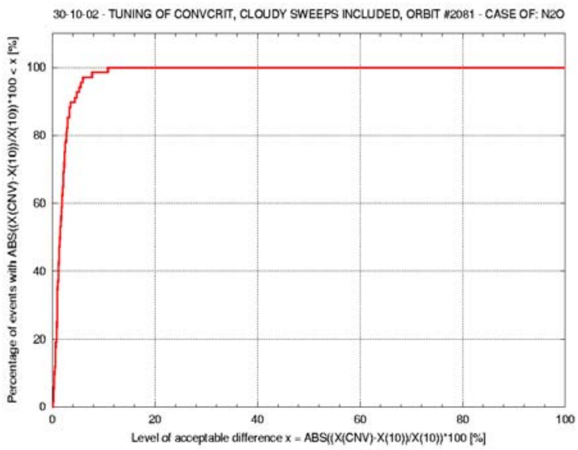

Fig.13: Convergence precision in case of N2O

Fig.14: Convergence precision in case of NO2

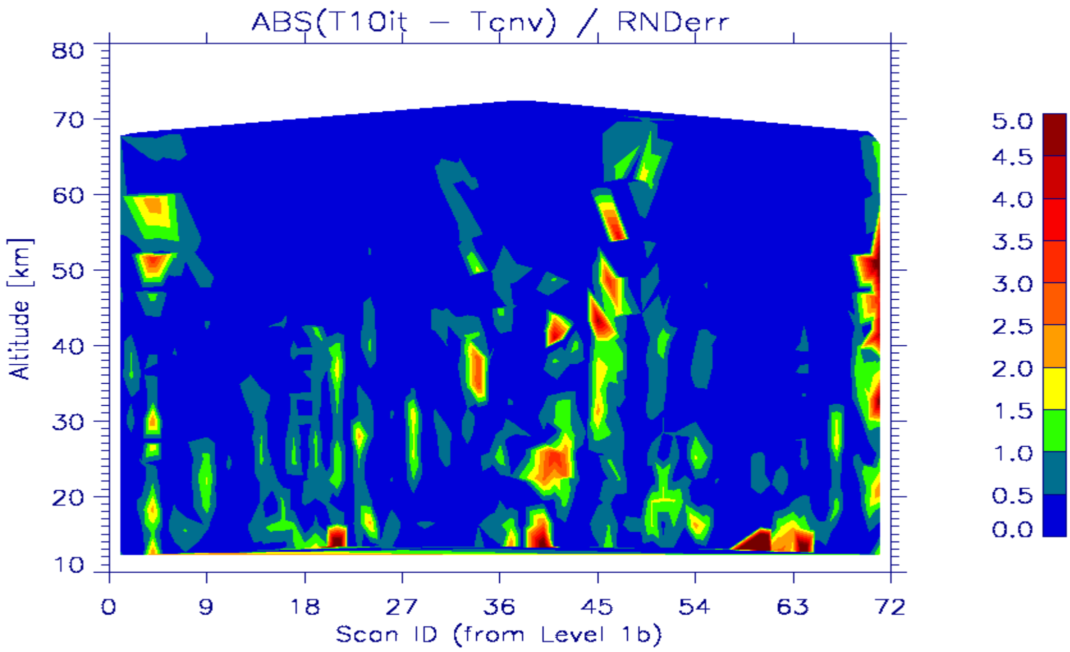

Fig.15: Convergence error quantified by the ESD-normalized difference between profiles at convergence and profiles after 10 iterations. Case of pT retrieval.

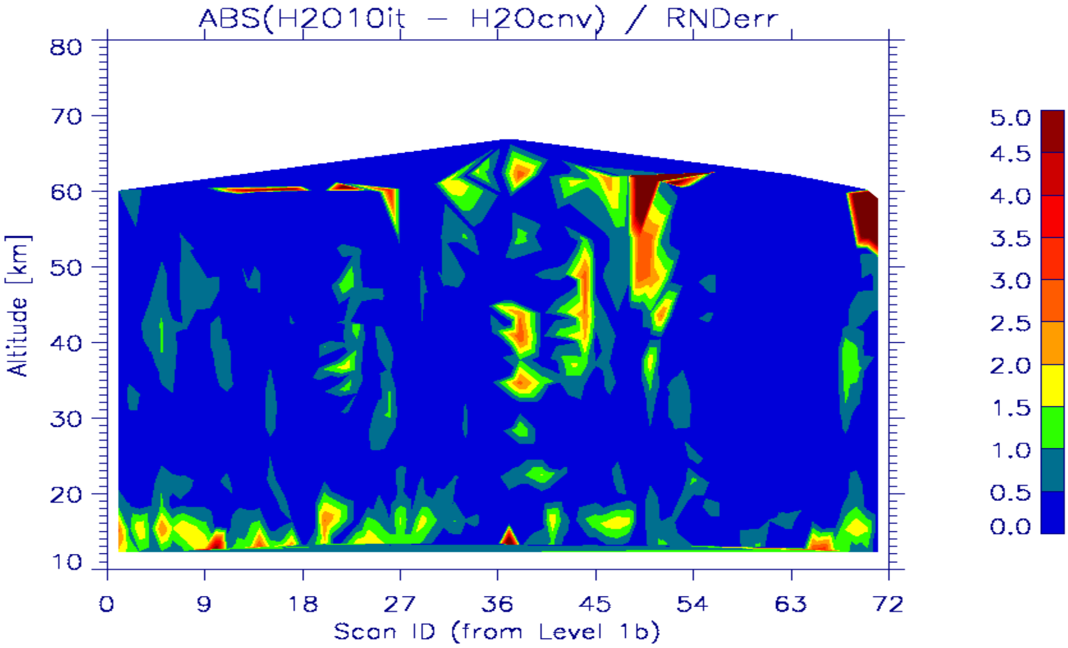

Fig.16: Convergence error quantified by the ESD-normalized difference between profiles at convergence and profiles after 10 iterations. Case of H2O retrieval.

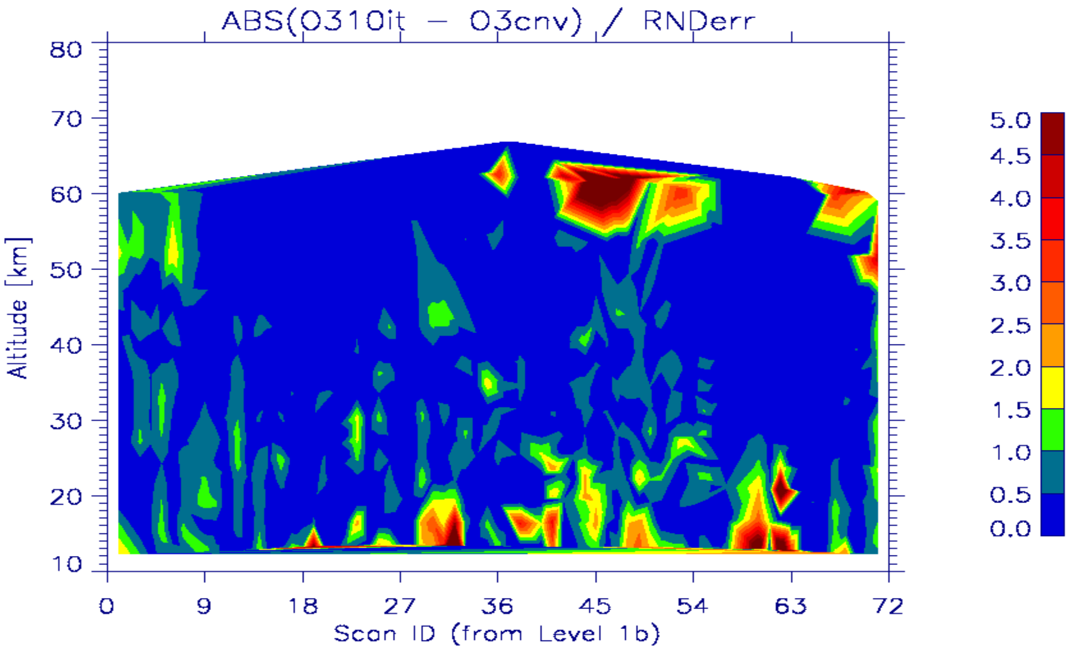

Fig.17: Convergence error quantified by the ESD-normalized difference between profiles at convergence and profiles after 10 iterations. Case of ozone retrieval.

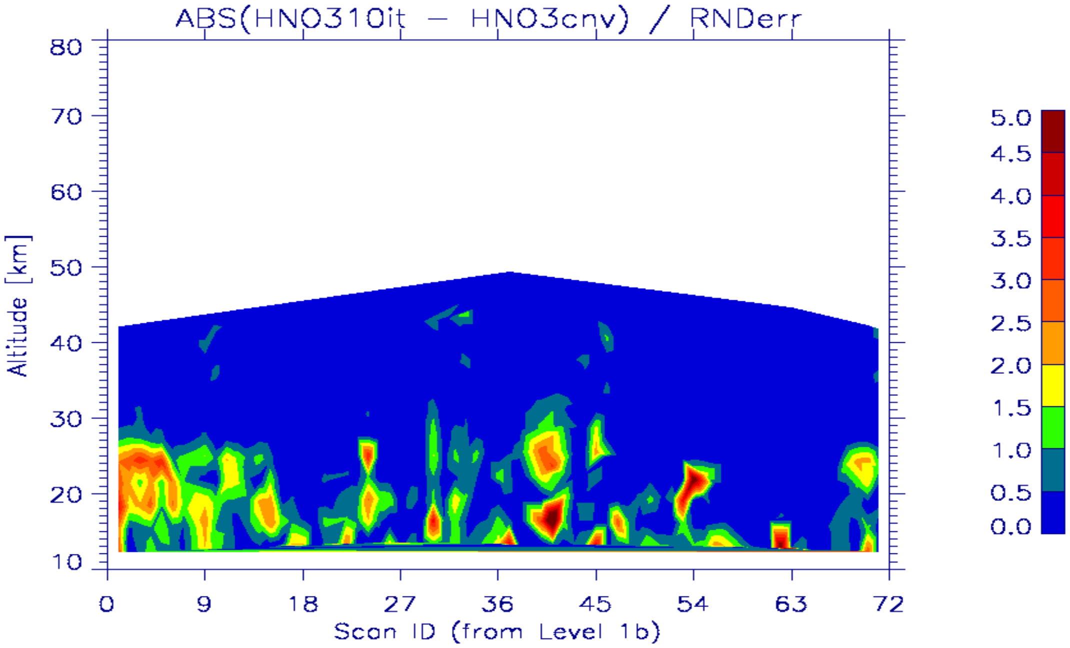

Fig.18: Convergence error quantified by the ESD-normalized difference between profiles at convergence and profiles after 10 iterations. Case of HNO3 retrieval.

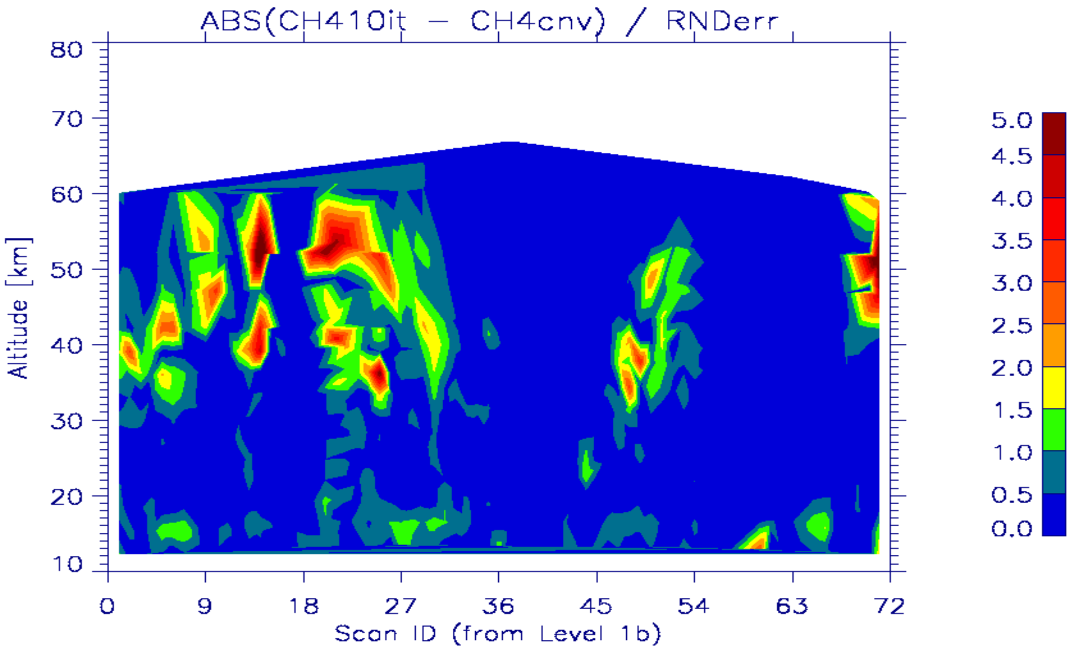

Fig.19: Convergence error quantified by the ESD-normalized difference between profiles at convergence and profiles after 10 iterations. Case of CH4 retrieval.

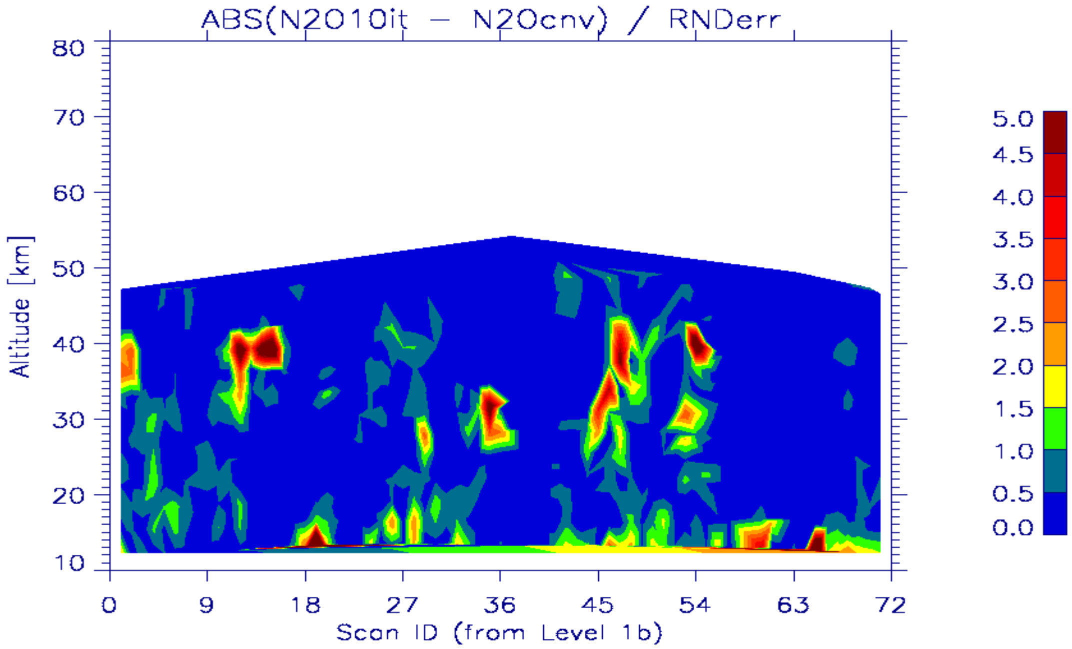

Fig.20: Convergence error quantified by the ESD-normalized difference between profiles at convergence and profiles after 10 iterations. Case of N2O retrieval.

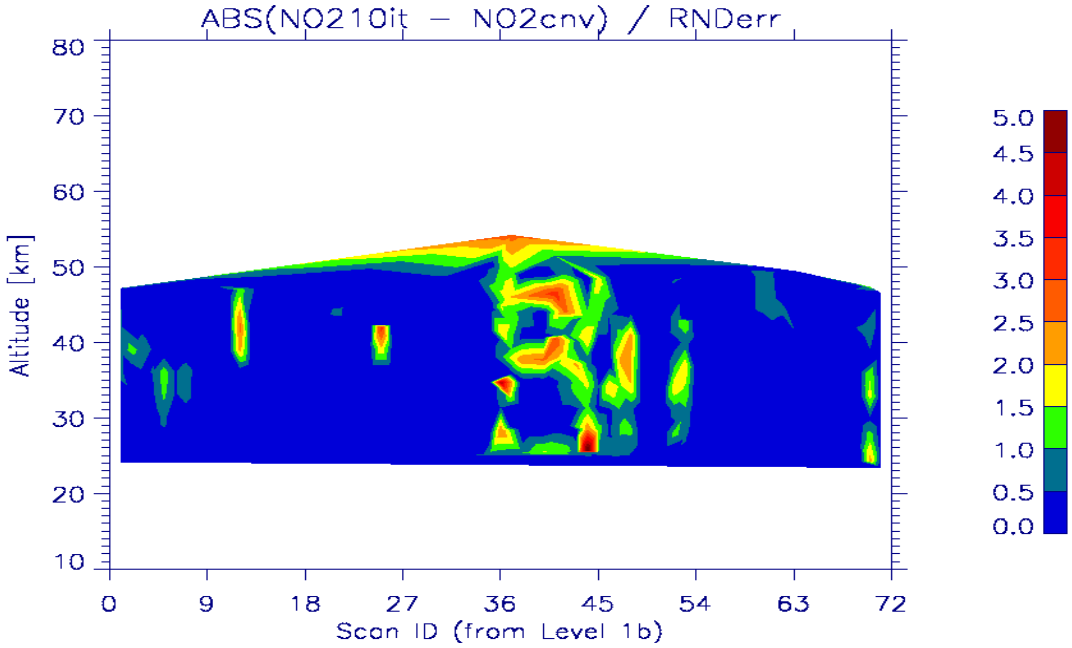

Fig.21: Convergence error quantified by the ESD-normalized difference between profiles at convergence and profiles after 10 iterations. Case of NO2 retrieval.

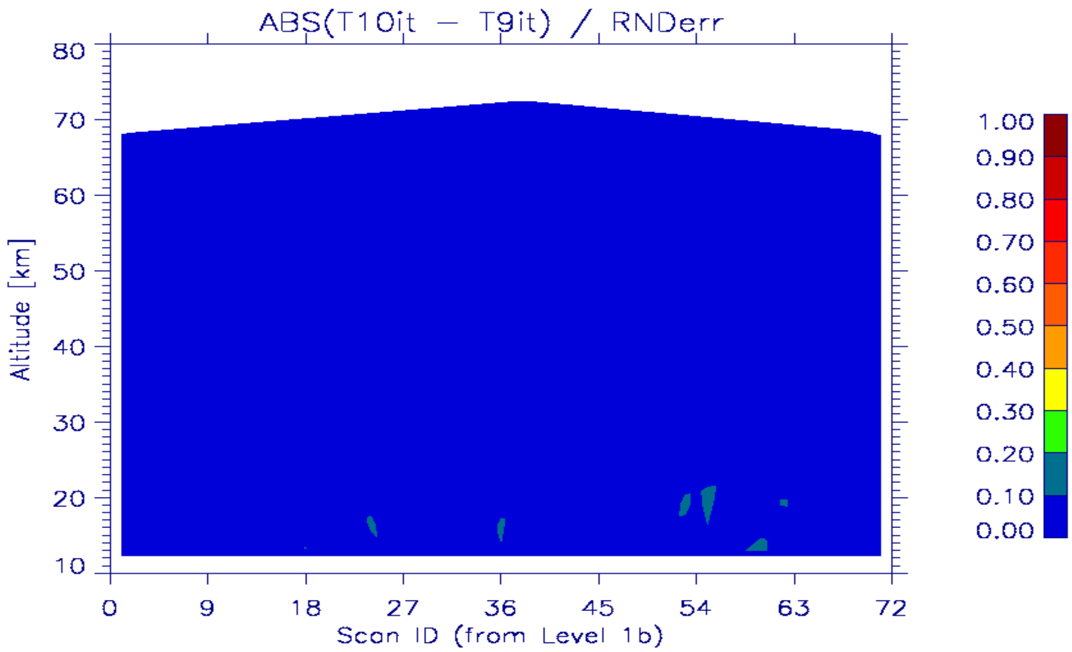

Fig. 22: Characterization of the stability of the retrieval. The map shows the ESD-normalized differences between profiles after 9 iterations and after 10 iterations. Case of PT retrieval.

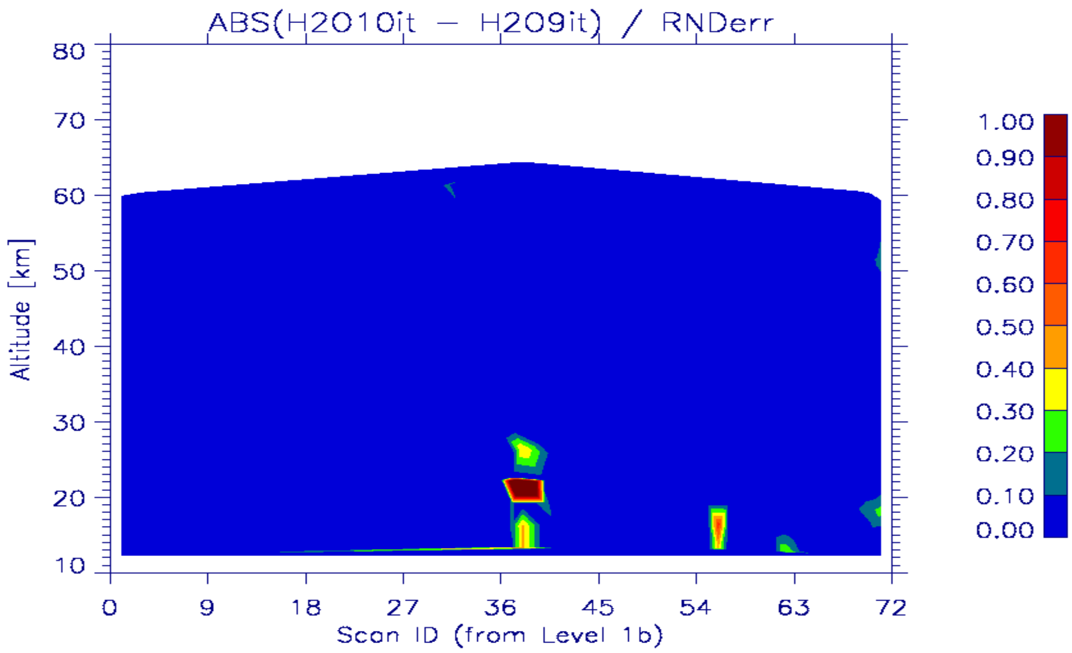

Fig. 23: Characterization of the stability of the retrieval. The map shows the ESD-normalized differences between profiles after 9 iterations and after 10 iterations. Case of H2O retrieval.

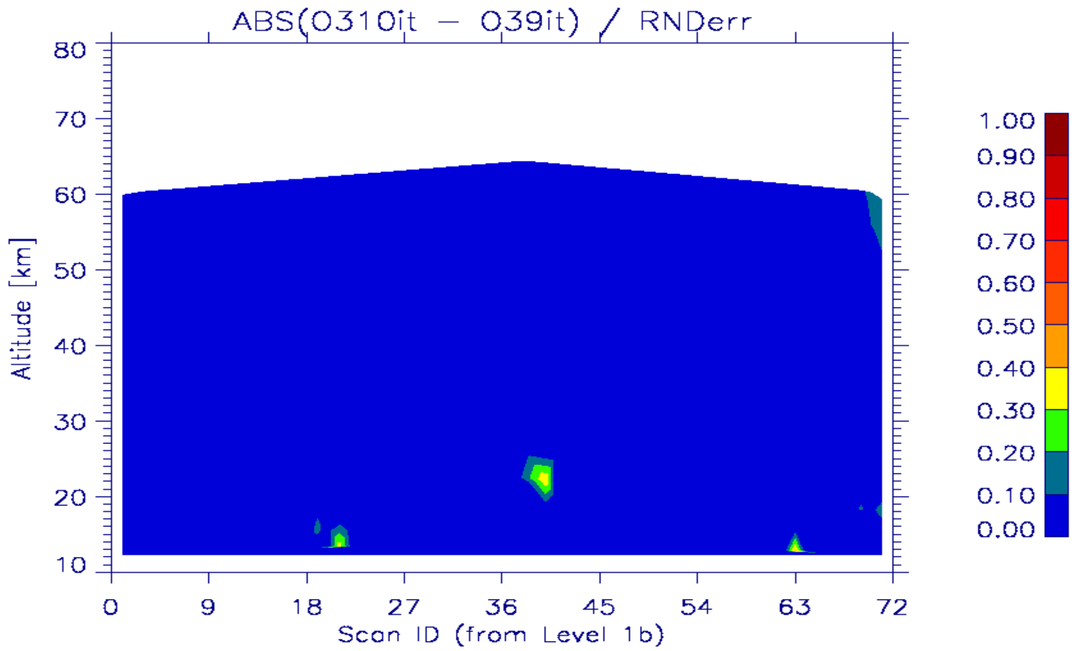

Fig. 24: Characterization of the stability of the retrieval. The map shows the ESD-normalized differences between profiles after 9 iterations and after 10 iterations. Case of O3 retrieval.

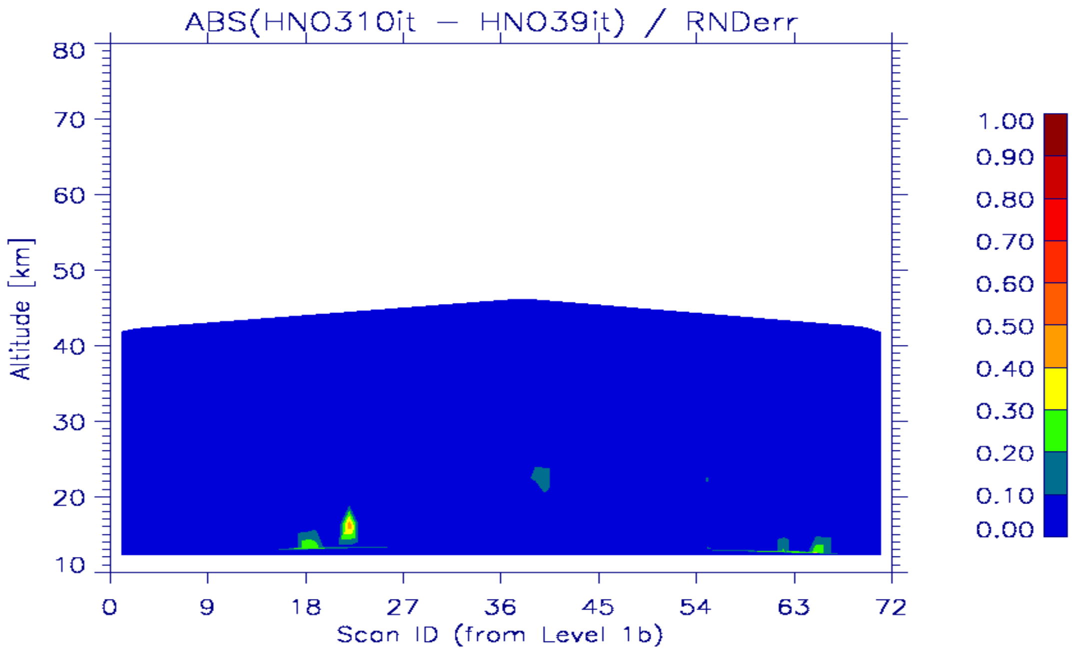

Fig. 25: Characterization of the stability of the retrieval. The map shows the ESD-normalized differences between profiles after 9 iterations and after 10 iterations. Case of HNO3 retrieval.

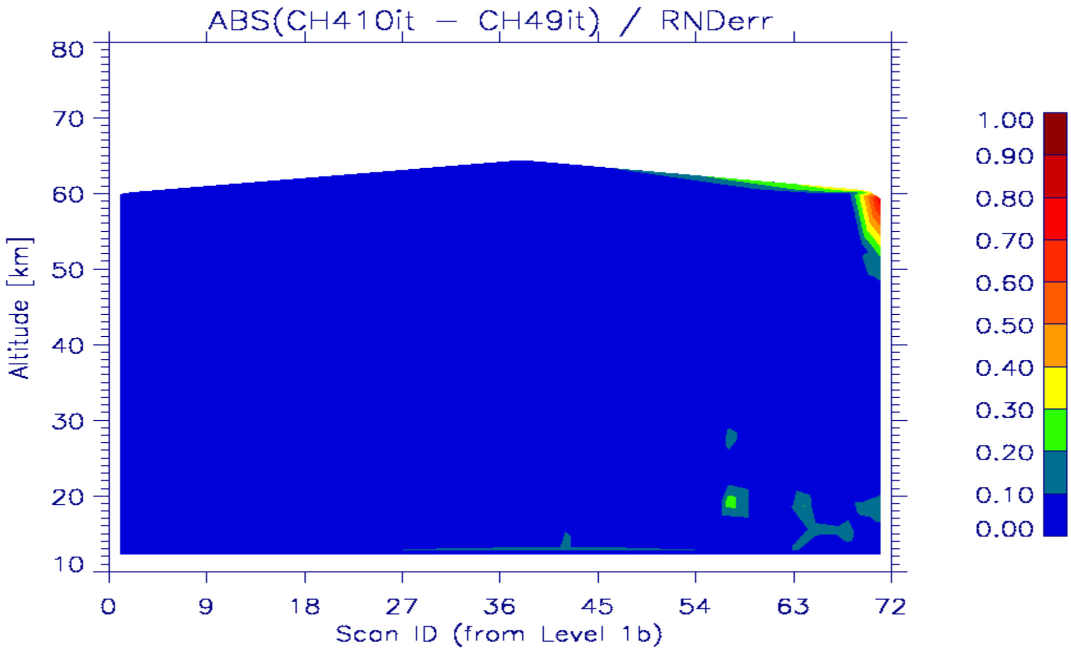

Fig. 26: Characterization of the stability of the retrieval. The map shows the ESD-normalized differences between profiles after 9 iterations and after 10 iterations. Case of CH4 retrieval.

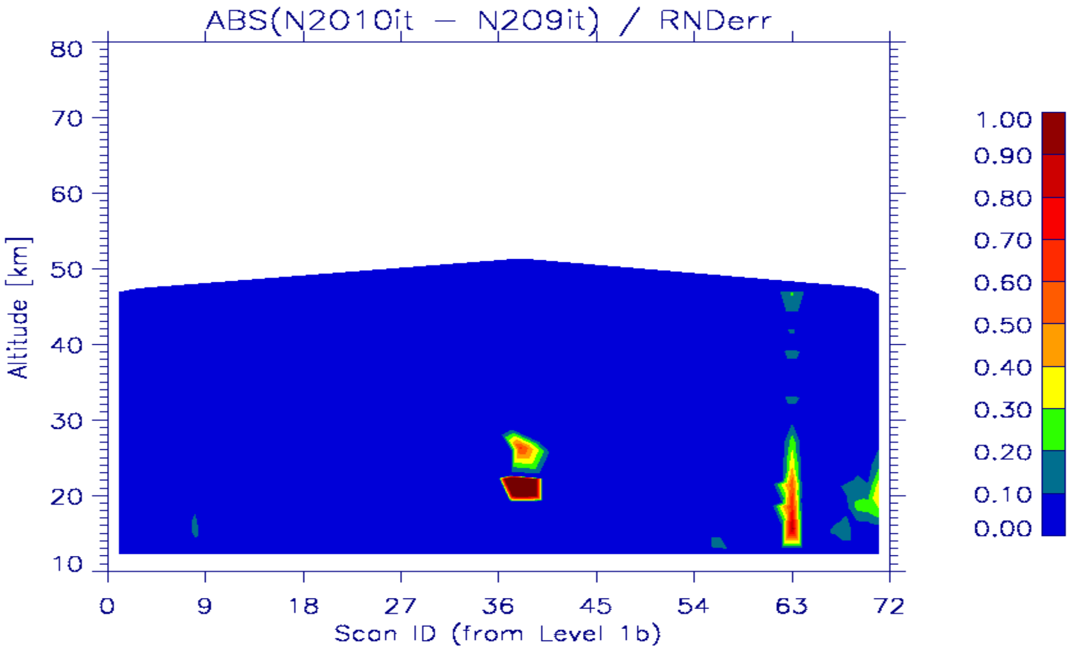

Fig. 27: Characterization of the stability of the retrieval. The map shows the ESD-normalized differences between profiles after 9 iterations and after 10 iterations. Case of N2O retrieval.

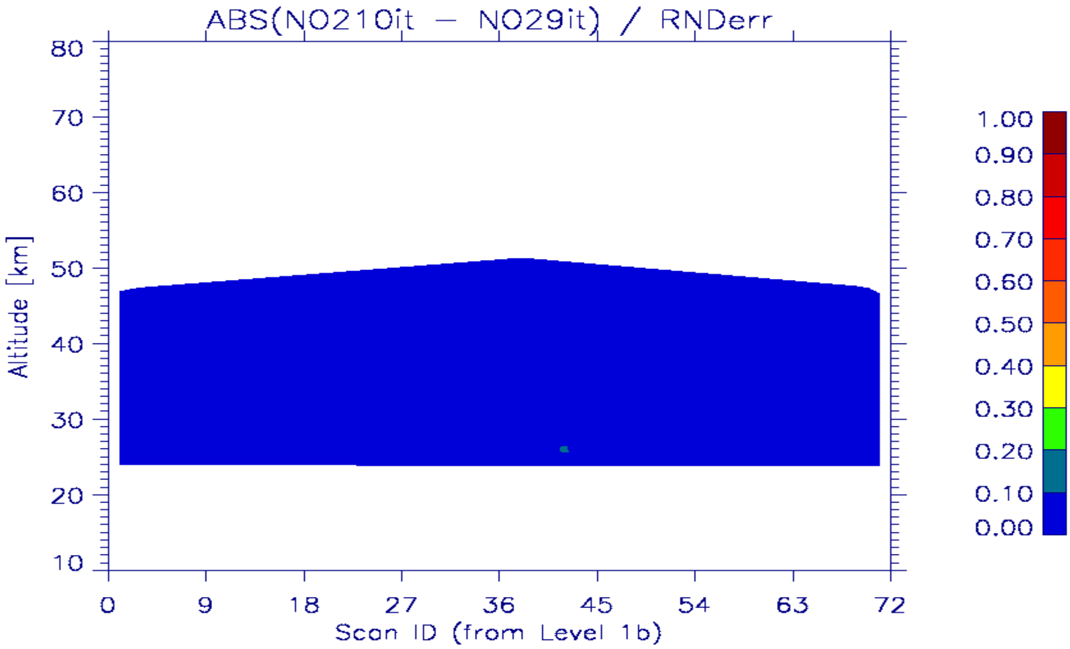

Fig. 28: Characterization of the stability of the retrieval. The map shows the ESD-normalized differences between profiles after 9 iterations and after 10 iterations. Case of NO2 retrieval.

Conclusions

Convergence criteria version 4 were determined on the basis of the analysis specified above and MIPAS measurements relating to orbit 2081, no cloud filtering was applied. Convergence criteria version 4 are very similar to the earlier version (Vers. 3) of convergence criteria that were determined on the basis of orbit 504 data with cloud filtering. The only exceptions are convergence criteria for O_3 and HNO_3. For these speciess version 4 criteria are less stringent due to the requirement of reaching convergence also in case of cloudy scans. Table 1 summarizes the optimized values of convergence thresholds version 4 and version 3.

Table 1: summary of convergence criteria version 3 and version 4.

Retrieval #	Convcrit V.3 based on # 504	Convcrit V.4 based on # 2081
PT	**0.144**	**0.118**
H_2O	**0.055**	**0.083**
O_3	**0.070**	**0.131**
HNO_3	**0.025**	**0.143**
CH_4	**0.050**	**0.041**
N_2O	**0.064**	**0.055**
NO_2	**0.040**	**0.047**

The convergence error highlighted in Figs. 15-21 is in several cases significant with respect to the ESD and is cause of some concern. As shown in Figs. 22-28 this error is not originated by a retrieval instability, but is

due to the fact that the current convergence criteria stop the retrieval significantly before the real minimum of the cost function has been reached.
In order to improve the retrieval accuracy and fully exploit the computing power presently available in the PDS we therefore recommend a further refinement of convergence criteria, in terms of both threshold values and type of required conditions.

3.4 Retrieval grid

Ref. [RD5]: Sect. 4.1.6; Ref. [RD9]: Sheet MIP_PS_2_5 - MIP_PS_2_6 /5

Introduction

The vertical resolution and the accuracy with which the retrieved profiles are determined are uncorrelated and are strongly dependent on the altitude grid where the retrieved points are represented (retrieval grid).
The retrieval range for each species has been defined together with the OM definition and the vertical resolution was assumed to be equal to the measurement resolution.
In the test for the assessment of the measurement altitude range we found that an extension of the retrieval range at altitudes where speciess have low concentration does not degrade the profiles in the nominal retrieval range. Here we try to assess the effect in the retrieved profile of a degradation of the vertical resolution at some altitudes (in the nominal range) characterised by big random noise.

Procedure and results

For each retrieval we selected the altitude that is characterised by the greatest random noise, and then we run retrieval excluding that altitude from the fit (the input parameter *lfit* was set to F in correspondence of that altitude).
We then compared the retrieved profiles obtained in the two cases. Figure 1 shows the retrieved profiles of o3 in case of nominal retrieval and when the VMR at altitude 15 km is not fitted.

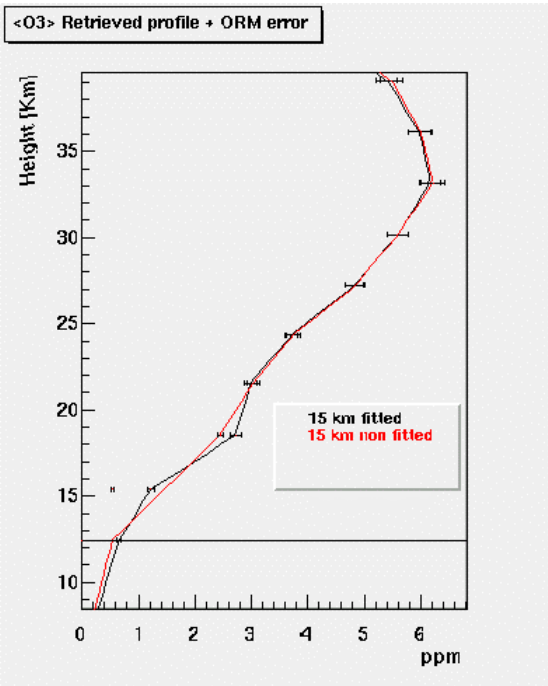

Figure 1 Comparison of O3 profile retrieved when the nominal retrieval range is used and when altitude 15 km is not included in the fit.

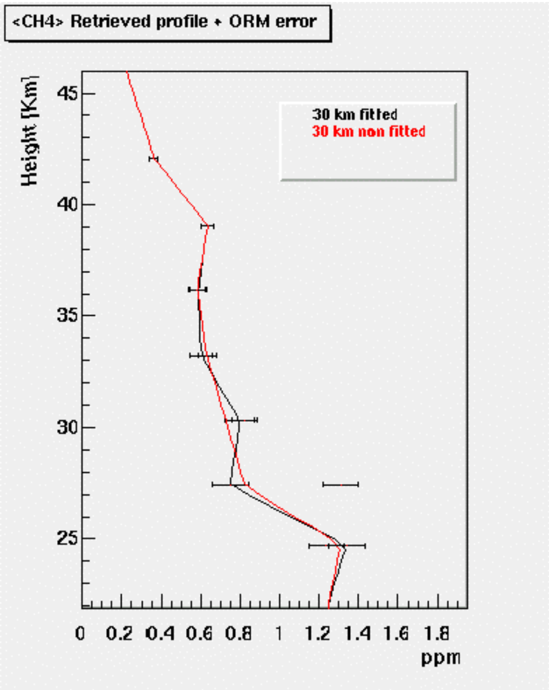

Figure 2 Comparison of CH4 profile retrieved when the nominal retrieval range is used and when altitude 30 km is not included in the fit.

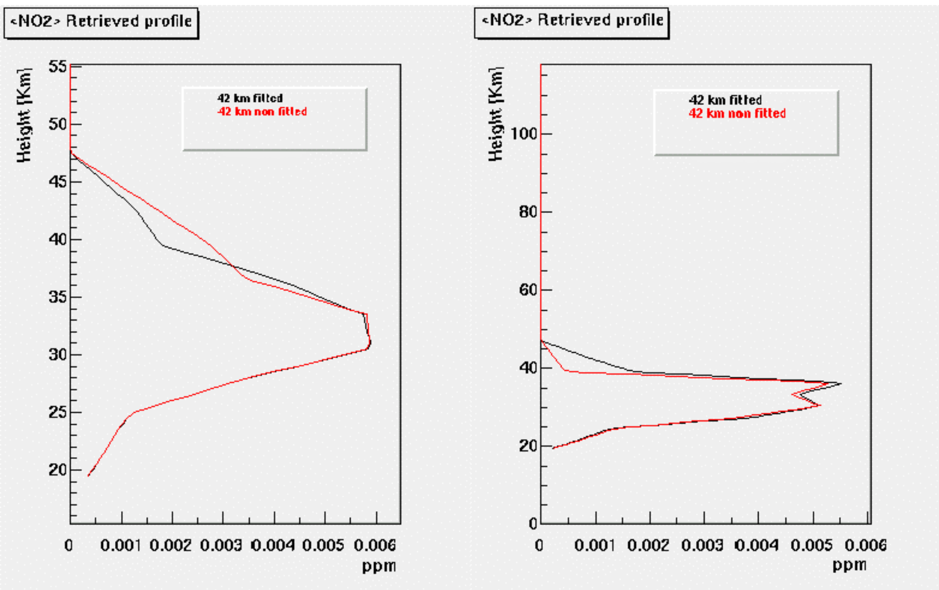

Figure 3 Comparison of NO2 profile retrieved when the nominal retrieval range is used and when altitude 42 km is not included in the fit for two representative scans.

Conclusions

In most cases we have verified that a degradation of the vertical resolution succeeds in reducing the oscillations in the retrieved profile, but the retrieved profile with a reduced vertical resolution could be obtained from the other just drawing a line through the two points contiguous to the altitude that is not fitted in one case.

This means that a degradation of the vertical resolution does not lead to an improvement of the retrieved profile and no relaxation of the present retrieval grid is recommended.

3.5 Tuning of the layering used in the forward model (linear-in-tau approximation)

Ref. [RD5]: Sect. 4.1.7; Ref. [RD9]: Sheet MIP_PS_2_5 - MIP_PS_2_6 /6

Introduction

In the radiative transfer of the ORM the Planck function is calculated in for a constant (frequency-independent) temperature equal to the Curtis-Godson temperature of the target gas of the retrieval. This approximation may turn out to be too rough for tangent layers in an opaque atmosphere. In some codes this problem is solved by assuming that the Planck function varies linearly with optical depth in the layer. This approach is usually referred to as the 'linear-in-tau' method and takes into account the fact that only a spectral element associated with small optical depth radiates with temperature determined in the Curtis-Godson approximation, while a spectral element with large optical depth radiates with a temperature characteristic of the layer at the boundary.
Due to the mentioned approximation, the parameters that control the automatic layering of the atmosphere (temperature and half-width variation thresholds) have been checked using the 'real' atmosphere as retrieved from MIPAS measurements. If the real atmosphere turned-out to be more opaque than that used for pre-flight tuning of the layering, the tuning operation may have lead to the selection of a layering finer than the optimized one determined (before the flight) with model atmospheres.

Procedure

The profiles retrieved on the basis of the layering determined before launch (43 levels) were compared with profiles retrieved using a very fine layering (80 levels). The differences between profiles determined in the two cases were compared with the profile ESD. For some scans the use of different layerings causes a different number of iterations required for convergence. Therefore in these cases differences between profiles would be due to different number of iterations rather than different layerings. For this reason it was decided, only for this test, to stop the retrievals after three iterations. No constrain was applied to micro-iterations.

Results

Figs 1 - 7 show the observed differences between the profiles retrieved with the layering determined before launch (43 levels) and the profiles retrieved using a fine layering (80 levels). These differences were normalized to the profile ESD for easier readability.
Generally the discrepancies are well below the random error associated with the retrieved profiles, however there are a few cases in which these discrepancies significantly exceed the random error, namely:

a) in correspondence of cloudy sweeps and
b) for pT retrieval, scan #7.

Case a) is well understood considering that clouds cause an enhancement of the opacity of the atmosphere. However this is not cause of concern because the retrieval performance is degraded in any case whenever cloudy sweeps are included in the analysis.

Also case b) is not cause of concern because, inspection of the pT retrieval for scan 7 reveals that a different number of micro-iterations occurs in the two run involved in the test. Therefore in this case the observed differences must be attributed to the different number of iterations rather than to the inadequacy of the atmospheric layering.

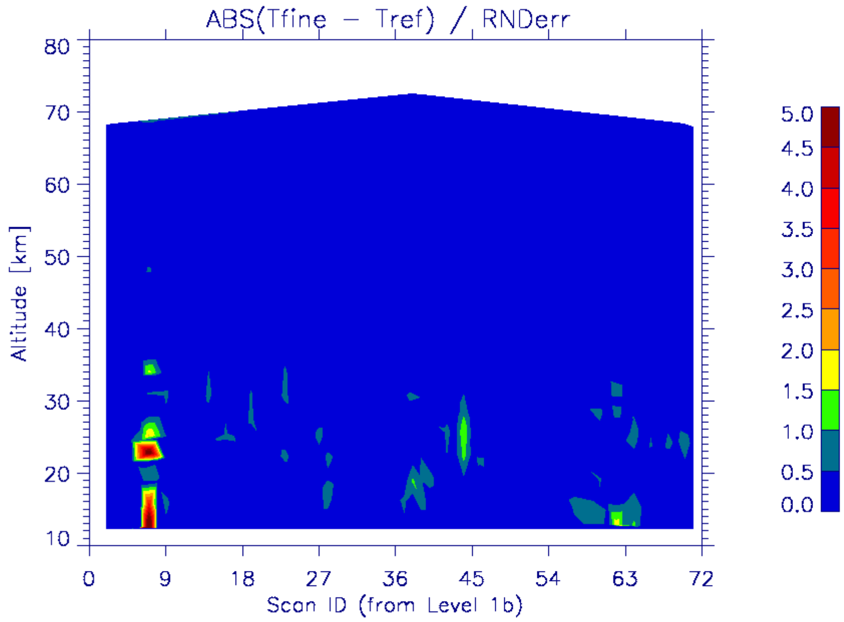

Fig. 1: ESD-normalized differences between temperature retrieved with a “fine” layering (80 levels) and the pre-flight optimized layering (43 levels). Large differences at scan 7 are attributed to the different number of micro-iterations occurred in the two retrievals runs involved in this test.

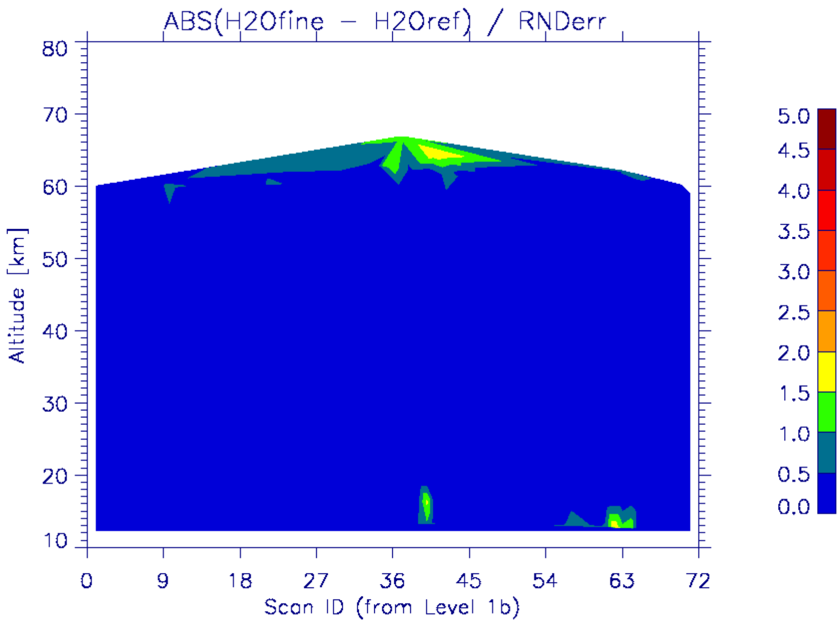

Fig. 2: ESD-normalized differences between H2O retrieved with a “fine” layering (80 levels) and the pre-flight optimized layering (43 levels).

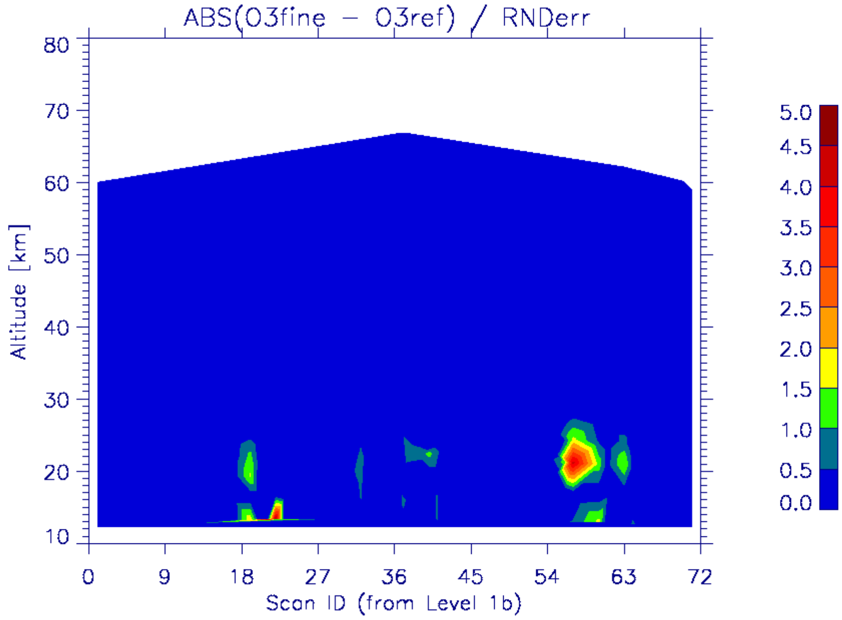

Fig. 3: ESD-normalized differences between O3 retrieved with a "fine" layering (80 levels) and the pre-flight optimized layering (43 levels).

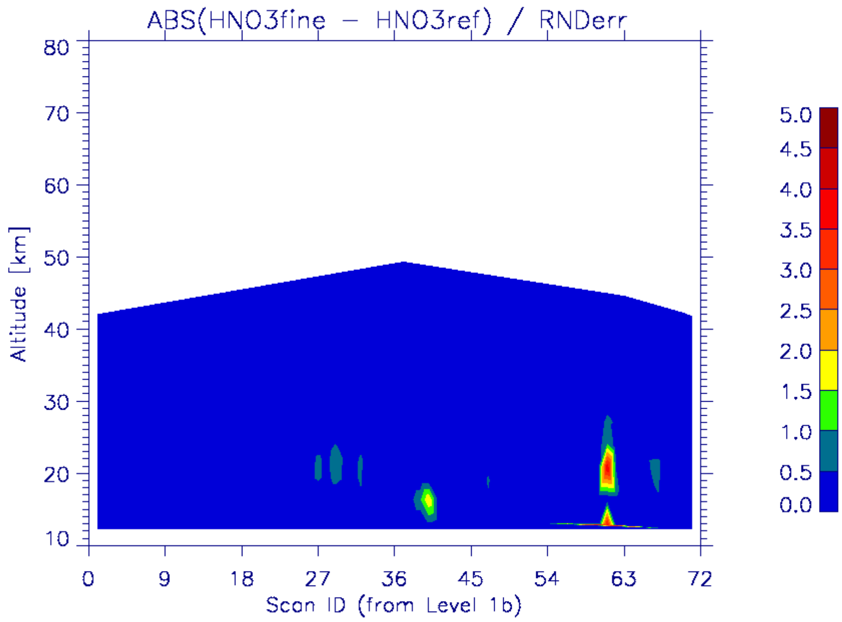

Fig. 4: ESD-normalized differences between HNO3 retrieved with a "fine" layering (80 levels) and the pre-flight optimized layering (43 levels).

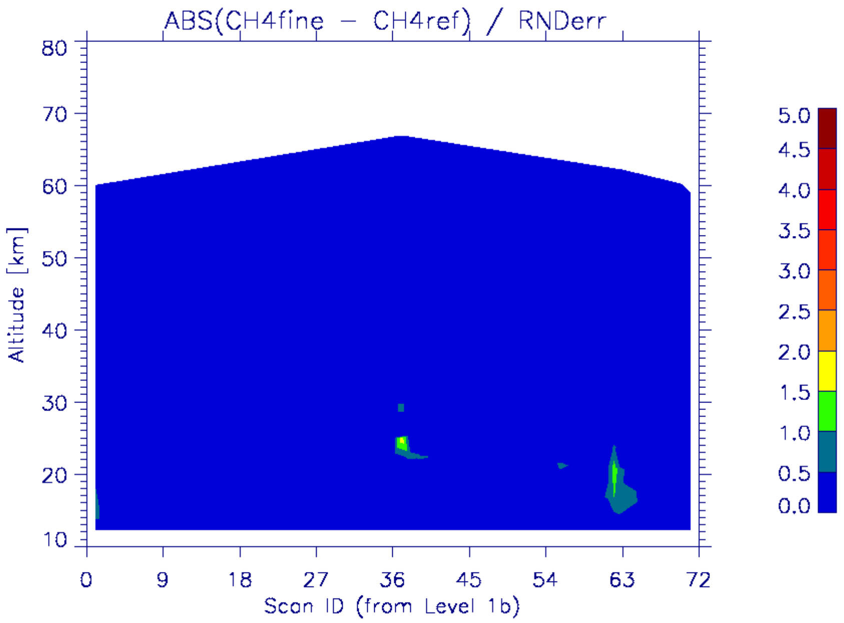

Fig. 5: ESD-normalized differences between CH4 retrieved with a "fine" layering (80 levels) and the pre-flight optimized layering (43 levels).

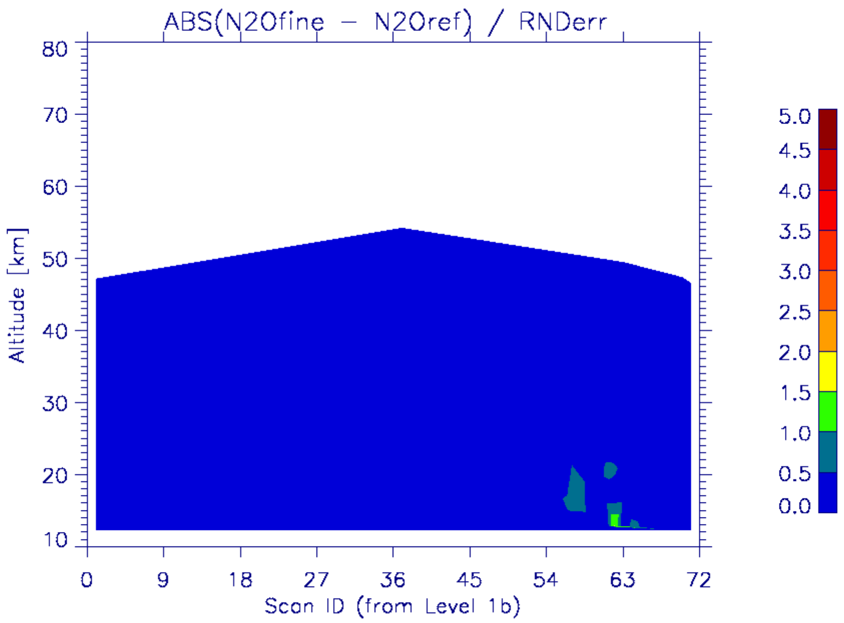

Fig. 6: ESD-normalized differences between N2O retrieved with a "fine" layering (80 levels) and the pre-flight optimized layering (43 levels).

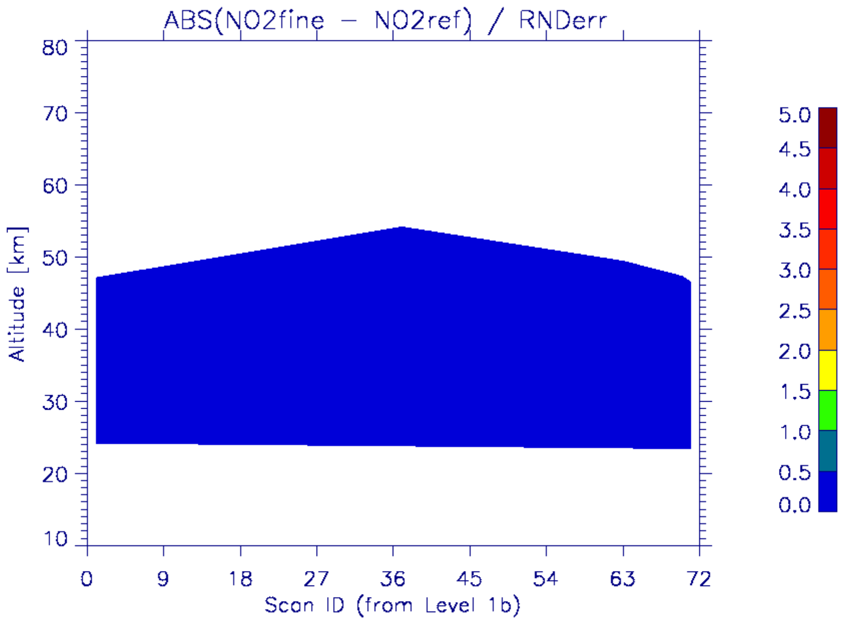

Fig. 7: ESD-normalized differences between NO2 retrieved with a "fine" layering (80 levels) and the pre-flight optimized layering (43 levels).

Conclusions

In conclusion the layering determined in the pre-launch phase and optimized on the basis of simulations was found to provide satisfactory accuracy also when dealing with real atmospheres.
The relatively large errors induced by a coarse layering in case of cloudy sweeps is not cause of concern because the retrieval performance is degraded in any case whenever cloudy sweeps are included in the analysis.
For the above reasons we recommend to keep using the layering determined before launch (on the basis of synthetic data) also for the analysis of real observations.
Frequent checks of the adequacy of the used layering are not considered necessary. A new check of the layering will be required only in case of special events having significant impact on the opacity of the atmosphere.

3.6 Tuning of FOV convolution

Ref. [RD5]: Sect. 4.1.9; Ref. [RD9]: Sheet MIP_PS_2_5 - MIP_PS_2_6 /8

Introduction

The effect of finite FOV is taken into account in the ORM by convolving the tangent altitude dependent spectrum with the FOV pattern. The forward model calculates spectra for a number of lines of sight that span the vertical range of the FOV around the tangent altitude. The continuous variation of the spectrum as a function of tangent altitude is determined by interpolation of a polynomial through the calculated spectra. The shape of the FOV is a piecewise linear altitude distribution tabulated in the processor input files. It is a measured instrument parameter.

The FOV convolution parameter that is subject to tuning is “rint”, i.e. the maximum separation between simulated spectra below a certain altitude (named “rint” altitude), chosen above the sharp vertical gradients of water vapour and temperature. The smaller is the tangent altitude separation between the simulated spectra, the smaller are the discretisation errors. However, a too large number of simulated spectra in the FOV convolution implies a too high order of the interpolating polynomial with another type of error source. The smaller is the tangent altitude separation between the simulated spectra the longer is the time requested to perform the calculation.

Description of the test

A retrieval in which the forward model calculates a spectrum every 200 metres below 20 km and uses a linear interpolation in between for the FOV convolution was performed. The profiles obtained from this retrieval are considered not affected by problems of FOV convolution and are used as reference truth to estimate the correctness of the calculation performed by ORM. The tuning was performed for the scans not affected by clouds of the orbit #2081.

The root mean square of deviation of the profiles, calculated with “rint”=1 km, 2 km, 4 km, with respect to the reference truth is compared with the averaged random error.

Another parameter to take into account for the choice of the “rint” values is the calculation time:

- the use of rint=2 km instead of rint=1 km allows to save about 15% of the calculation time
- the use of rint=4 km instead of rint=1 km allows to save about 20% of the calculation time.

Results

In the following figures the root mean square of deviations of the profiles, calculated with “rint”=1 km, 2 km, 4 km (respectively blue, red and green lines), with respect to the reference truth and the averaged random error are shown. The black solid line is the averaged random error corresponding to the reference truth. Dash, dash dot and dot black lines correspond respectively to the averaged random error obtained in the retrievals performed with rint=1 km, 2 km and 4 km

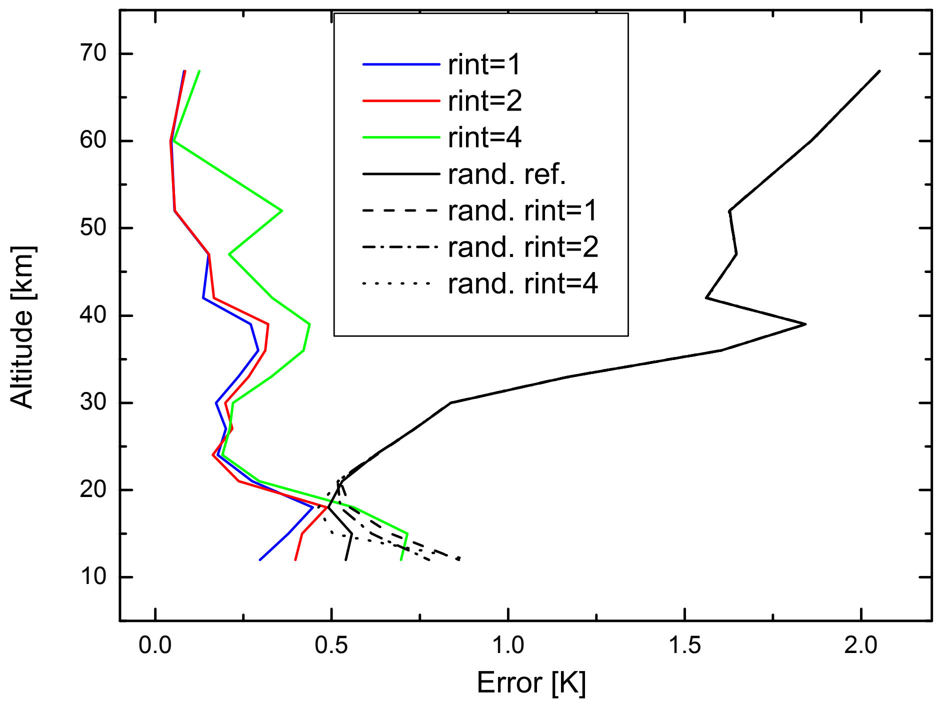

Fig. 1 Temperature

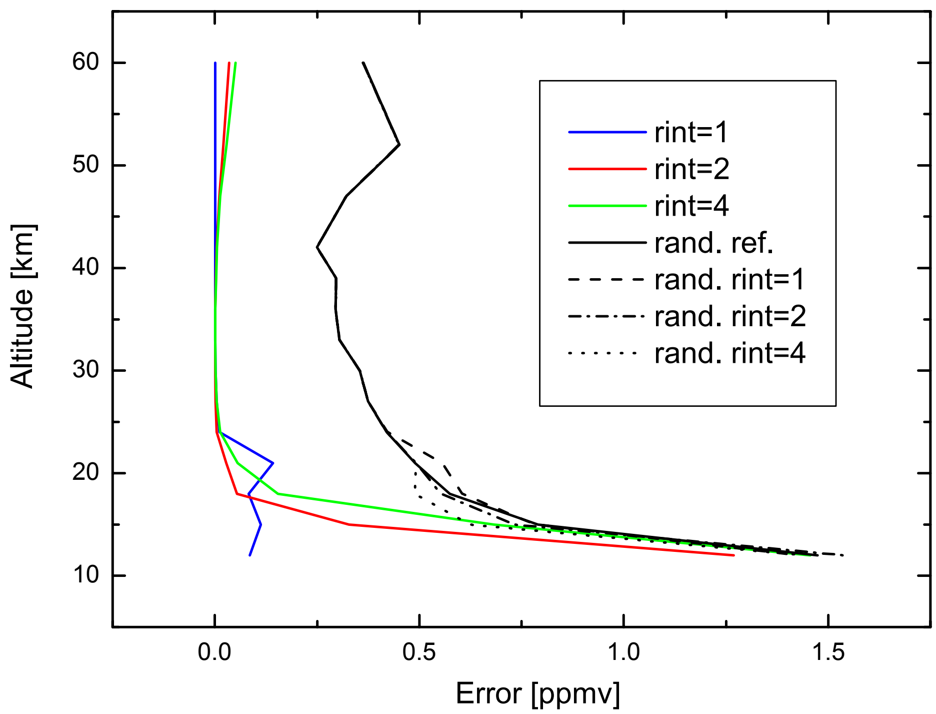

Fig. 2 Water vapour

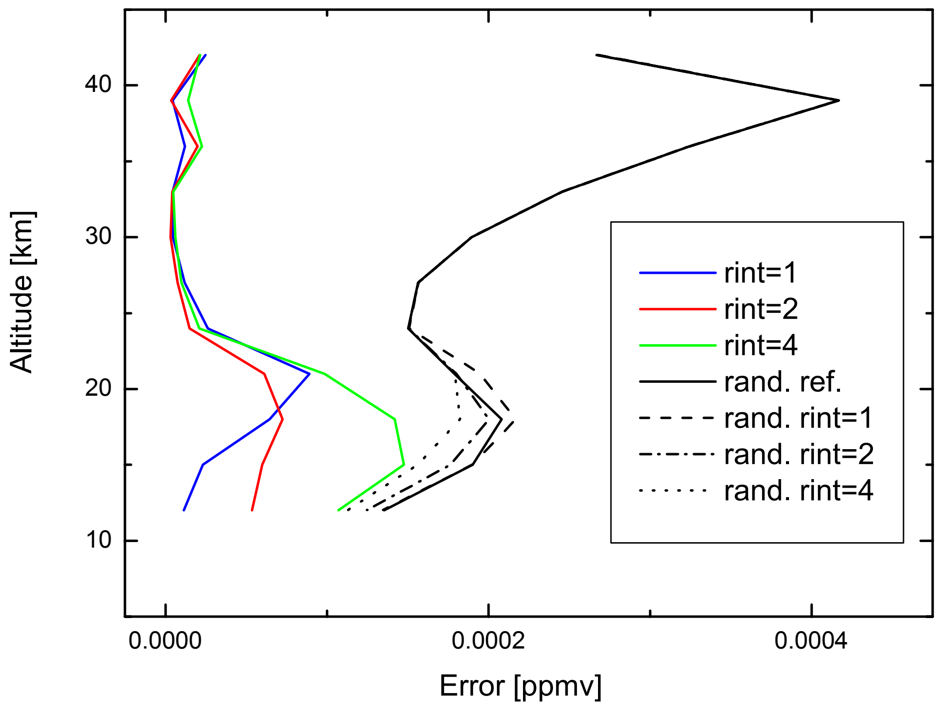

Fig. 3 Ozone

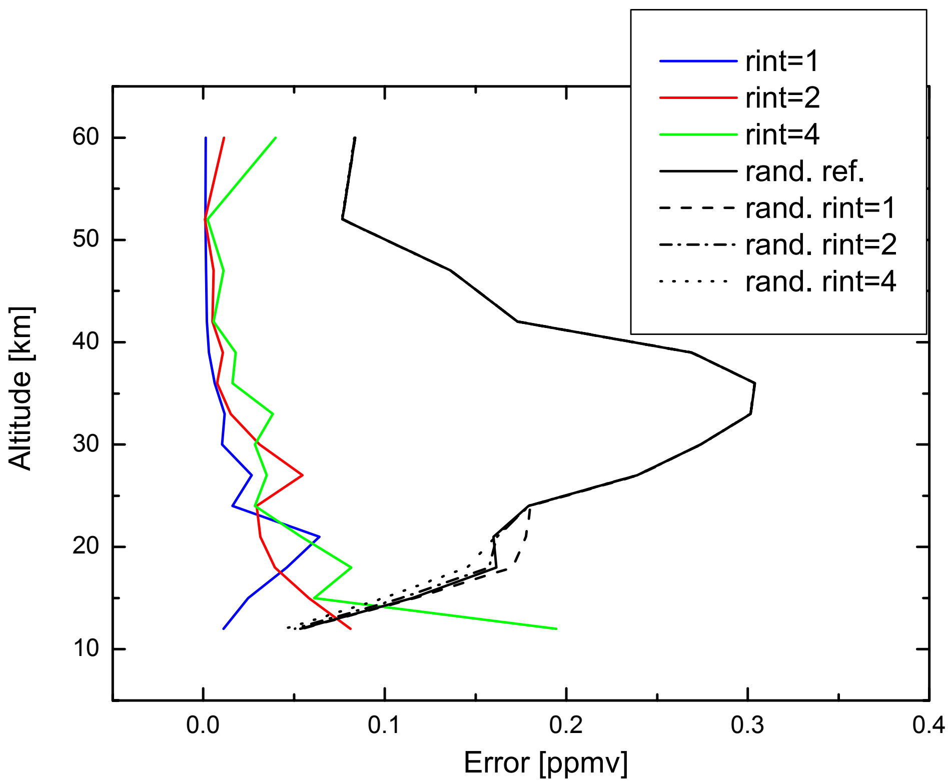

Fig. 4 Nitric Acid

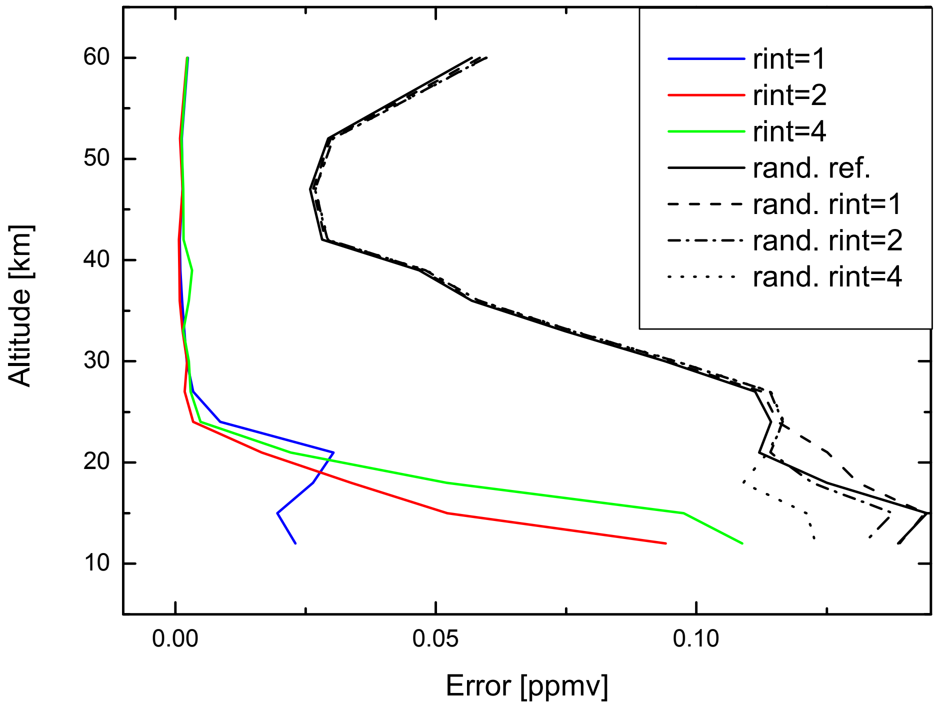

Fig. 5 Methane

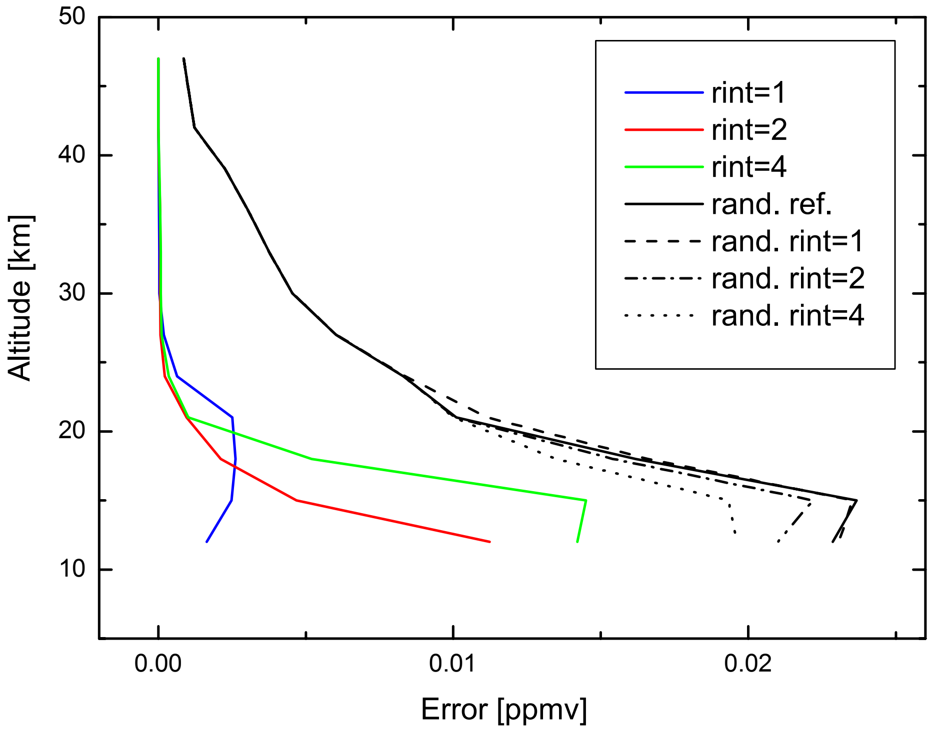

Fig. 6 Nitrous oxide

Conclusions

From the figures above we can see that a reduction of the differences with the reference profile is obtained with small values of rint.

The chosen values of "rint" on the basis of a compromise between accuracy and saving calculation time are:

T	rint = 2 km
H_2O	rint = 2 km
O_3	rint = 2 km
HNO_3	rint = 2 km
CH_4	rint = 4 km
N_2O	rint = 4 km

For NO_2 the minimum tangent altitude for which the retrieval is performed is 24 km that is above the "rint" altitude. So for the NO_2 retrieval the tuning of "rint" is not necessary.

3.7 Tuning of the error associated with engineering LOS information

Ref. [RD5]: Sect. 4.1.9; Ref. [RD9]: Sheet MIP_PS_2.5 – MIP_PS_2.6 - AX2.1

Introduction

The engineering LOS data are updated at each scan and therefore constitute an independent source of information which can be routinely used in p, T retrievals. In hydrostatic equilibrium atmosphere it is possible to derive from p, T retrieved quantities an estimate of the differences between the tangent altitudes of two contiguous sweeps. Furthermore, if one of the tangent altitudes provided by engineering measurements is assumed as perfectly known, an estimate of all tangent altitudes can be obtained. The differences between tangent altitudes obtained from p, T retrieval and the corresponding engineering estimates constitute the 'tangent heights corrections' vector. This is the correction to be applied to the assumed value of the tangent altitudes in order to obtain their correct value. The estimation of the tangent altitudes consists in weighting the retrieved tangent altitudes, with their covariance matrix (CM), with the engineering values, which are characterized by an a-priori CM. The CM associated to the engineering tangent altitudes is obtained from a simple algorithm that simulates MIPAS pointing performance specifications. The compliance of this algorithm with the actual MIPAS pointing performance must be assessed by characterizing the differences between the engineering estimate of tangent altitudes and the tangent altitudes retrieved by the ORM (without making use of engineering LOS data).

Procedure

The differences between the engineering estimate of tangent altitudes ($z_{eng}(h)$) and the tangent altitudes retrieved by the ORM without making use of engineering LOS data ($z_{sp}(h)$) have been characterized using the following approach. At each altitude *h*, the discrepancy between these two estimates can be evaluated using a chi-square test. We set:

$$\chi^2(h) = \sum_{i=1}^{N} \frac{\left(z_{sp}(h)_i - z_{eng}(h)_i\right)^2}{\sigma_{sp}^2(h)_i + \alpha(h)\sigma_{eng}^2(h)_i} = 1 \qquad (1)$$

Where:

σ_{sp}^2 =Total error of $Z_{sp}(h)_i$ estimated from pT retrieval when no LOS info is used, plus systematic error by Oxford team

σ_{eng}^2 =Variance of $Z_{eng}(h)_i$ estimated by the tool simulating MIPAS pointing performance (includes only drift and jitter, no offset, as the retrieval is not sensitive to vertical shifts of the altitude scale)

$\alpha(h)$=Factor to be determined, different from 1 only if σ_{sp}^2 and / or σ_{eng}^2 have not been correctly estimated

N =number of sweeps at altitude *h* in the considered orbit

The deviation of $\alpha(h)$ from 1 determines whether σ_{eng}^2 was under- or over- estimated.

The above mentioned method does not allow for an absolute evaluation of the accuracy of MIPAS pointing because pT retrieval is not sensitive (in the first order approximation) to vertical offsets of the altitude scale. In order to evaluate the absolute accuracy of MIPAS accuracy from Level 2 data, retrieved profiles were compared with co-located ECMWF measurements as a function of both altitude and pressure.

Results

A profile of $\alpha(h)$ was determined on the basis of tangent altitudes determined for orbit 2081 data without making use of LOS information in the retrieval.

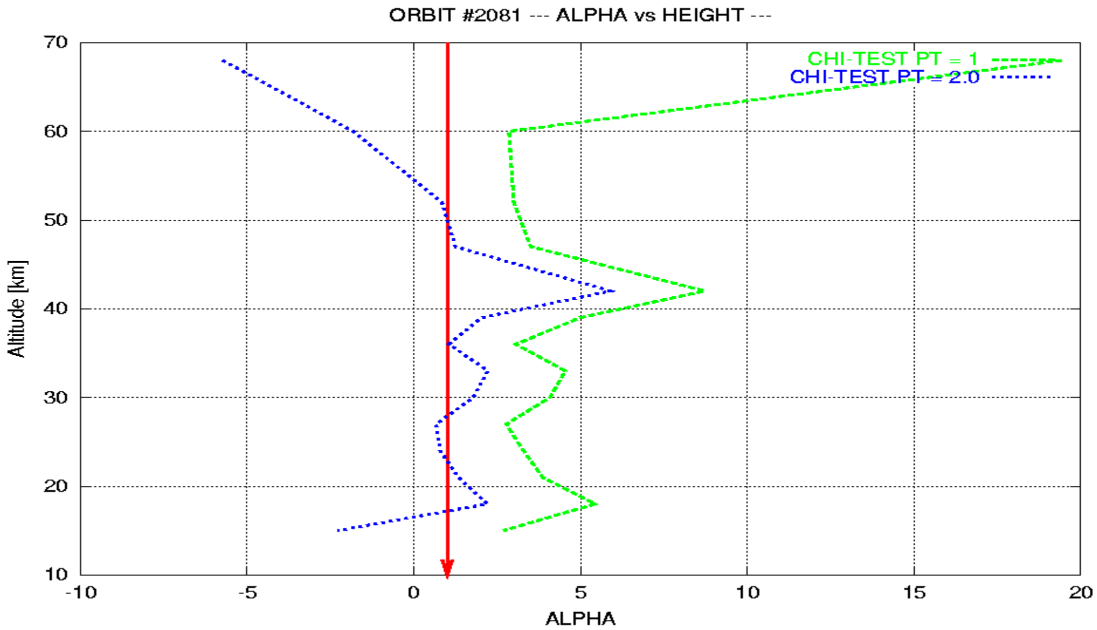

Fig. 1: Profiles of $\alpha(h)$ determined using Eq. 1. Green curve: σ_{sp}^2 determined from total error budget affecting retrieved altitudes in absence of LOS info. Bleu curve: $\sigma_{sp}^2 \rightarrow \sigma_{sp}^2 \cdot \sqrt{2}$, where "2" is the approximate value of the global chi2-test of pT retrieval.

Fig. 1 shows the profiles of $\alpha(h)$ determined using Eq. 1. In particular, the green curve was calculated by setting σ_{sp}^2 equal to the total error budget affecting retrieved altitudes in absence of LOS info, while the bleu curve was obtained by multiplying this value of σ_{sp}^2 by $\sqrt{2}$, where "2" is the approximate value of the chi2-test of pT retrieval (obtained from the spectral residuals). From this figure it is evident that the tool simulating MIPAS pointing performance is produces realistic estimates of MIPAS pointing error (correct order of magnitude). However it is not clear whether this tool underestimates the pointing drift + jitter (≈ 150 m) or we underestimate the systematic components of the error on retrieved pointing when no LOS info is used (not easy to discriminate from L2 results).

In order to evaluate the absolute pointing accuracy of MIPAS, the retrieved profiles relating to scan #12 of orbit 2081 were compared with related ECMWF data. In particular, in Figs. 2,3, 4 and 5 we compare retrieved pressure, temperature, H2O and O3 respectively with the corresponding ECMWF values. From these figures a +1.1km vertical shift of the ECMWF profiles with respect to MIPAS profiles is evident. Figures 6 and 7 show how (in case of temperature and ozone, respectively) the discrepancies between MIPAS and ECMWF are mitigated when the comparison takes place in the pressure domain, i.e. when profiles are plotted versus pressure.

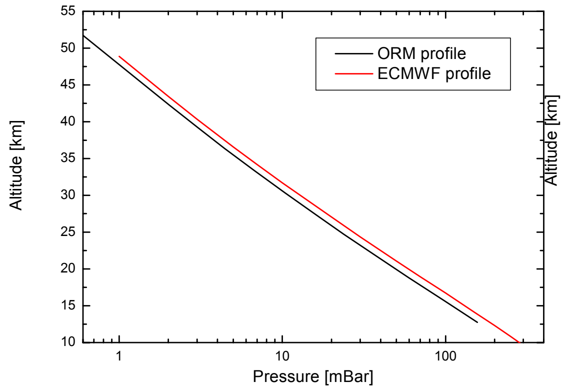

Fig. 2: MIPAS pressure profile compared with ECMWF profile, for scan #12, orbit 2081.

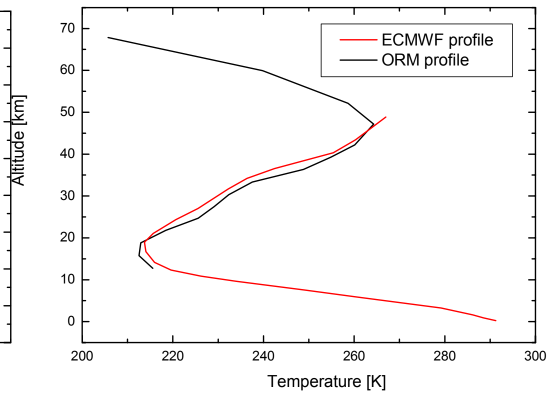

Fig. 3: MIPAS temperature profile compared with ECMWF profile, for scan #12, orbit 2081.

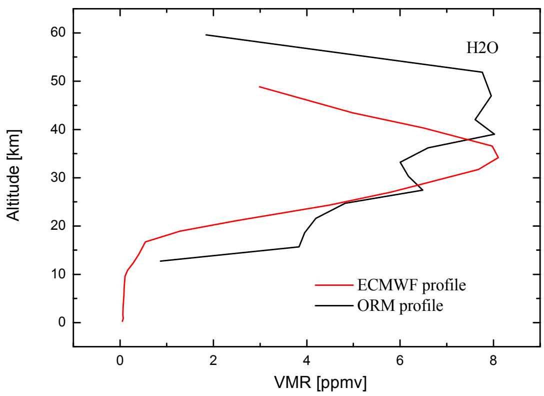

Fig. 4: MIPAS water profile compared with ECMWF profile, for scan #12, orbit 2081.

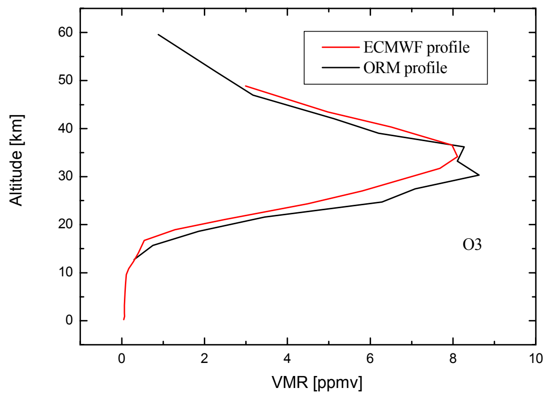

Fig. 5: MIPAS ozone profile compared with ECMWF profile, for scan #12, orbit 2081.

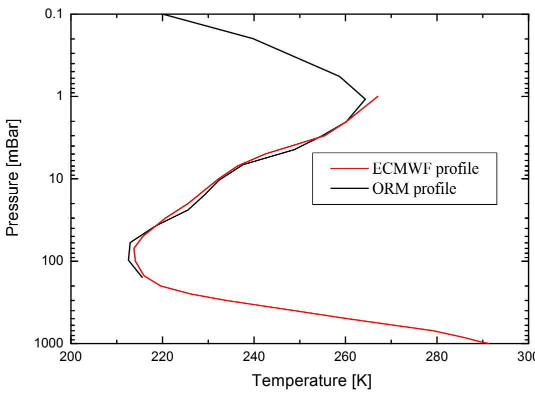

Fig. 6: MIPAS temperature profile compared with ECMWF profile, for scan #12, orbit 2081. Profiles plotted vs pressure

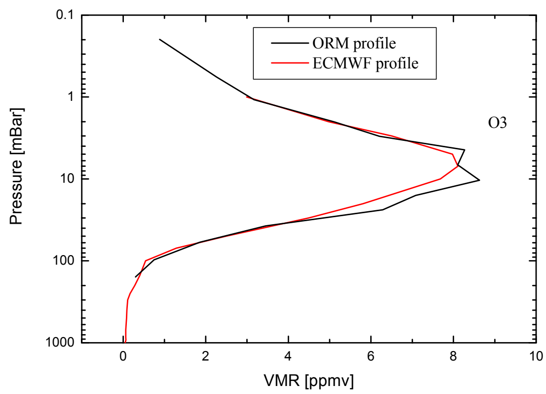

Fig. 7: MIPAS ozone compared with ECMWF profile, for scan #12, orbit 2081. Profiles plotted vs pressure

Conclusion

It is difficult to assess MIPAS pointing errors on the basis of inspection of Level 2 results. Nevertheless, the tests performed so far on Level 2 results pointed-out that:

- the tool simulating MIPAS pointing performance is produces realistic estimates of MIPAS pointing error (correct order of magnitude). However it is not clear whether this tool underestimates the pointing drift + jitter (≈ 150 m) or we underestimate the systematic components of the error on retrieved pointing when no LOS info is used (not easy to discriminate from inspection of Level 2 results).
- The analyzed data-set suffers of a pointing offset of about -1.1km. This is confirmed by the results of pointing characterization carried-out by ESA on the basis of dedicated measurements (see e.g E-mail from H.Nett to MICT group:

```
Date: Tue, 12 Nov 2002 15:37:23 +0100 (MET)
From: Herbert Nett <hnett@jw.estec.esa.nl>
To: mict@jw.estec.esa.nl
Subject: [ENVISAT:mict] MIPAS auxiliary data update
```

3.8 VCM of a-priori profiles for the computation of the IG profiles

Ref. [RD5]: Sect. 4.2.14; Ref. [RD9]: Sheet MIP_PS_2_5 - MIP_PS_2_6 /9

Introduction

Initial guess profiles are an important element in the inversion procedure: they are required to be as close as possible to the real atmosphere, in order to reduce the number of iterations needed to reach convergence, and smooth, because in this case the Marquardt method, used in the retrieval algorithm, provides also a weak 'regularisation' to the profile, since it mainly damps the ill-determined (and hence oscillating) components of the correction of the profile (i.e. the difference between retrieved profile at a given iteration and the one at the previous iteration).
In order to achieve these requirements, the Initial Guess (IG) profile is computed by the Level 2 operational processor as the weighted mean between the retrieved profile in the previous scan and the 'a-priori' profile (obtained by merging climatological and -if available- ECMWF profiles). The weight is provided by the VCM of each profile.
The VCM of the retrieved profiles is computed by the ORM and is a non-diagonal matrix, while the VCM of a-priori profiles (assumed to have only the diagonal and the first off-diagonal elements different from zero) is computed using the following input parameters: standard deviation at a reference pressure, gradient of the standard deviation with pressure, correlation. These input parameters have to be defined correctly in order to achieve our aim to obtain IG profile that are as close as possible to the reality and as smooth as possible.

The objectives of this test are the following ones:

- to verify the correctness of the diagonal values of the VCM associated to the a-priori profiles, by comparing the variance associated to the climatological profiles with the variance of the retrieved profiles computed in all the latitude bands;
- to investigate which is the most appropriate value and sign of the non-diagonal terms in order to have an non-oscillating IG profile.

Procedure and results

The validation of the correctness of the diagonal values of the VCM associated to the a-priori profiles has been performed using the orbit #2081 and comparing, for each latitude band and each species, the variance of the retrieved profiles (i.e. the square mean deviation of the retrieved profiles with respect to the mean retrieved profile in a given latitude band) with the variance of the climatological profile (equal to the square of the standard deviation used as input for the computation of the VCM of the climatological profile, PS2 file-GADS# 2-3 fields 82-84)
For each species, the variance profiles relative to all the latitude bands are plotted together with the corresponding climatological variance profile in **Figure 1(a-g).**

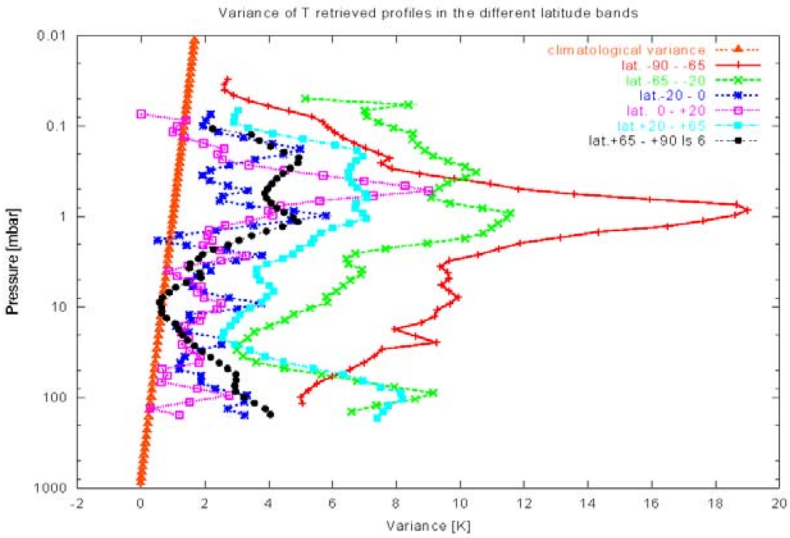

Figure 1a

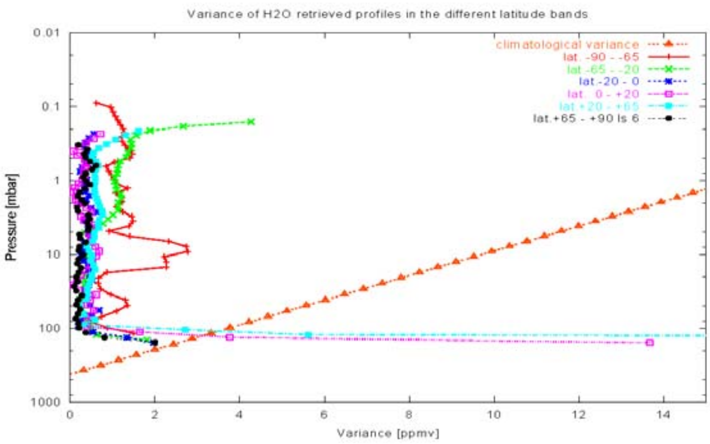

Figure 1b

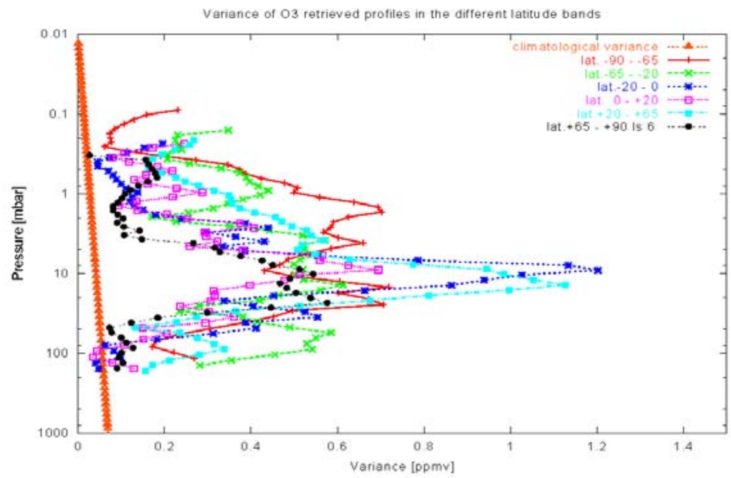

Figure 1c

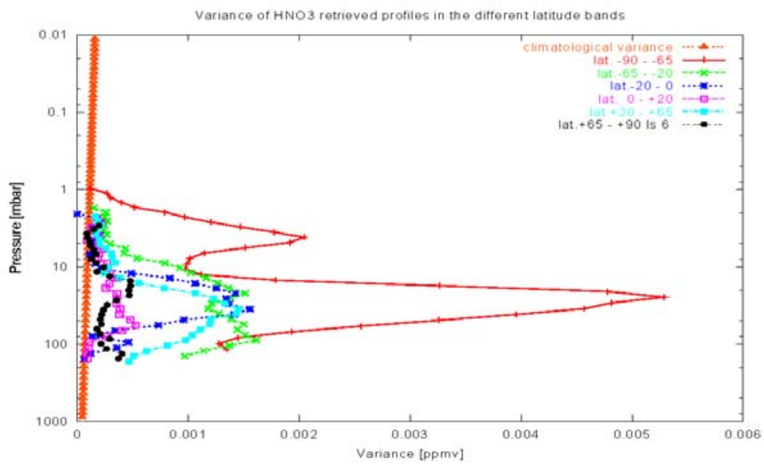

Figure 1d

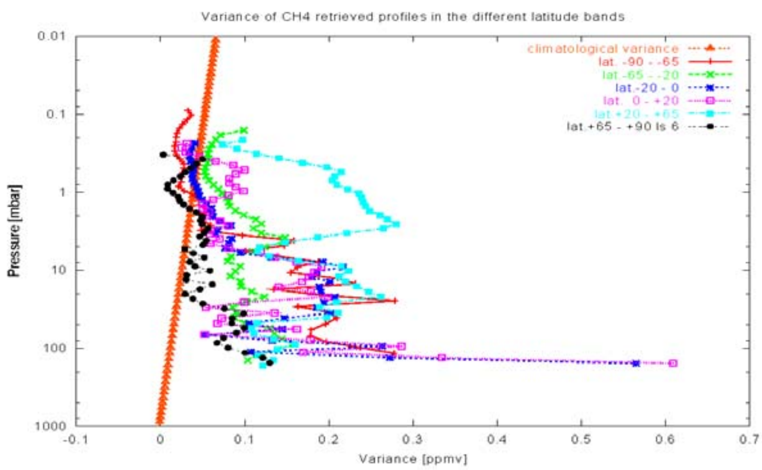

Figure 1e

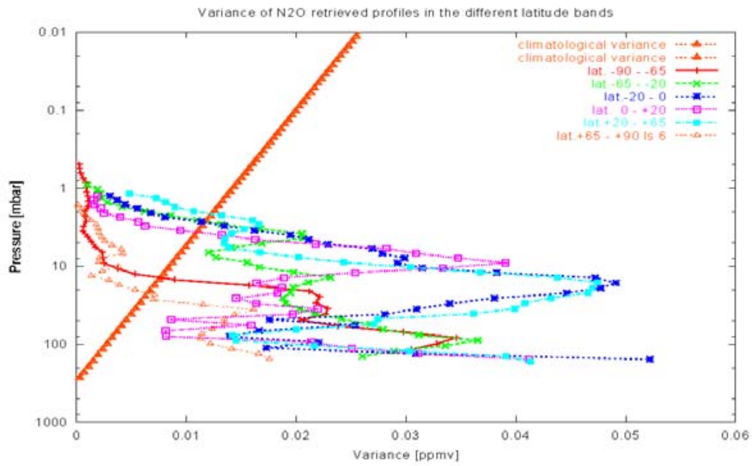

Figure 1f

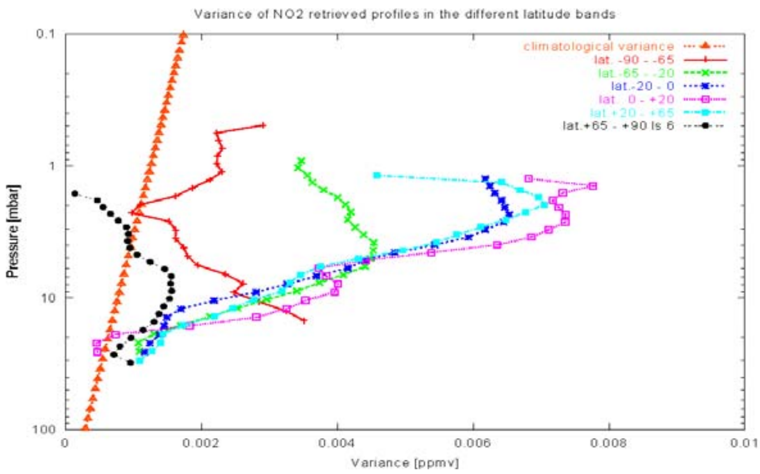

Figure 1g

The climatological variance is expected to be much greater than the retrieved one, because it should take into account the seasonal atmospheric variability, whereas the variance of the retrieved profiles has been obtained on the basis of a single orbit.

Against this expectation the climatological variance is in most cases (for T, O3,HNO3,CH4 and N2O) much smaller than the one associated to the retrieved profiles.

For this reason we believe that the climatogical variances supplied in the PS2 file are not very realistic and so realistic atmospheric variances are needed in order to draw any conclusion.

In order to determine the most appropriate value and sign of the non-diagonal term of the VCM of the climatological profiles, a small program has been developed that computes the weighted mean between the retrieved profile and the a-priori one. A very oscillating retrieved profile has been used for this test. The results of the weighted mean obtained using correlation equal to 0, -0.05 and +0.05 in the VCM of the a-priori profile are compared in Figure 2. Both negative and positive correlations increase the oscillations of the resulting profile (in case of negative correlations this is outside the scale). On the contrary, the resulting profile in case of correlations equal to 0 is a profile with oscillations smaller than the ones in the retrieved profile.

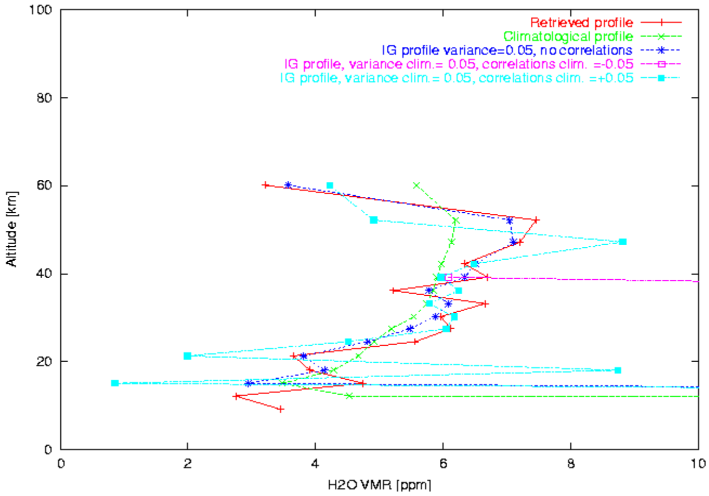

Figure 2 IG profiles obtained as the weighted mean of the retrieved profile (red curve) and the climatological profile (green curve) in case of no correlations in the VCM of the climatological profile (blue curve), negative correlation (pink curve) and positive correlations (pale-blue curve).

Conclusions

Concerning the diagonal elements of the VCM of the climatological profiles, this test has highlighted that the parameters currently used in the PS2 are not realistic, and hence realistic standard deviations have to be provided as soon as possible by the University of Leicester team.

Concerning the non-diagonal terms, we have verified that both negative and positive correlations in VCM increase the oscillations of IG profile. Besides, correlations between points of both climatological and ECMWF profiles are not known exactly. Therefore, even if in a smooth profile (as it is the a-priori profile) correlations are expected to be positive, the most appropriate value for the correlations in the VCM of the a-priori profile is 0. The auxiliary file PS2 provided to ESA on 31 Oct. 2002 has already been modified accordingly to this result.

3.9 Verification of frequency calibration & determination of coefficients for second order polynomial frequency correction

Ref. [RD5]: Sect. 4.2.9; Ref. [RD9]: Sheet MIP_PS_2_3-MV_2_15

The original scope of this test was just a validation of frequency calibration of MIPAS spectra, but since an improvement in frequency calibration was proved to be possible, the tuning of the input parameters providing a non-linear shift to the ILS for compensating the systematic shift in MIPAS measurements was also performed.

Introduction

Frequency calibration of MIPAS measurements is performed by Level 1 processor.
The objective of this test is to verify the correctness of the frequency calibration by fitting the residual band dependent frequency shift in MIPAS spectra. The fit of the frequency shift scaling factor led in most cases to a significant reduction of the residuals indicating the possibility for an improvement of the frequency calibration. A systematic difference was observed in the frequency shift of the different bands suggesting the need for a frequency dependent correction.
In order to make this correction MIPAS Level 2 pre-processor capability of shifting the ILS according to a second order frequency dependent polynomial was exploited and the coefficients of the second order polynomial for ILS shift were determined. After the verification that the non-linear spectral correction succeeded in eliminating the band dependent frequency shift, the impact of a bias in frequency calibration on χ^2 and retrieved profiles was assessed.

Procedure and results

Together with nominal MIPAS target parameters, an additional parameter k_{band} equal to a band dependent and altitude independent frequency shift scaling parameter can be fitted by the ORM_ORB program for each scan of the orbit and for each retrieval (pT, h2o, o3, etc.).

$$k_{band} = \Delta\omega / \omega_c,$$

where ω_c is the central frequency of the microwindow in consideration, k_{band} is the fitted value for the band the microwindow belongs to. For each microwindow, the ILS provided by Level1 is convoluted with a shifted sinc function (with resolution equal to the unapodized resolution of MIPAS spectra), and the shift is given by the fitted parameter k_{band} time the central frequency of the microwindow. The microwindows used for this fit are the ones selected for the nominal retrievals (no dedicated microwindows are used).
Each retrieval (one retrieval for each species and for each sequence) provides the values of the frequency shift scaling parameters for all the spectral bands used in the microwindow selection of that species. Comparison of the results obtained by different retrievals for the same band provides an indication of the consistency of the retrieved values.
The retrieved frequency shift scaling parameters obtained by the analysis of orbit # 2081 are reported in Figure 1 as a function of scan ID for bands A, AB, B and C (no microwindows in band D are used). In general, variations along the orbit are visible but small, and the retrieved frequency shift presents a systematic behaviour with frequency: from negative values of the order of 10^{-6} in band A, to positive values of the same order of magnitude in band C, with 0 located somewhere between band AB and B. This behaviour with frequency indicates that the instrument has a small

non-linear distortion in the frequency scale. Since this effect is not modelled in Level1 it leads to a bias in the determination of the linear scaling factor.

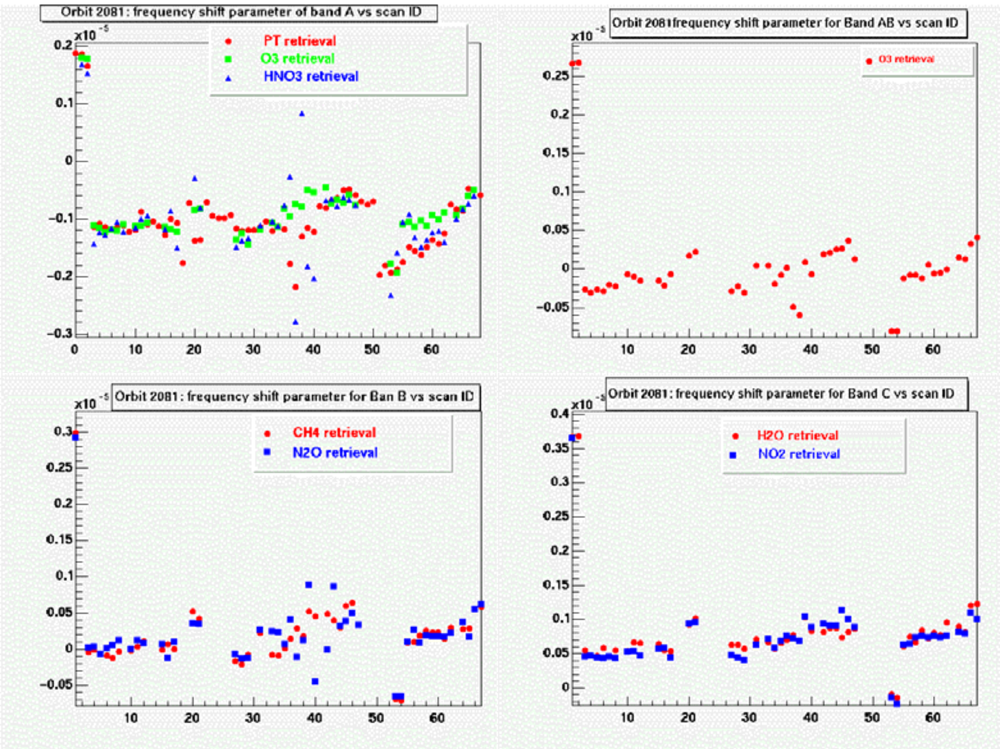

Figure 1 Retrieved frequency shift scaling parameter vs scan ID for bands A, AB, B and C obtained by the analysis of orbit #2081 acquired on 24th July 2002.

Considering that Level 2 pre-processor has the capability of applying a frequency dependent shift to the ILS (with a second order polynomial), we tried to determine the optimal coefficients in order to reduce the detected frequency shift. The average along the orbit of the frequency shift scaling factors retrieved for the different spectral bands by the different retrievals were fitted to a second order polynomial with the constant term set to 0: $f(\omega)=b\omega+c\omega^2$. Since spectral bands are wide, the retrieved frequency shift scaling parameter obtained by each retrieval for a particular band was associated not to the central frequency of the band, but to the central frequency of the microwindows belonging to that band used for that retrieval.
The obtained second order polynomial is the following one:

$$f(\sigma) = -2.60511.e-6\,\sigma + 2.140841.e-9\,\sigma^2$$

The fitted frequency shift scaling parameter in orbit #2081 obtained after this spectral correction are reported in Figure 2.

It is evident that the particular behaviour of the frequency shift with frequency has been removed and the detected residual frequency shift, apart from some scans around scan #36 and #54 is within $\pm 5\ 10^{-7}$.
The frequency shift scaling factors obtained for each band by the different retrievals are consistent each other, with the only exception of the ones retrieved by h2o retrieval in band A (reported in green in Figures 2, 3 and 4). The cause of this inconsistency has to be sought in the small number of spectral points used by h2o retrieval in band A (only a microwindow with a small number of spectral points, i.e. 52 points, taking into account all the measured altitudes).

In order to check whether the detected frequency shift is constant for different orbits, the spectral correction obtained by the analysis of orbit #2081 was applied to orbits #2082 and #2083.
Results are reported in Figure 3 and Figure 4.

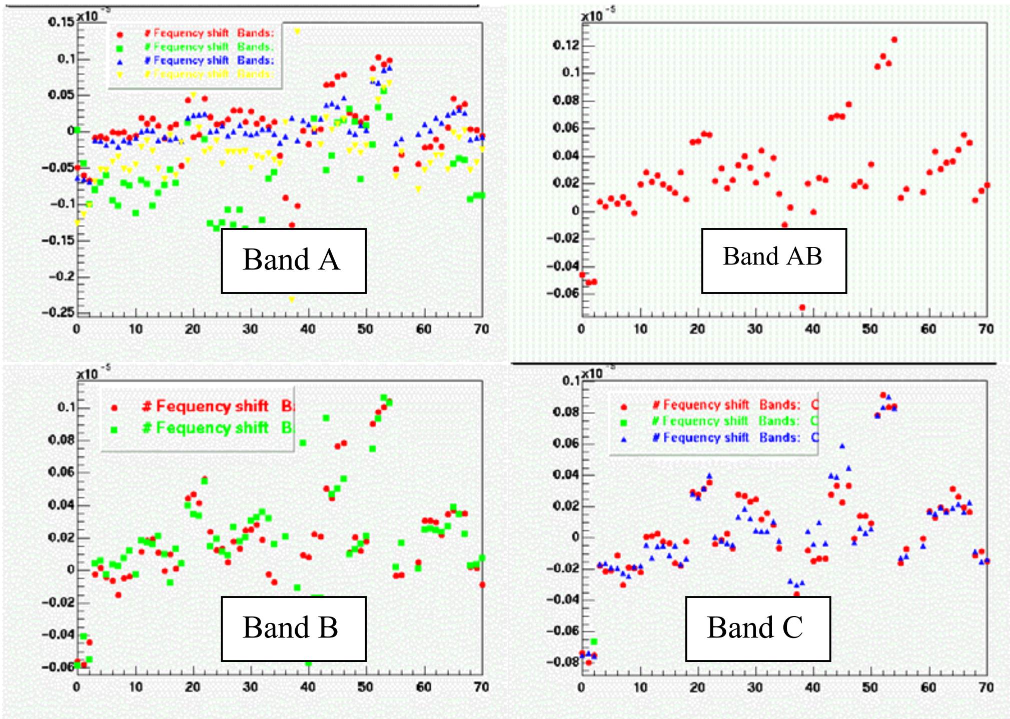

Figure 2 Residual frequency shift scaling parameter retrieved by the different retrievals in the different bands for orbit #2081 after the non-linear spectral correction.

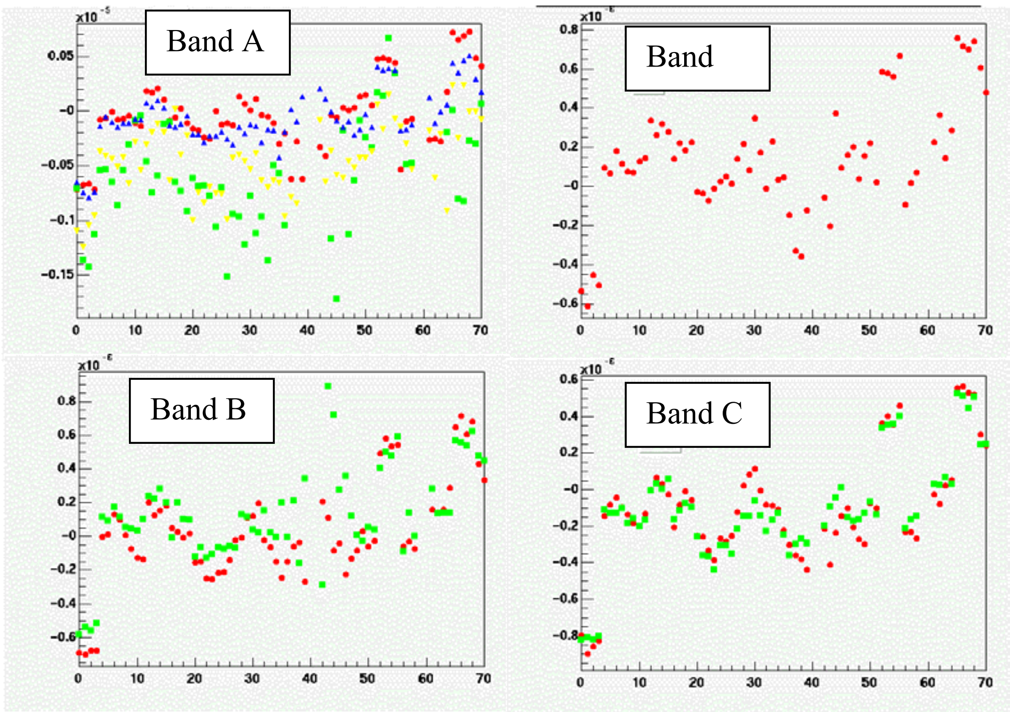

Figure 3 Residual frequency shift scaling parameter retrieved by the different retrievals in the different bands for orbit #2082 after the non-linear spectral correction (the coefficients used for the spectral correction were determined considering the frequency shift detected in orbit #2081).

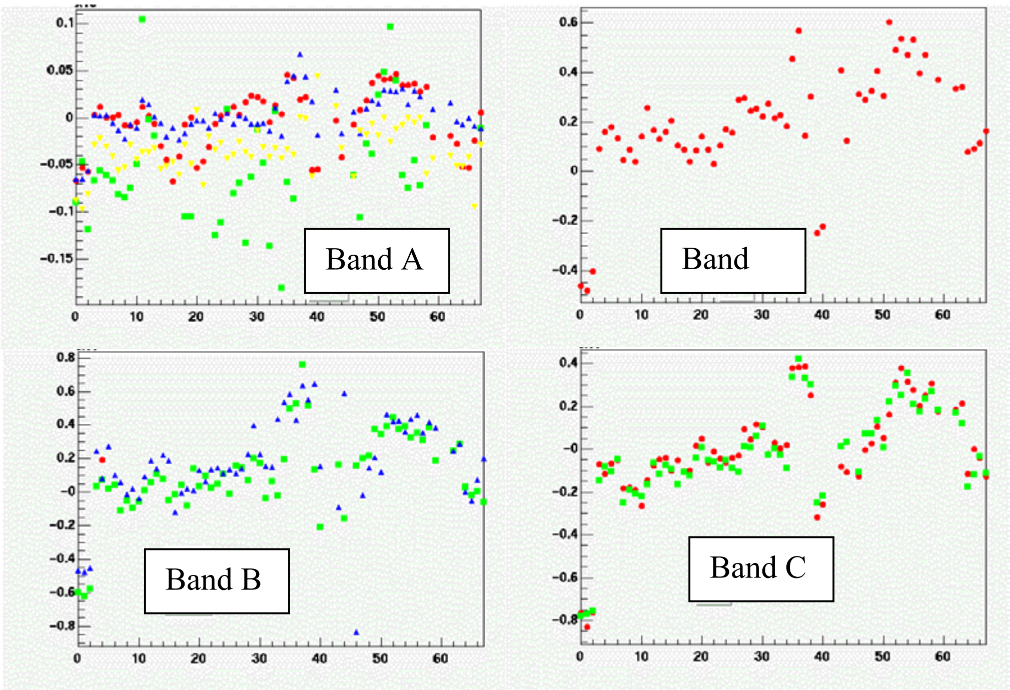

Figure 4 Residual frequency shift scaling parameter retrieved by the different retrievals in the different bands for orbit #2083 after the spectral correction (the coefficients used for the spectral correction were determined considering the frequency shift detected in orbit #2081). The values on the y-axis have to be multiplied by the factor 10^{-6}.

The consistency of results obtained for different speciess and bands is shown in Fig.5, where the residual frequency shift scaling factor after spectral correction is plotted vs scan ID for a few different retrievals and bands. Different colours are used depending on the number of spectral points used in the fit: green is used for fits that use less than 100 points, red for fits that use less than 1300 points, and blue is used for fits that use more than 1300 points. As expected the internal agreement of the curves depends on the accuracy of the retrieval as determined by the number of fitted points. Different corrections are obtained for different sequences.

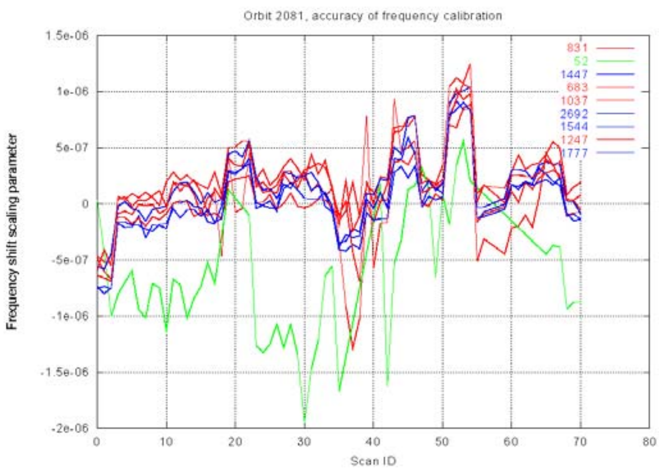

Figure 5 Retrieved frequency scaling factor for different bands and different retrievals as a function of the sequence number

Impact of frequency shift on residuals and retrieved profiles.

After the implementation of a spectral correction in MIPAS spectra, the impact of the frequency shift on residuals and retrieved profiles was assessed comparing the results with and without the spectral correction. The results for residuals are shown in Figure 6: frequency shift has a strong impact on residuals and hence on χ^2. Since χ^2 is used as an indicator of the presence of systematic errors in the spectra, the contribution of the frequency shift should be eliminated in order not to mask other systematic errors under investigation.

The impact of frequency shift on retrieved profiles is less critical (see Figure 7): differences between retrieved profiles with and without the spectral correction are in general within 2 sigma with the only exception of water vapour profile, that seems to be affected by a more general instability of this retrieval.

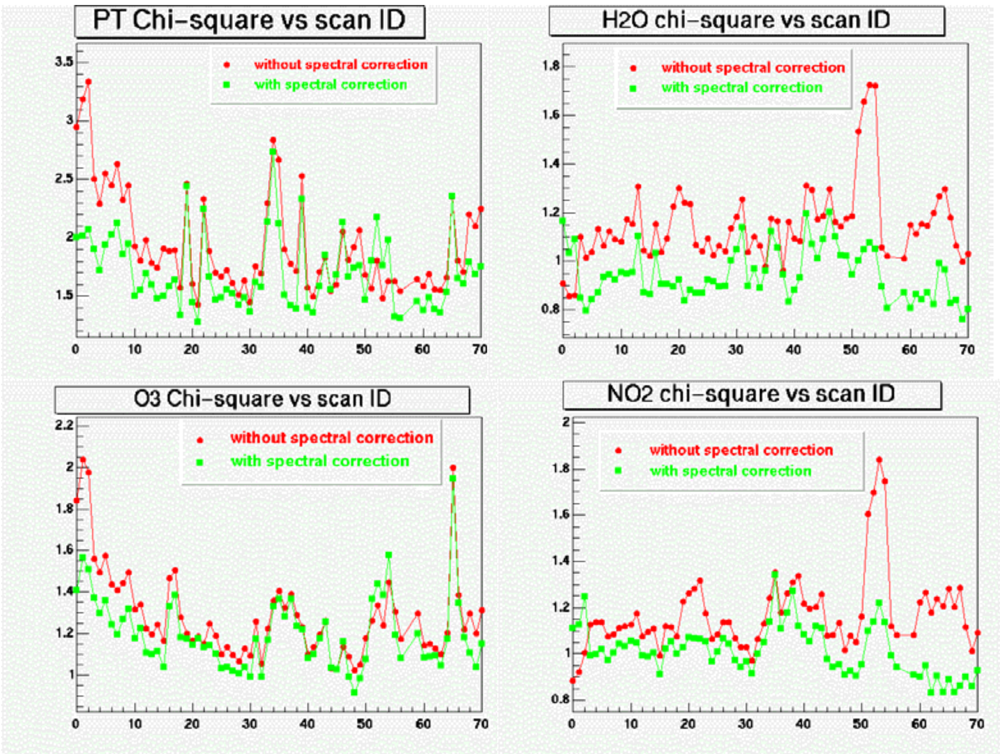

Figure 6 Impact of frequency shift on χ^2

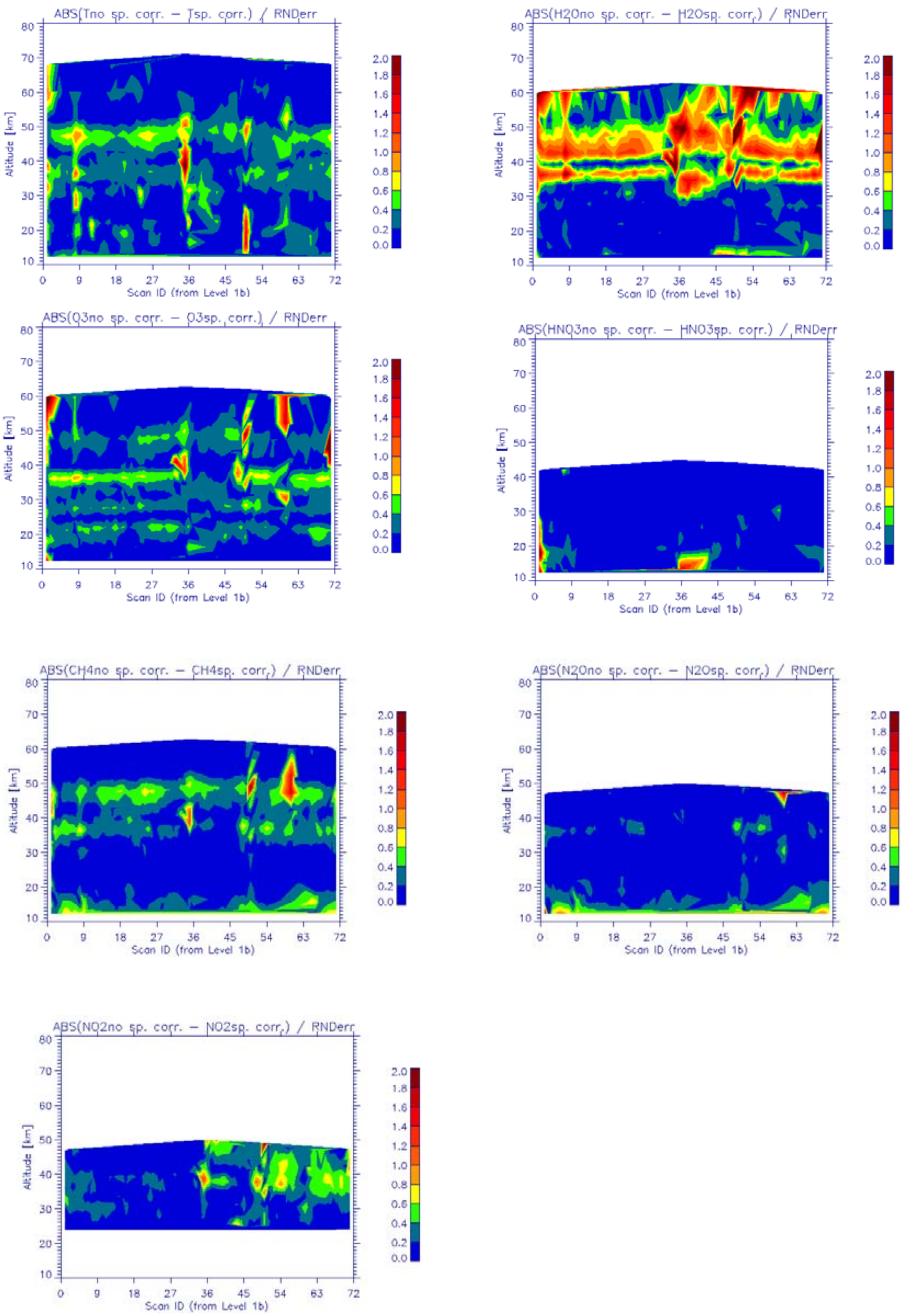

Figure 7 Impact of frequency shift on retrieved profiles: maps of the differences between profiles obtained with and without the spectral correction, normalized by the random error.

Conclusions

The following conclusions can be drawn:

- Frequency shift affects significantly the residuals but not the retrieved profiles (an exception is observed in the case of water vapour, but is related to a more general instability of this retrieval)
- Correction is necessary to eliminate from the residuals this strong contribution of systematic error that may cover other systematic errors under investigation
- The second order polynomial shift of the ILS successfully correct the small non-linear distortion of the instrument in the frequency scale.
- After the spectral correction a residual frequency shift of the order of 10^{-6} is detected for a small number of orbits, whose location changes by orbit to orbit.
- The same correction is valid in three consecutive orbits.

4 Verification of critical baselines

The second group of tests deals with the verification of critical level2 baseline. The outputs of these tests consist in either an assessment of the impact of some critical approximations on the retrieved profiles, or recommendation for modifications in the code, or suggestions for improvements of the quality of data products.

4.1 Verification of extrapolation rules

Ref. [RD5]: Sect. 4.2.12; Ref. [RD9]: Sheet MIP_MV_2_25/1

Introduction

In ORM the retrieved discrete values of the vertical profile are determined in correspondence of the so-called "retrieval grid", equal to the grid of the measured tangent altitudes (or to a subset of it). The retrieved profile above the highest tangent altitude used in the retrieval is obtained scaling the initial guess profile by the same quantity used for the highest fitted point. The assumptions made on the shape of the initial guess profiles may therefore affect the quality of the retrievals.

Procedure and results

To assess the impact of the extrapolation rules used by ORM, we have analysed the 71 sequences of orbit 2081 using different profile shapes.
The reference retrieval has been performed with the same initial guess profiles used by the ML2PP code.
Then the shape of the ML2PP initial guess profiles above the highest fitted altitude has been changed 5 times, in order to have a minimum of statistics.
For each altitude the resulting retrieved values have been compared with the reference value calculating the averaged deviation with the following expression:

$$Dev(z) = \sqrt{\frac{\sum_{i=1}^{5}\left(P_i(z) - P_{ref}(z)\right)^2}{5}}$$

where $P_i(z)$ is the retrieved value at altitude z using the i shape, $P_{ref}(z)$ is the value obtained at altitude z with the reference retrieval.
The obtained averaged deviations have been compared with the random errors of the reference retrieval using the following expression

$$NDev(z) = \frac{Dev(z)}{esd(z)}$$

The attached plots report, for each target quantity, the 5 assumed profile shapes and the resulting normalised deviations.

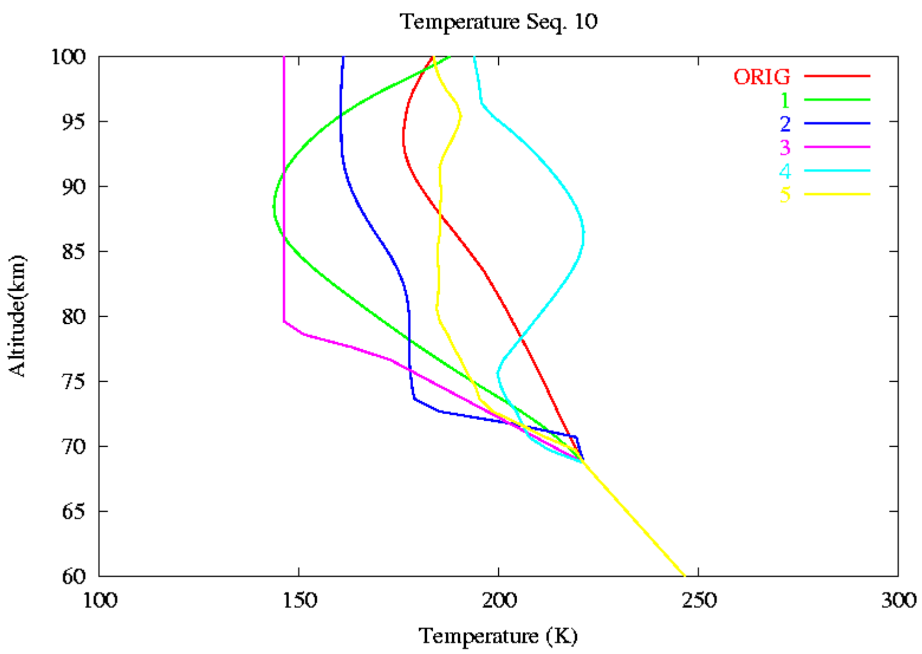
Temperature Seq. 10
ORIG
1
2
3
4
5
Altitude(km)
Temperature (K)
100
95
90
85
80
75
70
65
60
100
150
200
250
300

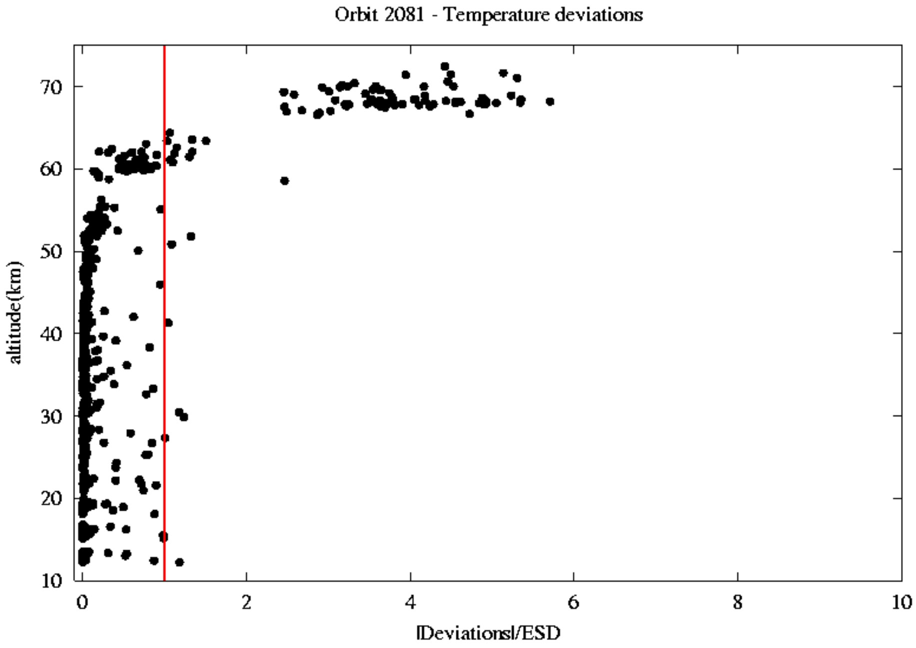
Orbit 2081 - Temperature deviations
altitude(km)
|Deviations|/ESD
70
60
50
40
30
20
10
0
2
4
6
8
10

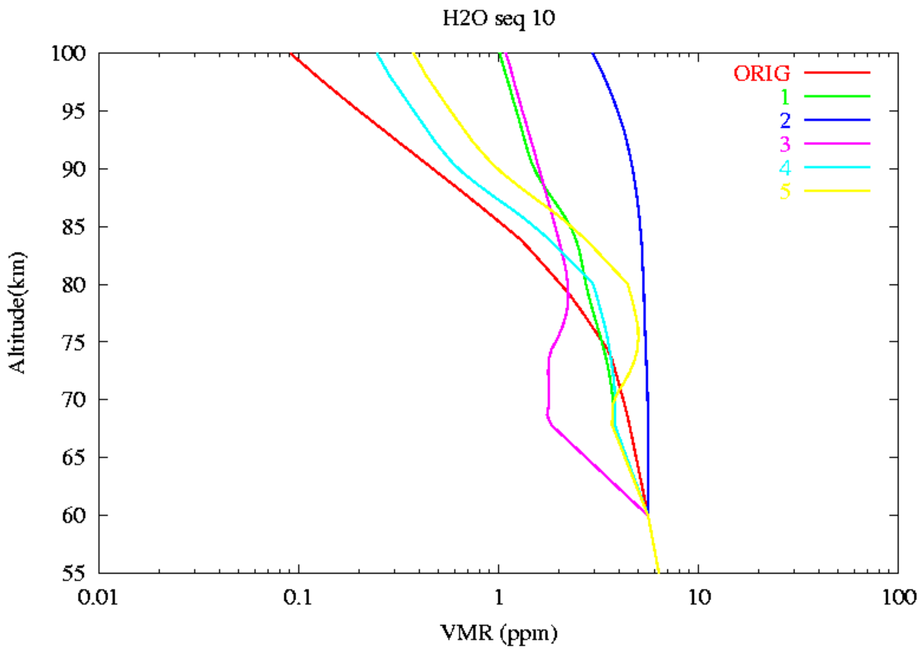
H2O seq 10
Altitude(km)
VMR (ppm)
ORIG
1
2
3
4
5
100
95
90
85
80
75
70
65
60
55
0.01
0.1
1
10
100

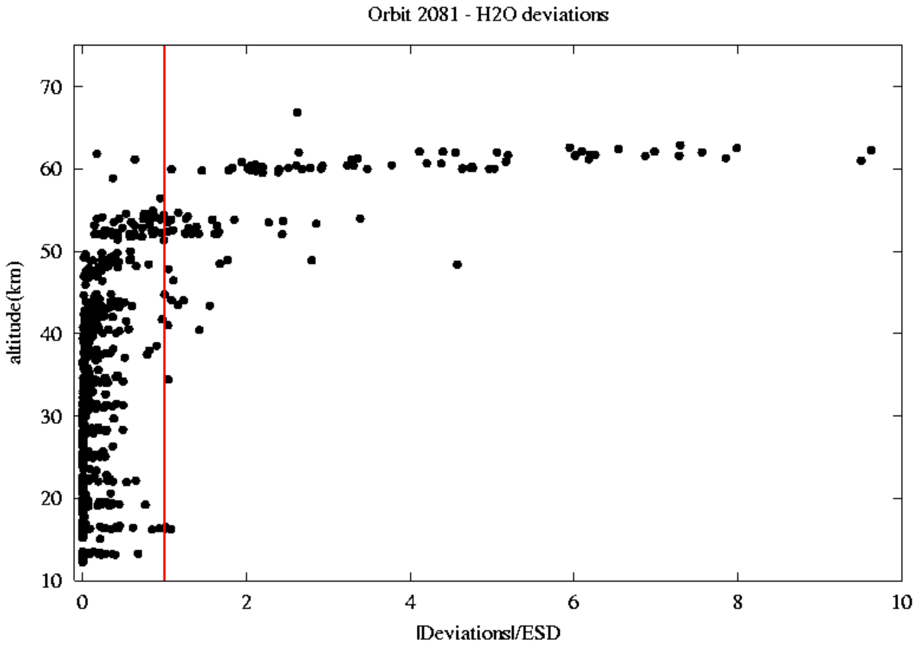
Orbit 2081 - H2O deviations
altitude(km)
|Deviations|/ESD
70
60
50
40
30
20
10
0
2
4
6
8
10

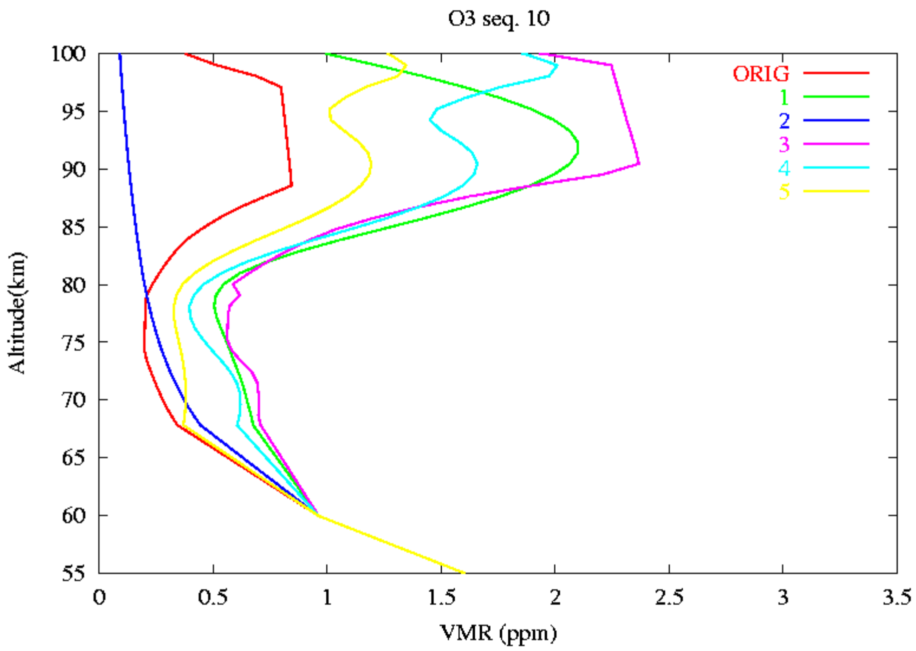
O3 seq. 10
ORIG
1
2
3
4
5
Altitude(km)
VMR (ppm)
100
95
90
85
80
75
70
65
60
55
0
0.5
1
1.5
2
2.5
3
3.5

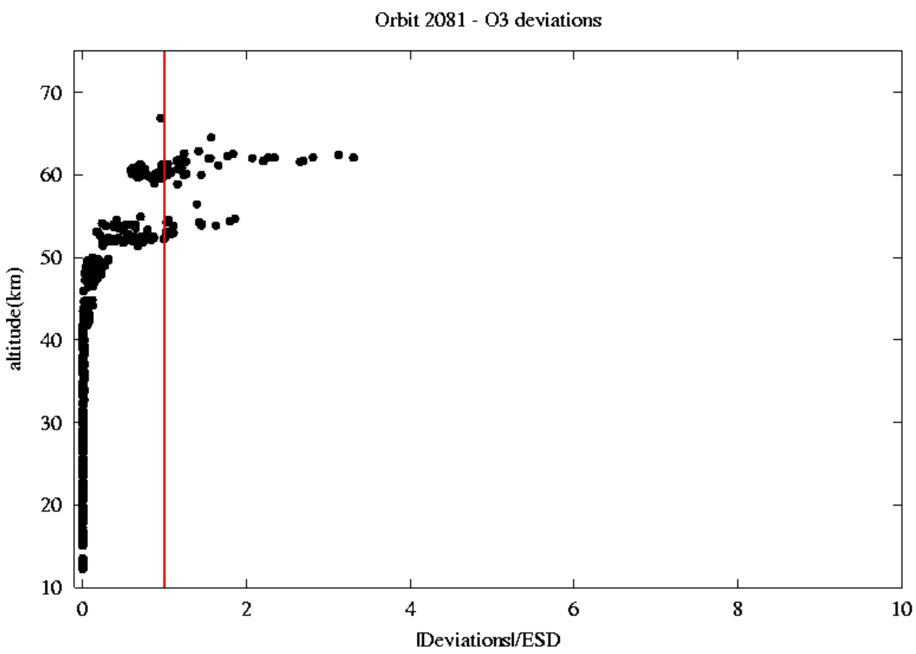
Orbit 2081 - O3 deviations
altitude(km)
|Deviations|/ESD
70
60
50
40
30
20
10
0
2
4
6
8
10

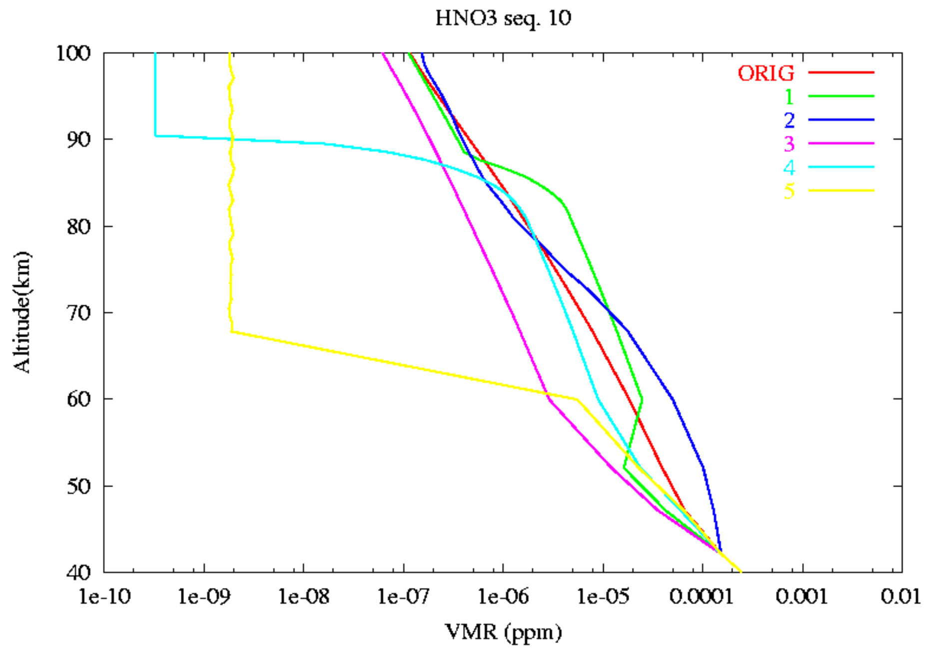
HNO3 seq. 10
ORIG
1
2
3
4
5
Altitude(km)
VMR (ppm)
100
90
80
70
60
50
40
1e-10
1e-09
1e-08
1e-07
1e-06
1e-05
0.0001
0.001
0.01

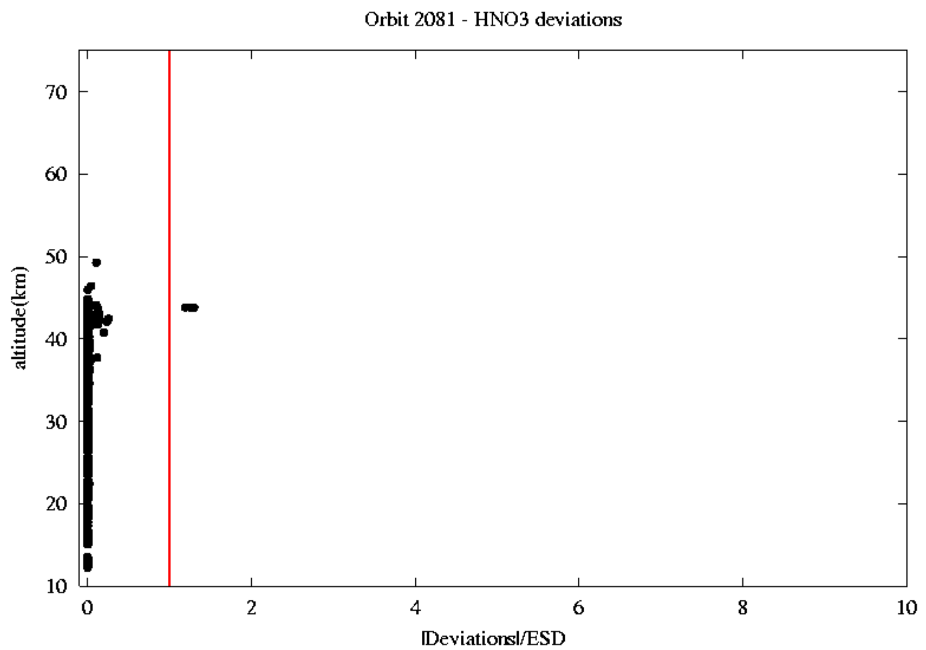
Orbit 2081 - HNO3 deviations
altitude(km)
|Deviations|/ESD
70
60
50
40
30
20
10
0
2
4
6
8
10

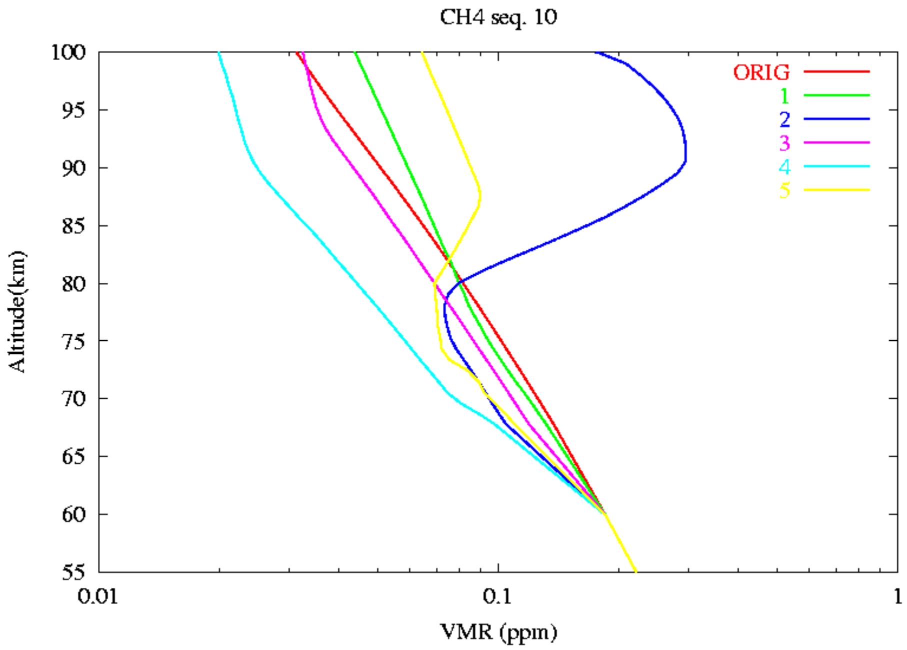
CH4 seq. 10
Altitude(km)
VMR (ppm)
ORIG
1
2
3
4
5
100
95
90
85
80
75
70
65
60
55
0.01
0.1
1

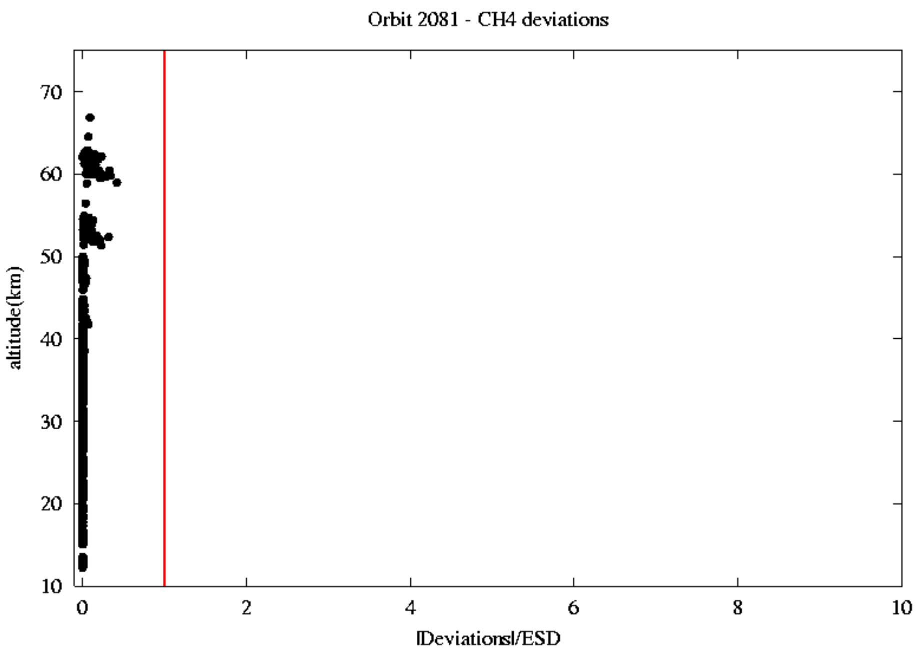
Orbit 2081 - CH4 deviations
altitude(km)
|Deviations|/ESD
70
60
50
40
30
20
10
0
2
4
6
8
10

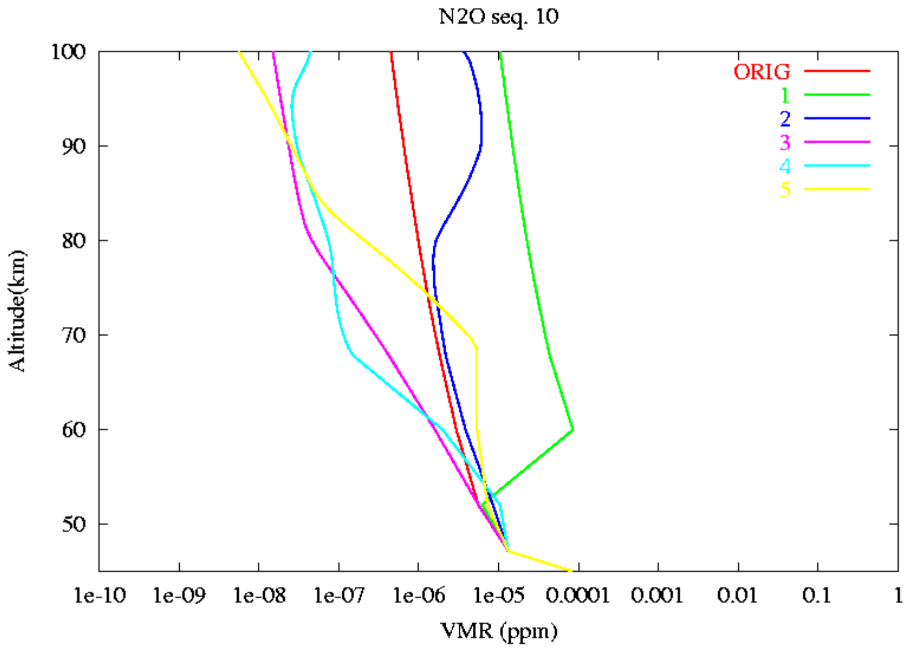
N2O seq. 10
ORIG
1
2
3
4
5
Altitude(km)
VMR (ppm)
100
90
80
70
60
50
1e-10
1e-09
1e-08
1e-07
1e-06
1e-05
0.0001
0.001
0.01
0.1
1

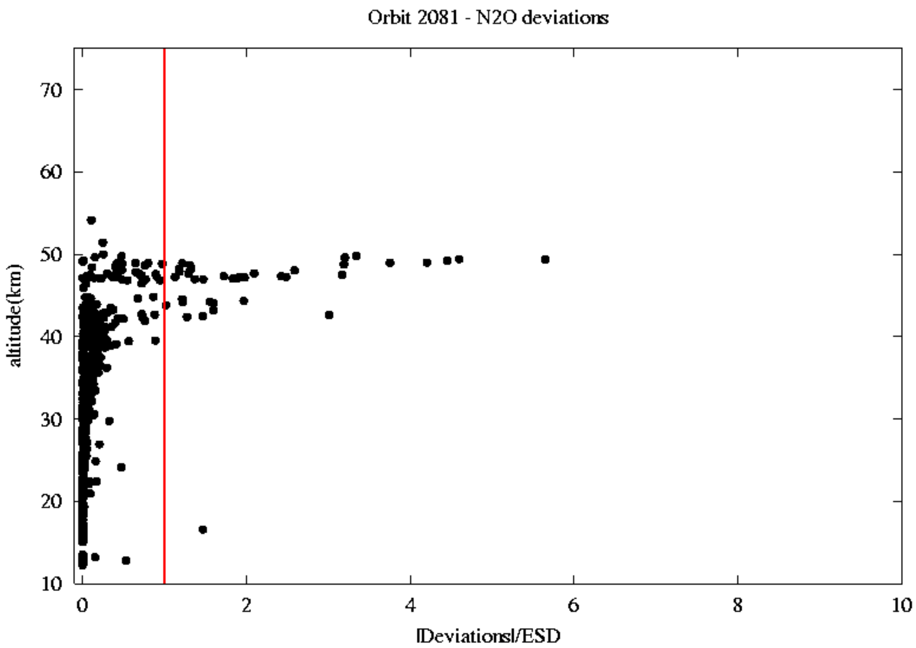
Orbit 2081 - N2O deviations
altitude(km)
|Deviations|/ESD
70
60
50
40
30
20
10
0
2
4
6
8
10

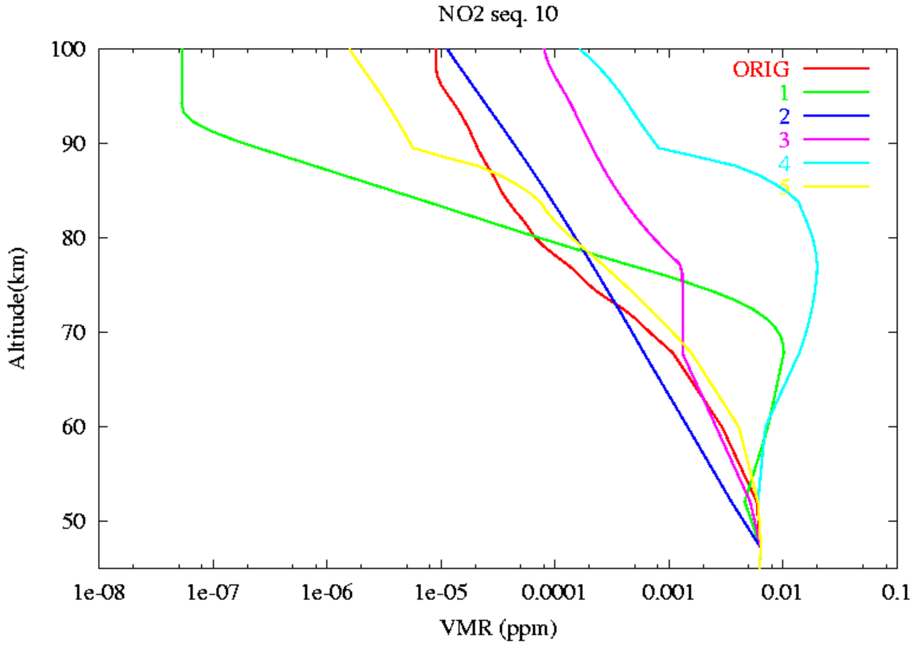
NO2 seq. 10
ORIG
1
2
3
4
5
100
90
80
70
60
50
Altitude(km)
1e-08
1e-07
1e-06
1e-05
0.0001
0.001
0.01
0.1
VMR (ppm)

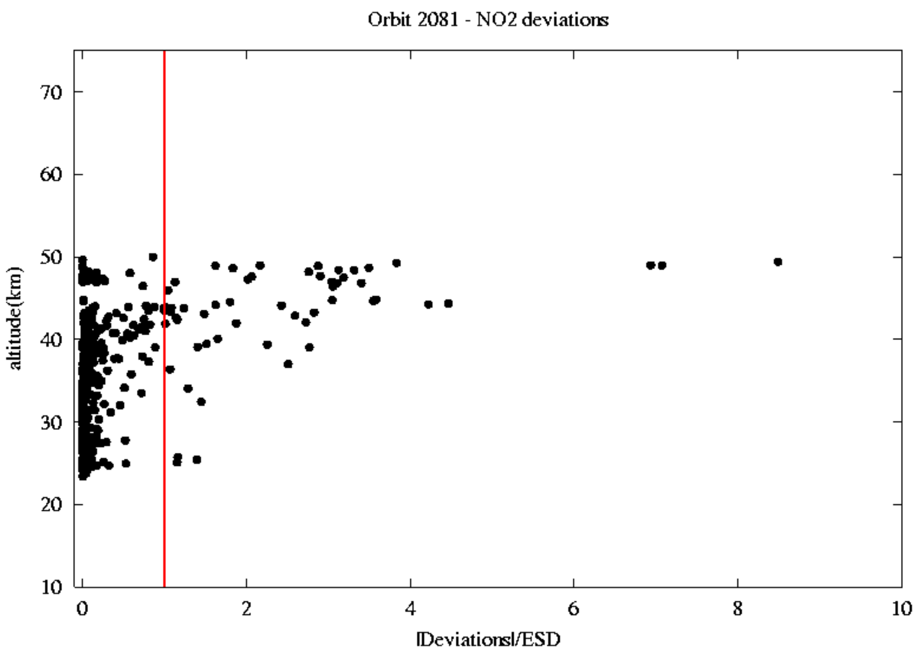
Orbit 2081 - NO2 deviations
70
60
50
40
30
20
10
altitude(km)
0
2
4
6
8
10
|Deviations|/ESD

Conclusions

In general the retrieved profiles at high altitudes depend on the assumed shape of the profile above them.
Temperature and H_2O retrieved profiles are the most affected by the shape of the profile above the highest fitted altitude, with deviations bigger than 3 times the estimated standard deviation. For the molecules whose VMR is very low above the highest retrieved point, such as HNO_3 and CH_4, these deviations are lower than the retrieval esd.
The whole NO_2 profile depends on the assumed shape above the highest retrieved altitude. This can be explained by the fact that the altitude range where NO_2 VMR is retrieved is very limited, and the assumption on the shape of the profiles weights much more on the few retrieved points.
It is therefore recommended to perform the retrievals over the whole measured range (see Sect. 3.2) and to include the extrapolation of the assumed profile among the sources of systematic errors.

4.2 Measurement altitude range

Ref. [RD5]: Sect. 4.1.10; Ref. [RD9]: Sheet MIP_MV_2_25/2

Introduction
MIPAS nominal limb scanning sequence consists of 17 spectra with tangent altitudes between 6 and 68 km (steps of 3 km from 6 to 42 km, steps of 5 km between 42 to 52 km and steps of 8 km from 52 to 68 km).
Retrieval of profiles at very low altitudes can be affected by the following problems: possible lack of information below a certain altitude (e.g.: due to low concentration of target species or to very opaque atmosphere), large horizontal gradients (e.g. temperature and water vapour), extra absorption and / or scattering due to clouds that are not modeled in the ORM.
At high altitudes, retrieval of the species having low concentration can result in strongly oscillating profiles that may induce problems also in the nominal range. Furthermore, systematic errors can increase significantly at high altitudes due to non-LTE.
In order to avoid these problems, it was decided not to exploit all spectra of a MIPAS scan, but to perform operational retrievals only between 12 and 68 km. Furthermore, within this range, a customized retrieval range was defined for each species, according to the information content of each species in MIPAS measurements. The nominal retrieval ranges for the different retrievals are reported in Table 1.

Table 1 Nominal retrieval range for the different retrievals

Retrieval	P, T	H_2O	O_3	HNO_3	CH_4	N_2O	NO_2
Retrieval range [km]	12-68	12-60	12-60	12-42	12-60	12-47	24-47

On the other hand, retrievals on the whole measurement range would allow:
_ to derive information on tropospheric profiles from MIPAS measurements;
_ to extend the height range in which the profiles are not affected by the assumption on the initial guess profile outside the retrieval range (see results on test on extrapolation, Sect. 4.1);
_ to get information on species whose concentration is significant only for particular latitudes and seasons (ex. NO2 significant above 47 km only in the winter pole).

Tests have been done in order to understand whether retrieval on the whole MIPAS measurement range are feasible and whether downward and upward propagation of errors affects retrieved profiles in the nominal retrieval range.

The results of this test is connected with the results of the test on extrapolation rules (see Sect. 4.1): since the highest and lowest values of the retrieved profiles are affected by the assumption on initial guess profile respectively above and below, an extension of the retrieved profile helps at least in providing a better profile in the nominal range.

Procedure

The first test is meant to evaluate the possibility of retrieving profiles down to 6 km, by checking if the inclusion of spectra at low altitudes that can be affected by big systematic errors induces an upward propagation of the retrieval error at high altitudes. In order to do this, the nominal Occupation Matrices (OM) of all the species (except NO_2) were modified extending down to 6 km the range where the microwindows included in the OM is used, if allowed by the altitude range of each microwindow. The OM used for N_2O retrieval was extended only down to 9 km, since no microwindows in the nominal OM are allowed to be used below 9 km.
In order to avoid problems coming from clouds in the line of sight, this test was performed with the cloud filtering activated, so that the retrieval range is extended only if clouds are not present in the line of sight. Orbit #2081, acquired on 24th July 2002, was used for this test.
Retrievals were performed in both the nominal case and for the extended retrieval range, and comparisons between the profiles retrieved in the two cases were made.

The second test is meant to evaluate the possibility to retrieve profiles up to 68 km. Also in this case, nominal OM of all the species (except N_2O, for which no microwindow in the nominal OM is allowed to be used up to 68 km) were extended.
The extension of NO_2 is of great interest, because it would allow to detect a significant increase of NO_2 concentration in the polar winter.

Results

Figure 1 shows the maps of the difference between profiles retrieved down to 12 km and profiles retrieved down to 6 km (if clouds are not present) for the different species. In the maps the differences are normalized by the random error.
Differences are mainly observed in T and h2o retrievals.
The T and h2o vmr profiles retrieved down to 12 km and 6 km in a single selected sequence are shown in Figure 2 (where profiles are plotted vs altitude) and in Figure 3 (where profiles are plotted vs pressure). As expected, differences are reduced when the profiles are plotted vs pressure, because retrieved tangent altitudes depend on the value of the lowest tangent altitude, that is assumed as known and that is different in the two cases.
For water retrieval, big differences are visible at low altitudes. One cause of these differences is surely the fact that the lowest retrieved value is affected by the slope of water profile assumed below the lowest retrieved tangent altitude. If the retrieval is performed down to 6 km, the value of VMR retrieved at 12 km is less affected by the assumption of the initial guess profile below 6 km.
Big differences are visible also at high altitudes, but their cause has to be searched not in the upward propagation of retrieval error, but in inherent water profile oscillations, whose cause is still under investigation (see Sect. 5).

The differences in the retrieved profiles of the other species between the 12 km case and the 6 km case are mainly induced by differences in temperature and h2o (the retrieval of each species is performed using as assumed profiles the profiles obtained in the previous retrievals). Furthermore, some differences (for example at scan #10 and scan #28) are due to difference in the selected OMs (since only the nominal OMs have been extended to 6 km, if for any reason the nominal OM cannot be used below 12 km, an OM having some skipped sweeps above 12 km is selected in the 6 km case). Difference can also be induced by the fact that a different number of iterations are needed to reach convergence in the two cases.

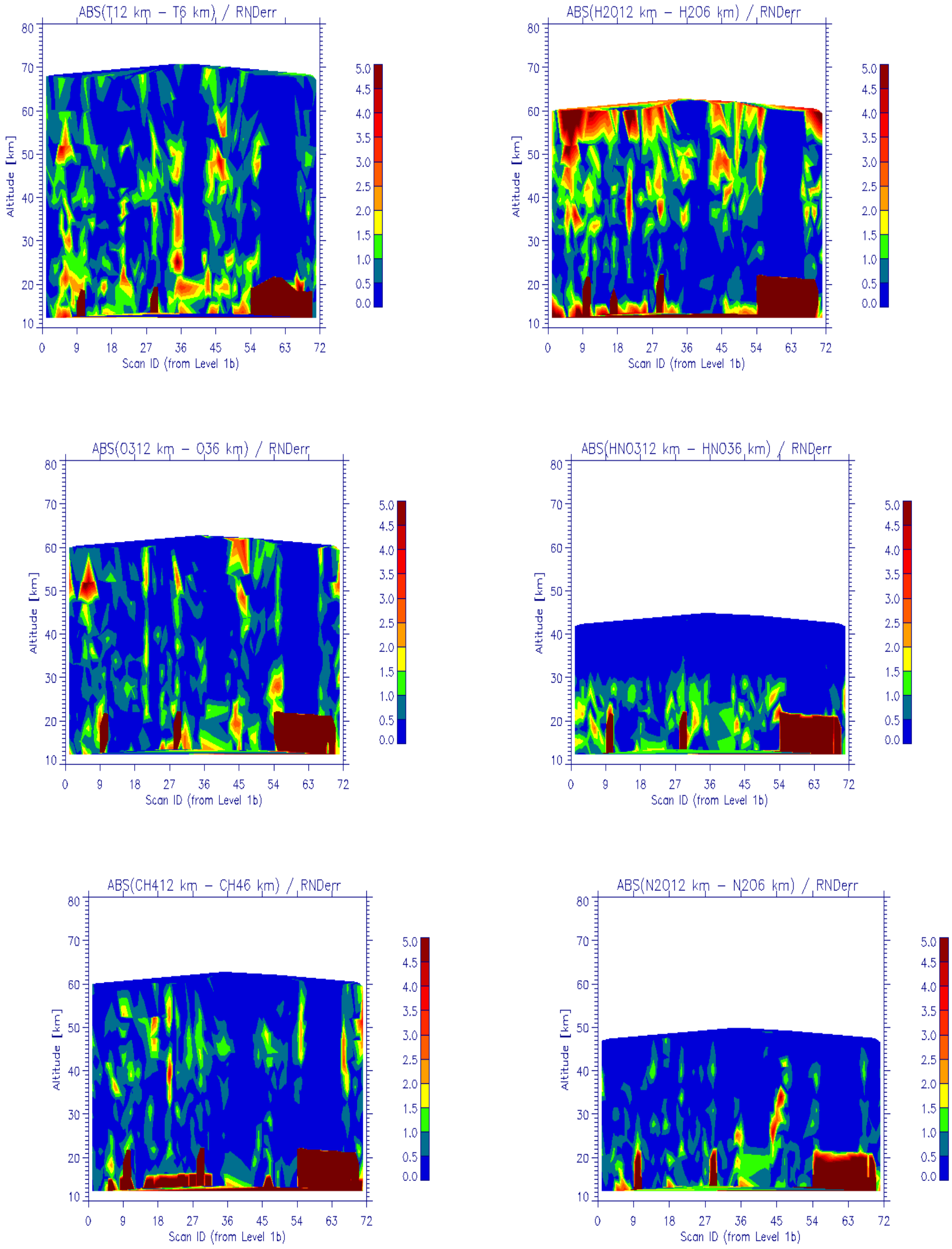

Figure 1 Map of the difference, in the common retrieval range, between profiles retrieved down to 12 km and down to 6 km for the different species. The maps are normalized by the random error. In abscissa the scan ID is reported. The red rectangle at low altitudes for scans 54-70 does not represent real differences since it corresponds to cloudy scans.

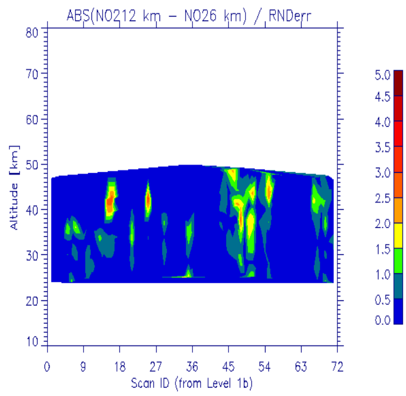

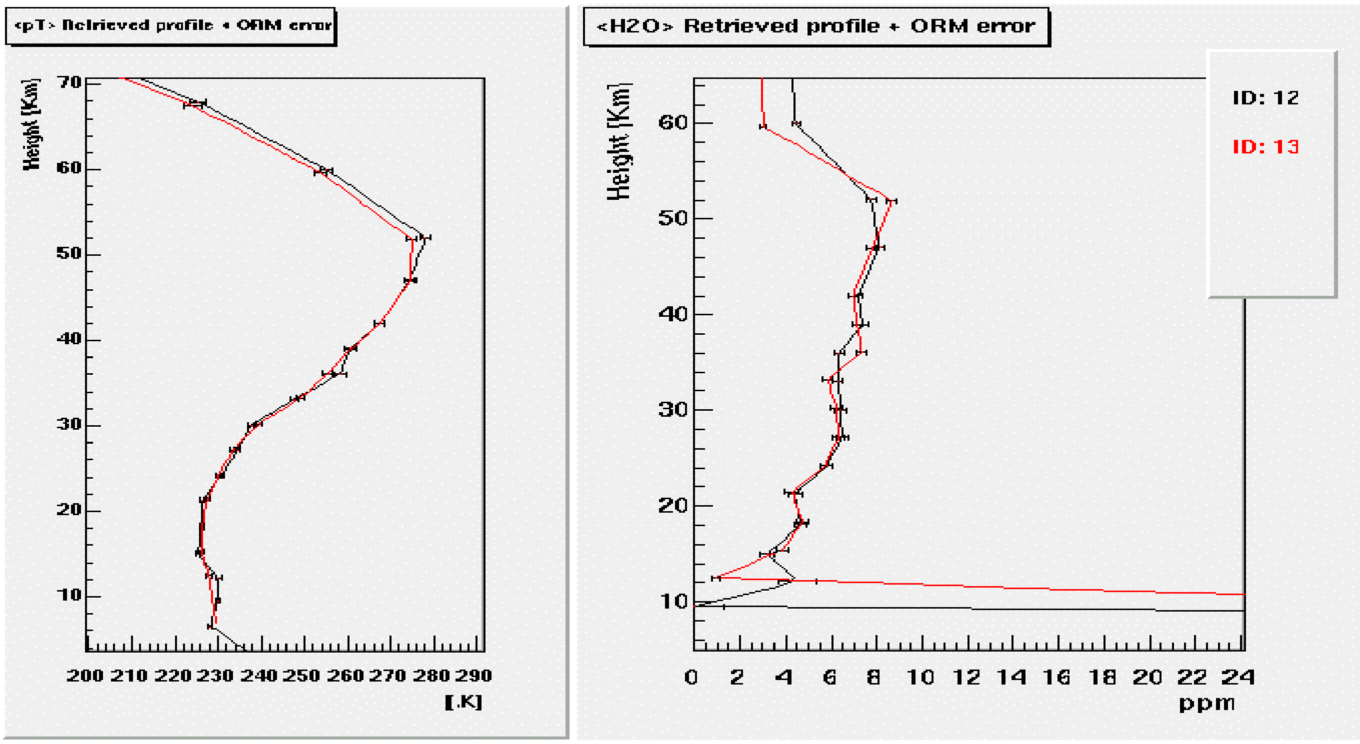

Figure 2 Extension of the retrieval down to 6km: comparison between retrieved profiles down to 12 km and retrieval to 6 km in scan 7 for T and H2O

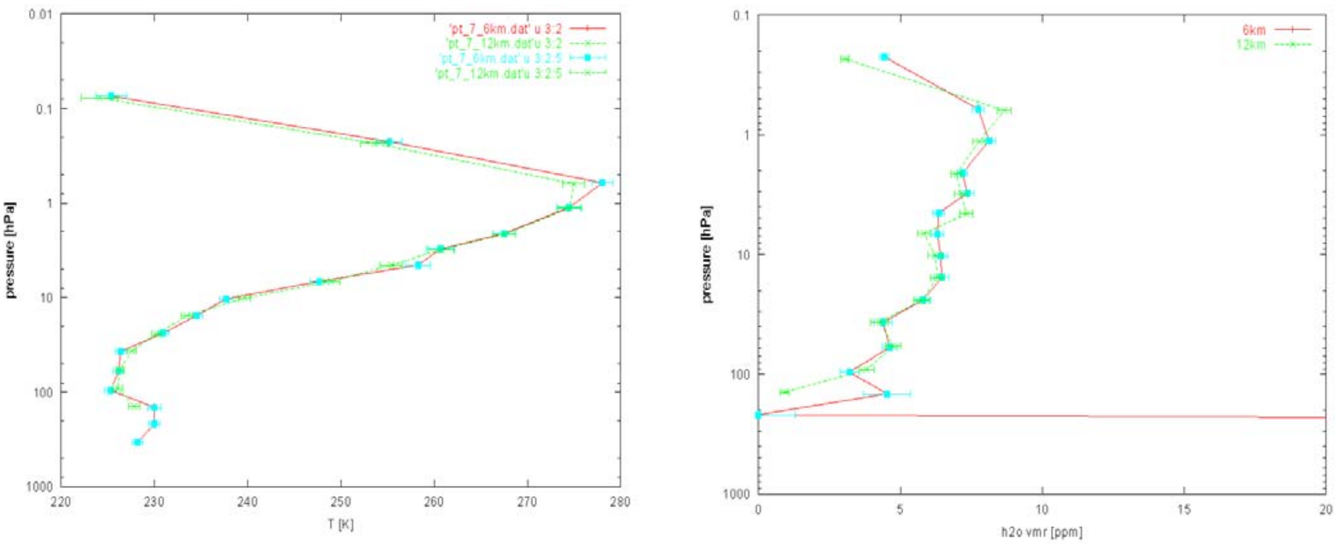

Figure 3 Same as Figure 2, but profiles reported vs pressure

In the second test the altitude range of the retrieval was extended at high altitudes. In Figure 4 the maps of no2 obtained up to 47 km and up to 68 km are shown. In the map up to 68 km is clearly visible the high concentration of no2 above 50 km around sequence #40, corresponding to the South Pole in winter (orbit #2081 was acquired on the 24th July 2002).
The absolute difference, in the common retrieval range, of the maps obtained using the nominal retrieval range and the extended one, normalized by the random error, is also reported in the lower panel of Figure 4. This map shows that no significant differences are found in the retrieved profiles below 47 km except in the South Pole. This means that outside the polar vortex, where the concentration of n2o is low at altitudes above 47 km, the oscillations in the retrieved profile from 47 to 68 km do not affect retrieved profiles below 47 km (see also the lowest panel of Figure 5, where comparison of no2 profiles retrieved far from the South Pole when using two different retrieval ranges are shown); on the contrary, in the South Pole, retrieved profiles in the range 12-47 km are strongly affected by the assumption of the profile above 47 km, if retrieval is stopped at that altitude: in this case, downward propagation of the error strongly affects the retrieved profile down to very low altitudes (see upper panels of Fig.5, where profiles obtained in 4 different scans in the polar vortex are shown).

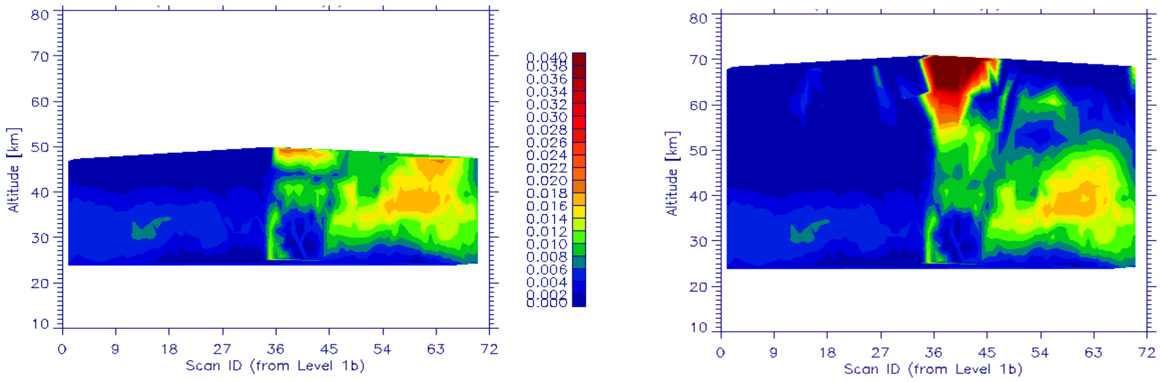

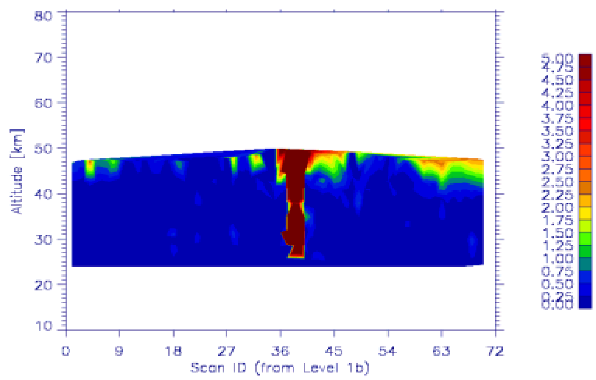

Figure 4 Plots above: maps of NO2 up to 47 km and up to 68 km. Plot on the right: map of the absolute value of the difference between the two maps above, normalized by random error.

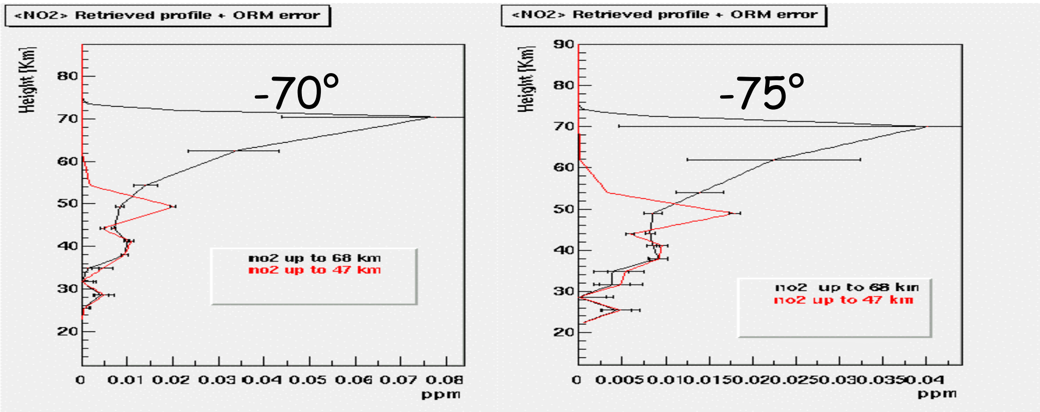

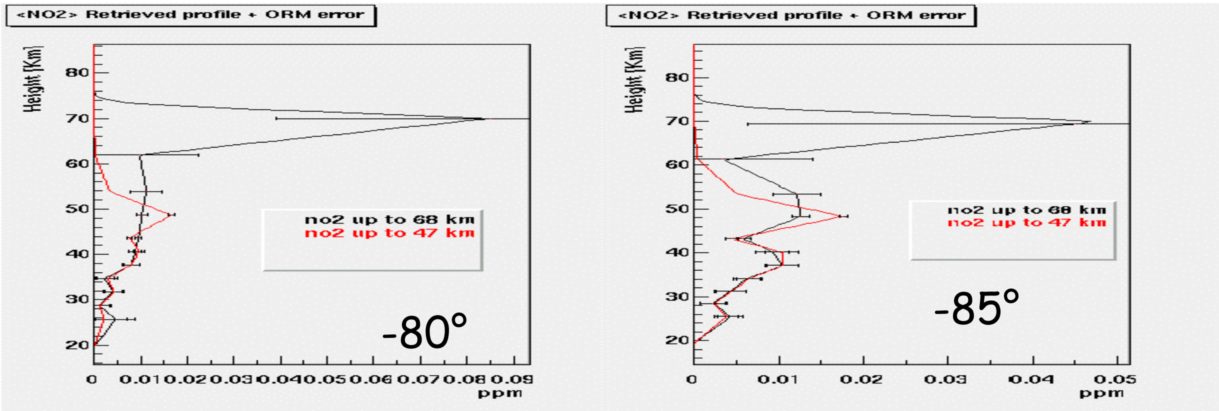

Figure 5 – Comparison between no2 retrieved up to 47 km and up to 68 km for different scans of orbit #2081. The 4 upper plots refers to scans inside the polar vortex (latitude is reported), the plot on the right refers to a scan far from the polar vortex

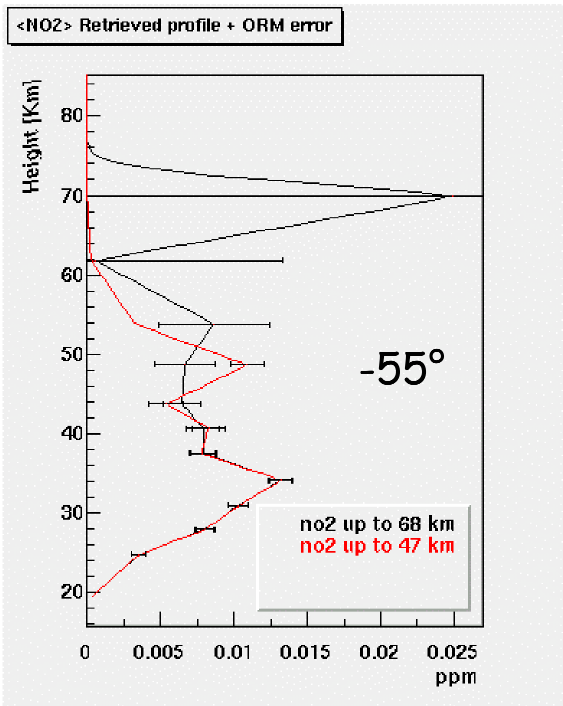

The same test performed for no2 was repeated for all the other species. In Figure 6 the results are shown for h2o retrieval. Also in this case the main differences are located in the South Pole.

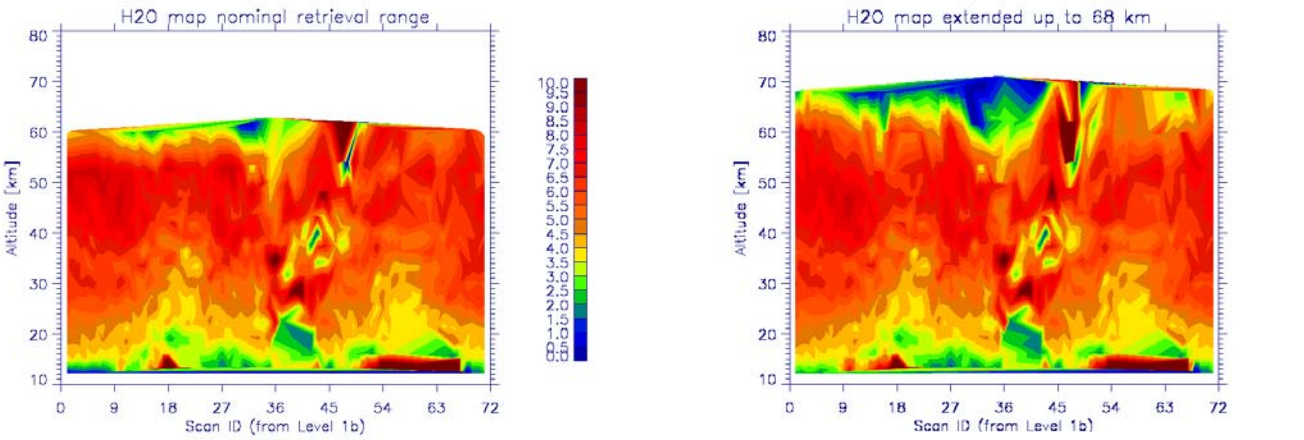

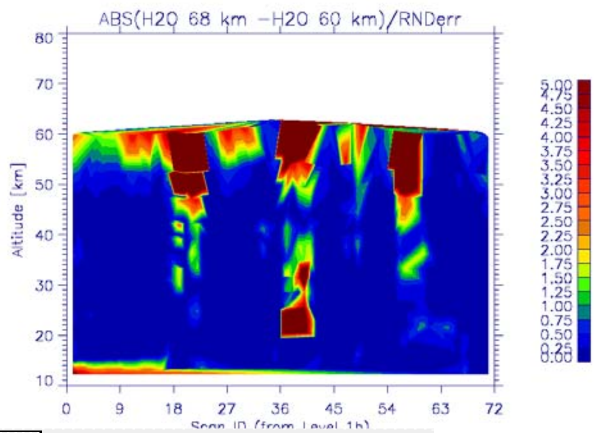

Figure 6 Plots above: maps of H_2O up to 47 km and up to 68 km. Plot on the right: map of the absolute value of the difference between the two maps above, normalized by random error.

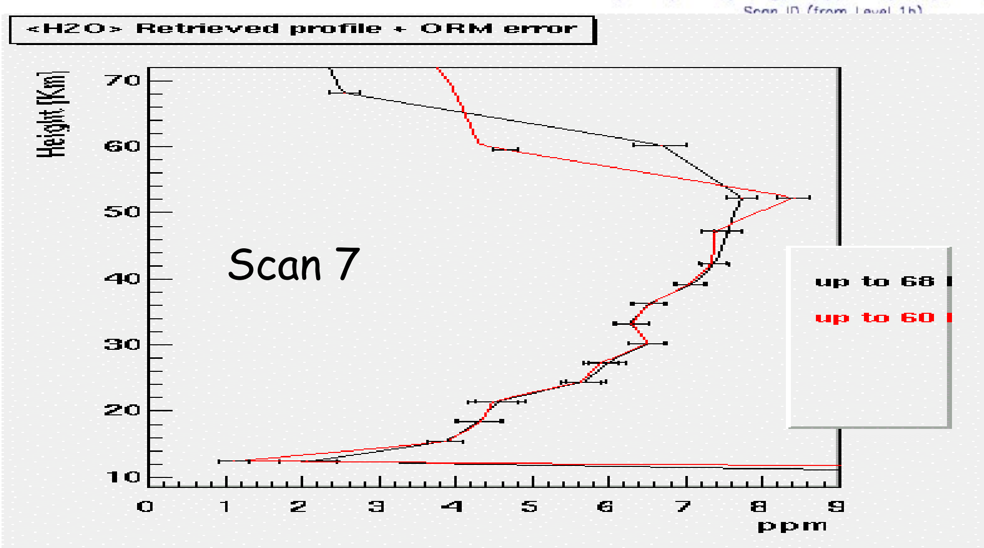

Figure 7 Water vapour retrieved VMR in case of nominal retrieval range (12-60 km, red curve) and extended one (12-68 km, black curve)

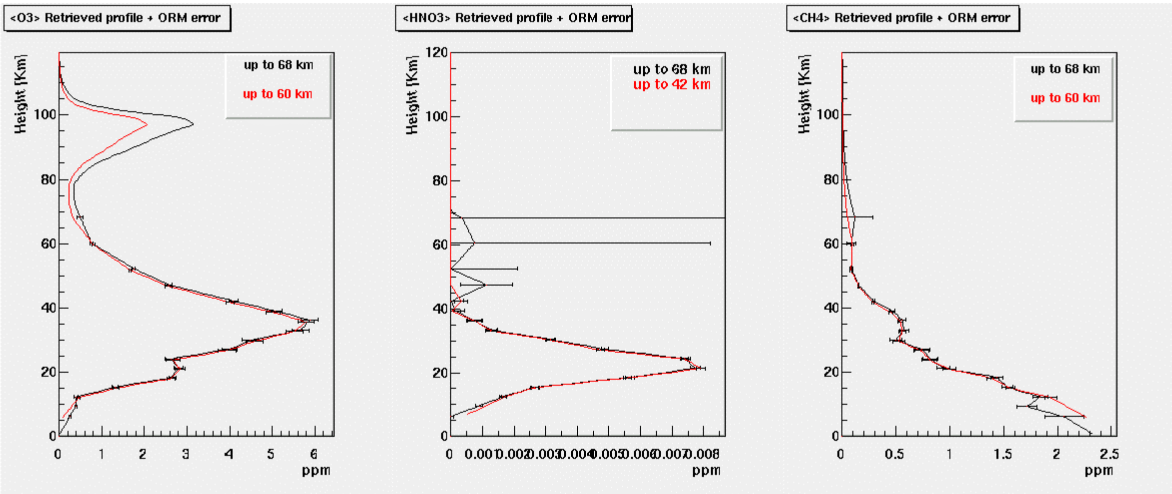

Figure 8 Retrieved profiles of O3 (left panel), HNO3 (central panel) and CH4 (right panel) obtained in case of nominal retrieval range and extended retrieval range.

The extension of the retrieval range up to 68 km for retrieval of O3, HNO3 and CH4 does not degrade the retrieved profiles in the nominal range, as is shown in Fig. 8.

Conclusions

Test retrievals have shown that, whenever cloud free conditions are observed, the altitude range of the retrieval can be extended to altitudes lower than 12 km: if insufficient information is present large errors are found in the retrieved values, but the errors generally do not propagate in a negative way to higher altitudes: however further investigations are needed to understand the impact of some approximations below 12 km (water independent refractive index, pressure shift, self-broadening, refraction-independent FOV)
Main differences are observed for T and H2O.

A similar situation is encountered at high altitudes where the retrieval can be extended to the maximum altitude of 68 km also for those species that do not have a measurable concentration at this altitude.
NO2 retrieval up to 68 km is feasible and it is very useful in the polar vortex. ESDs are acceptable, however NLTE error is expected to play an important role above 47 km.

In general, for all species the extension of the retrieval range up to 68 km does not seem to degrade the retrieved profiles in the range originally selected for the retrieval. Further investigations has to be made in order to assess the contribution of systematic errors to the total error in the extended altitude range. The recommendation is to perform retrieval on the whole MIPAS altitude range.

4.3 Local thermodynamic equilibrium (LTE)

Ref. [RD5]: Sect. 4.2.1; Ref. [RD9]: Sheet MIP_MV_2_1

Introduction

ORM assumes the atmosphere in local thermodynamic equilibrium (LTE). This means that the temperature of the Boltzmann distribution is equal to the kinetic temperature and the source function is the Planck function at the local kinetic temperature. This LTE model is usually valid at low altitudes where kinetic collisions are frequent.

Non-LTE effects cause a radiance higher or lower than that modeled in LTE. Non-LTE effects can sometimes be discriminated by the fact that they tend to decrease during the night.

Description of the test

χ^2 corresponding to the day scans are compared with the χ^2 corresponding to the night scans of orbit #2081.

Partial χ^2 in correspondence of the speciess and altitudes which have the highest non-LTE error quantifiers are reported for day and night measurements for orbit #2081.

Results

The comparison between χ^2 corresponding to day and night scans are reported in the table below:

	day	**night**
PT	1.71	1.70
H_2O	0.94	0.96
O_3	1.19	1.20
HNO_3	1.31	1.13
CH_4	1.06	1.06
N_2O	1.01	1.05
NO_2	1.02	1.01

The error analysis has identified significant non-LTE error for the following speciess and altitudes:

gas	**altitude**	**Non-LTE error**
H_2O	60 km	39.1%
CH_4	60 km	12.4 %
NO_2	47 km	62.5 %
NO_2	42 km	12.2 %

In the following figures the partial χ^2 corresponding to these speciess and altitudes as a function of the orbital coordinate are shown. The orbital cordinate is an angular coordinate that is equal 0 on the equator when the satellite is moving toward north, is 90 on the north pole, 180 on the equator when the satellite is moving toward south and 270 on the south pole. The day measurements are reported with red points and the night measurements are reported with bleu points.

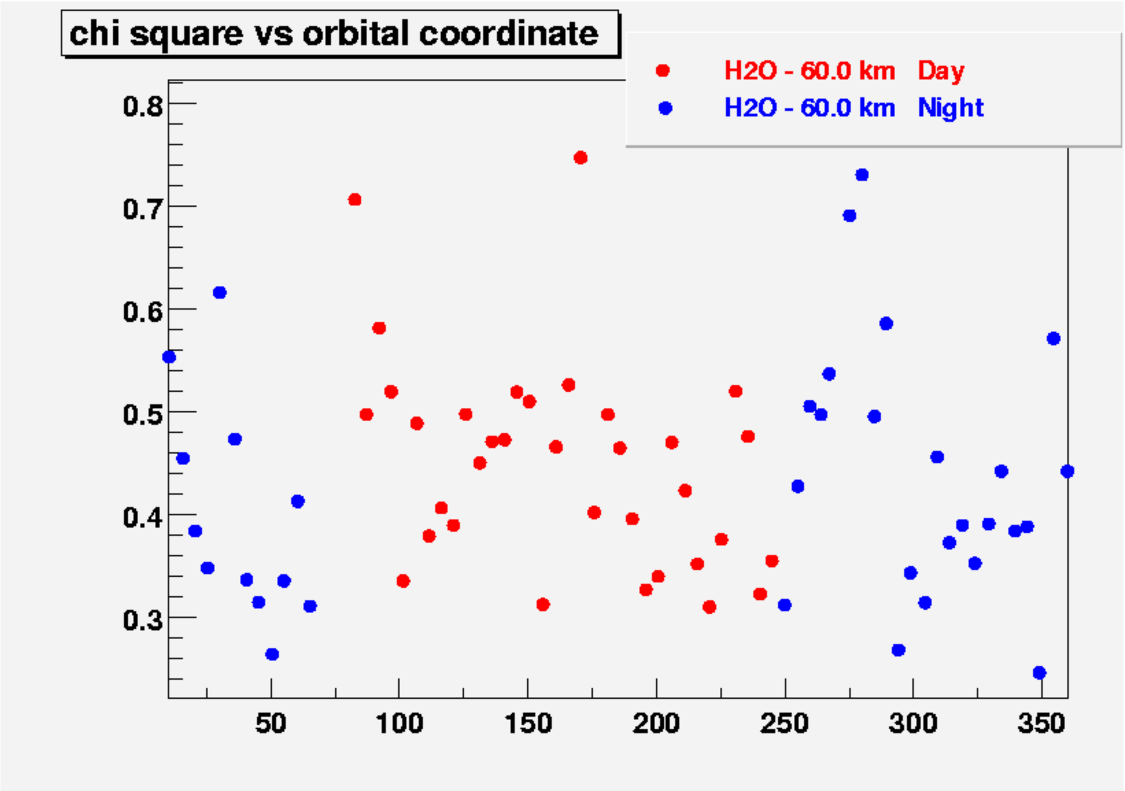
chi square vs orbital coordinate
H2O - 60.0 km Day
H2O - 60.0 km Night
0.8
0.7
0.6
0.5
0.4
0.3
50
100
150
200
250
300
350

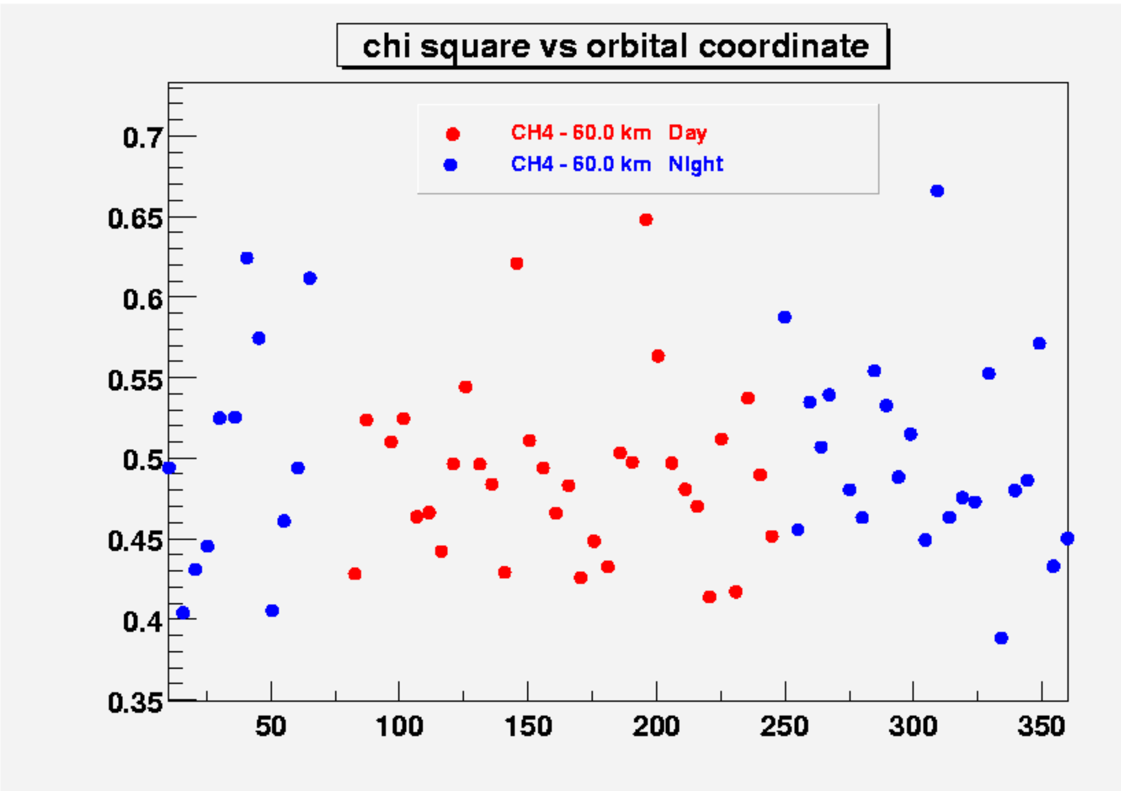
chi square vs orbital coordinate
CH4 - 60.0 km Day
CH4 - 60.0 km Night
0.7
0.65
0.6
0.55
0.5
0.45
0.4
0.35
50
100
150
200
250
300
350

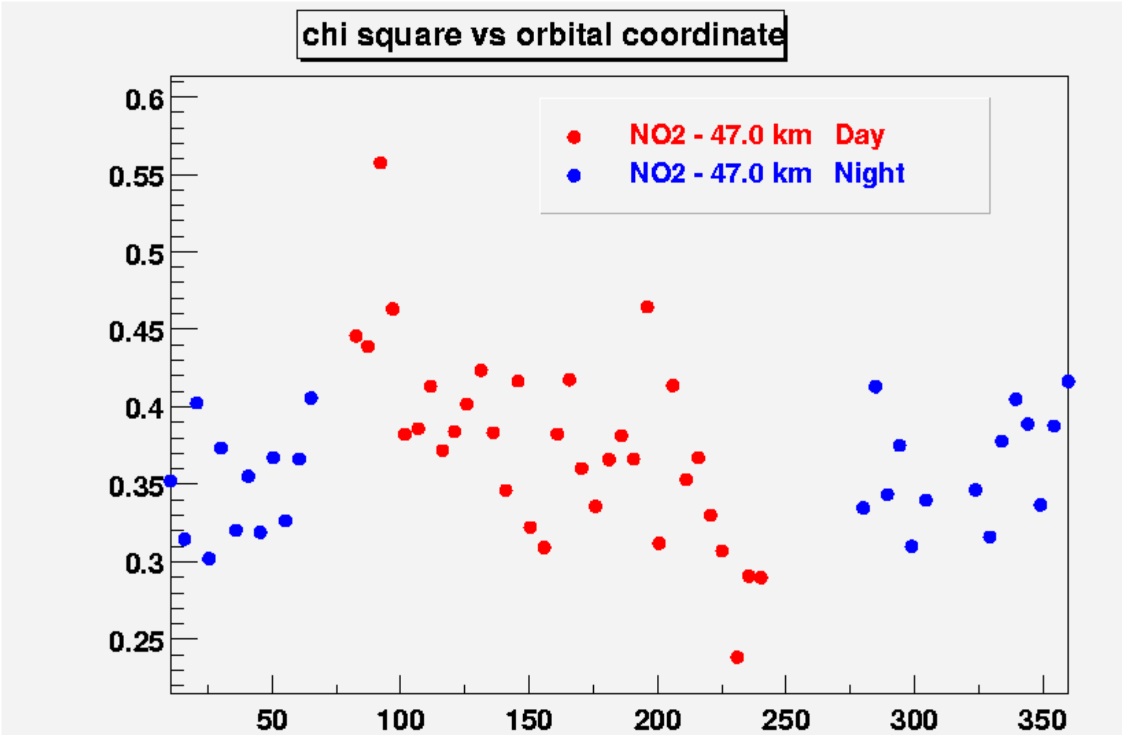

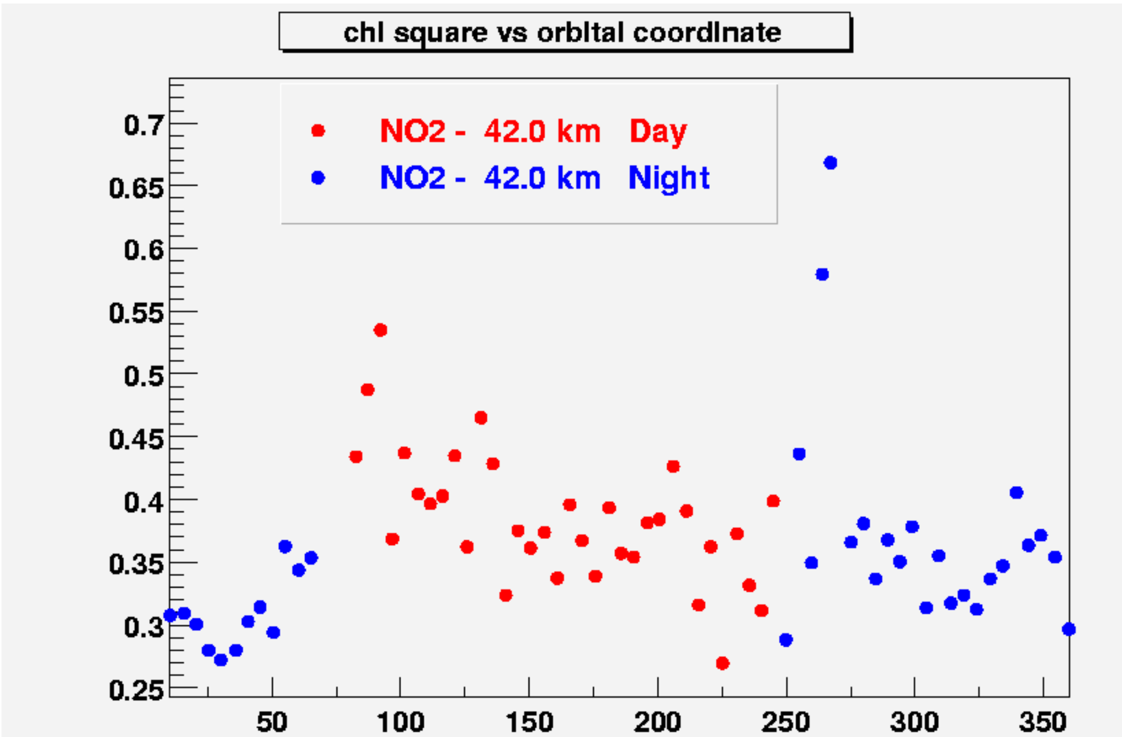

Conclusions

The analysis of the partial χ^2 corresponding to these species and altitudes has evidenced no significant variation between χ^2 obtained in day or night measurements. This does necessarily mean that NLTE does not influence the retrieval, because the effect of NLTE could be compensated by wrong values of the VMR. So a deeper analysis of this problem is necessary and for it we refer to the one performed by the team of Manuel Lopez Puertas.

4.4 Verification of horizontal homogeneity assumption

Ref. [RD5]: Sect. 4.2.2; Ref. [RD9]: Sheet MIP_MV_2_2

Introduction

Limb sounding attains good sensitivity due to the long path length of the observation, but this necessarily implies measurements of the average atmosphere over long horizontal distances. The horizontal length scale, for a typical limb sounding experiment, is of the order of several hundreds of kilometers and the assumption that the atmosphere is horizontally homogeneous over this distance may fail in some cases. The retrieval accuracy is particularly sensitive to horizontal temperature gradients (see [R10]).
The problem causes systematic errors and possibly large chi-squares in correspondence of large latitudinal gradients (poles and equator). The amplitude of the horizontal gradients can be calculated from the difference between profiles retrieved from subsequent scans.

Procedure

The following procedures have been adopted to verify the assumption of homogeneous atmosphere:

1. Assessment of the correlations between chi-square of the fit at a given tangent altitude and latitudinal variation of temperature, H_2O and O_3 at the same altitude,
2. Comparison of the profiles for different scans with 'external' information (ECMWF, correlative measurements, chemical models, etc.) in areas where large gradients occur,
3. REC analysis of the residuals (includes only the effect of T gradients)

The output of procedure 1. is a set of scatter plots correlating horizontal gradient and total chi-square at a given altitude. Each plot contains as many points as many are the scans of the considered orbit. The correlation between the considered quantities is quantified by the linear correlation coefficient. The most important effects of the tested assumption are expected to arise from H_2O, O_3 and T gradients at low altitudes, therefore the correlation, if any, is expected to be significant especially at low altitudes. If the mentioned plots do not highlight a correlation between chi-square and gradient, it means that most likely the horizontal homogeneity assumption is compensated by a systematic deviation of the retrieved VMR from its true value. In this case test 2. provides useful insights regarding the correlation between horizontal gradients and systematic VMR error. The output of tests 1. and 2. is an assessment of the impact of horizontal homogeneity assumption on MIPAS retrievals.

Results

Procedures 1. and 2. were tested on observations relating to orbit 2081, with no cloud filtering.
Procedure 1. did not highlight significant correlations between chi-square and horizontal gradient at the individual altitudes. Figs. 1-5 show the correlation between the absolute value of temperature horizontal gradient and the chi-square at several altitudes. Fig. 6 also shows the correlation between the absolute value of temperature horizontal gradient and the chi-square but in this case all the sweeps of the nominal scans of the orbit 2081 have been merged in a single plot. In Fig. 7 we report the behavior of the measured correlations as a function of altitude, for the three retrievals that are expected to be most affected by horizontal variability, i.e. pT, H2O and O3. The measured correlations are generally less than 40%, only for water retrieval at 12 km the value of the correlation approaches 50%. Furthermore the measured correlations do not show any particular trend as a function of altitude (see Fig. 7).

Procedure 2. was tested only on some specific scans of orbit 2081, however the intercomparisons with ECMWF data carried-out so far did not point-out discrepancies localized where horizontal structures are present. Figures relating to intercomparison with ECMWF data are reported in the section dedicated to " Tuning of the error associated with engineering LOS information".

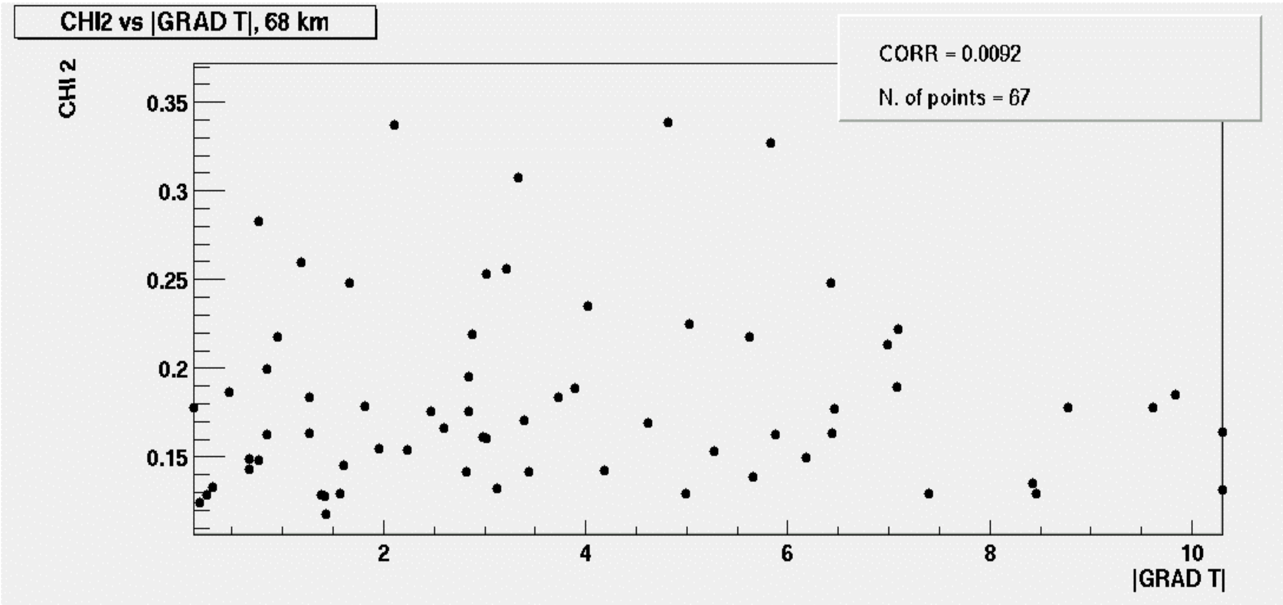

Fig. 1: Scatter plot of χ^2 @ 68 km versus absolute value of horizontal temperature gradient at the same altitude.

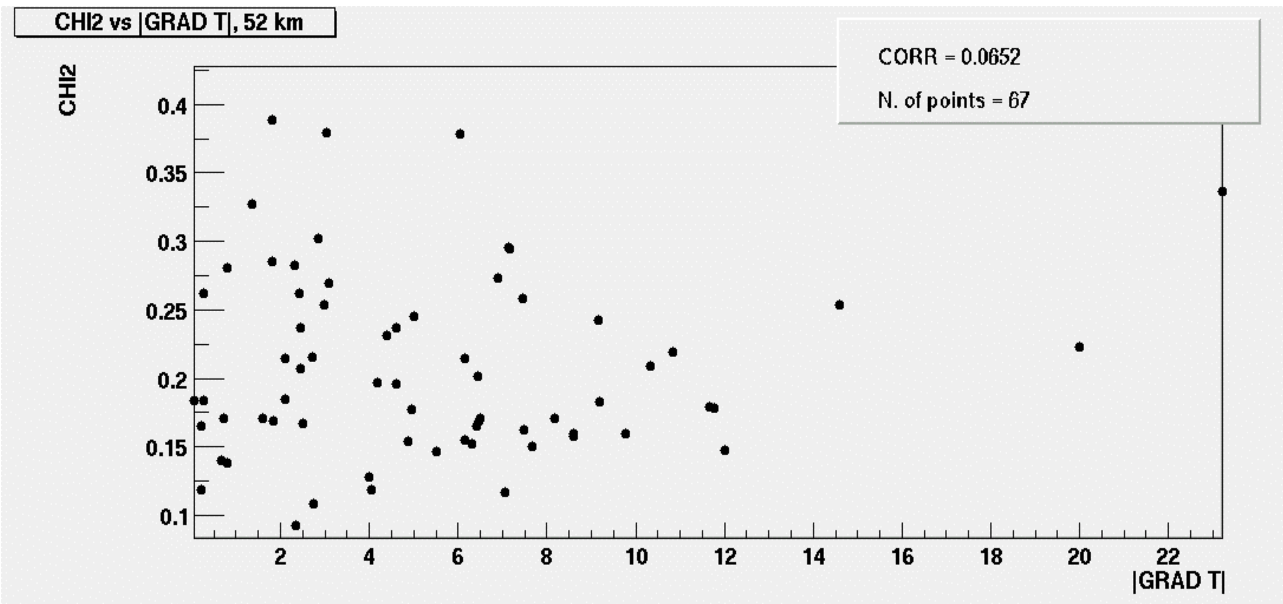

Fig. 2: Scatter plot of χ^2 @ 52 km versus absolute value of horizontal temperature gradient at the same altitude.

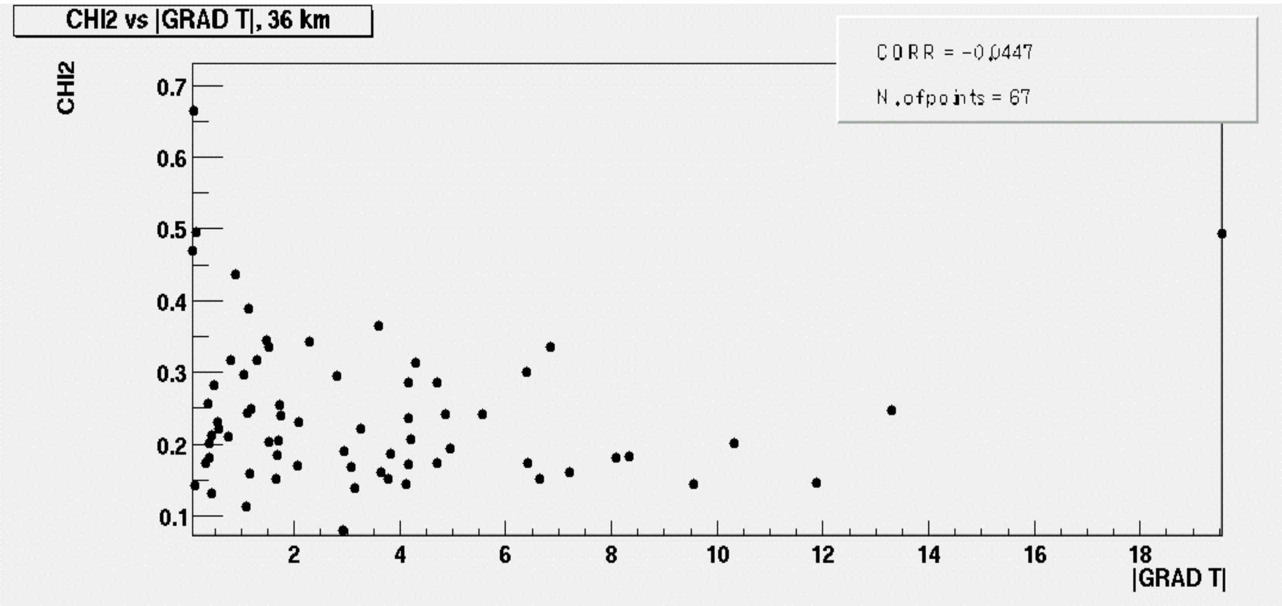

Fig. 3: Scatter plot of χ^2 @ 36 km versus absolute value of horizontal temperature gradient at the same altitude.

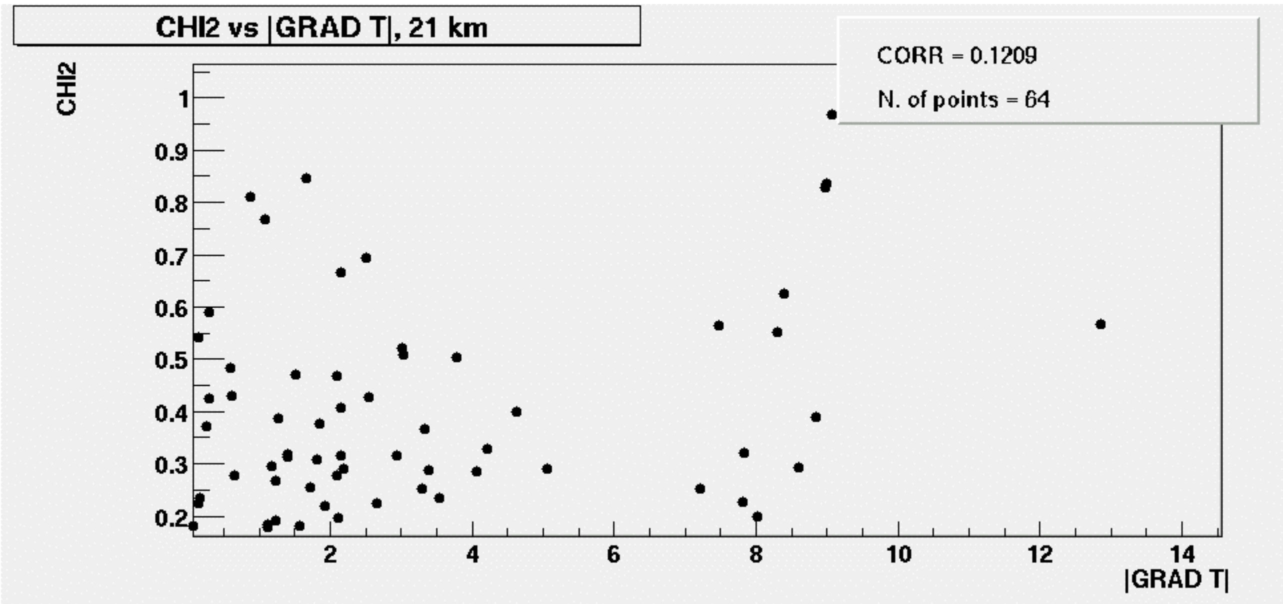

Fig. 4: Scatter plot of χ^2 @ 21 km versus absolute value of horizontal temperature gradient at the same altitude.

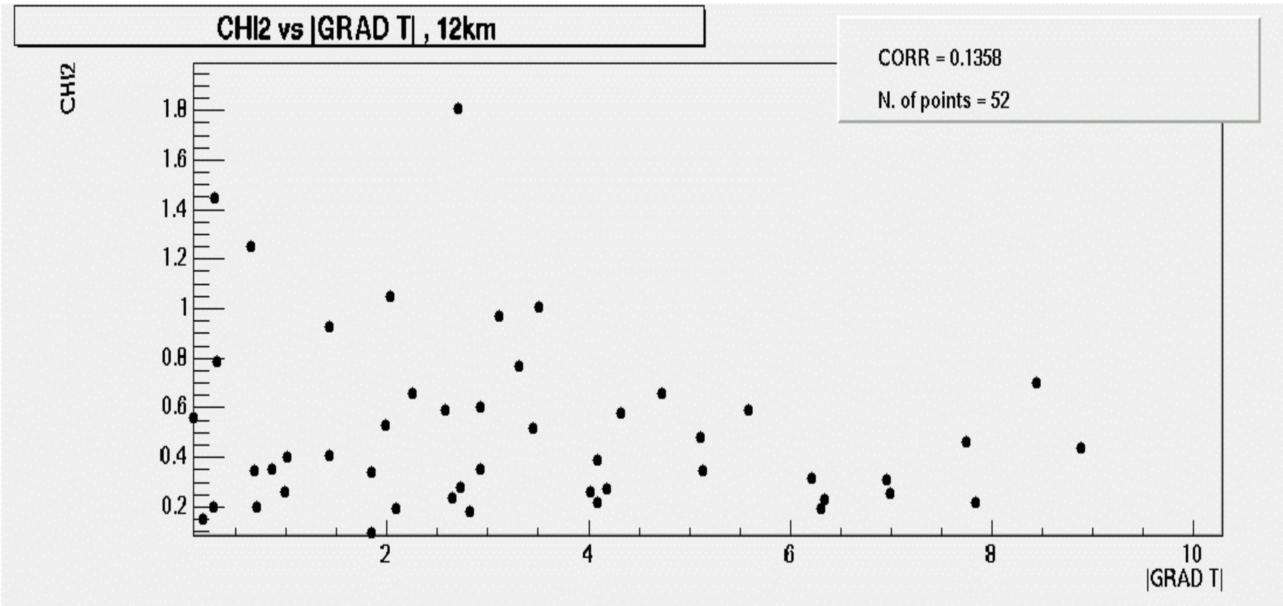

Fig. 5: Scatter plot of χ^2 @ 12 km versus absolute value of horizontal temperature gradient at the same altitude.

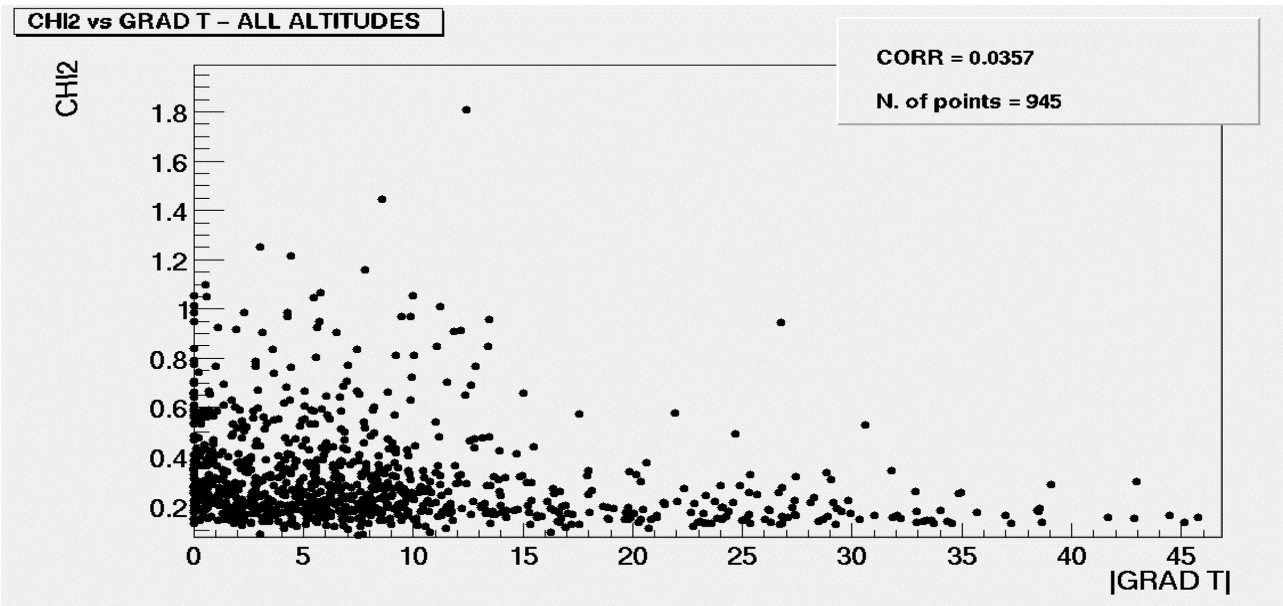

Fig. 6: Scatter plot of χ^2 at the different tangent altitudes versus absolute value of horizontal temperature gradient at the same altitude. All altitudes are included in this scatter plot.

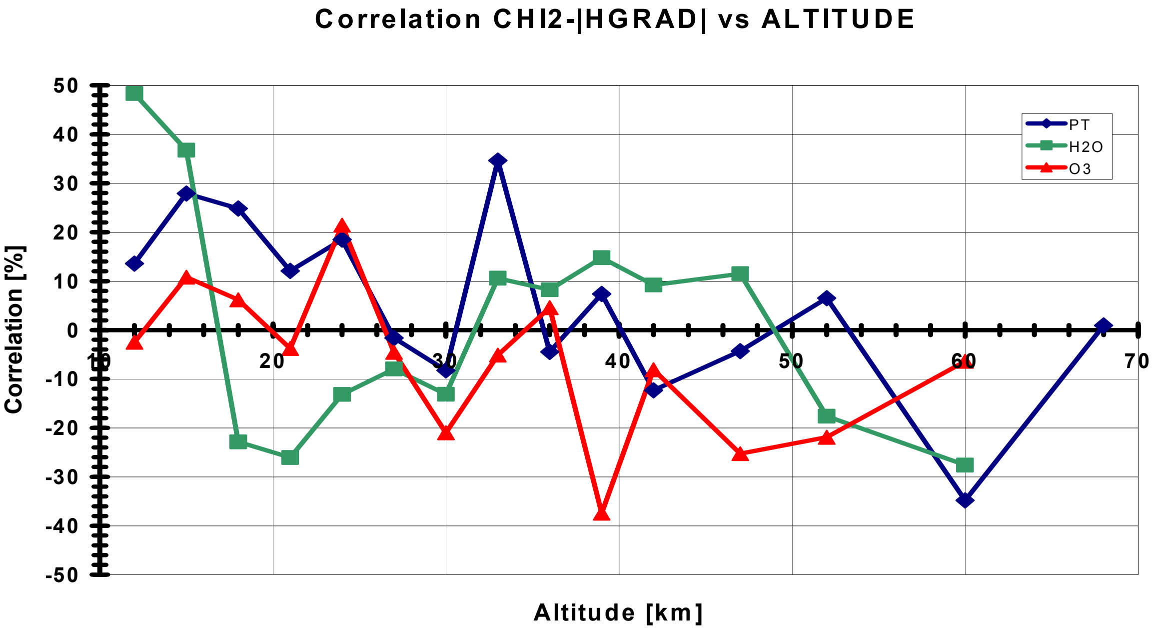

Fig. 7: Altitude distribution of the correlation between horizontal gradient of some target quantities (temperature, H2O and O3 as indicated in the key of the plot) and chi-square at the same altitudes.

Conclusion

The measured correlations between horizontal gradients of temperature, H2O, O3 with the chi-square at the individual altitudes are generally small (possible exception for H2O below 15 km). The observed behavior of these correlations as a function of altitude does not show particular trends. This result confirms the findings of [R10], suggesting that most likely the horizontal homogeneity assumption does not lead to large spectral residuals but to a systematic bias in the retrieved profiles.

So far intercomparisons with ECMWF data were restricted to a very limited number of scans of orbit 2081. Therefore these intercomparisons were not able to point-out discrepancies localized in correspondence of horizontal structures.

For the future, more extensive intercomparisons with ECMWF data are recommended and the observed discrepancies should be correlated with the horizontal gradients in the atmosphere.

A further test that should be done consists in comparing Level 2 retrieved profiles with profiles retrieved by a 2D retrieval algorithm such as the GEOFIT [R10].

4.5 Verification of hydrostatic equilibrium (assumption of vertical profiles)

Ref. [RD5]: Sect. 4.2.3; Ref. [RD9]: Sheet MIP_MV_2_3

Introduction

Hydrostatic equilibrium provides a relationship between temperature, pressure and geometrical altitude and is generally fulfilled in normal atmospheric conditions (especially in the stratosphere). However it should be noted that, with limb scanning, the profile of acquired tangent points is a slant profile. This is due both to the variation of the tangent point position with the elevation angle and because of the satellite motion (most important factor). The Level 2 algorithm assumes retrieved profiles as "vertical" to apply the hydrostatic balance and this approximation could have a significant impact on the accuracy of the retrieved tangent altitude corrections.

Procedure

The test procedure consists in the assessment of the correlations between the horizontal temperature gradients and the tangent altitude corrections (i.e. the difference between engineering and retrieved estimates of the tangent altitude separation) obtained from p,T retrieval, when no engineering pointing information is used. A scatter plot (see Fig. 1) was built correlating the horizontal temperature gradients with the tangent altitude correction at the same altitude. The plot contains as many points as many are the sweeps measured along the considered orbit (orbit 2081). The correlation between the considered quantities is quantified by the linear correlation coefficient.

Results

The correlation between tangent altitude corrections and temperature gradients is not zero but is small (around 9%, see Fig. 1).
Given the heterogeneity of the considered sample of tangent altitude corrections (considered tangent altitude corrections are different due to real differences in MIPAS pointings along the orbit rather than to horizontal variability of temperature) it is not possible to compare this empirical correlation with its theoretically expected value.

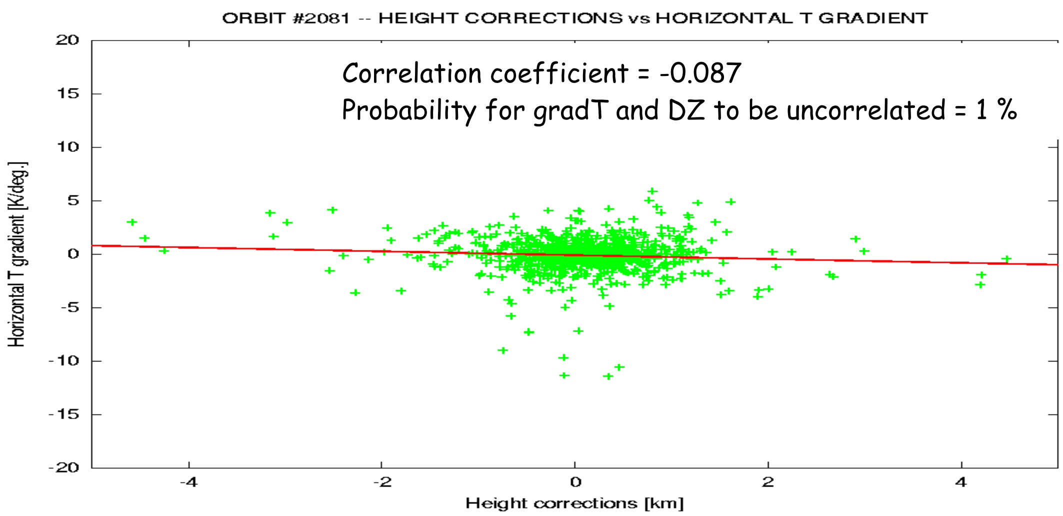

Fig. 1: scatter plot correlating tangent height corrections and absolute temperature gradients.

Conclusion

The assumption of "vertical" profiles is justified and does not have significant impact on the accuracy of retrieved tangent altitude corrections.

4.6 Verification of error in the VMR profiles of interfering speciess

Ref. [RD5]: Sect. 4.2.4; Ref. [RD9]: Sheet MIP_MV_2_4

Introduction

ORM first performs the retrieval of pressure and temperature, then the VMRs of the target speciess in sequence. This means that in each retrieval the VMR of the interfering speciess, i.e. the speciess whose VMR is not fitted in the current retrieval, are assumed as known, acting as a systematic error source. In particular, tests have shown that a "wrong" H_2O profile may cause problems in the p,T retrieval.

Procedure and results

To assess the impact of the assumed H_2O profile on the p,T retrieval the following procedure was followed:

1. For each sequence, the p,T and H_2O retrievals have been performed on orbit 2081 using the initial guess profiles coming from ML2PP processor (iteration 0) with no cloud detection
2. The retrieved profiles have been used as initial guess in a new retrieval
3. The loop has been repeated until the retrieved profiles were consistent (within their error) with the profiles at the previous step.

The retrievals have been performed using version 3 of the settings. The maximum number of these loops has been set to 9 in order to limit the computing time.
The attached plots report the results of this test. The maps (figs 1 and 2) report the absolute differences between the profiles obtained in the first p,T + H_2O loop and the ones obtained at the last iterations, normalized to the esd of the retrievals. The number of needed iterations to reach convergence for each measured sequence is plotted in figure 3.
A part few exceptions, consistent profiles have been found after 2 p,T+H_2O loops. This means that, on average, the loops have to be repeated at least once per sequence in order to reach stable results.
This instability may be explained by either the use in the retrievals of a wrong initial guess profiles or by the fact that the adopted convergence criteria are too "weak".
In order to check if the reported behaviour was due to 'weak' convergence criteria, the test was repeated using IG of ML2PP with cloud detection and forcing each p,T and H_2O retrievals to perform always 10 Gauss Newton iterations. The results of this test (plotted in fig. 4) showed that in the majority of cases consistent results are now obtained after the first loop.
This means that in general there is no need for a p,T + H_2O loop if true convergence has been reached. However, the loop is useful if one of the two retrievals did not reach convergence.

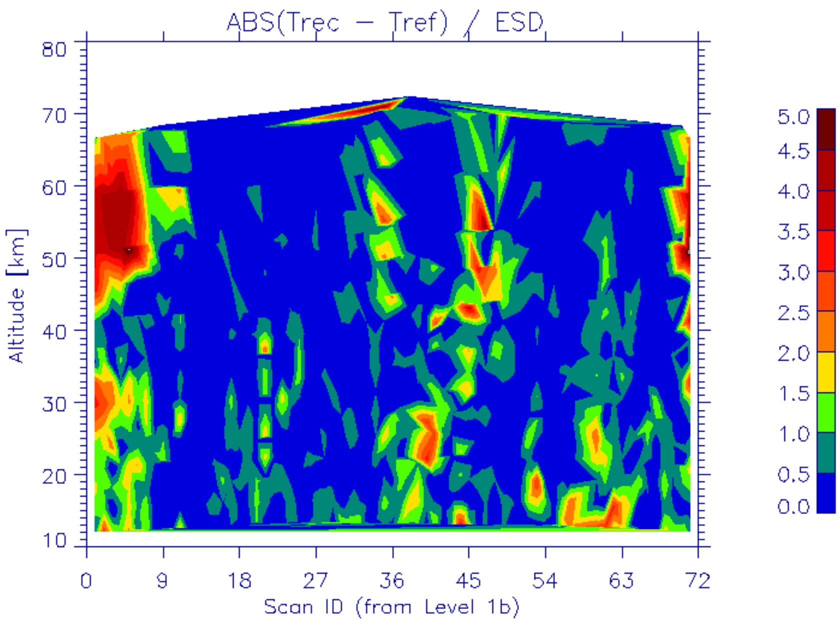

Figure 1 Comparison between Temperature profiles obtained with and without performig p,T + H_2O loops

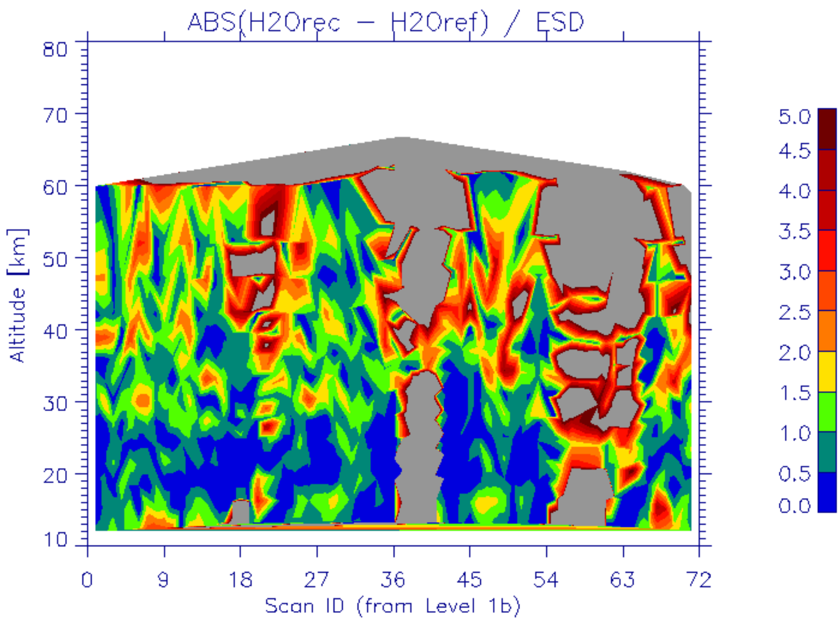

Figure 2 Comparison between Water profiles obtained with and without performig p,T + H_2O loops

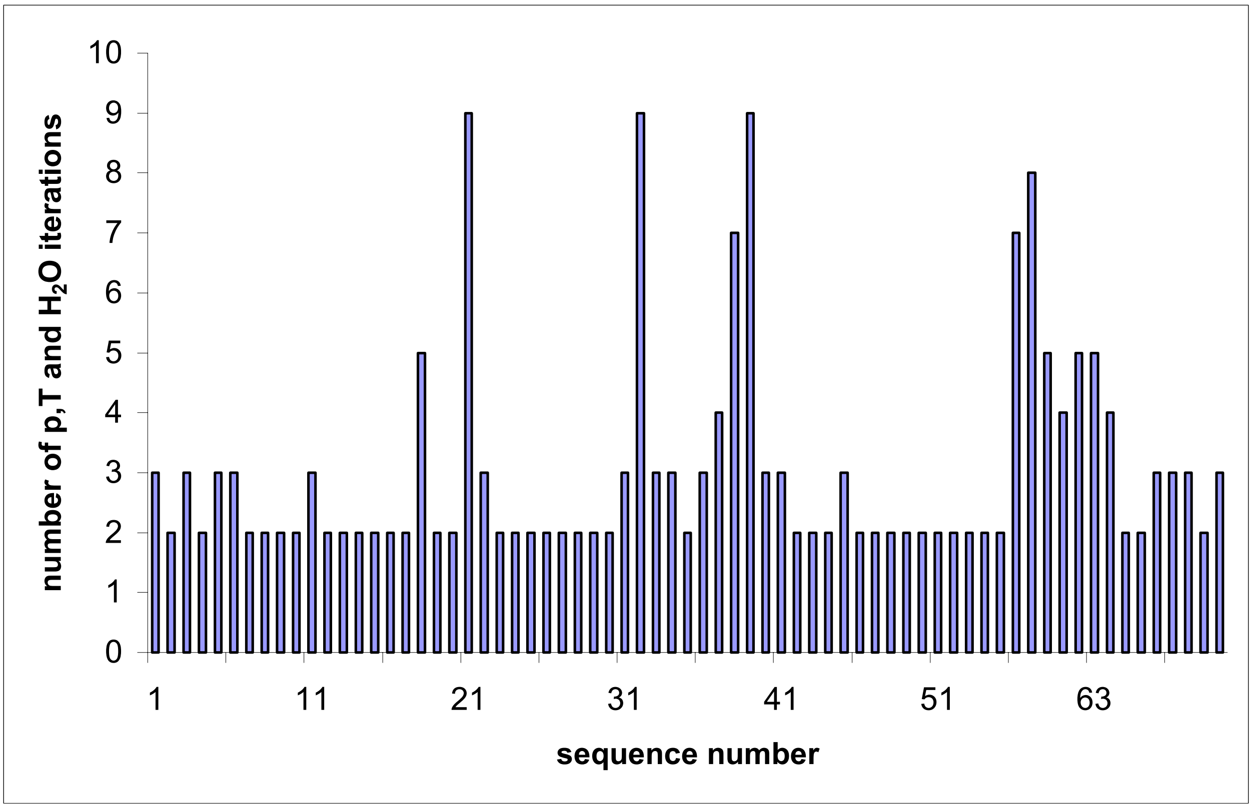

Figure 3 Number of p,T + H_2O loops needed to reach consistent profiles in case of convergence criteria as in settings version 3

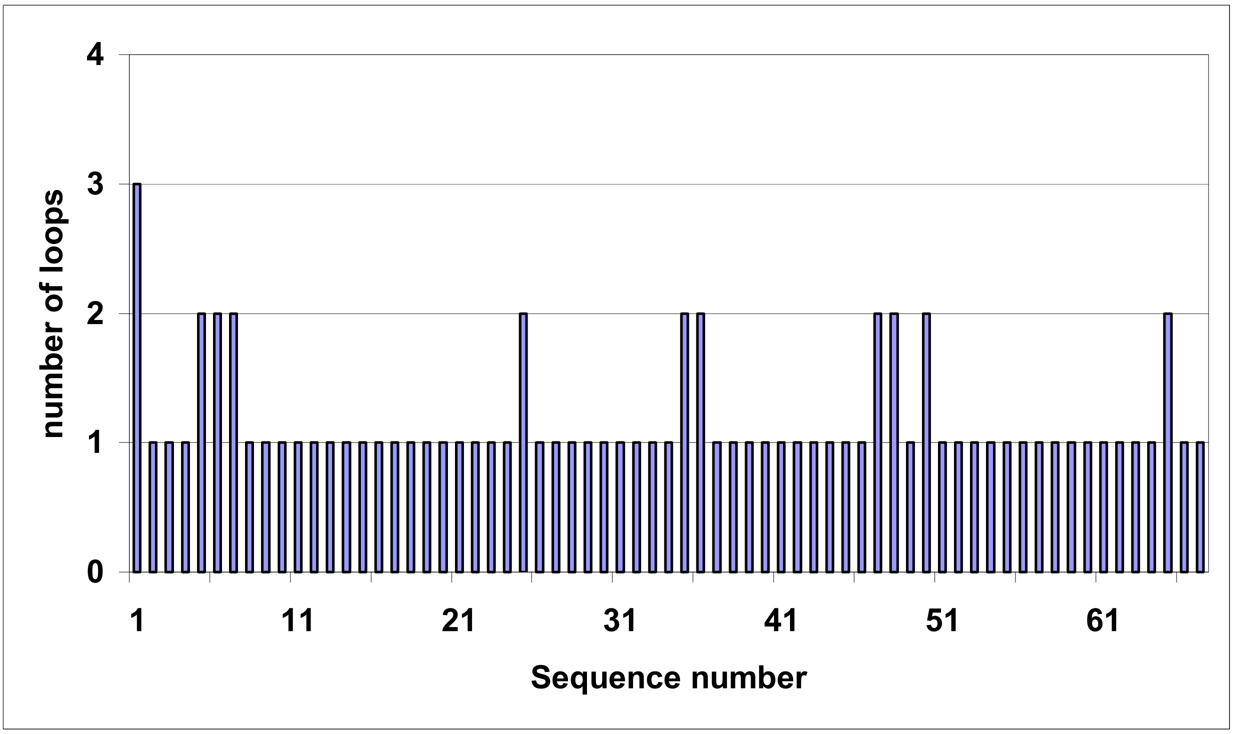

Figure 4 Number of p,T + H_2O loops needed to reach consistent profiles in case of 10 Gauss Newton iterations forced in each retrieval

Conclusions

We recommend to use strong convergence criteria and implement p,T + H_2O loops to help ORM cope with p,T retrievals that do not converge

4.7 Verification of the assumptions related to the line-mixing for CO_2 Q-branches

Ref. [RD5]: Sect. 4.2.6; Ref. [RD9]: Sheet MIP_MV_10

Introduction

Line mixing corresponds to the deviation of measured line shape from the Voigt function. This effect occurs when collisions between a radiating molecule and the broadening gas molecules cause the transfer of population between rotational-vibrational states. Line mixing affects especially the Q-branches where transitions between rotational-vibrational energy levels closer than K_BT (K_B is the Boltzmann constant, T is the temperature) are packed together. The most apparent effect of line-mixing is a reduction of the cross-section in the wings of the branch. The impact of line-mixing effects, mainly significant for CO_2 lines, is reduced in ORM by using an appropriate selection of microwindows.

Description of the test

By inspection of the CO_2 line mixing error spectra provided by the University of Oxford four spectral ranges (in the range measured by MIPAS) have been found where the error introduced by ignoring line mixing can be significant:

708 cm^{-1} – 768 cm^{-1}
780 cm^{-1} – 804 cm^{-1}
1905 cm^{-1} – 1964 cm^{-1}
2047 cm^{-1} – 2160 cm^{-1}

In the nominal occupation matrix used by ORM there are four microwindows inside the spectral ranges written above:

PT0004	728.300 cm^{-1} – 729.125 cm^{-1}
PT0006	741.975 cm^{-1} – 742.250 cm^{-1}
PT0002	791.375 cm^{-1} – 792.875 cm^{-1}
O30021	763.375 cm^{-1} – 766.375 cm^{-1}

The averaged residuals corresponding to the microwindows indicated above have been compared with the random error (NESR) and with the CO_2 line mixing error spectra.

Results

In the following pages three figures are shown for each microwindow at a few relevant altitudes. The top figure shows the averages on all orbit of the spectra observed and simulated. The middle figure shows the averages of the residuals with the random error (NESR of the average). The bottom figure shows the CO_2 line mixing error spectra corresponding to the microwindows indicated above. The triangles indicate the points used by ORM for the retrieval.

PT0004 15 km

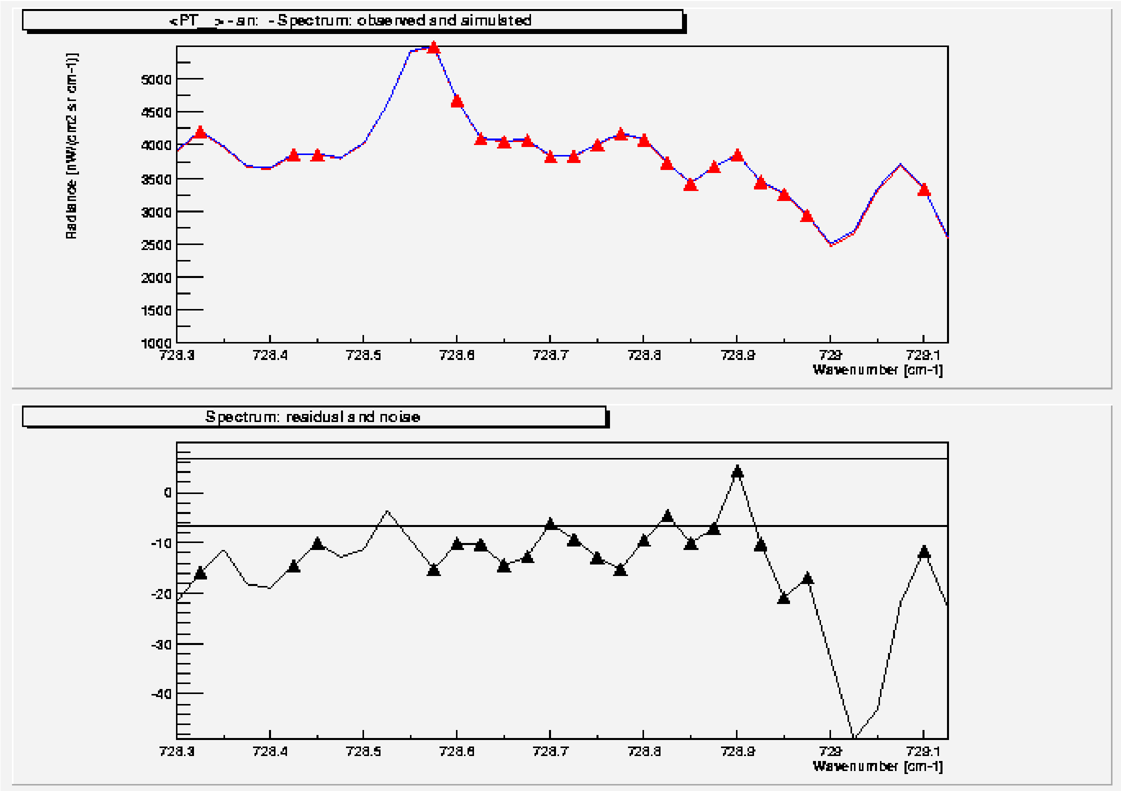
<PT__>-an: -Spectrum: observed and simulated
Radiance [nW/(cm2 sr cm-1)]
Wavenumber [cm-1]
Spectrum: residual and noise
Wavenumber [cm-1]

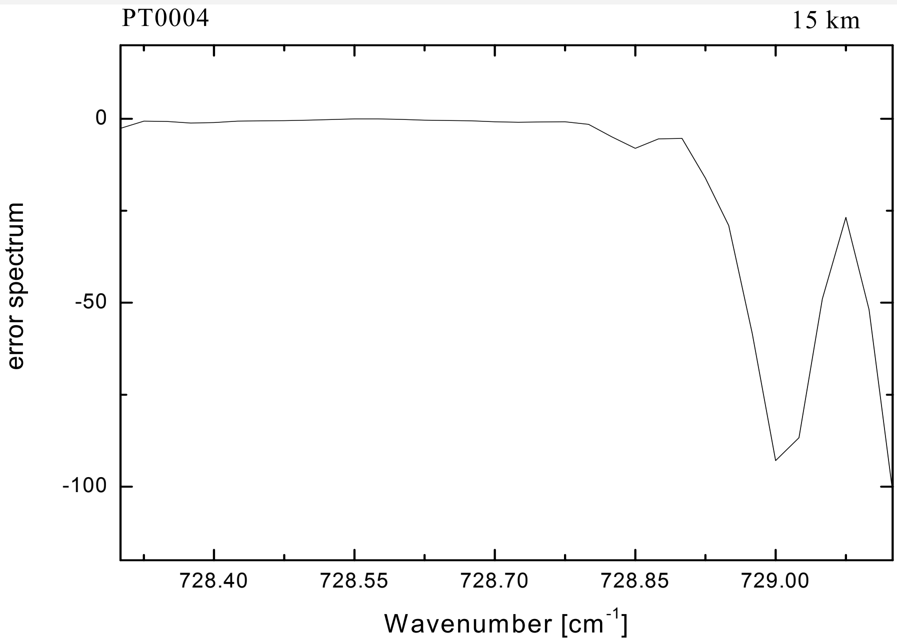
PT0004
15 km
error spectrum
Wavenumber [cm-1]

PT0004 18 km

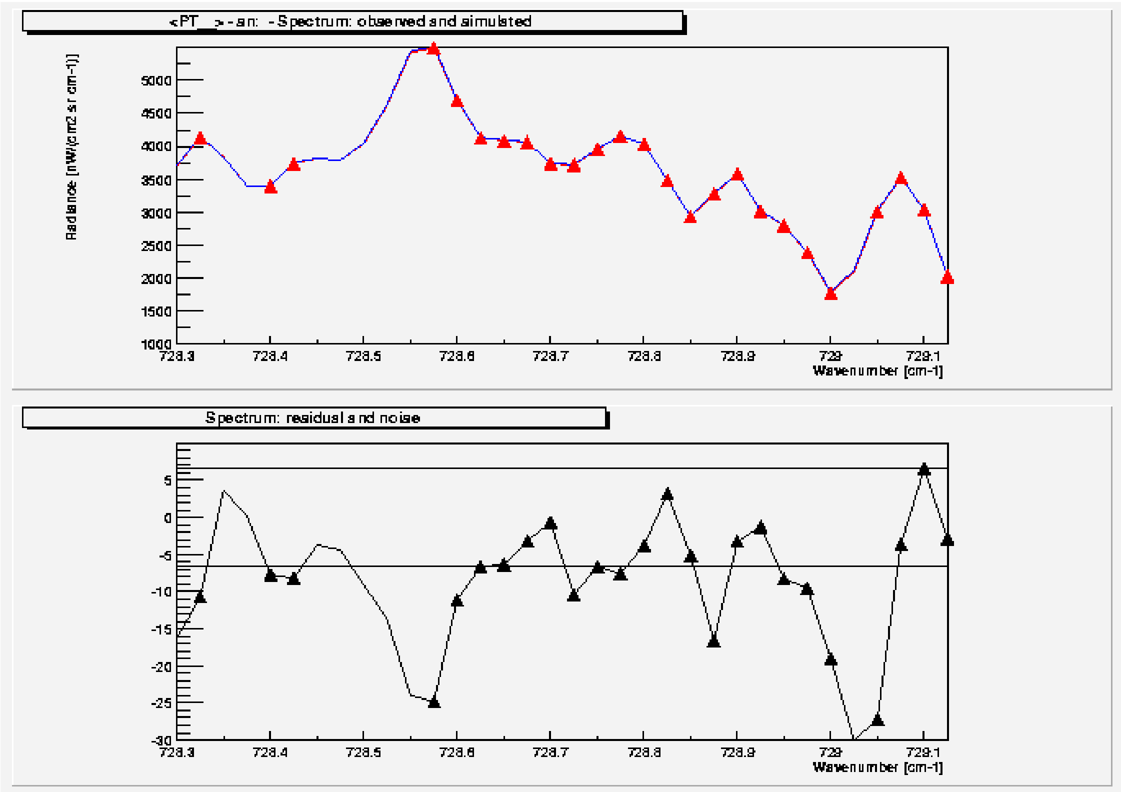
Spectrum: observed and simulated
Radiance [nW/(cm2 sr cm-1)]
Wavenumber [cm-1]
Spectrum: residual and noise
Wavenumber [cm-1]

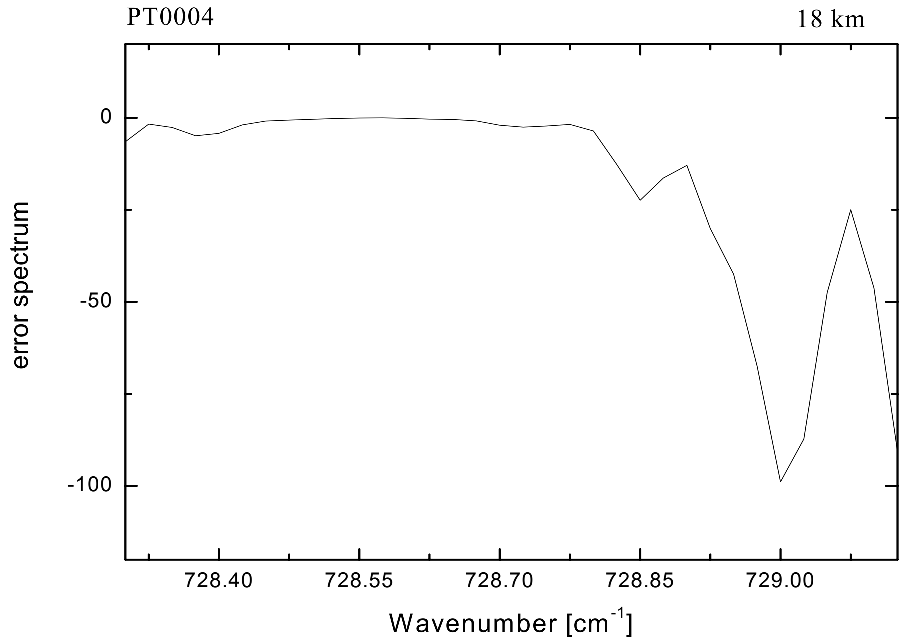
PT0004
18 km
error spectrum
Wavenumber [cm^{-1}]

PT0004 21 km

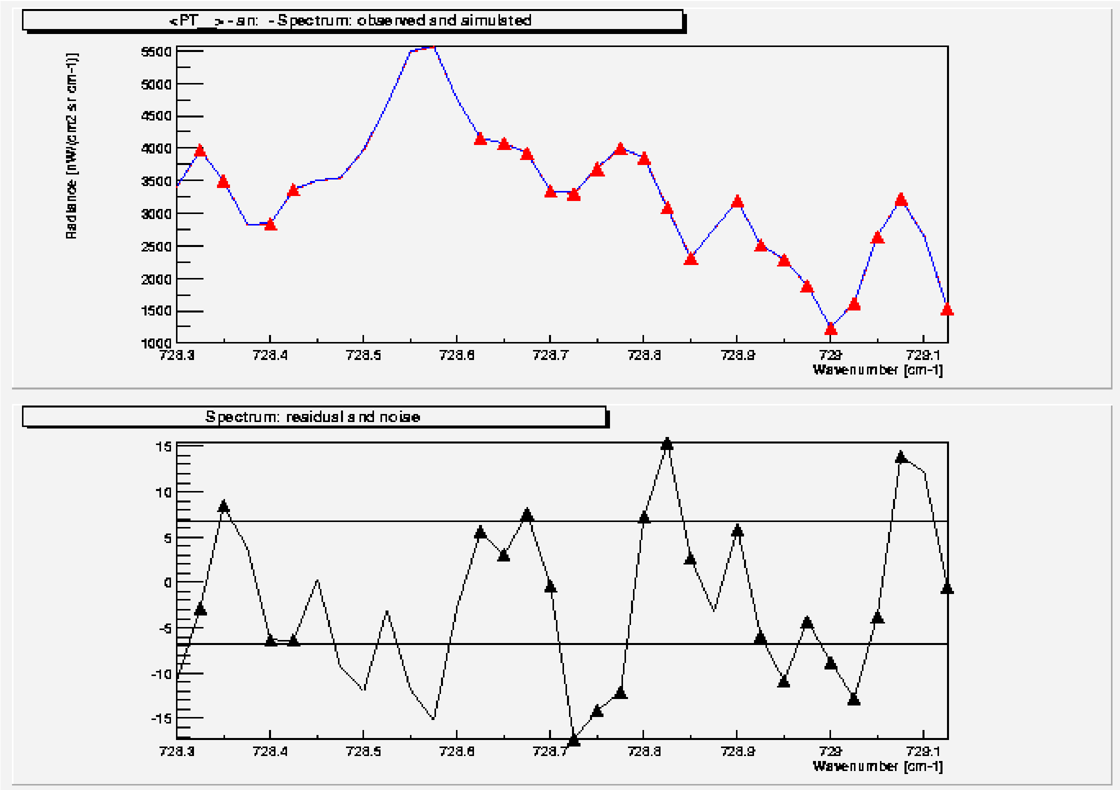
Spectrum: observed and simulated
Radiance [nW/(cm2 sr cm-1)]
Wavenumber [cm-1]
Spectrum: residual and noise
Wavenumber [cm-1]

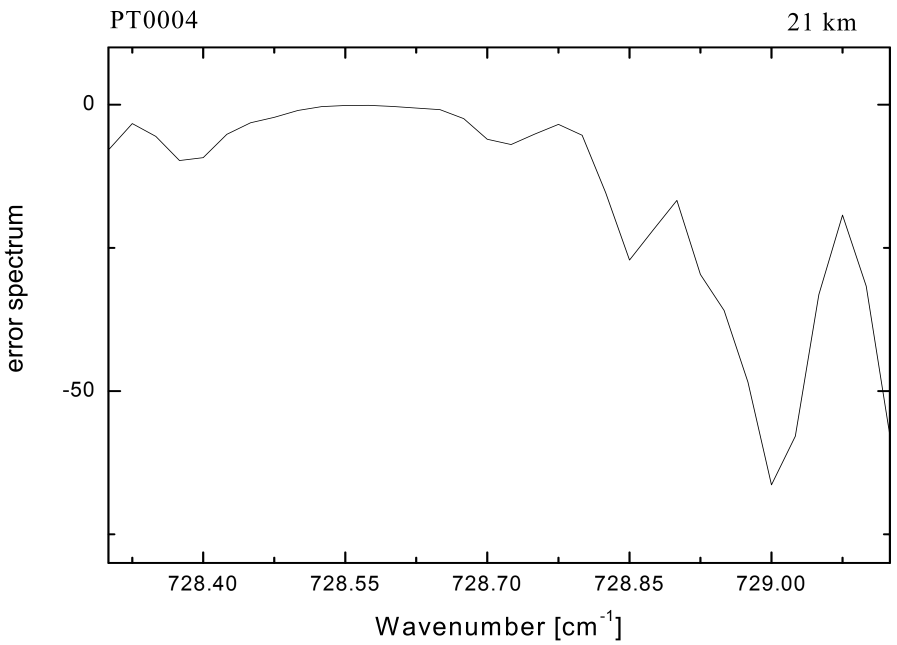
PT0004
21 km
error spectrum
Wavenumber [cm-1]

PT0004 24 km

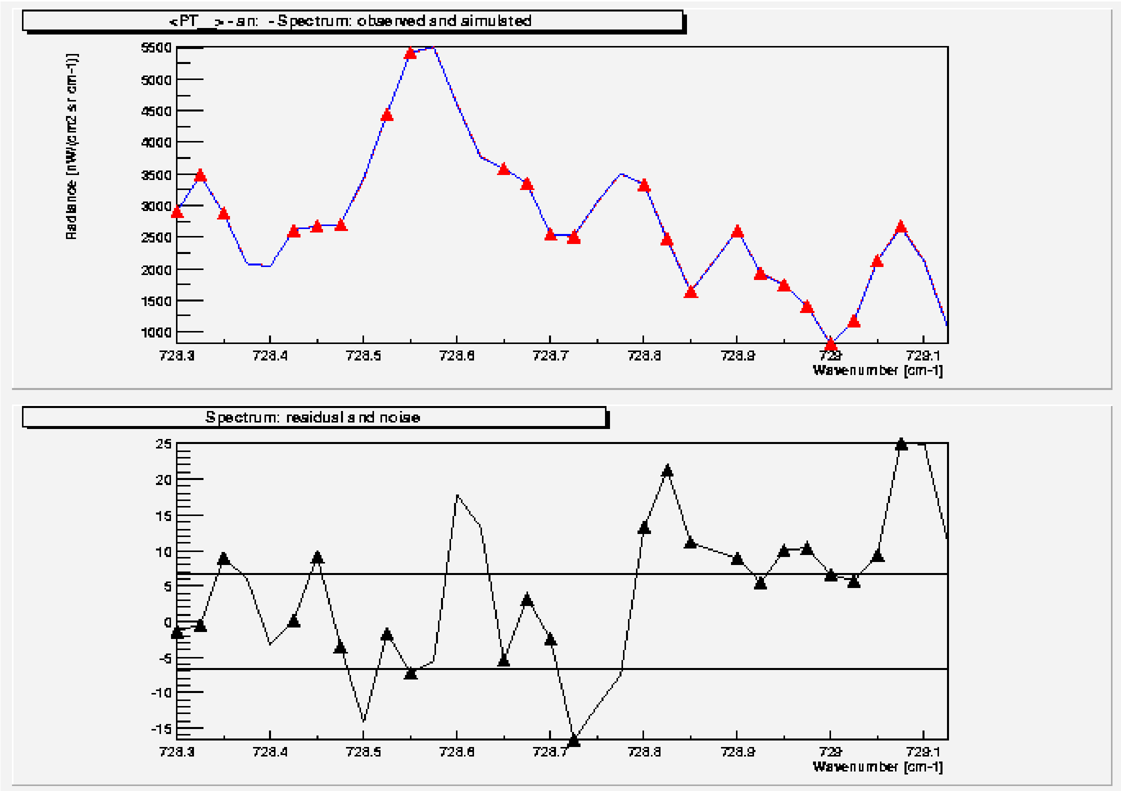
<PT_ >-an: -Spectrum: observed and simulated
Radiance [nW/(cm2 sr cm-1)]
Wavenumber [cm-1]
Spectrum: residuals and noise
Wavenumber [cm-1]

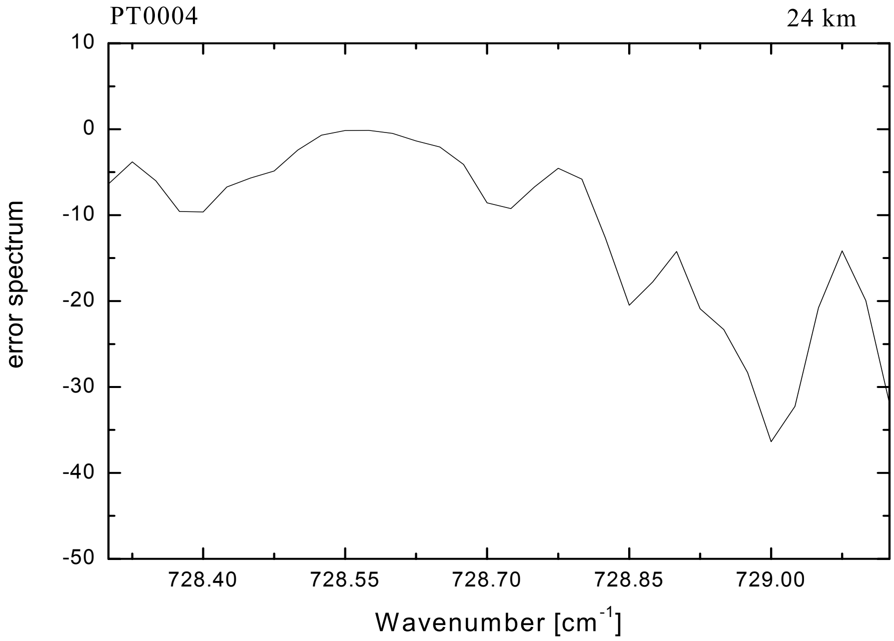
PT0004
24 km
error spectrum
Wavenumber [cm-1]

PT0004 27 km

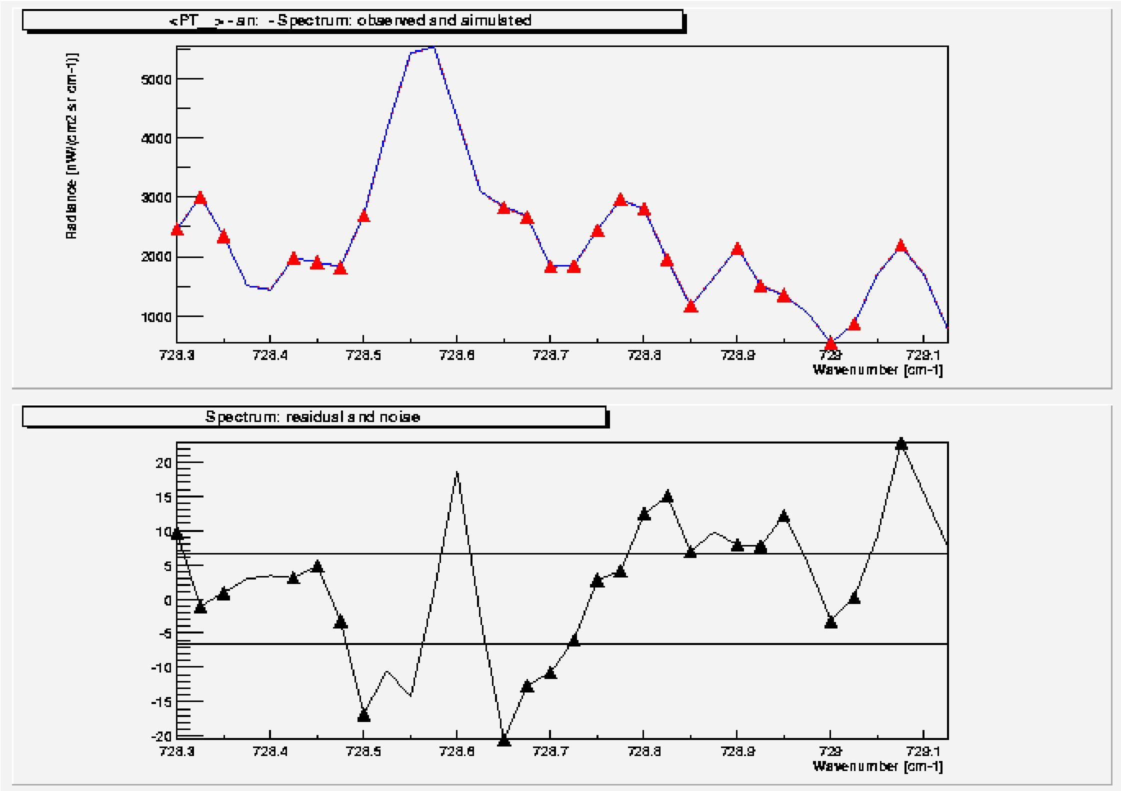
Spectrum: observed and simulated
Radiance [nW/(cm2 sr cm-1)]
Wavenumber [cm-1]
Spectrum: residual and noise
Wavenumber [cm-1]

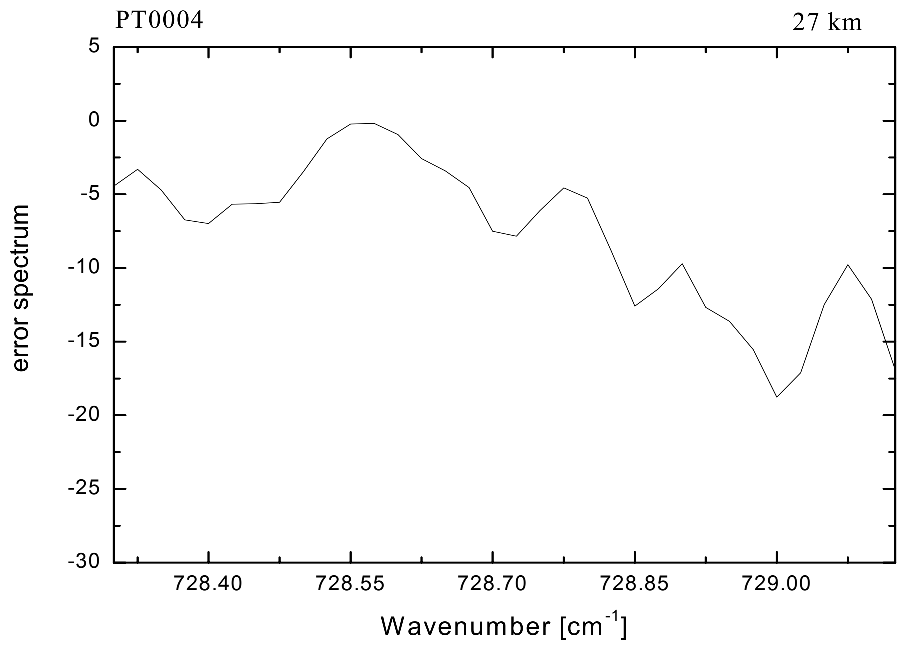
PT0004
27 km
error spectrum
Wavenumber [cm^{-1}]

PT0006 15 km

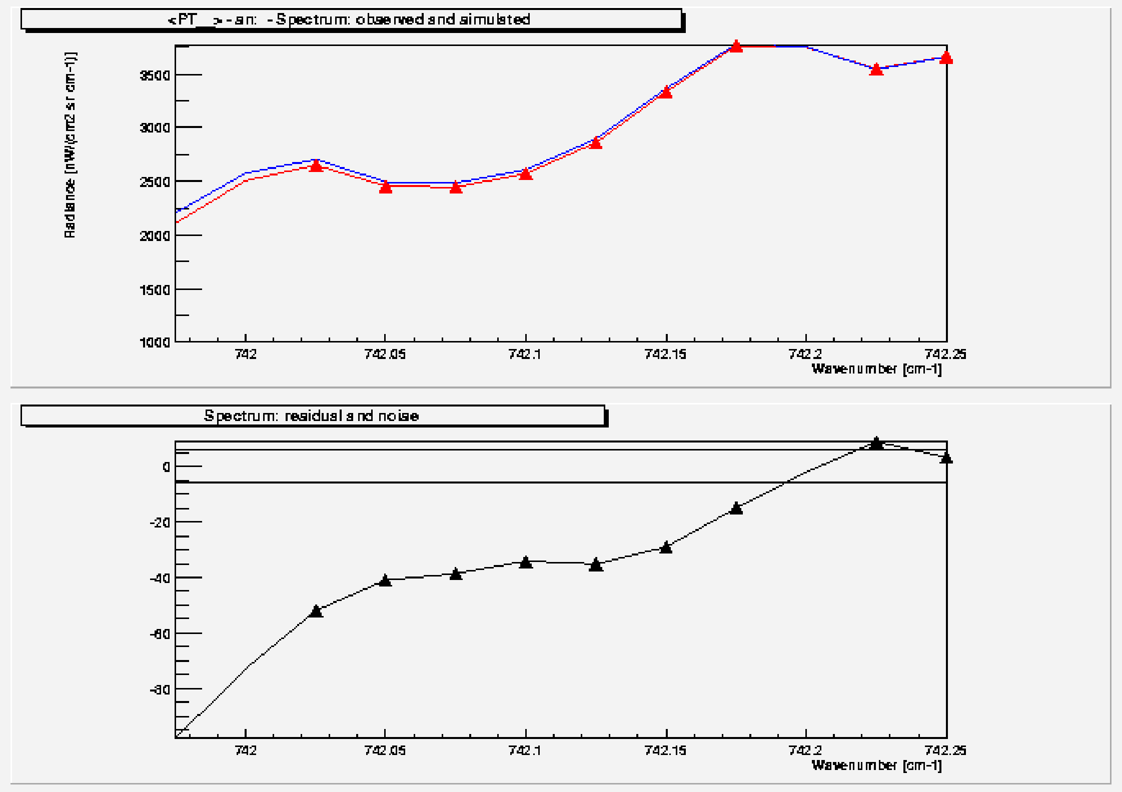
<PT_ >-an: - Spectrum: observed and simulated
Radiance [nW/(cm2 sr cm-1)]
3500
3000
2500
2000
1500
1000
742
742.05
742.1
742.15
742.2
742.25
Wavenumber [cm-1]
Spectrum: residual and noise
0
-20
-40
-60
-80
742
742.05
742.1
742.15
742.2
742.25
Wavenumber [cm-1]

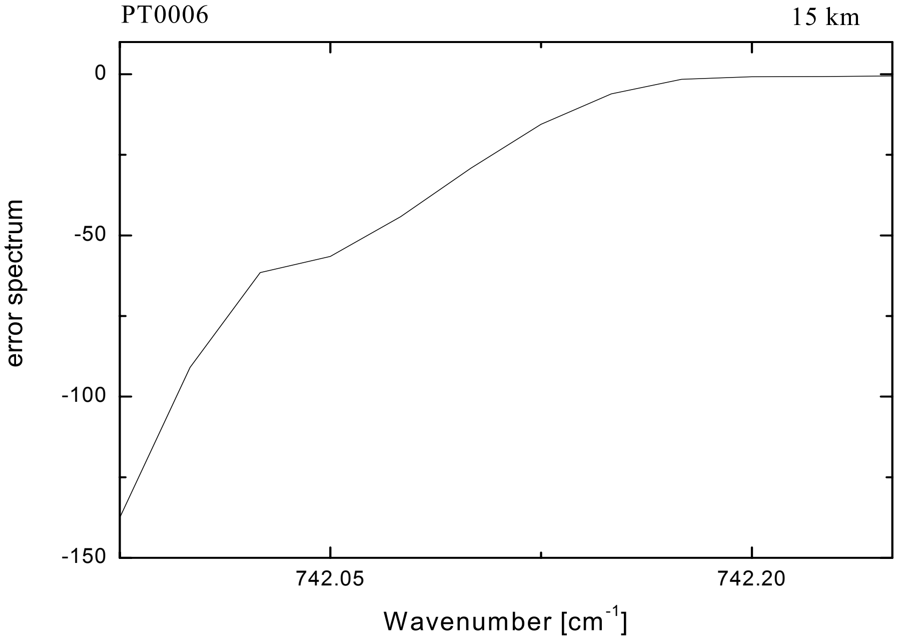
PT0006
15 km
0
-50
-100
-150
error spectrum
742.05
742.20
Wavenumber [cm-1]

PT0006 18 km

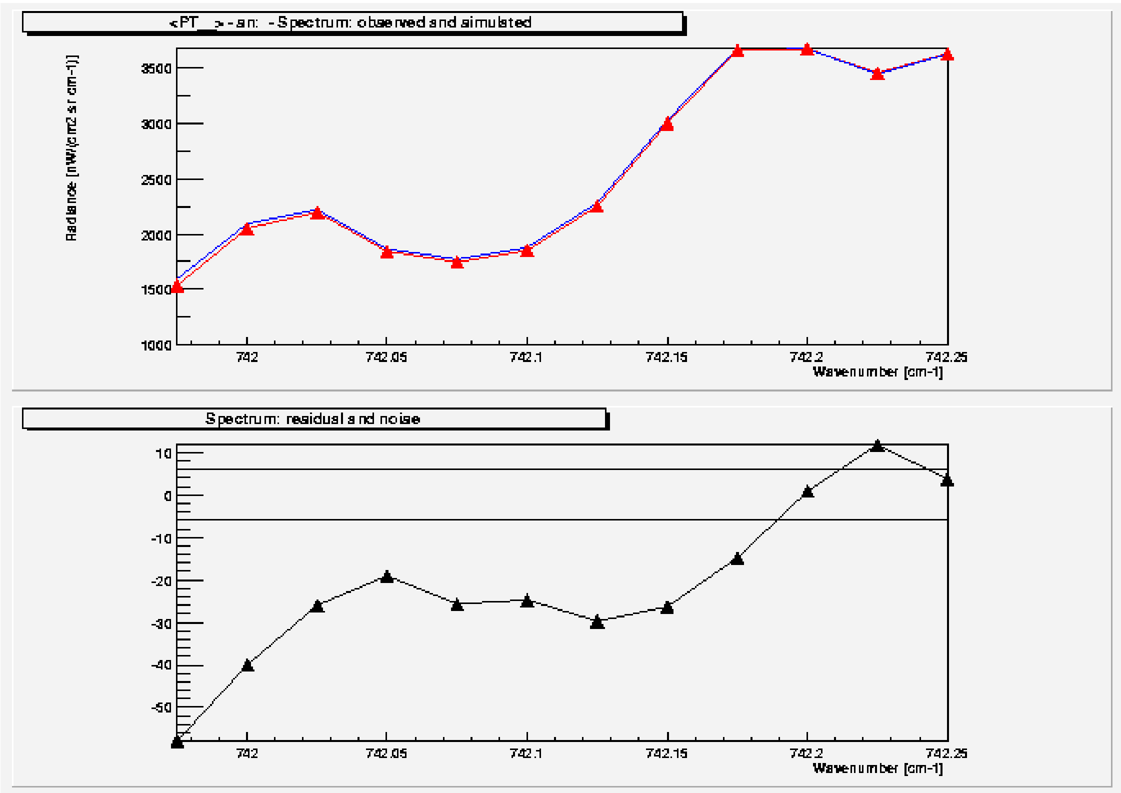
<PT_ > - an: - Spectrum: observed and simulated
Radiance [nW/(cm2 sr cm-1)]
3500
3000
2500
2000
1500
1000
742
742.05
742.1
742.15
742.2
742.25
Wavenumber [cm-1]
Spectrum: residual and noise
10
0
-10
-20
-30
-40
-50
742
742.05
742.1
742.15
742.2
742.25
Wavenumber [cm-1]

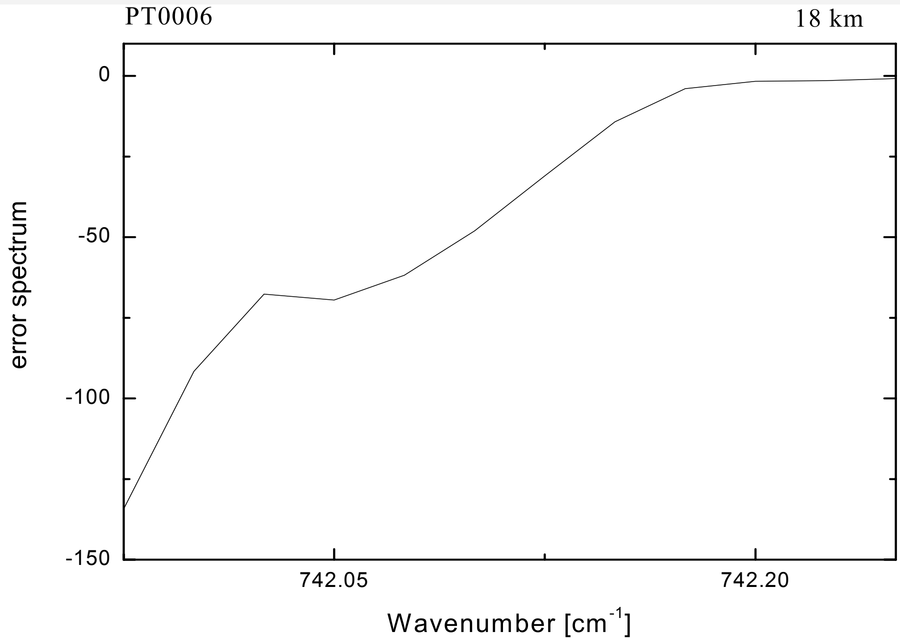
PT0006
18 km
error spectrum
0
-50
-100
-150
742.05
742.20
Wavenumber [cm-1]

PT0006 21 km

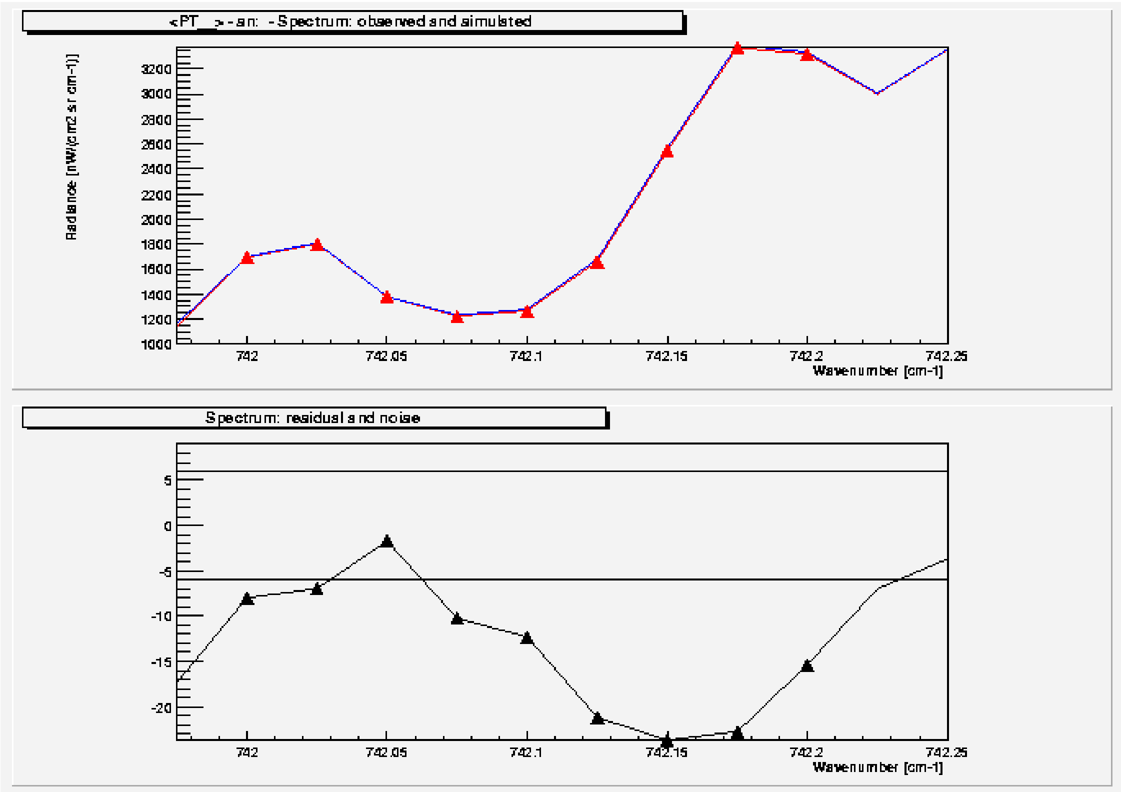
<PT_ _>-an: -Spectrum: observed and simulated
Radiance [nW/(cm2 sr cm-1)]
Wavenumber [cm-1]
Spectrum: residual and noise
Wavenumber [cm-1]

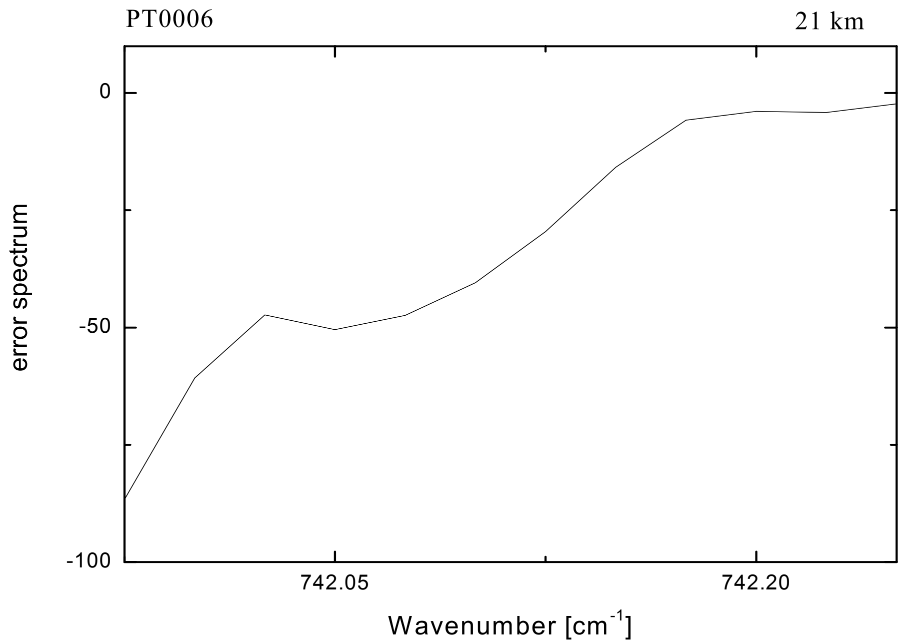
PT0006
21 km
error spectrum
Wavenumber [cm-1]

PT0006 24 km

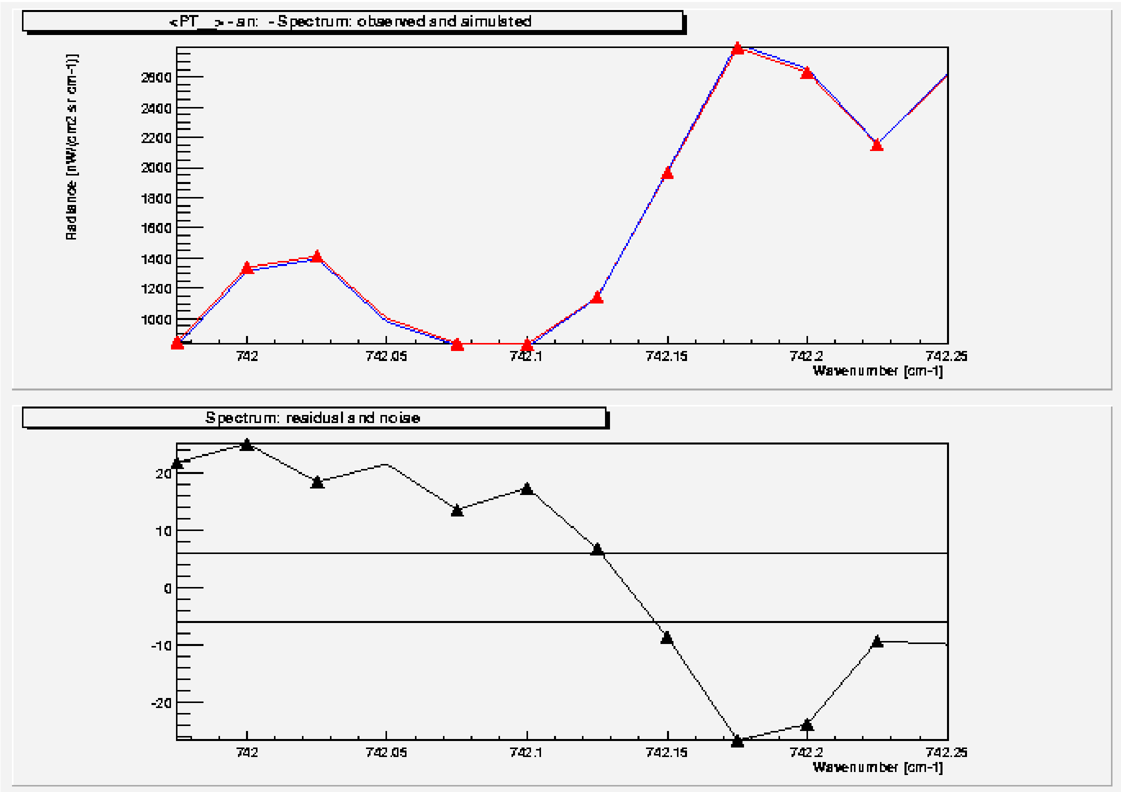
<PT__> - an: - Spectrum: observed and simulated
Radiance [nW/(cm2 sr cm-1)]
2600
2400
2200
2000
1800
1600
1400
1200
1000
742
742.05
742.1
742.15
742.2
742.25
Wavenumber [cm-1]
Spectrum: residual and noise
20
10
0
-10
-20
742
742.05
742.1
742.15
742.2
742.25
Wavenumber [cm-1]

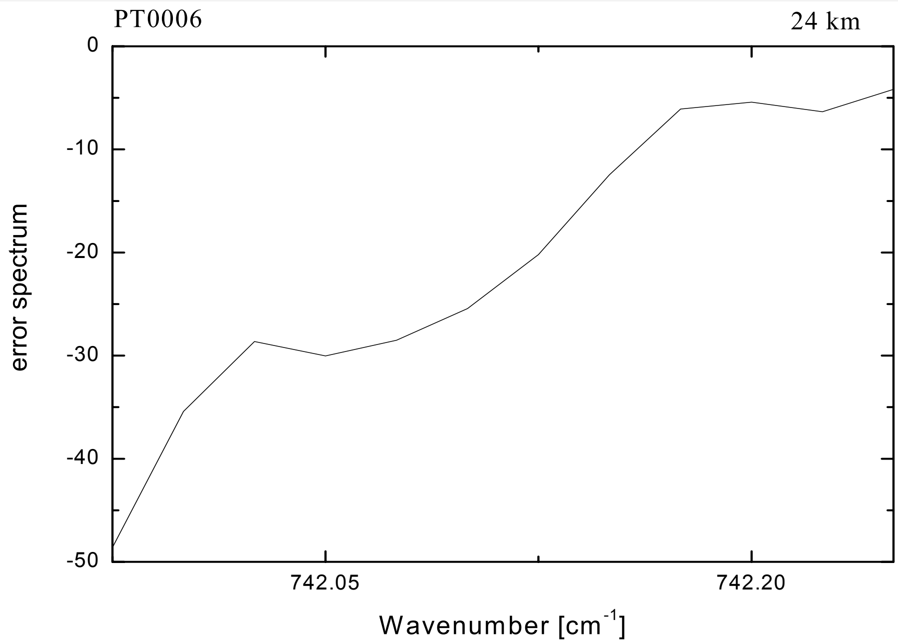
PT0006
24 km
error spectrum
0
-10
-20
-30
-40
-50
742.05
742.20
Wavenumber [cm-1]

PT0002 12 km

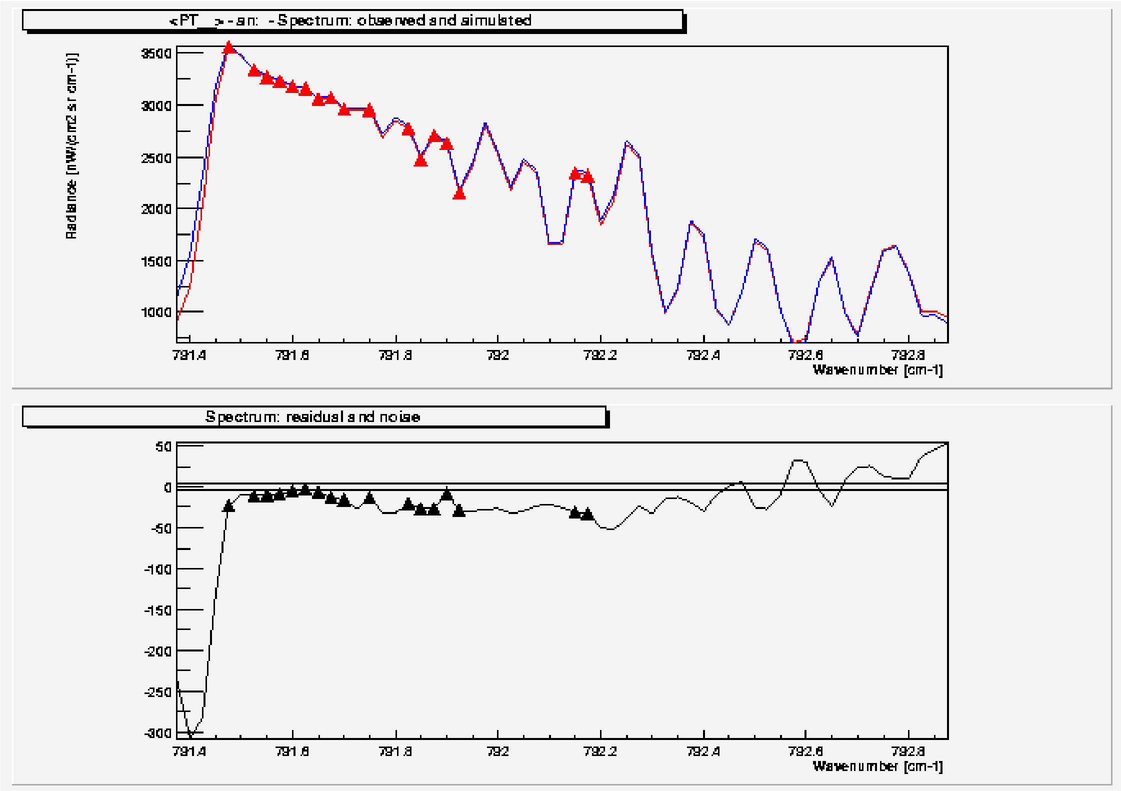
Spectrum: observed and simulated
Radiance [nW/(cm2 sr cm-1)]
3500
3000
2500
2000
1500
1000
791.4
791.6
791.8
792
792.2
792.4
792.6
792.8
Wavenumber [cm-1]
Spectrum: residual and noise
50
0
-50
-100
-150
-200
-250
-300
Wavenumber [cm-1]

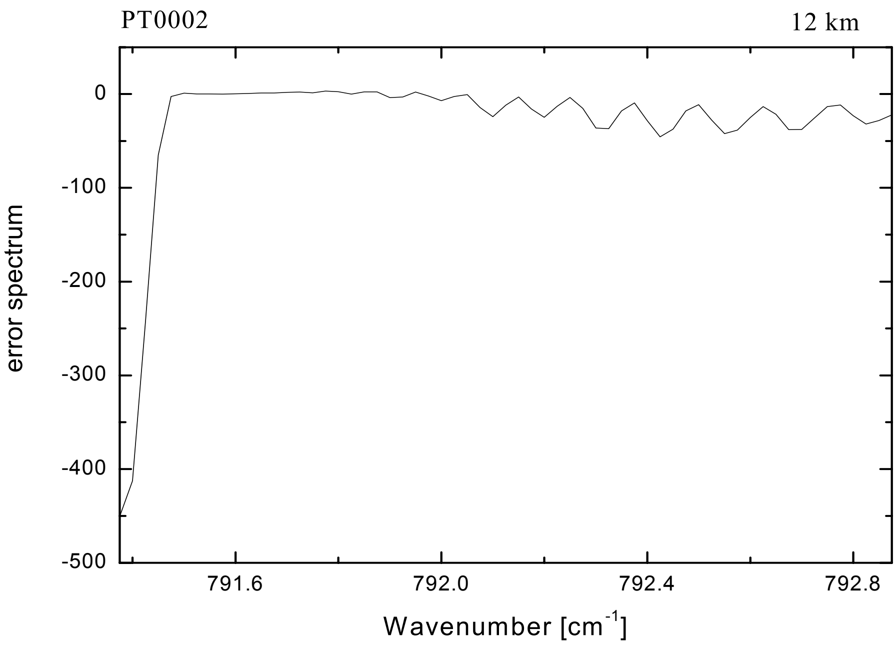
PT0002
12 km
error spectrum
0
-100
-200
-300
-400
-500
791.6
792.0
792.4
792.8
Wavenumber [cm^{-1}]

PT0002 15 km

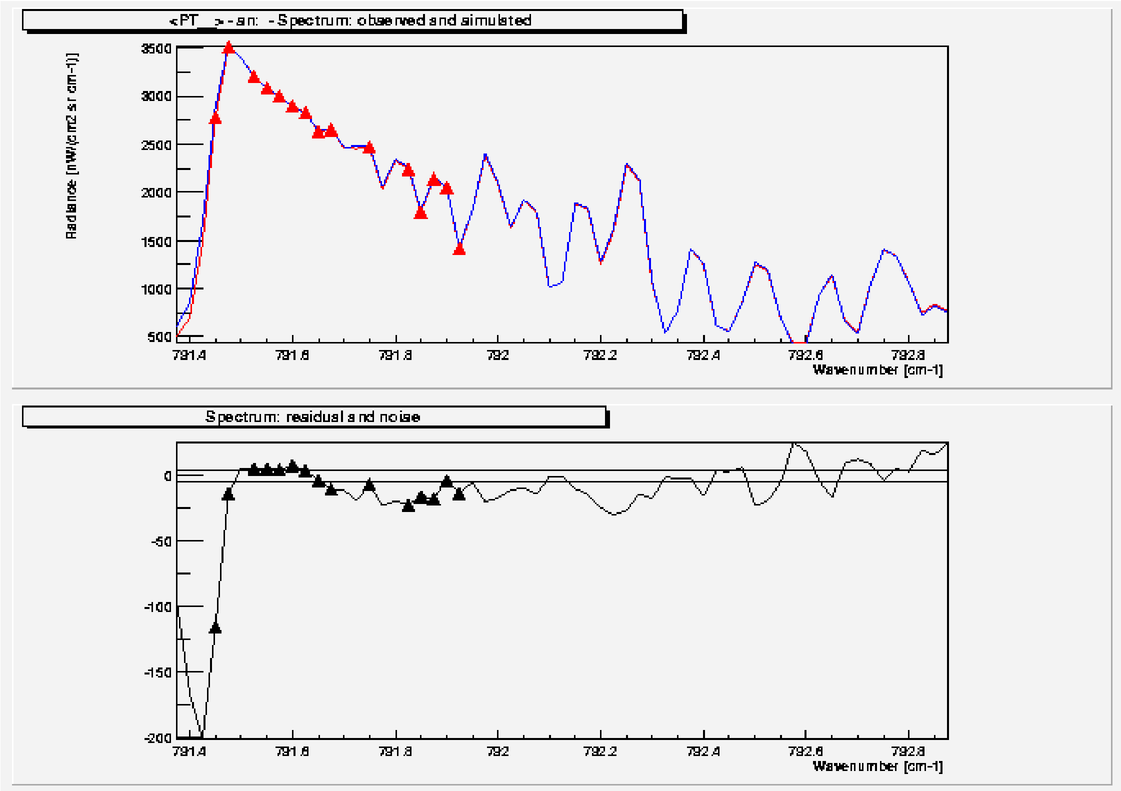

PT0002 15 km

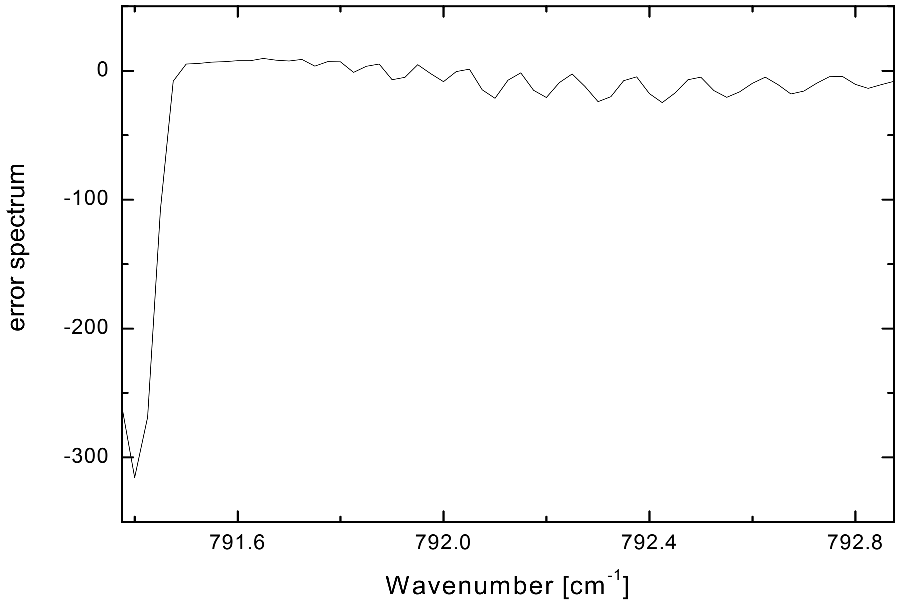

PT0002 18 km

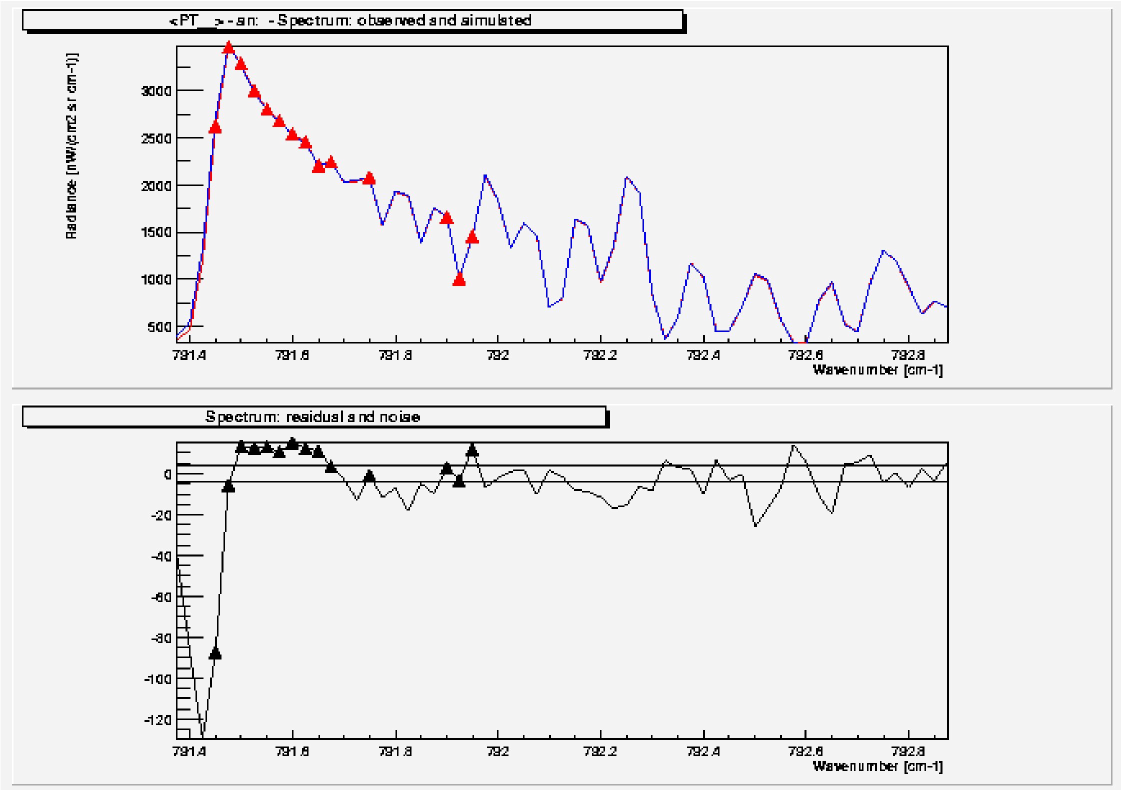
<PT__>-an: -Spectrum: observed and simulated
Radiance [nW/(cm2 sr cm-1)]
3000
2500
2000
1500
1000
500
791.4
791.6
791.8
792
792.2
792.4
792.6
792.8
Wavenumber [cm-1]
Spectrum: residual and noise
0
-20
-40
-60
-80
-100
-120

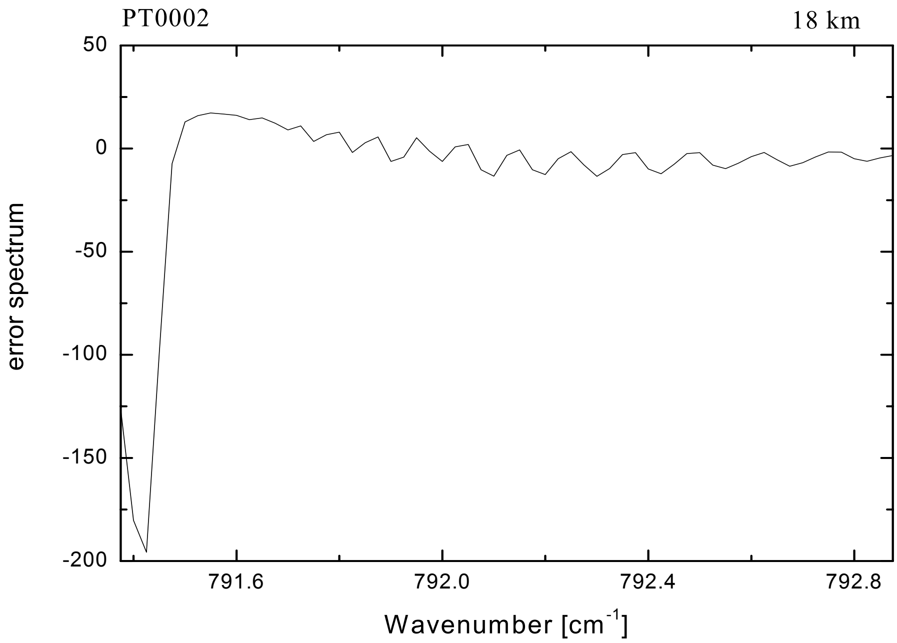
PT0002
18 km
50
0
-50
-100
-150
-200
error spectrum
791.6
792.0
792.4
792.8
Wavenumber [cm^{-1}]

PT0002 21 km

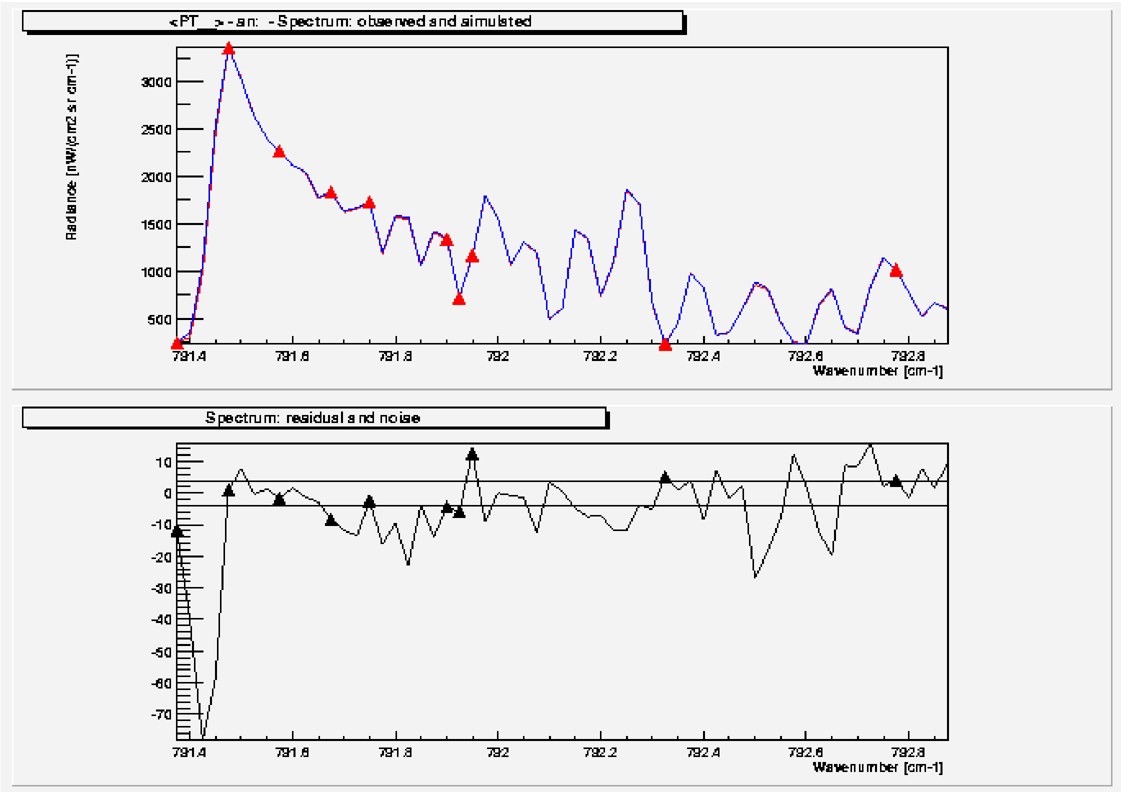
<PT__>-an: -Spectrum: observed and simulated
Radiance [nW/(cm2 sr cm-1)]
3000
2500
2000
1500
1000
500
791.4
791.6
791.8
792
792.2
792.4
792.6
792.8
Wavenumber [cm-1]
Spectrum: residual and noise
10
0
-10
-20
-30
-40
-50
-60
-70
791.4
791.6
791.8
792
792.2
792.4
792.6
792.8
Wavenumber [cm-1]

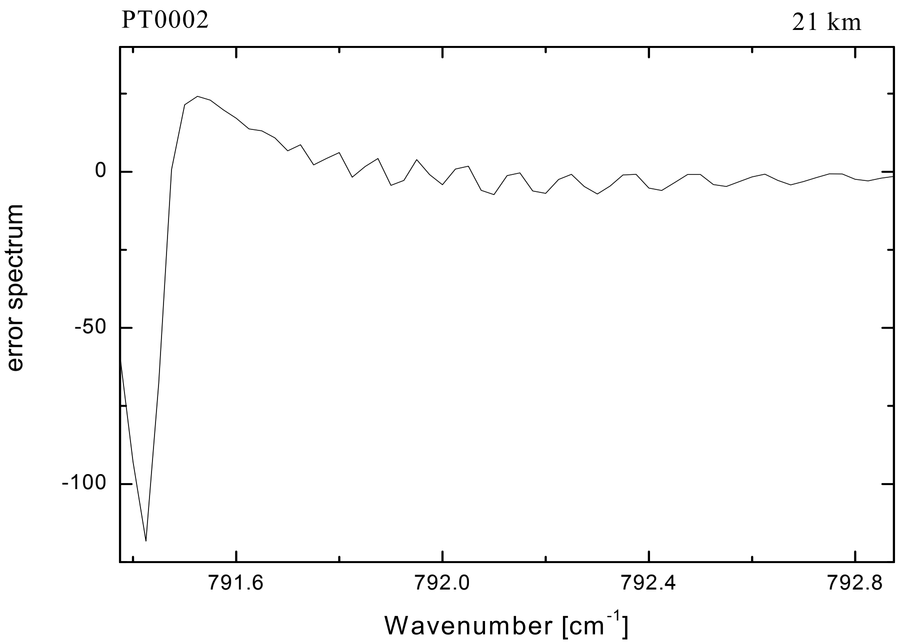
PT0002
21 km
error spectrum
0
-50
-100
791.6
792.0
792.4
792.8
Wavenumber [cm^{-1}]

PT0002 24 km

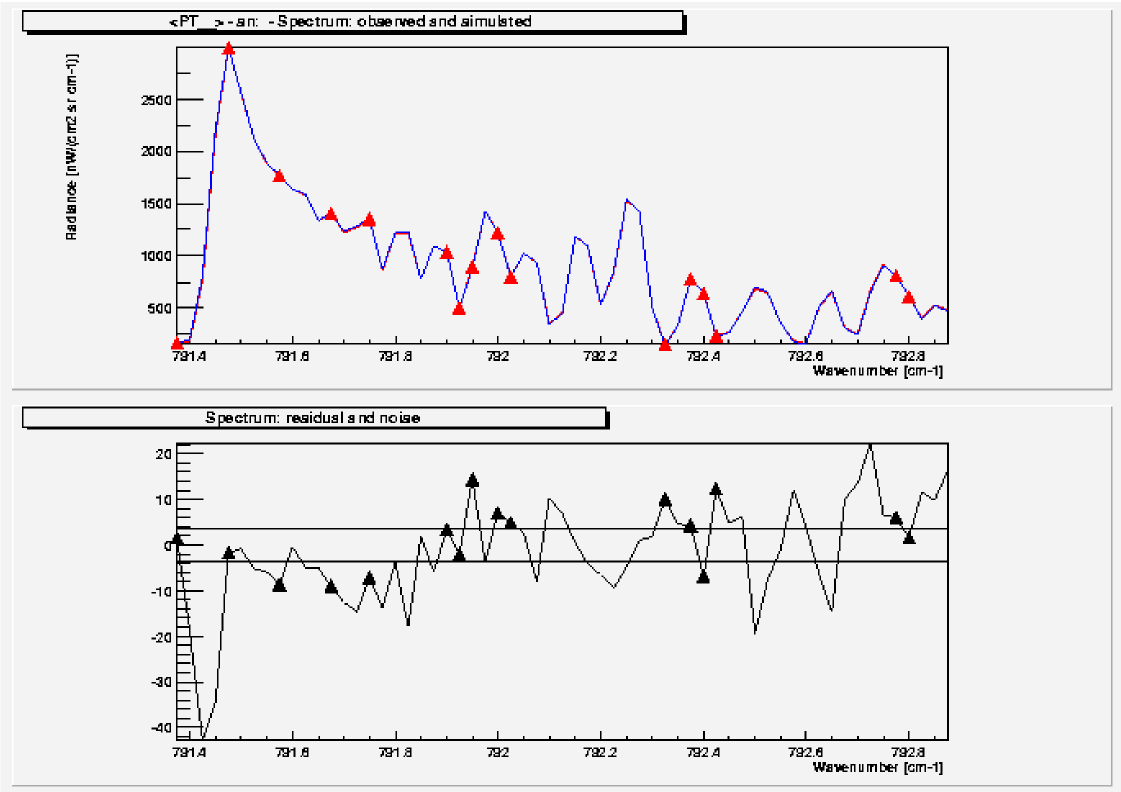
<PT_ >-an: - Spectrum: observed and simulated
Radiance [nW/(cm2 sr cm-1)]
2500
2000
1500
1000
500
791.4
791.6
791.8
792
792.2
792.4
792.6
792.8
Wavenumber [cm-1]
Spectrum: residual and noise
20
10
0
-10
-20
-30
-40
791.4
791.6
791.8
792
792.2
792.4
792.6
792.8
Wavenumber [cm-1]

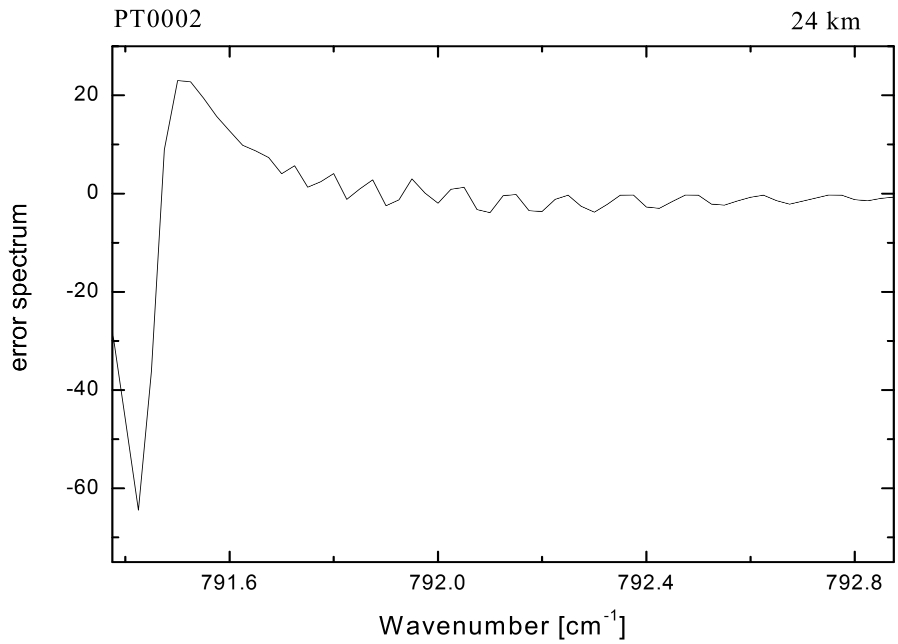
PT0002
24 km
error spectrum
20
0
-20
-40
-60
791.6
792.0
792.4
792.8
Wavenumber [cm-1]

PT0002 27 km

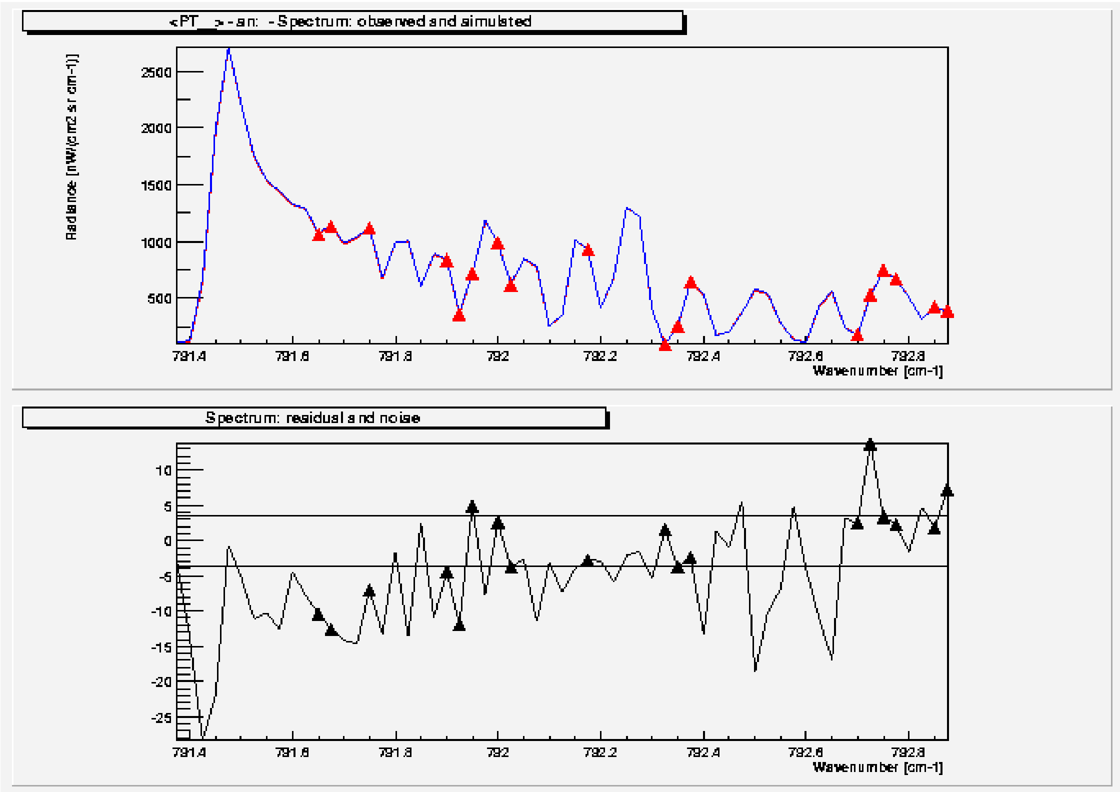
Spectrum: observed and simulated
Radiance [nW/(cm2 sr cm-1)]
Wavenumber [cm-1]
Spectrum: residual and noise
Wavenumber [cm-1]

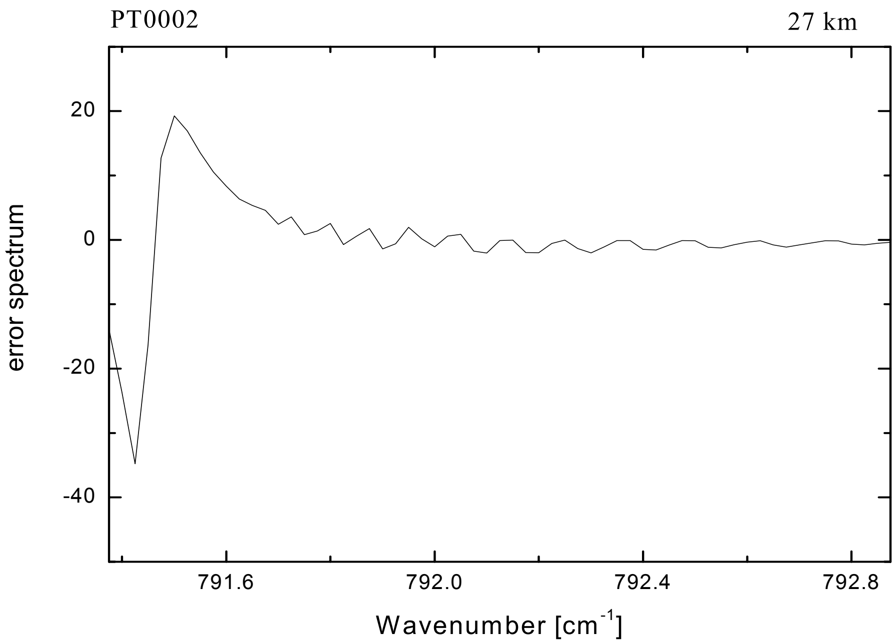
PT0002
27 km
error spectrum
Wavenumber [cm-1]

PT0002 30 km

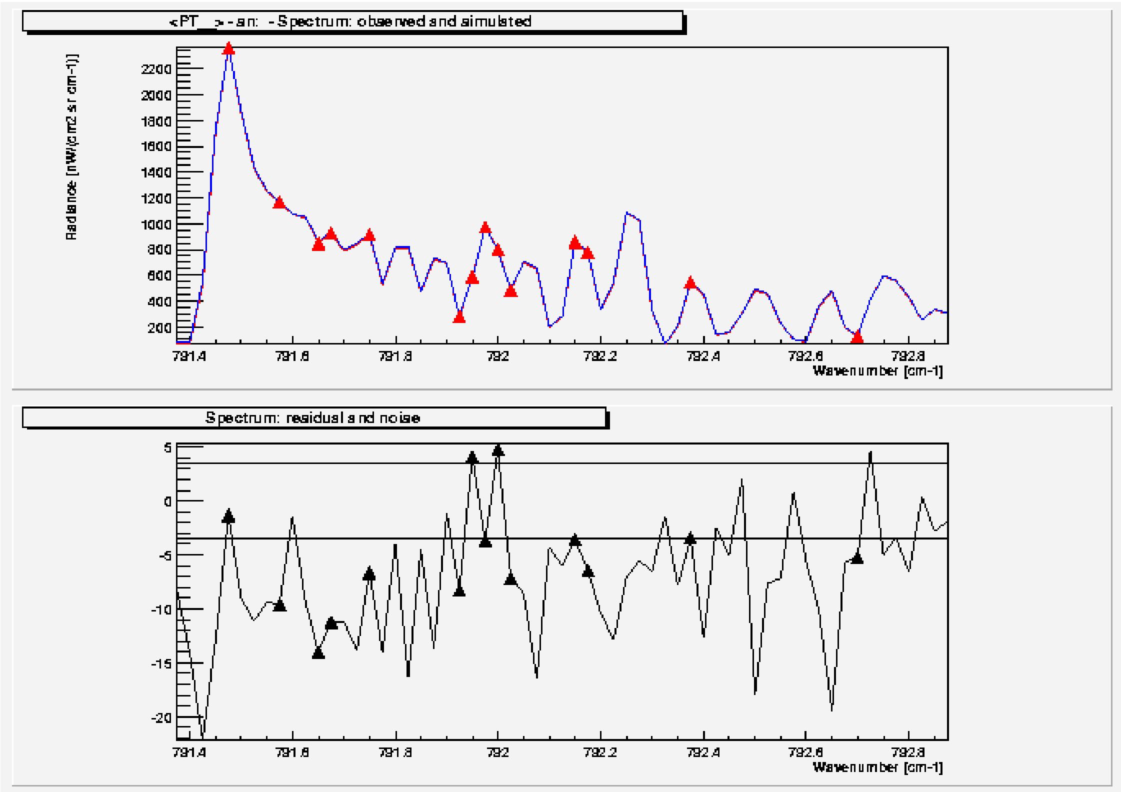
<PT__>-an: -Spectrum: observed and simulated
Radiance [nW/(cm2 sr cm-1)]
Wavenumber [cm-1]
Spectrum: residual and noise
Wavenumber [cm-1]

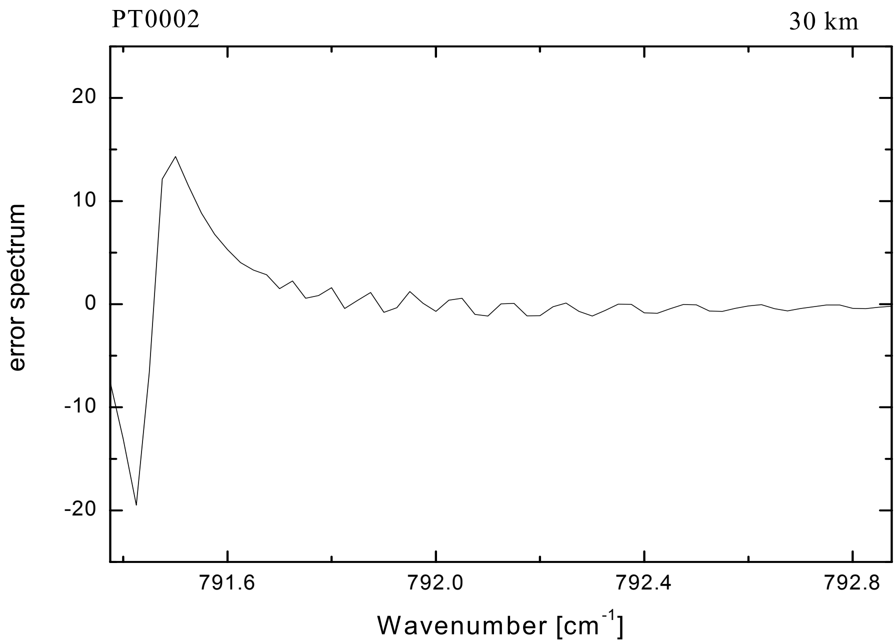
PT0002
30 km
error spectrum
Wavenumber [cm-1]

PT0002 33 km

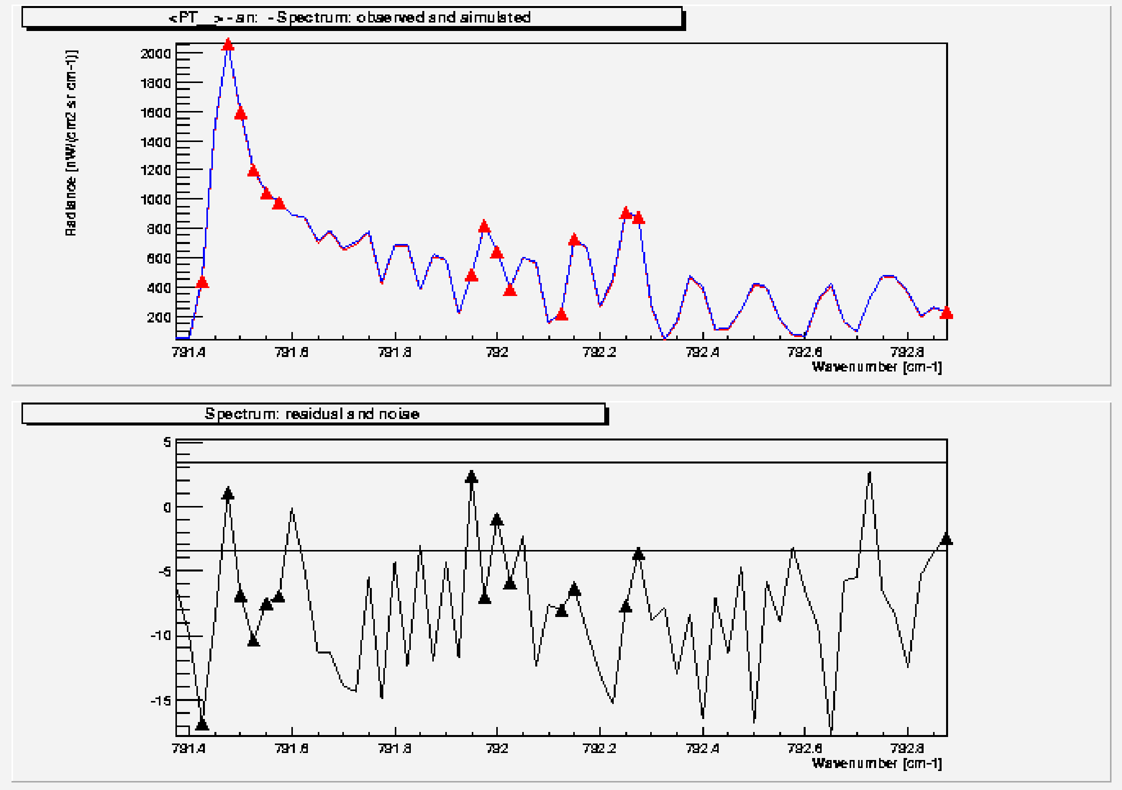
<PT__>-an: -Spectrum: observed and simulated
Radiance [nW/(cm2 sr cm-1)]
2000
1800
1600
1400
1200
1000
800
600
400
200
791.4
791.6
791.8
792
792.2
792.4
792.6
792.8
Wavenumber [cm-1]
Spectrum: residual and noise
5
0
-5
-10
-15
791.4
791.6
791.8
792
792.2
792.4
792.6
792.8
Wavenumber [cm-1]

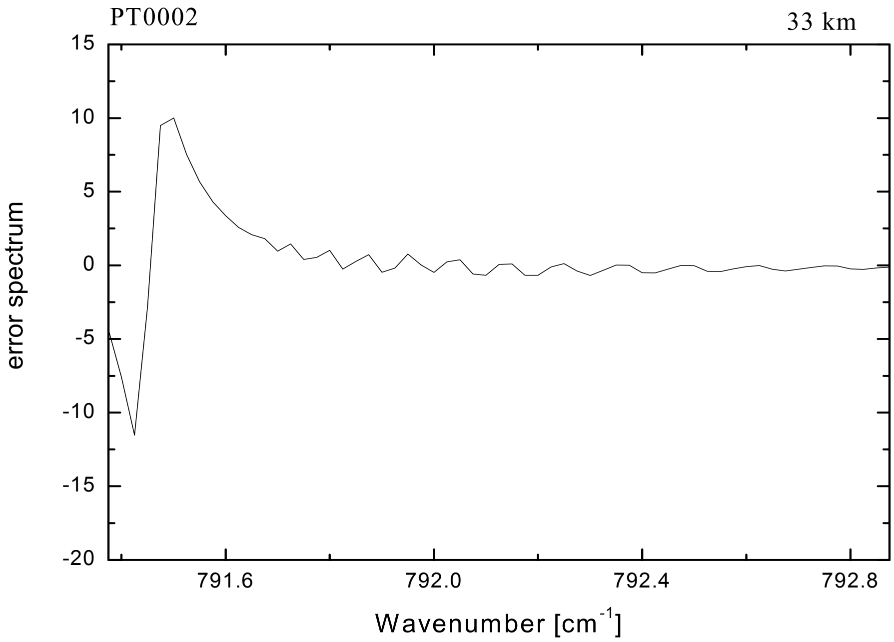
PT0002
33 km
15
10
5
0
-5
-10
-15
-20
error spectrum
791.6
792.0
792.4
792.8
Wavenumber [cm^{-1}]

O30021 12 km

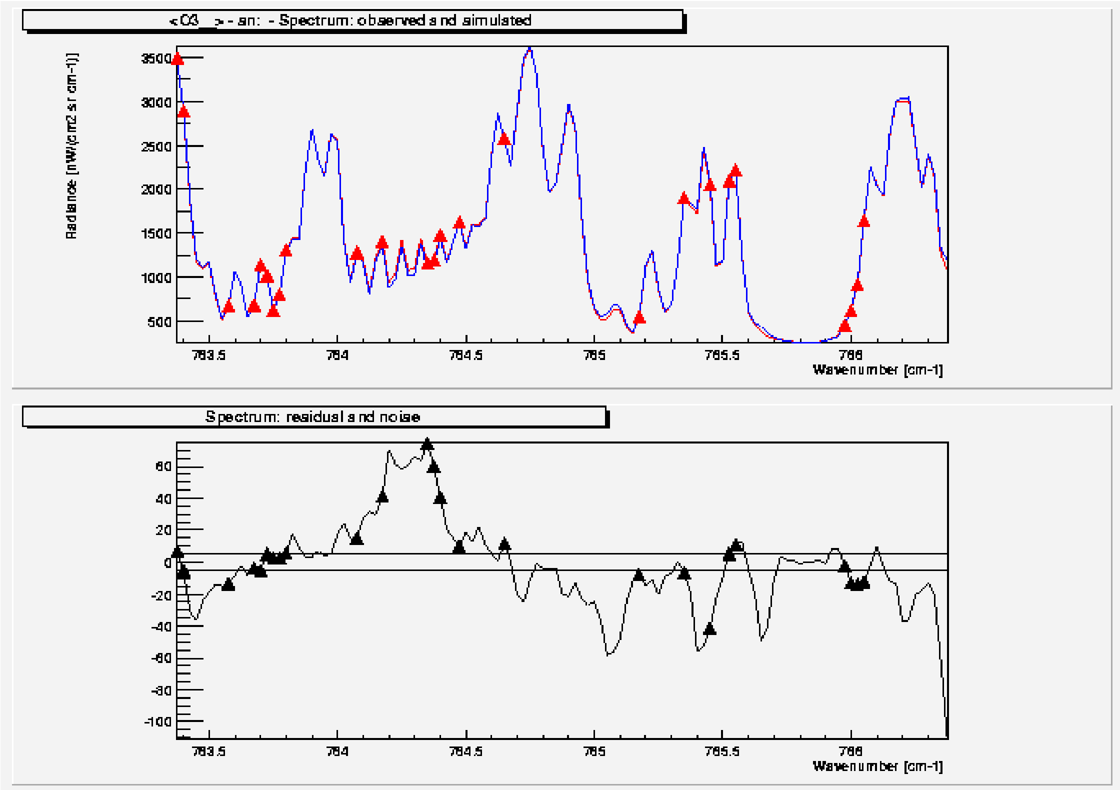

O30021 12 km

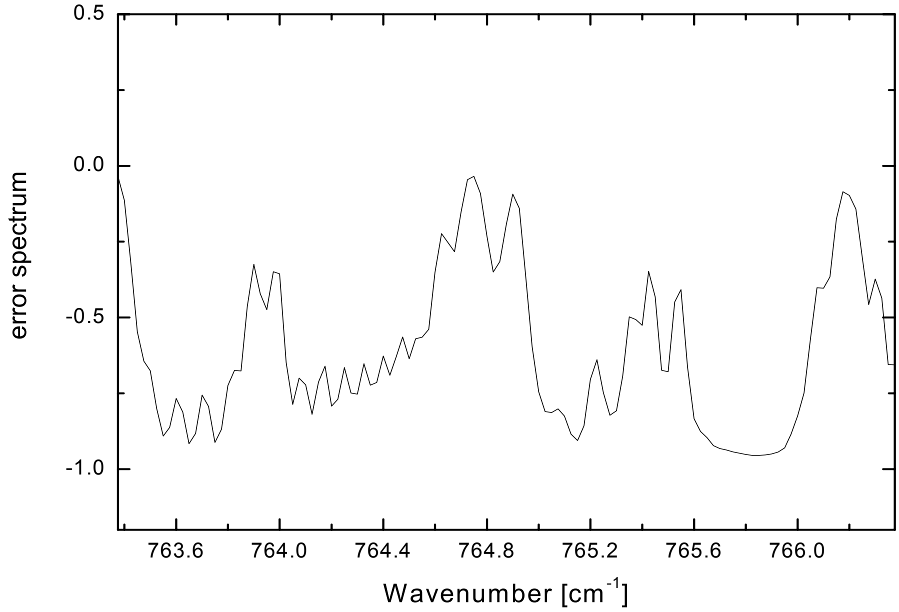

O30021 15 km

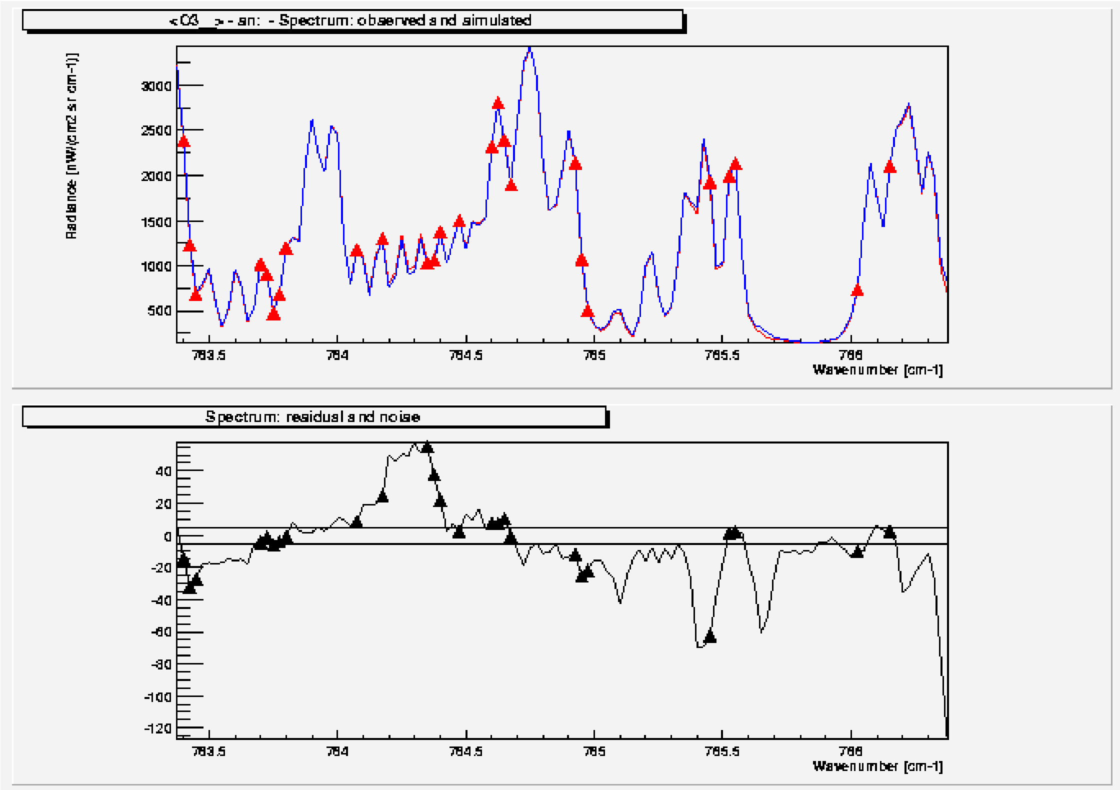
Spectrum: observed and simulated
Radiance [nW/(cm2 sr cm-1)]
Wavenumber [cm-1]
Spectrum: residual and noise
Wavenumber [cm-1]

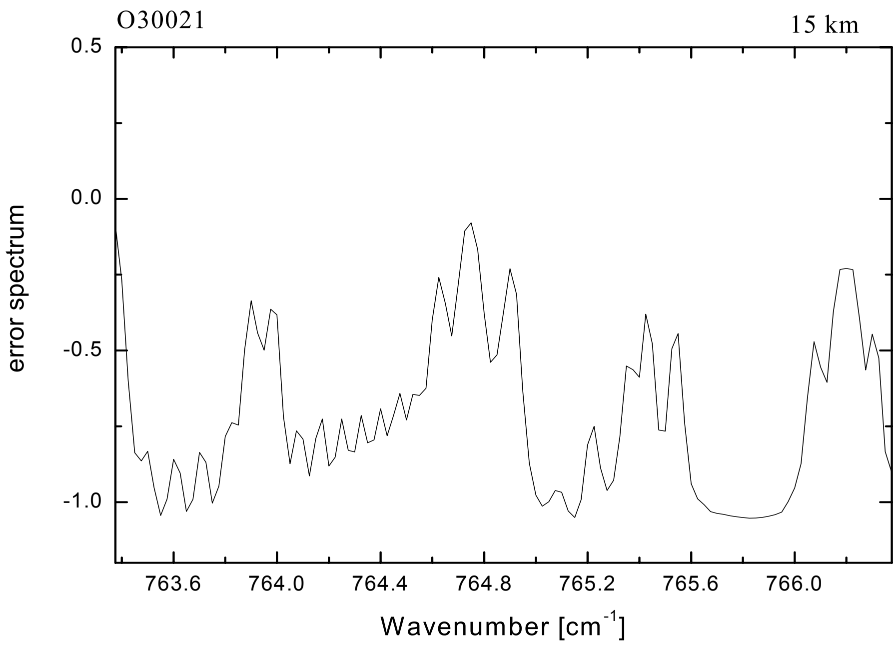
O30021
15 km
error spectrum
Wavenumber [cm-1]

O30021 18 km

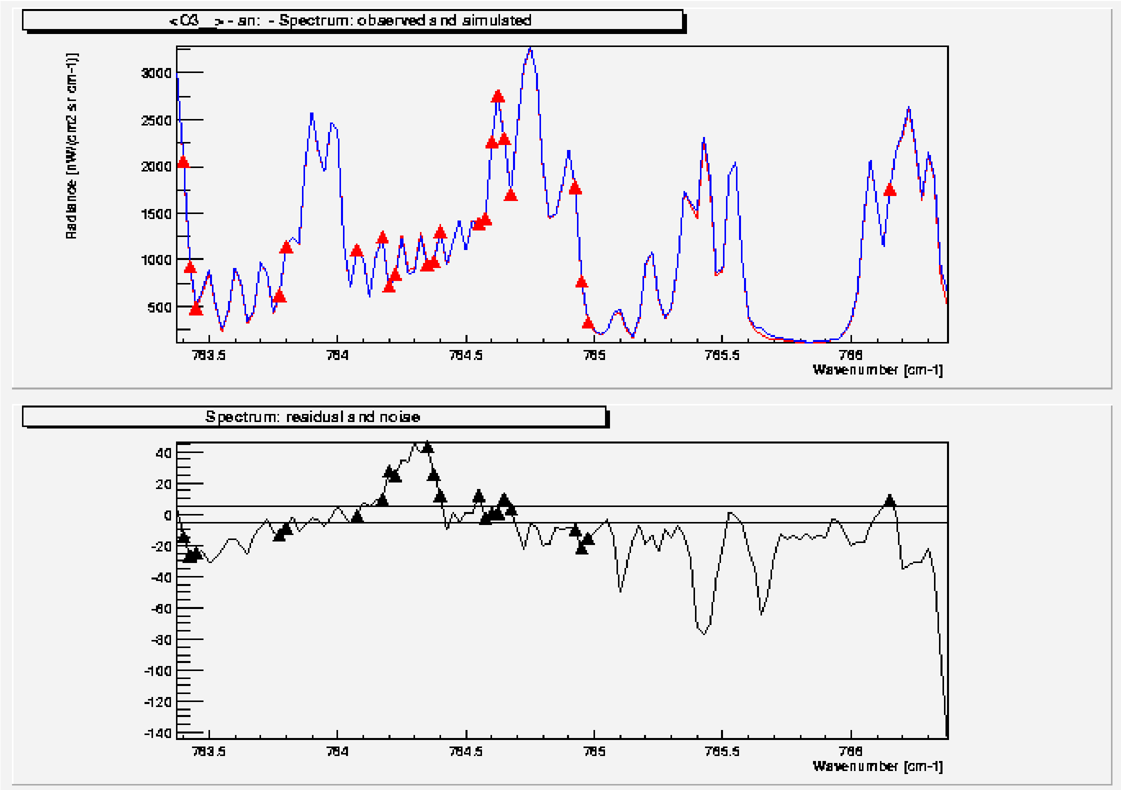
<O3__> - an: - Spectrum: observed and simulated
Radiance [nW/(cm2 sr cm-1)]
3000
2500
2000
1500
1000
500
763.5
764
764.5
765
765.5
766
Wavenumber [cm-1]
Spectrum: residual and noise
40
20
0
-20
-40
-60
-80
-100
-120
-140
763.5
764
764.5
765
765.5
766
Wavenumber [cm-1]

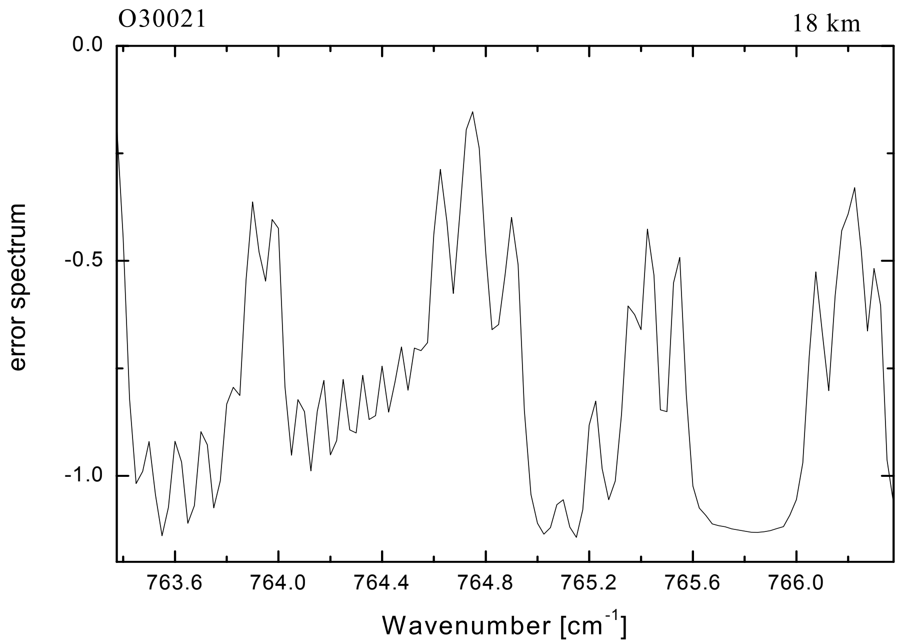
O30021
18 km
error spectrum
0.0
-0.5
-1.0
763.6
764.0
764.4
764.8
765.2
765.6
766.0
Wavenumber [cm-1]

O30021 21 km

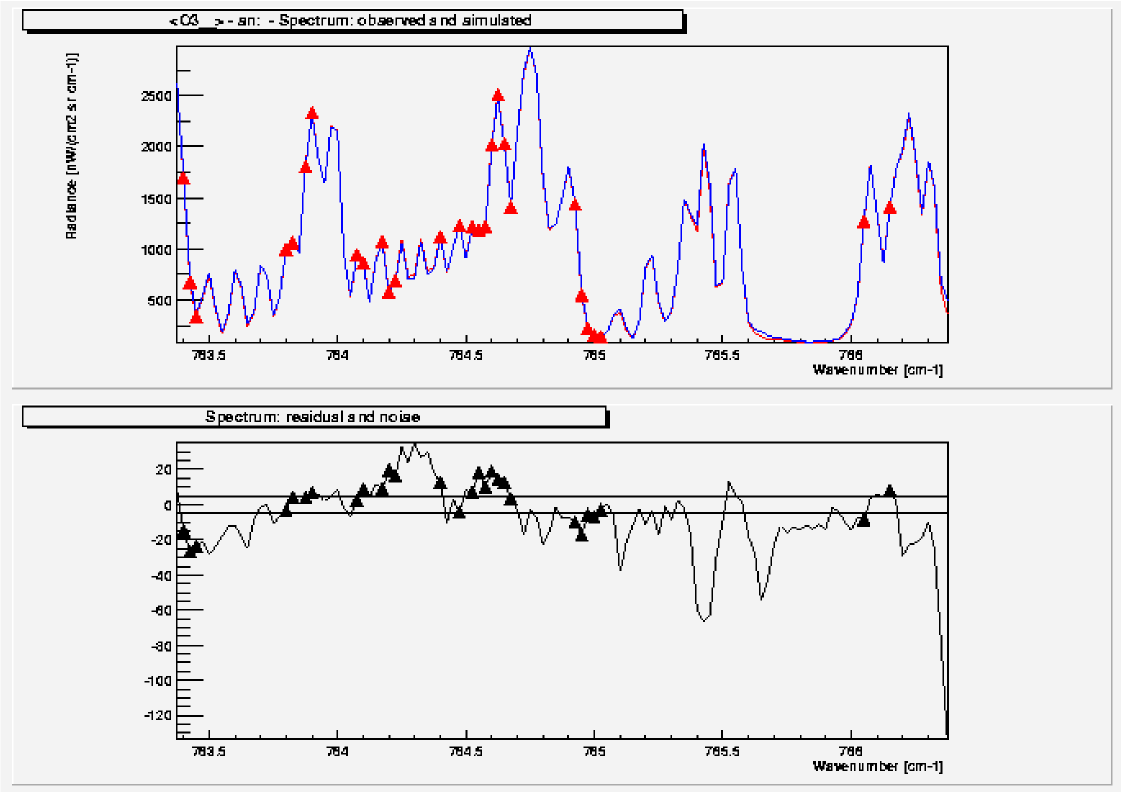
<O3__>- an: - Spectrum: observed and simulated
Radiance [nW/(cm2 sr cm-1)]
Wavenumber [cm-1]
Spectrum: residual and noise
Wavenumber [cm-1]

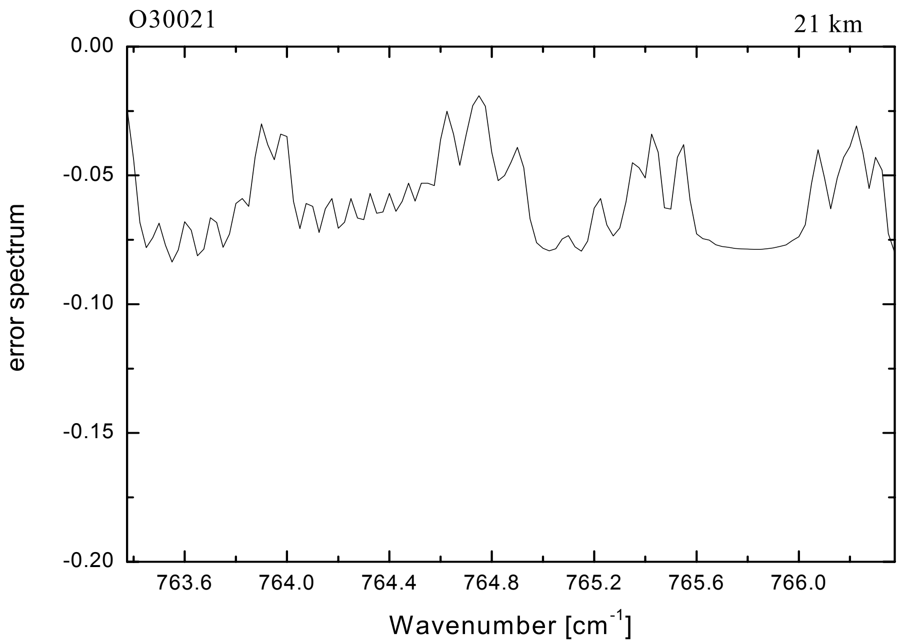
O30021
21 km
error spectrum
Wavenumber [cm-1]

Conclusions

A clear correlation between averaged residuals and line mixing error is noticed in particular for the following microwindows and altitudes:

PT0004	15, 18 km
PT0006	15, 18 km
PT0002	12, 15, 18, 21, 24, 27 km

We have found that the values of averaged residuals are a little smaller than the error spectra indicating an overestimation of the error spectra.

The systematic error caused by line mixing must be compared with the NESR of the individual measurement that is about 7 times greater than the NESR of the average shown in the figures.

In some microwindows the error on the simulated spectrum introduced by line-mixing is comparable with the random error on the single measurement. On the basis of these results we can conclude that line-mixing error is not a major problem but is significant and can introduce a bias in analyses involving the calculation of averages of the profiles.

4.8 Verification of Instrument Line Shape (ILS)

Ref. [RD5]: Sect. 4.2.8; Ref. [RD9]: Sheet MIP_MV_2_12

Introduction

The ILS is determined in Level 1 with an empirical expression that is used in Level 2 for the simulation of the observations.

The objective of this test is to verify the correctness of the width of the ILS provided by Level 1 processor by fitting a band dependent ILS broadening parameter from MIPAS spectra.

Procedure and results

The ORM_ORB code is able to fit, together with the nominal MIPAS target parameters, a band-dependent parameter used to modify the width of the ILS provided by Level 1. The ILS provided by Level 1 is convoluted with an additional function that is equal to a linear combination of a *sinc* function (with resolution equal to the unapodized resolution of MIPAS spectra) with a $sinc^2$ function that is twice as large as than the *sinc*. The two functions correspond respectively to the ILS of a box-car apodization and of a triangular apodization. The combination of the two corresponds to trapezoid apodization of value one at zero path difference and of value one minus c at maximum path difference, where c is the fitted parameter. This parameter is the ILS broadening parameter that measures the requirement for either a broader ILS (positive values) or a narrower ILS (negative values).

The microwindows used for this fit are the ones selected for the nominal retrievals (no dedicated microwindows are used).
Each species retrieval provides the values of the ILS broadening parameters relative to all the spectral bands of the microwindows used for the analysis. Comparison of the results obtained by different retrievals for the same band provides an indication of the consistency of the retrieved values.
The fit of this parameter leads to some but not important reduction of the residuals (see Fig. 1)

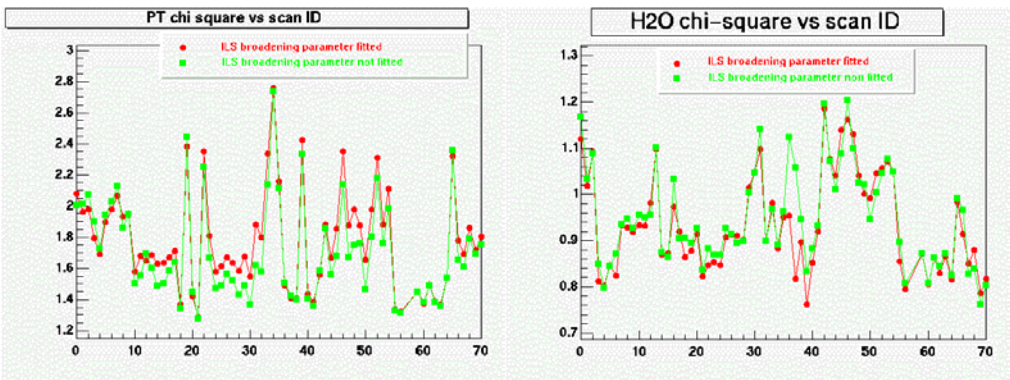

Figure 1 χ^2 as a function of scan ID for pt retrieval (left plot) and h2o retrieval (right plot).

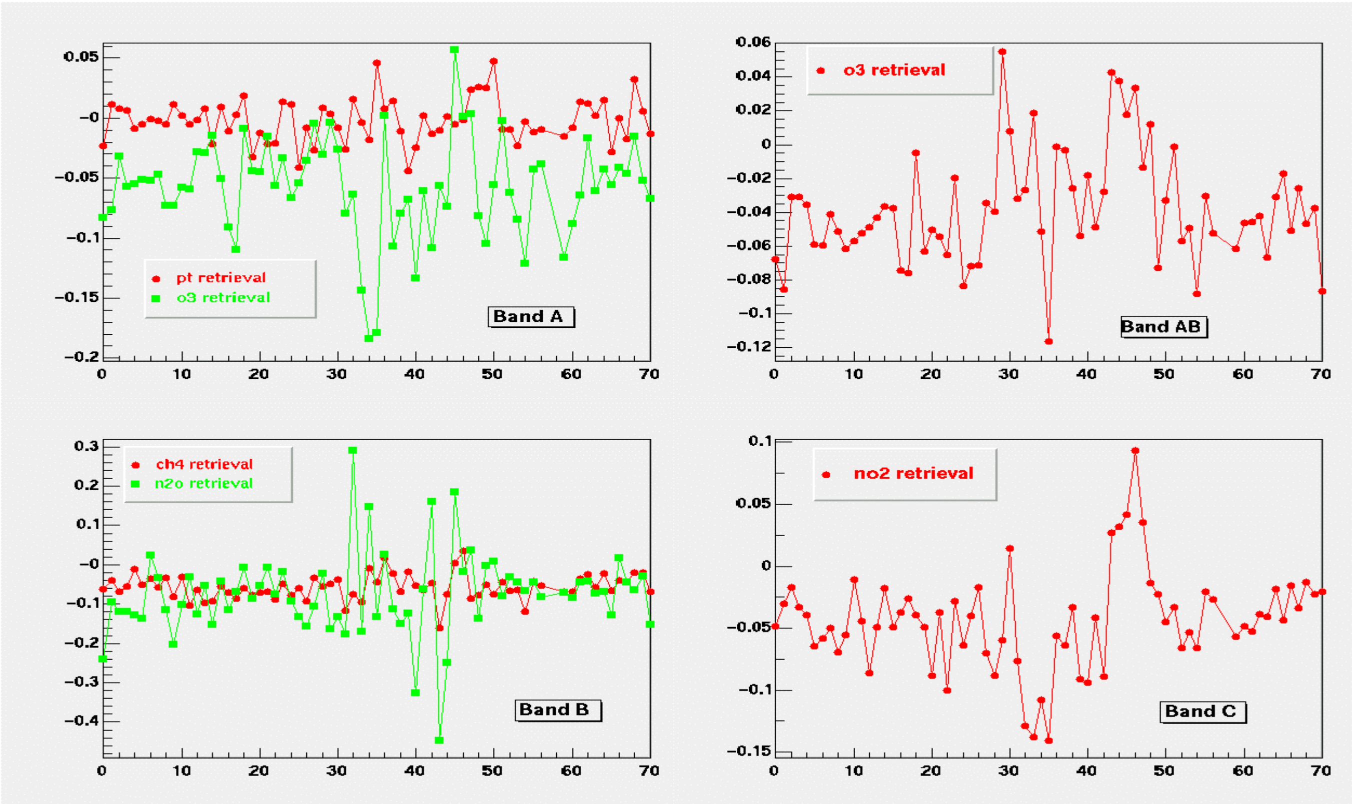

Figure 2 Retrieved ILS broadening parameter for the different bands (only spectra above 40 km are included in the fit)

Furthermore the ILS broadening parameter has a high correlation with pressure retrievals. This correlation with pressure is the reason for the requirement of an accurate ILS, and is also the cause of the difficulties in the retrieval of the ILS from the atmospheric measurements.
In order to avoid this problem it is necessary to limit the interference of the atmospheric broadening that occurs mainly at low altitudes. Therefore, special sensitivity tests were made with retrieval limited to altitudes above 40 km. The retrieved ILS broadening parameters obtained by the analysis of orbit # 2081 are reported in Figure 2 as a function of scan ID for bands A, AB, B and C (no microwindows in band D have been used).

Significant variations are observed as a function of the sequence number, and on average the broadening parameter is negative, suggesting that the real ILS may be sharper than the one provided by Level 1.

Conclusions

An error in the width of the ILS provided by Level 1is measured with statistically significant accuracy.
We obtain on average an indication for a sharper ILS, but the large variability of the results leaves the suspicion that other modelling effects may be interfering with this test.

4.9 Verification of intensity calibration.

Ref. [RD5]: Sect. 4.2.10; Ref. [RD9]: Sheet MIP_MV_16

Introduction

Intensity calibration of MIPAS measurements is performed by Level 1 processor and is crucial because of the strong correlation between intensity calibration parameters and temperature and VMR profiles (a wrong intensity calibration leads to a wrong retrieved profile).
The objective of this test is to try to assess, by the analysis of the spectra, the correctness of the intensity calibration by fitting a band dependent and altitude independent intensity scaling parameter. Due to the correlations of this parameter with temperature and VMR, it is not possible to provide an absolute verification of the intensity calibration, but in case that microwindows belonging to different bands are used in the fit, the ratio between the intensity calibration parameters of different bands is expected to be determined.

Procedure and results

A band dependent and altitude independent intensity scaling parameter can be fitted by the ORM_ORB program for each scan of the orbit and for each retrieval (pT, h2o, o3, etc.).

The microwindows used for this fit are the ones selected for the nominal retrievals (no dedicated microwindows are used).
The fit of this parameter does not lead to a significant reduction of the residuals (see Fig. 1, where the χ^2 as a function of scan ID is shown for 3 different retrievals in the nominal case and when the fit of the intensity calibration parameter is performed) .

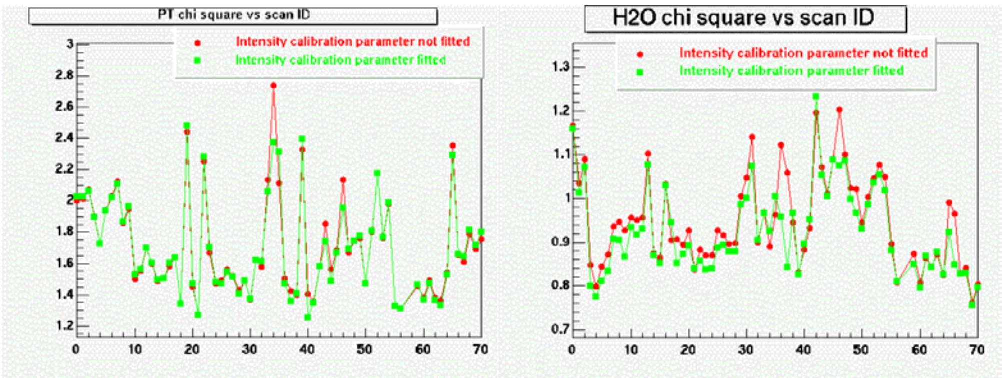

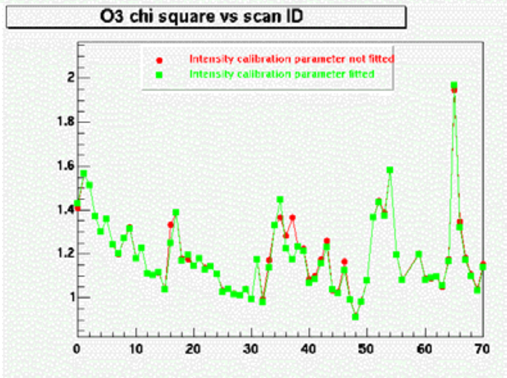

Figure 1 $\chi 2$ vs scan ID for different retrievals obtained in the nominal case and when the intensity scaling parameter is fitted.

In order to increase statistics we performed a fit using, for each retrieval, an OM containing all microwindows of the microwindow database. Only 17 scans of orbit #2081 could be processed with these occupation matrices. In Table 1 the mean value of the intensity scaling parameters for the different bands and the different retrievals are reported. The last column contains the ratio between intensity scaling parameter retrieved in band A and band B. Not very consistent results are obtained for the ratio A/B.

Table 1 Retrieved intensity scaling parameter for the different bands and retrievals

Band → Retrieval ↓	A	AB	B	C	A/B
PT	.997± .0014		.996± .0025		1.001±.003
H2O	.980± .0127		.998± .0010	1.009± .0009	.982±.01
O3	1.00± .0004	.998± .0005			
HNO3	1.027± .0016		.994± .0009		1.033±.002

Conclusions

The fit of an intensity scaling factor varies only marginally the residuals. Furthermore, a reduction of the residuals is observed only in the cases of sequences that have large residuals.

The intensity scaling factor strongly correlates with the retrieved geophysical quantities and it is difficult to discriminate the two effects.

No positive evidence is observed of a intensity calibration error.

4.10 Zero-level calibration

Ref. [RD5]: Sect. 4.2.11; Ref. [RD9]: Sheet MIP_MV_17

Introduction

Causes of instrument zero level offset are internal emission of the instrument, scattering of light into the instrument or third order non-linearity of the detectors. All these causes of offset are corrected during the calibration step in Level 1b data processing.
In the ORM, a limb scanning angle independent offset is fitted for each microwindow in order to compensate for the residual uncorrected instrument offset. If the instrument has a limb angle dependent offset, the ORM corrects only partially for it.
An altitude dependent offset probably can not be seen in the residuals because cross talks are possible with intensity calibration errors and atmospheric continuum retrieval. The evidence is hidden in the inconsistency of the retrieved quantities.

Description of the test

A fit of the instrumental offset as a function of both tangent altitude and microwindow has been done and compared with the nominal retrieval.

A retrieval without the fit of the instrumental offset has been performed and compared with the nominal retrieval.

Results

In the following 7 figures the comparison between the χ^2 obtained in the nominal retrieval (altitude independent offset) and the χ^2 obtained when the instrumental offset is fitted as a function of both tangent altitude and microwindow (altitude independent offset) is shown for all the retrieved species as a function of the scan ID.

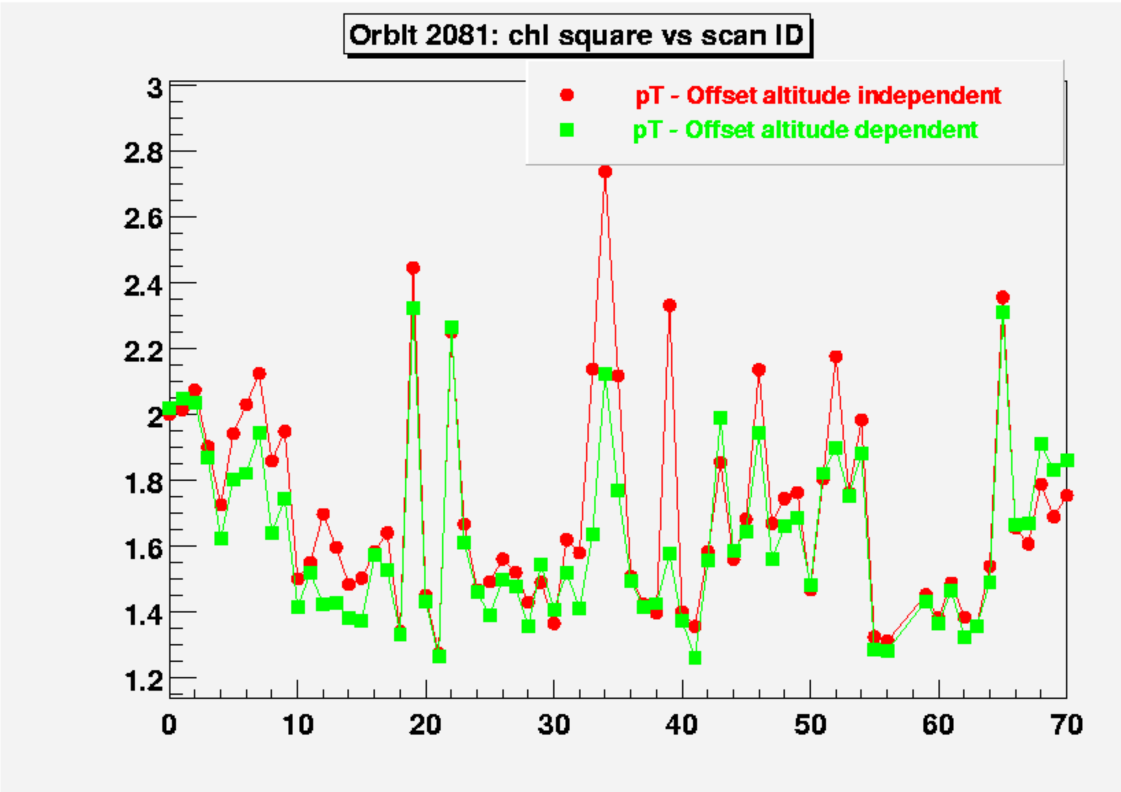
Orbit 2081: chi square vs scan ID
pT - Offset altitude independent
pT - Offset altitude dependent
3
2.8
2.6
2.4
2.2
2
1.8
1.6
1.4
1.2
0
10
20
30
40
50
60
70

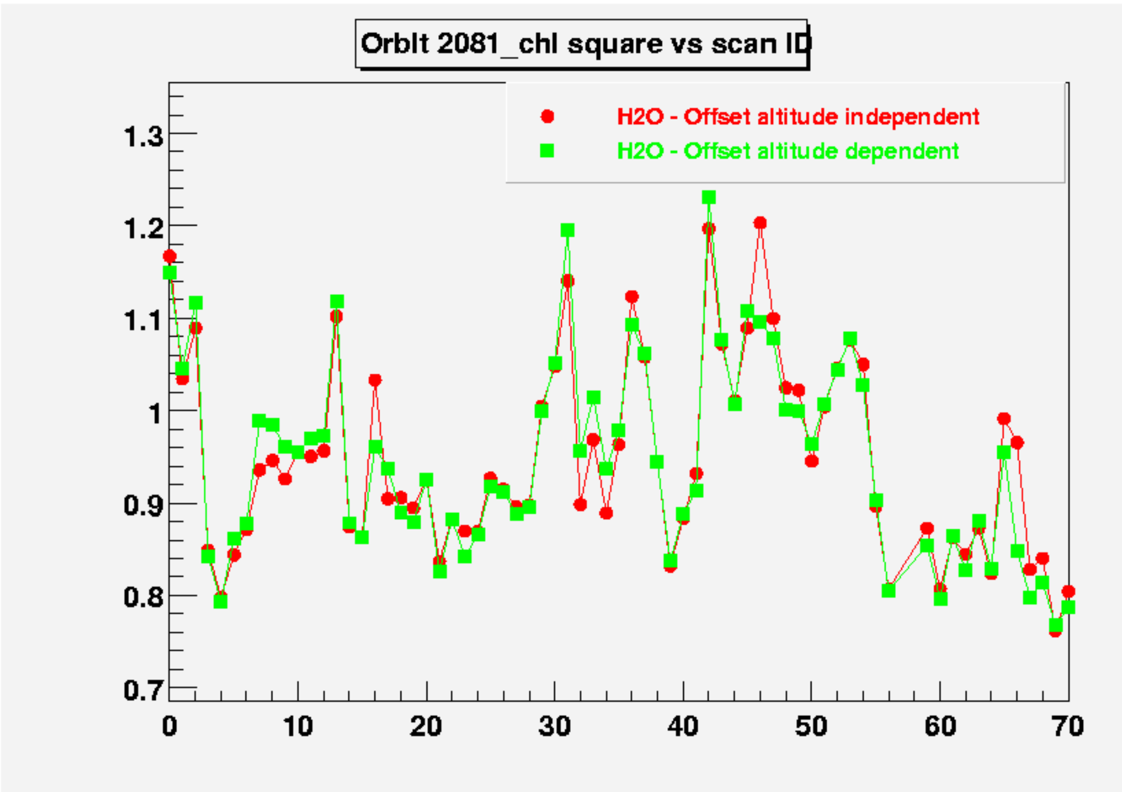
Orbit 2081_chi square vs scan ID
H2O - Offset altitude independent
H2O - Offset altitude dependent
1.3
1.2
1.1
1
0.9
0.8
0.7
0
10
20
30
40
50
60
70

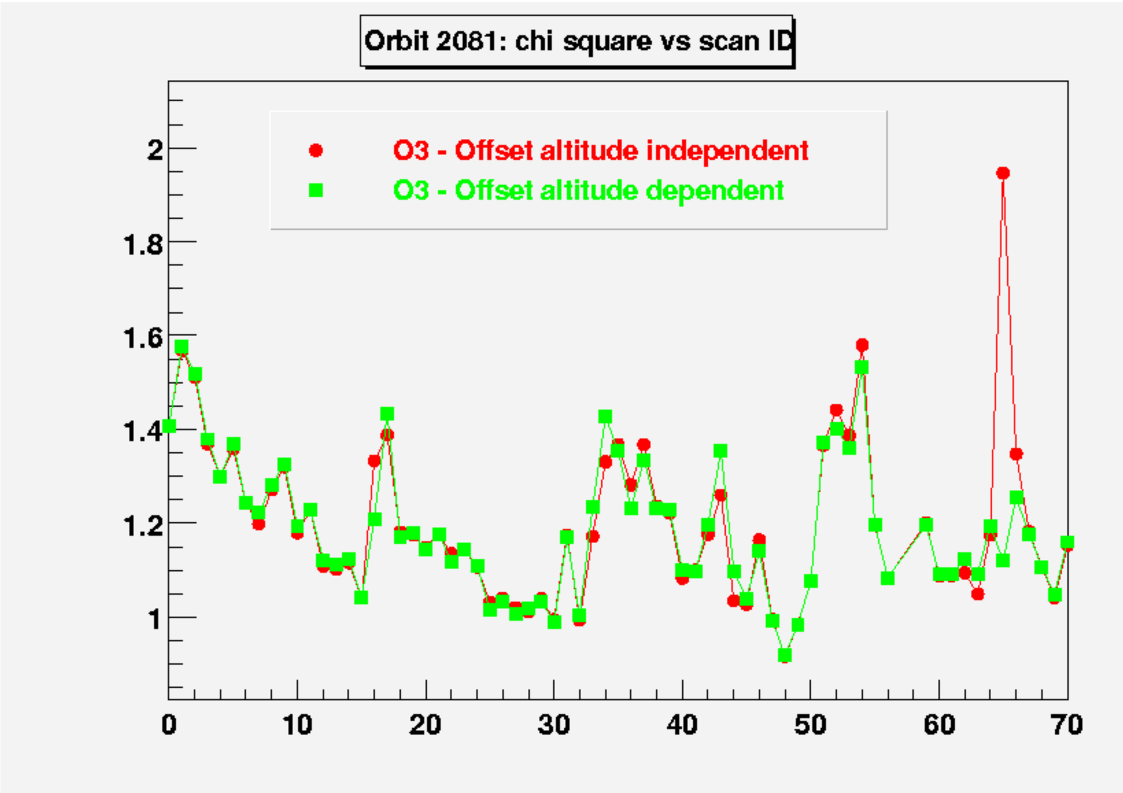
Orbit 2081: chi square vs scan ID
O3 - Offset altitude independent
O3 - Offset altitude dependent
2
1.8
1.6
1.4
1.2
1
0
10
20
30
40
50
60
70

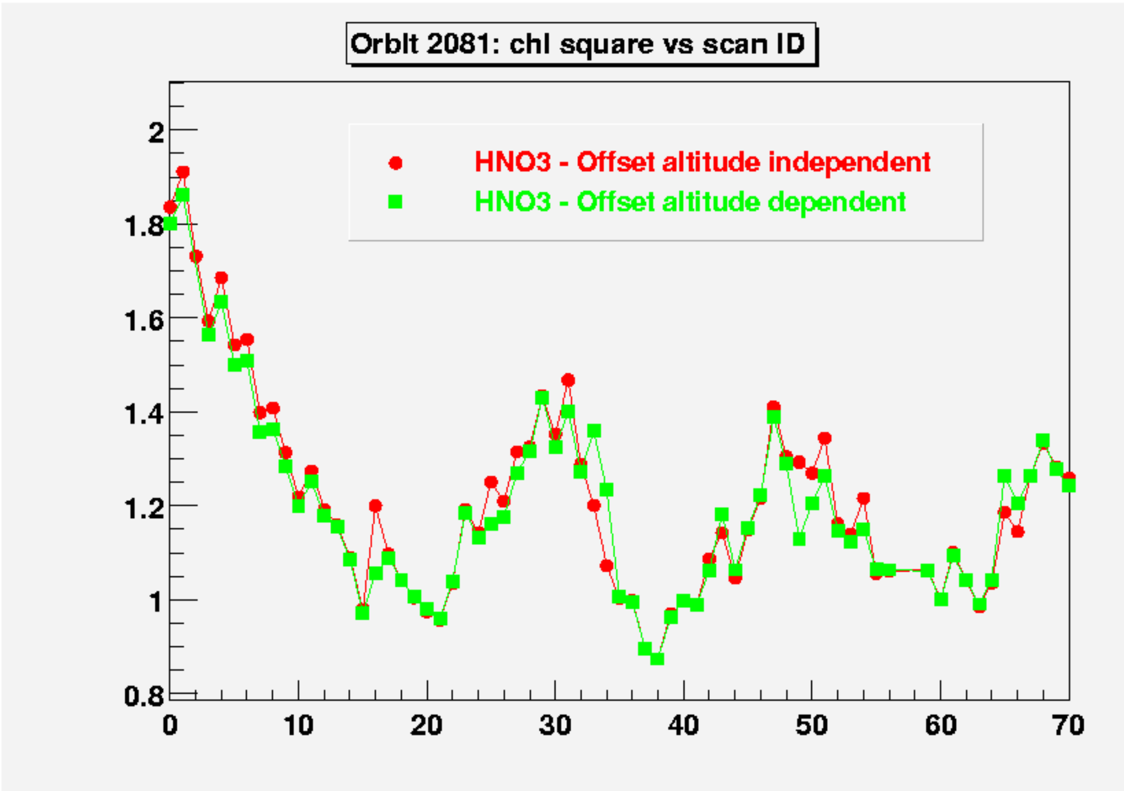
Orbit 2081: chi square vs scan ID
HNO3 - Offset altitude independent
HNO3 - Offset altitude dependent
2
1.8
1.6
1.4
1.2
1
0.8
0
10
20
30
40
50
60
70

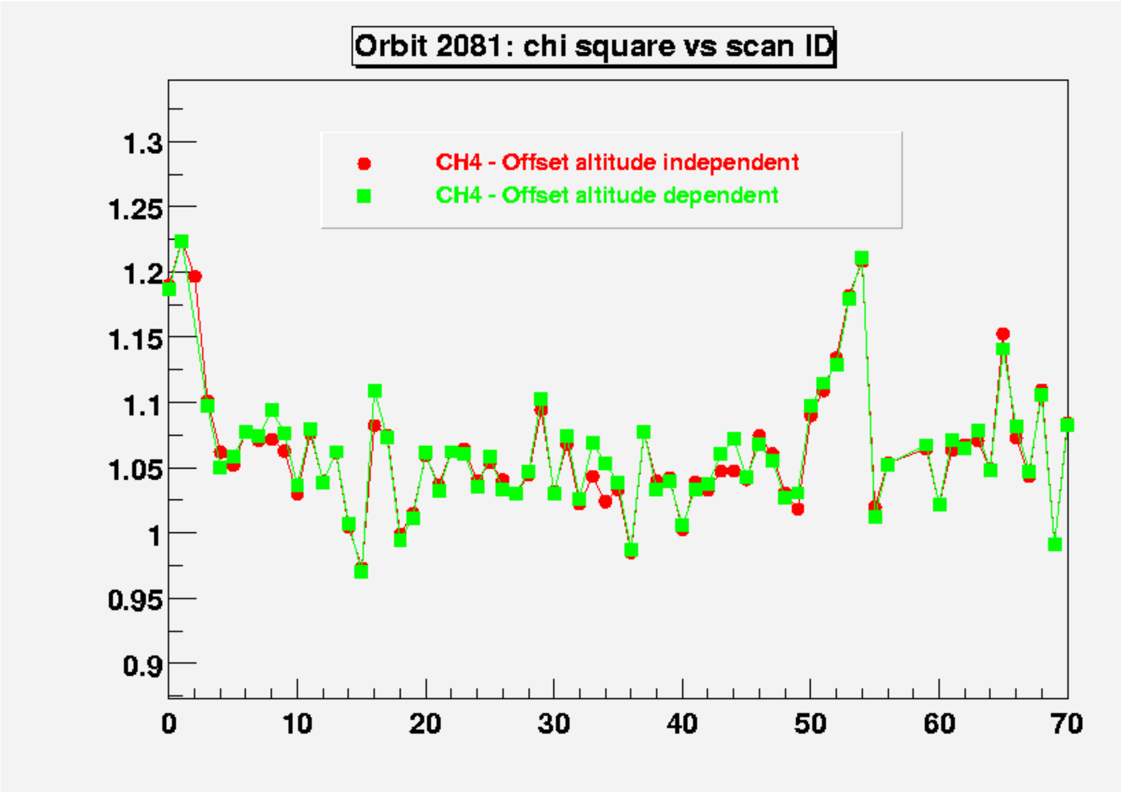
Orbit 2081: chi square vs scan ID
CH4 - Offset altitude independent
CH4 - Offset altitude dependent
1.3
1.25
1.2
1.15
1.1
1.05
1
0.95
0.9
0
10
20
30
40
50
60
70

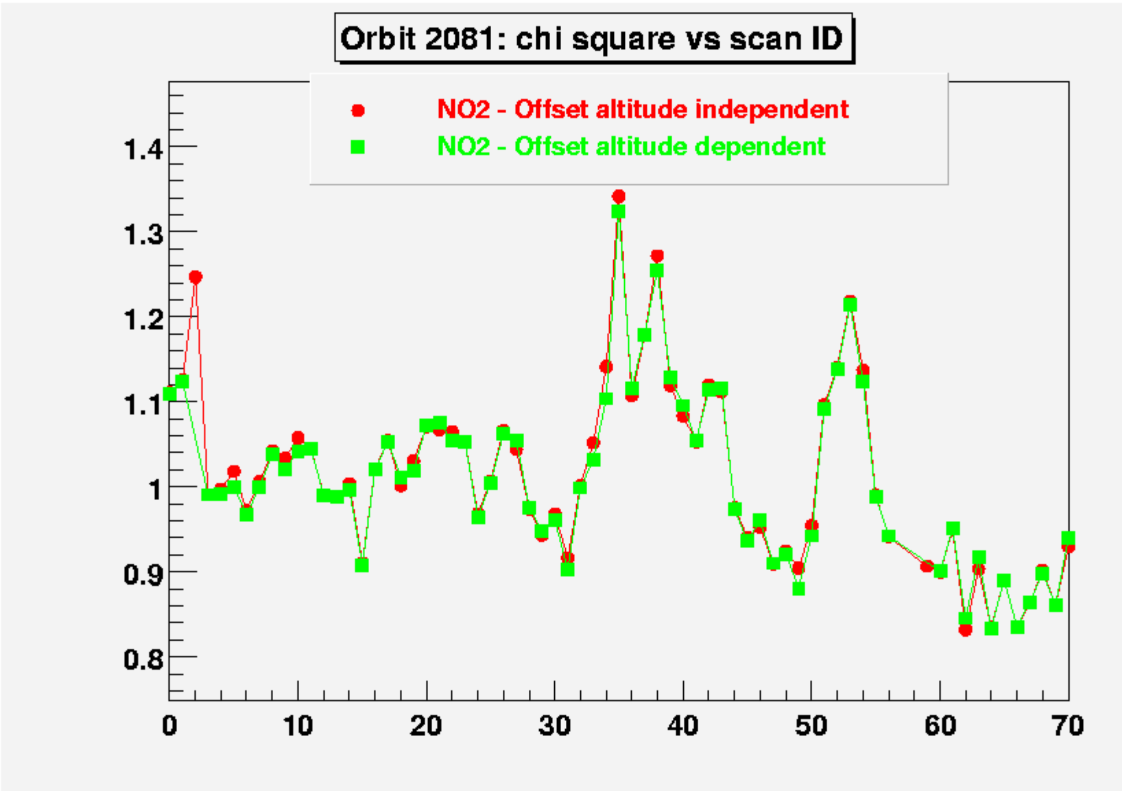
Orbit 2081: chi square vs scan ID
NO2 - Offset altitude independent
NO2 - Offset altitude dependent
1.4
1.3
1.2
1.1
1
0.9
0.8
0
10
20
30
40
50
60
70

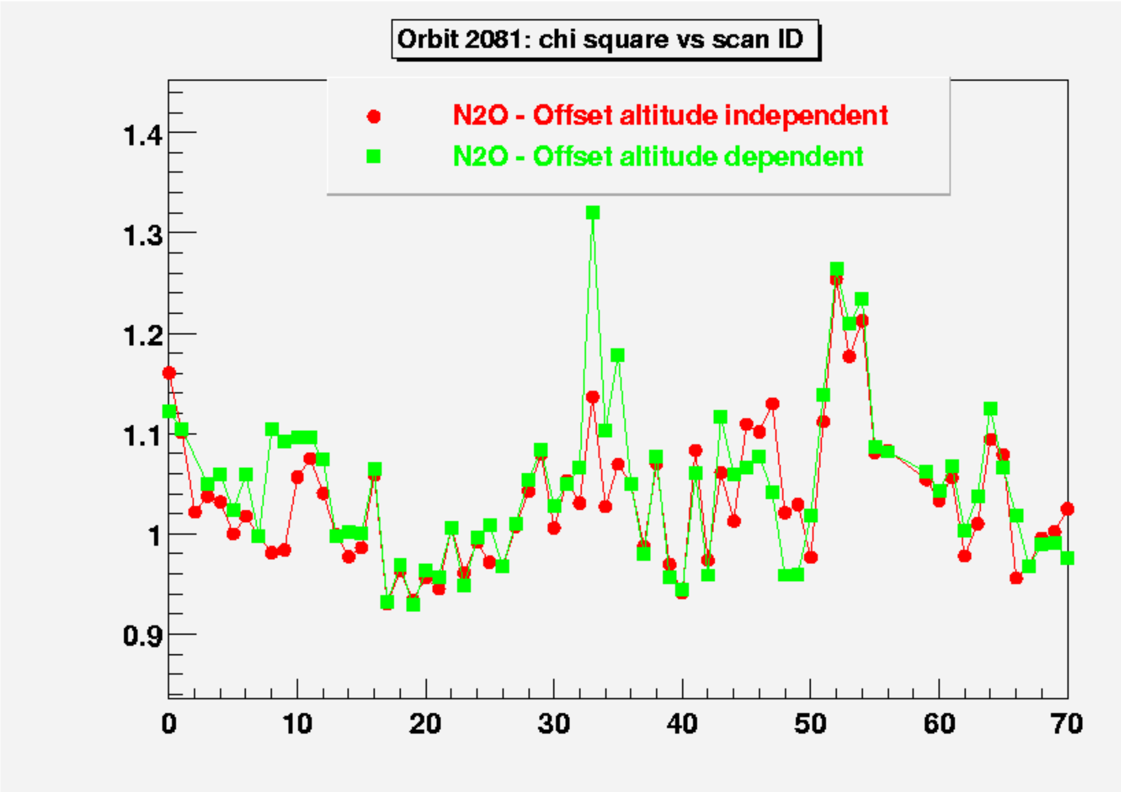

A small reduction of the χ^2 is observed in the second case.

In the following 2 figures the values of the retrieved offset as a function of the wavenumber are compared with the random error in both cases when the retrieved offset is altitude independent and altitude dependent.

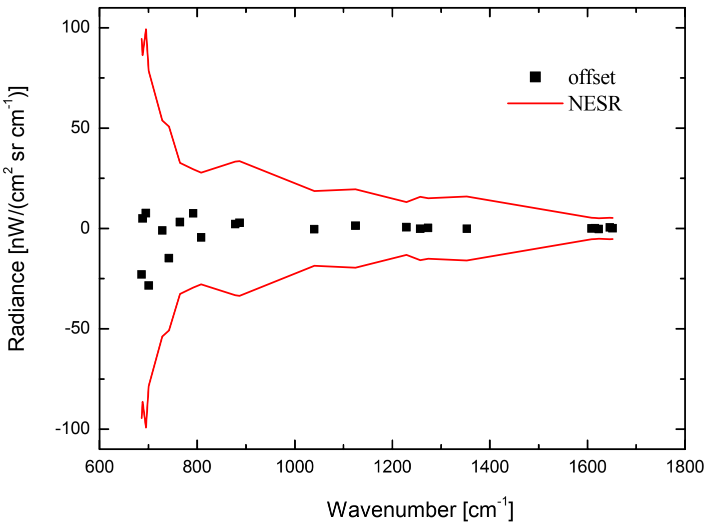
offset
NESR
Radiance [nW/(cm2 sr cm-1)]
100
50
0
-50
-100
600
800
1000
1200
1400
1600
1800
Wavenumber [cm-1]

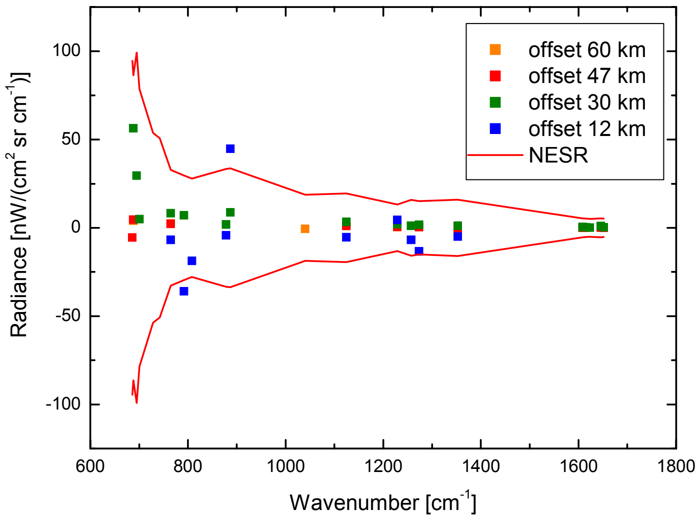

In the following 7 figures the comparison between the profiles obtained fitting an instrumental offset altitude dependent and altitude independent is shown for every speciess. The absolute value of the difference between the two profiles divided by the random error is represented in colour maps as a function of the altitude and the scan ID.

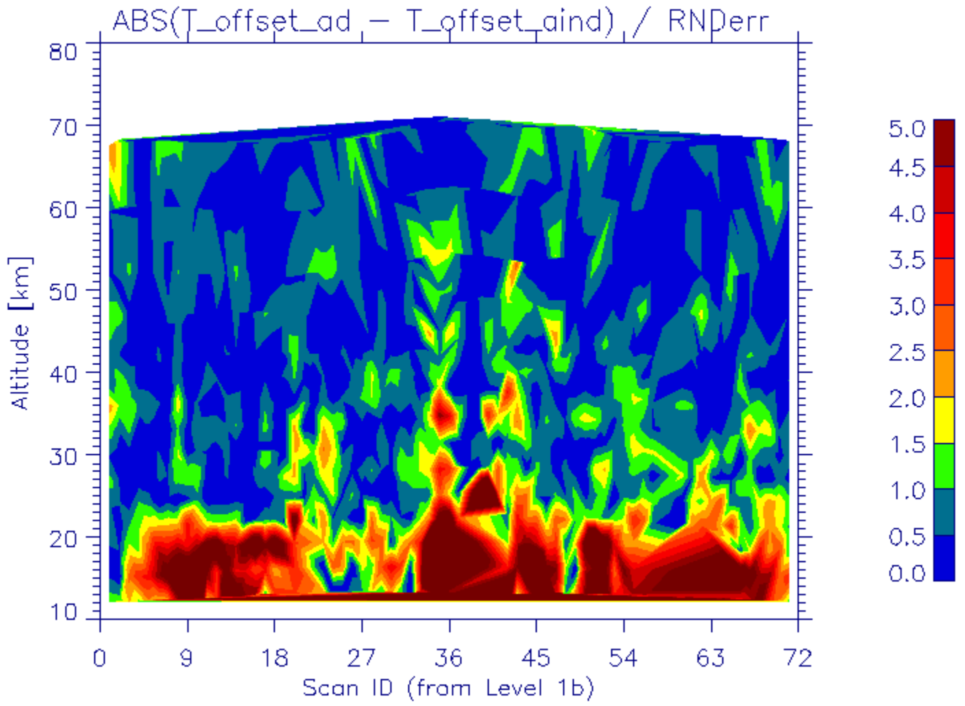
ABS(T_offset_ad − T_offset_aind) / RNDerr
Altitude [km]
80
70
60
50
40
30
20
10
0
9
18
27
36
45
54
63
72
Scan ID (from Level 1b)
5.0
4.5
4.0
3.5
3.0
2.5
2.0
1.5
1.0
0.5
0.0

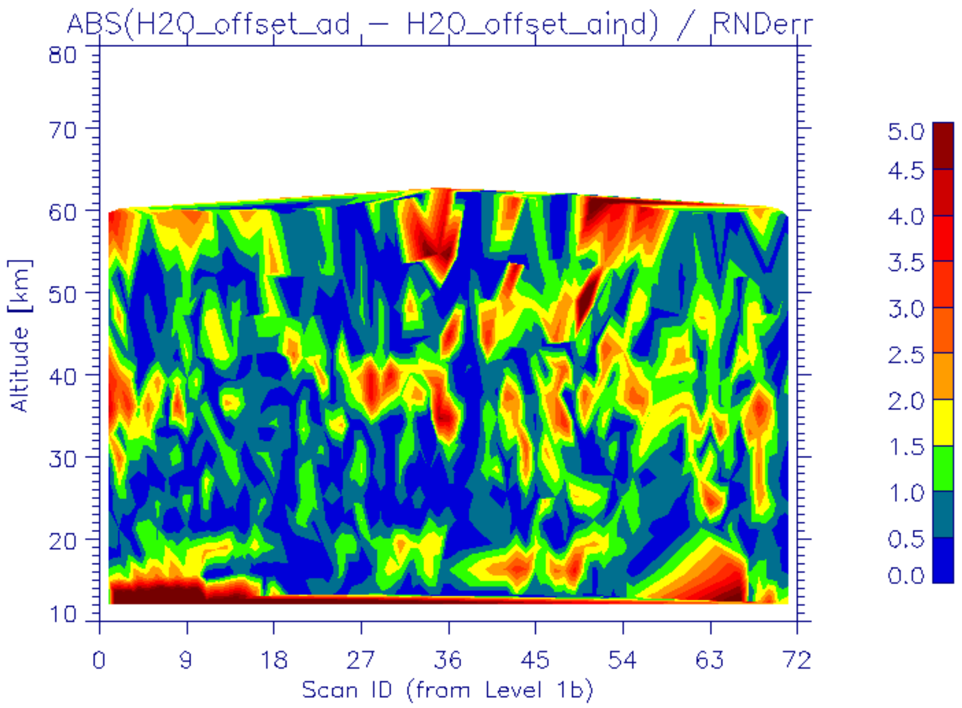
ABS(H2O_offset_ad − H2O_offset_aind) / RNDerr
Altitude [km]
80
70
60
50
40
30
20
10
0
9
18
27
36
45
54
63
72
Scan ID (from Level 1b)
5.0
4.5
4.0
3.5
3.0
2.5
2.0
1.5
1.0
0.5
0.0

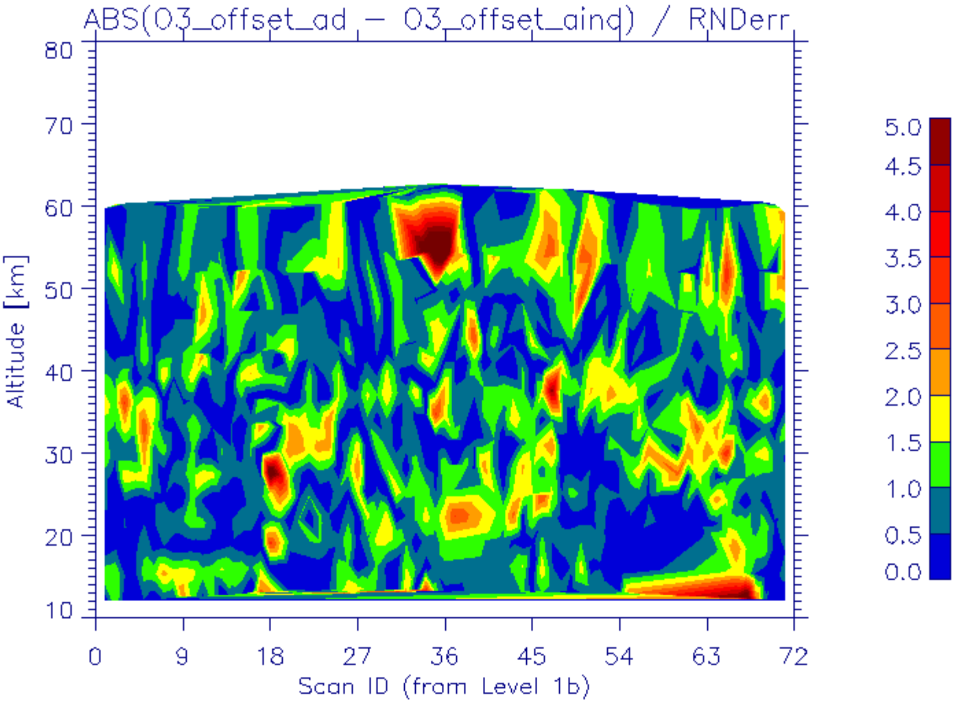
ABS(O3_offset_ad − O3_offset_aind) / RNDerr
Altitude [km]
Scan ID (from Level 1b)
80
70
60
50
40
30
20
10
0
9
18
27
36
45
54
63
72
5.0
4.5
4.0
3.5
3.0
2.5
2.0
1.5
1.0
0.5
0.0

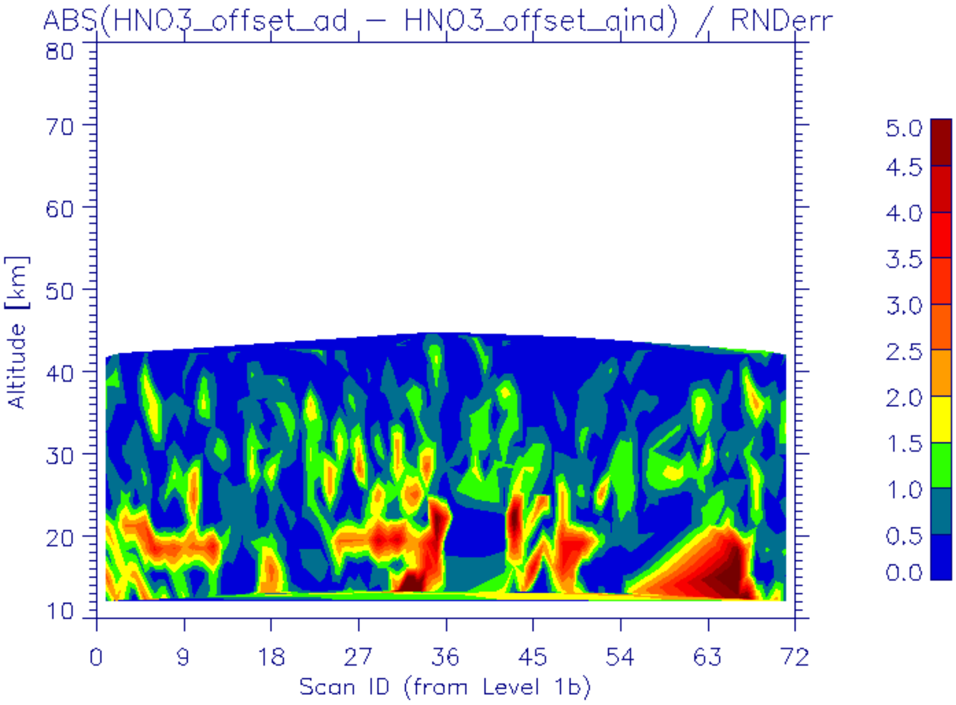
ABS(HNO3_offset_ad − HNO3_offset_aind) / RNDerr
Altitude [km]
Scan ID (from Level 1b)
80
70
60
50
40
30
20
10
0
9
18
27
36
45
54
63
72
5.0
4.5
4.0
3.5
3.0
2.5
2.0
1.5
1.0
0.5
0.0

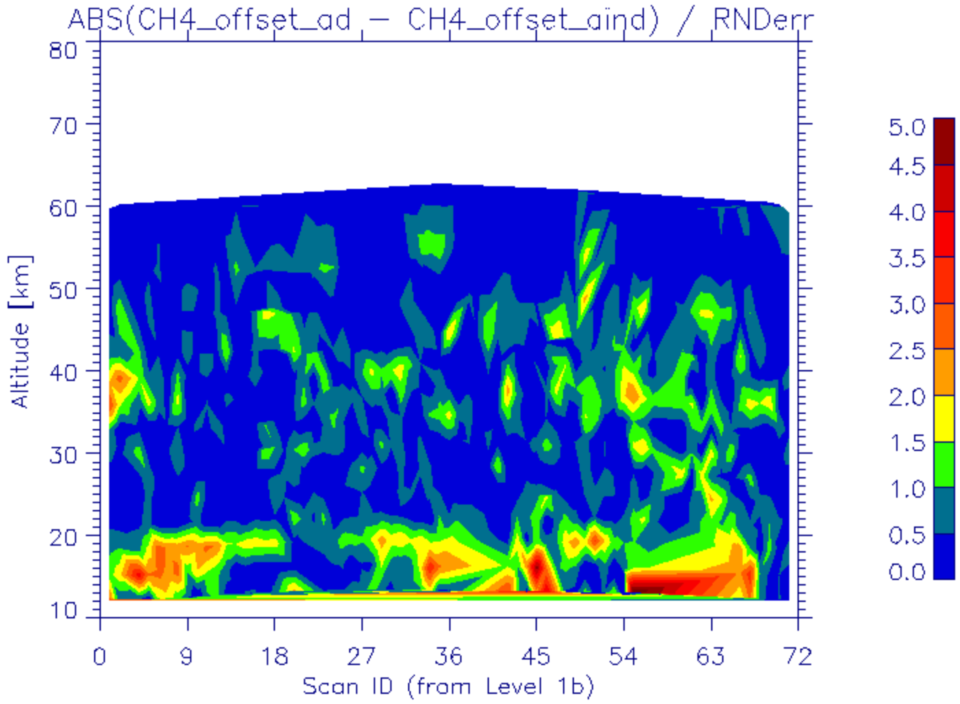
ABS(CH4_offset_ad − CH4_offset_aind) / RNDerr
Altitude [km]
80
70
60
50
40
30
20
10
0
9
18
27
36
45
54
63
72
Scan ID (from Level 1b)
5.0
4.5
4.0
3.5
3.0
2.5
2.0
1.5
1.0
0.5
0.0

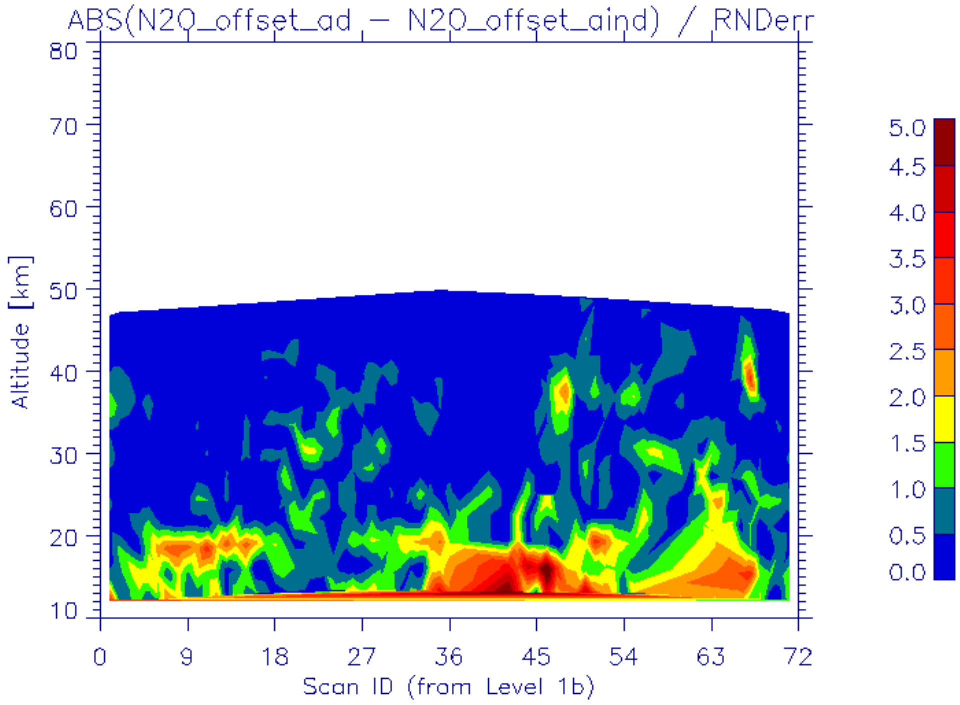
ABS(N2O_offset_ad − N2O_offset_aind) / RNDerr
Altitude [km]
80
70
60
50
40
30
20
10
0
9
18
27
36
45
54
63
72
Scan ID (from Level 1b)
5.0
4.5
4.0
3.5
3.0
2.5
2.0
1.5
1.0
0.5
0.0

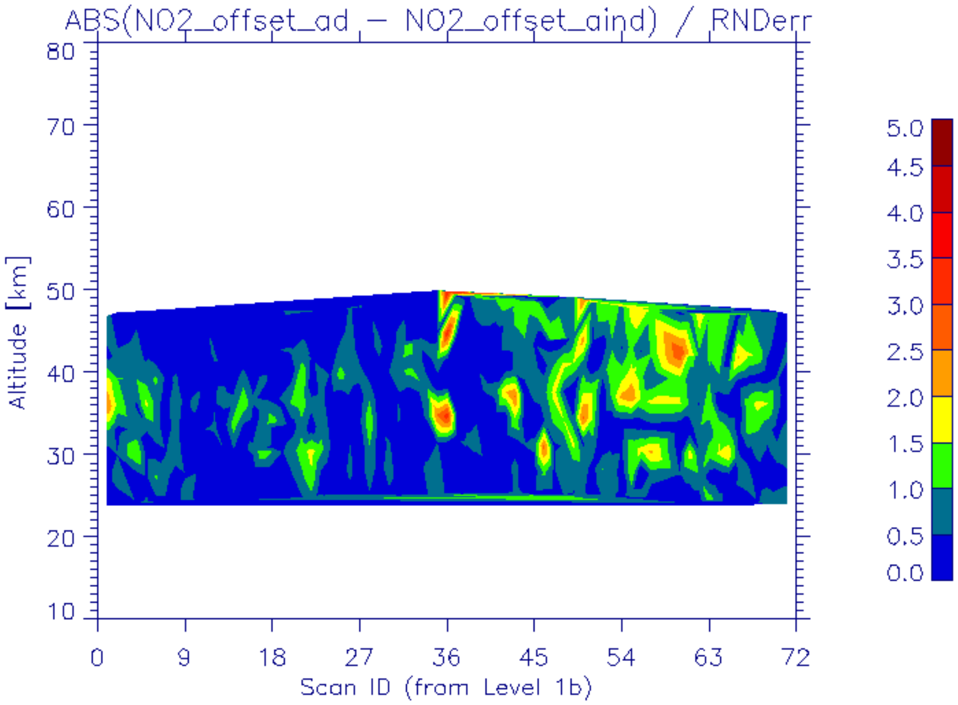

In the following 7 figures the comparison between the χ^2 obtained in the nominal retrieval and the χ^2 obtained when the fit of the instrumental offset is not performed is shown for all the retrieved speciess as a function of the scan ID.

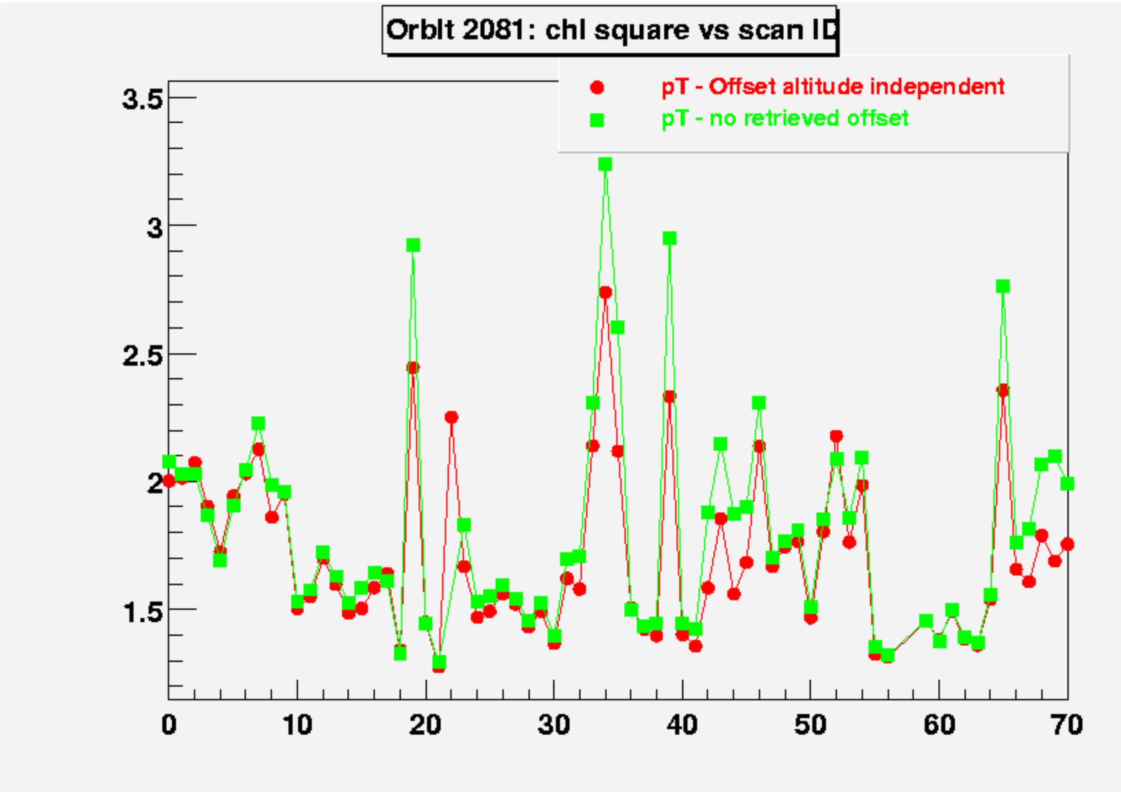
Orbit 2081: chi square vs scan ID
pT - Offset altitude independent
pT - no retrieved offset
3.5
3
2.5
2
1.5
0
10
20
30
40
50
60
70

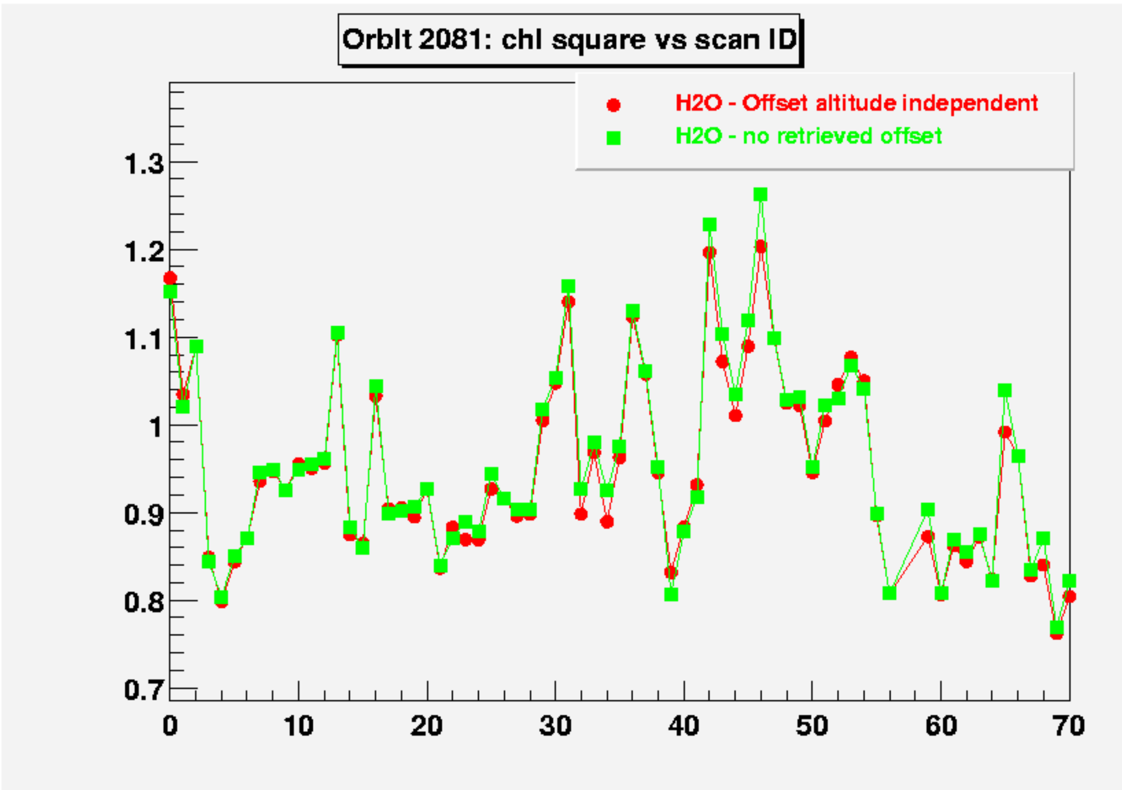
Orbit 2081: chi square vs scan ID
H2O - Offset altitude independent
H2O - no retrieved offset
1.3
1.2
1.1
1
0.9
0.8
0.7
0
10
20
30
40
50
60
70

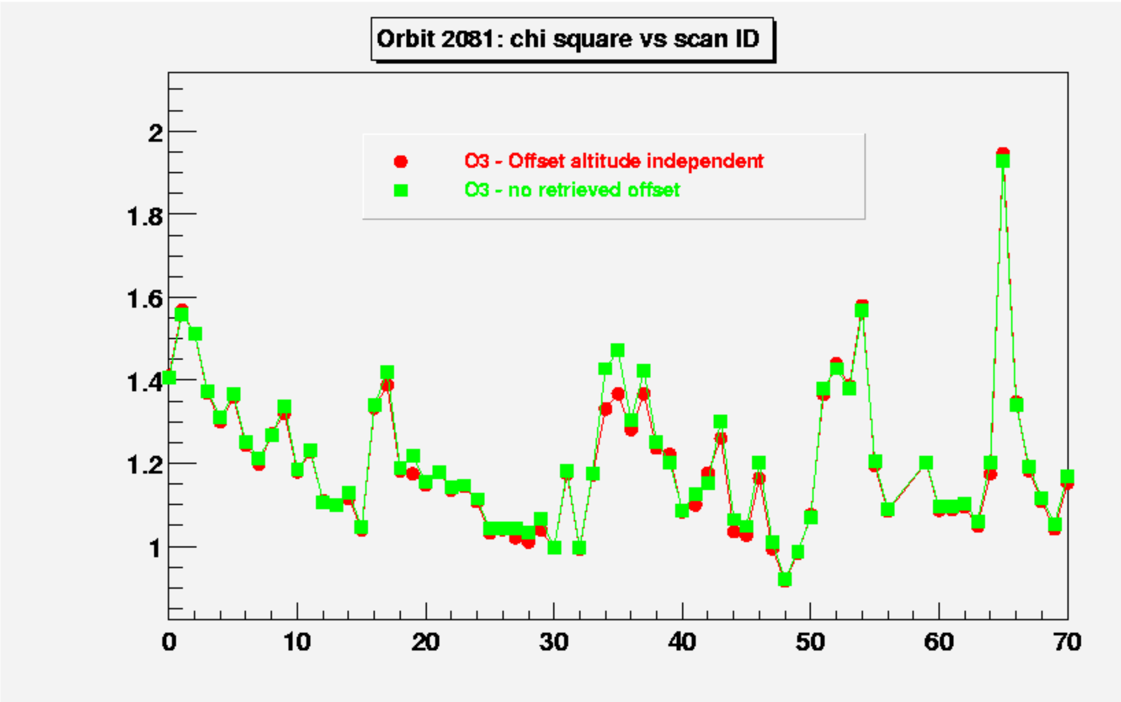
Orbit 2081: chi square vs scan ID
O3 - Offset altitude independent
O3 - no retrieved offset
2
1.8
1.6
1.4
1.2
1
0
10
20
30
40
50
60
70

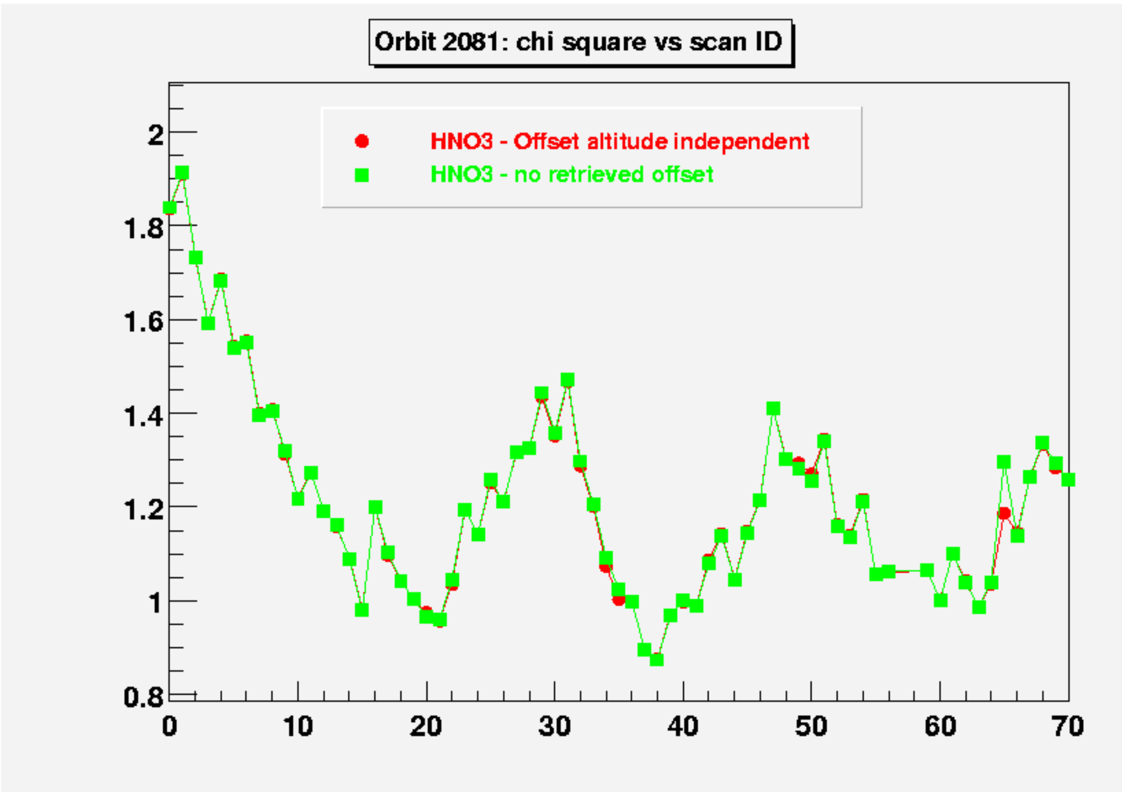
Orbit 2081: chi square vs scan ID
HNO3 - Offset altitude independent
HNO3 - no retrieved offset
2
1.8
1.6
1.4
1.2
1
0.8
0
10
20
30
40
50
60
70

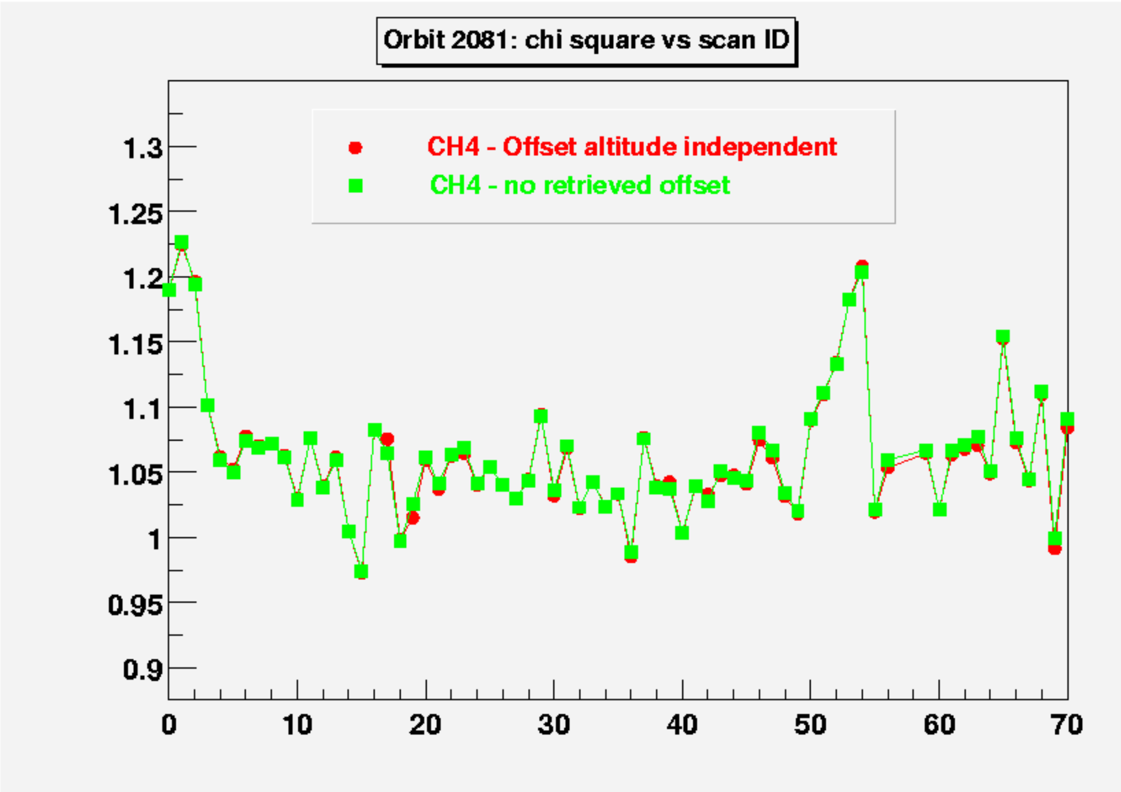
Orbit 2081: chi square vs scan ID
CH4 - Offset altitude independent
CH4 - no retrieved offset
1.3
1.25
1.2
1.15
1.1
1.05
1
0.95
0.9
0
10
20
30
40
50
60
70

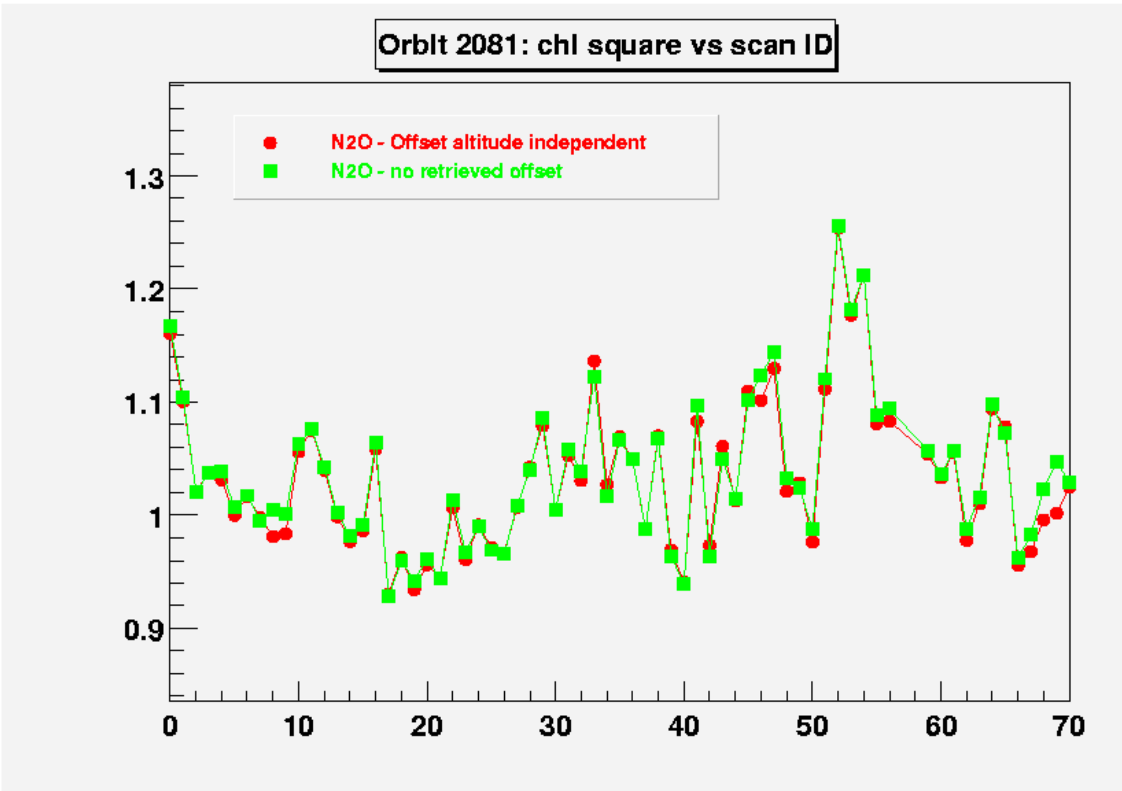
Orbit 2081: chi square vs scan ID
N2O - Offset altitude independent
N2O - no retrieved offset
1.3
1.2
1.1
1
0.9
0
10
20
30
40
50
60
70

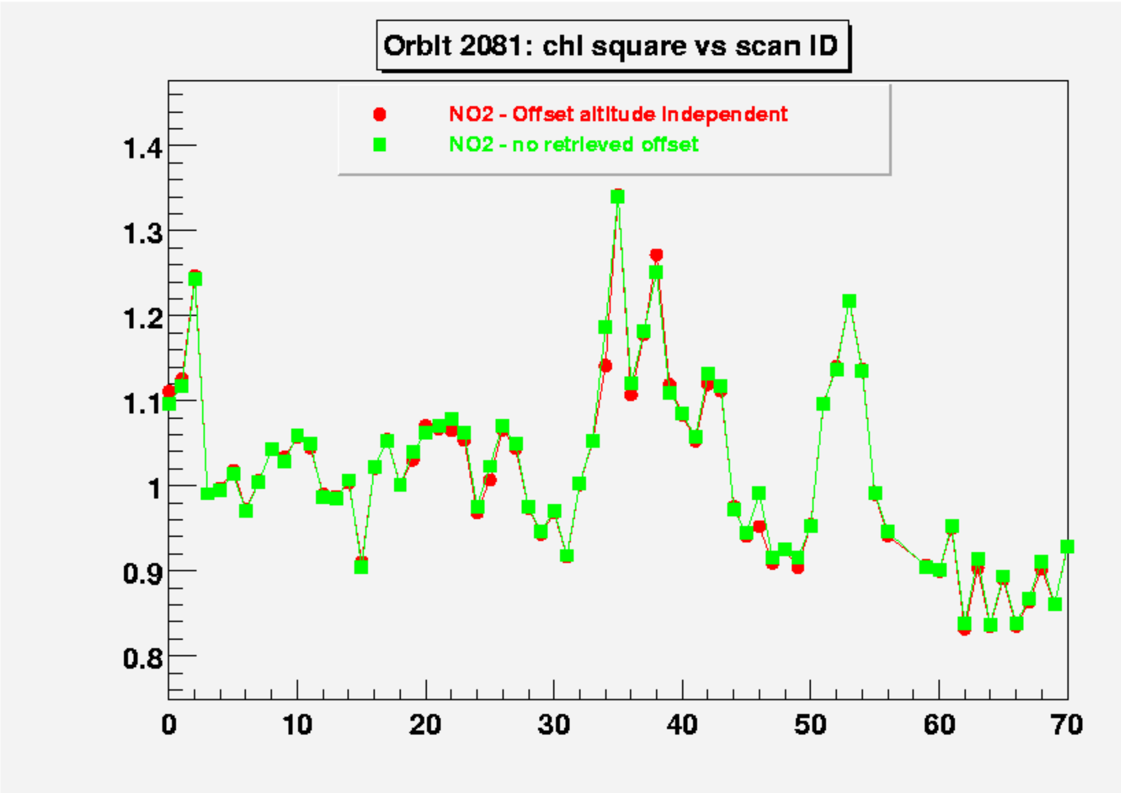

In the following 7 figures the comparison between the profiles obtained in the nominal retrieval and in the case where no instrumental offset is fitted is shown for every speciess. The absolute value of the difference between the two profiles divided by the random error is represented in colour maps as a function of the altitude and the scan ID.

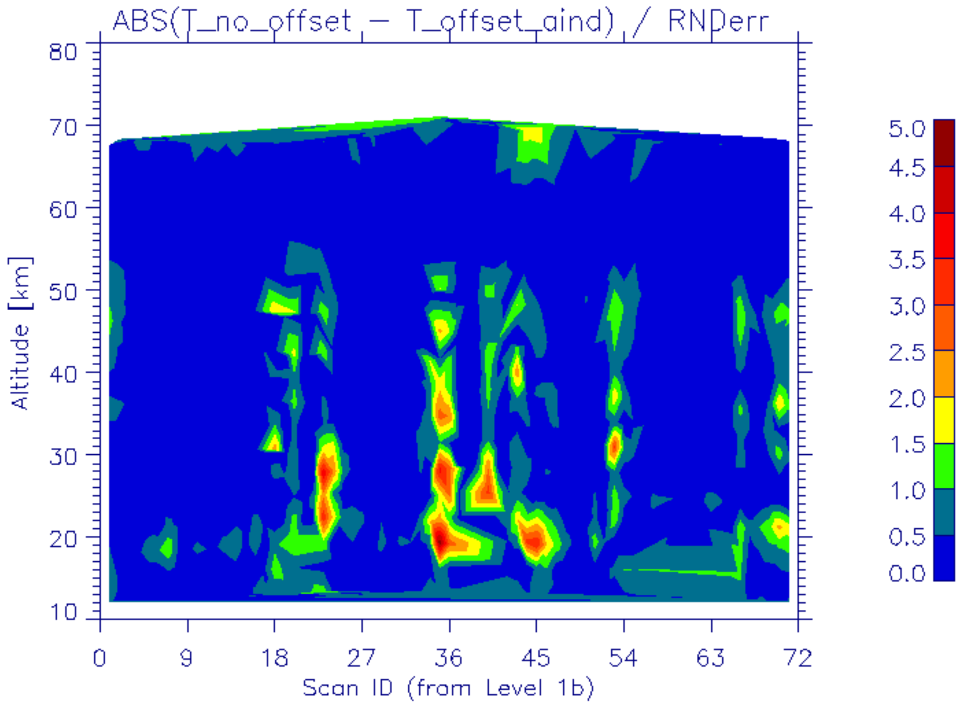
ABS(T_no_offset − T_offset_aind) / RNDerr
Altitude [km]
80
70
60
50
40
30
20
10
0
9
18
27
36
45
54
63
72
Scan ID (from Level 1b)
5.0
4.5
4.0
3.5
3.0
2.5
2.0
1.5
1.0
0.5
0.0

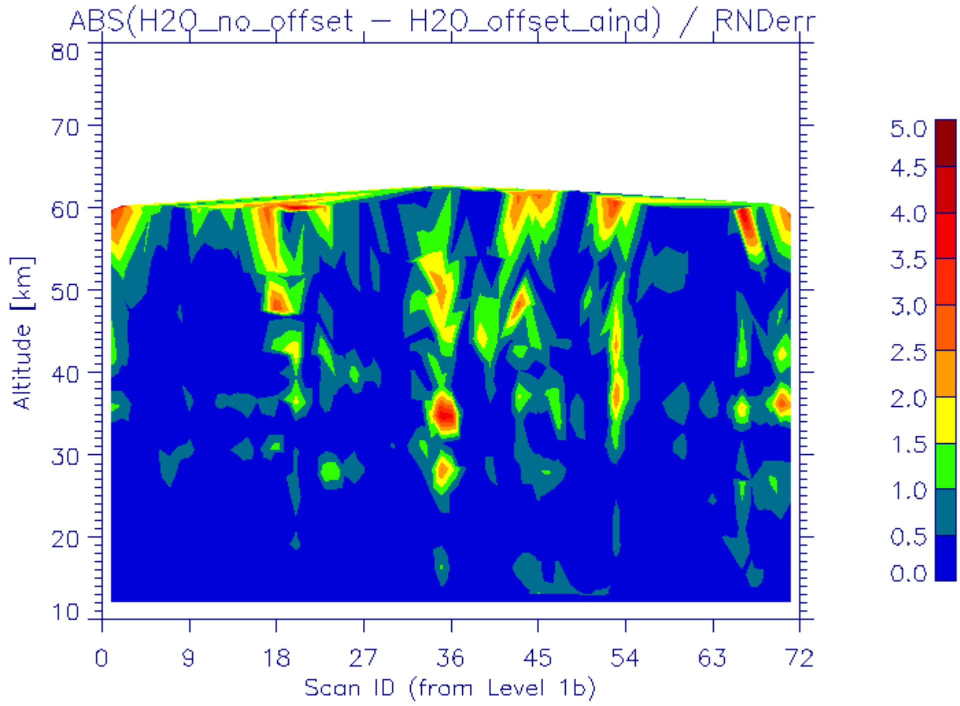
ABS(H2O_no_offset − H2O_offset_aind) / RNDerr
Altitude [km]
80
70
60
50
40
30
20
10
0
9
18
27
36
45
54
63
72
Scan ID (from Level 1b)
5.0
4.5
4.0
3.5
3.0
2.5
2.0
1.5
1.0
0.5
0.0

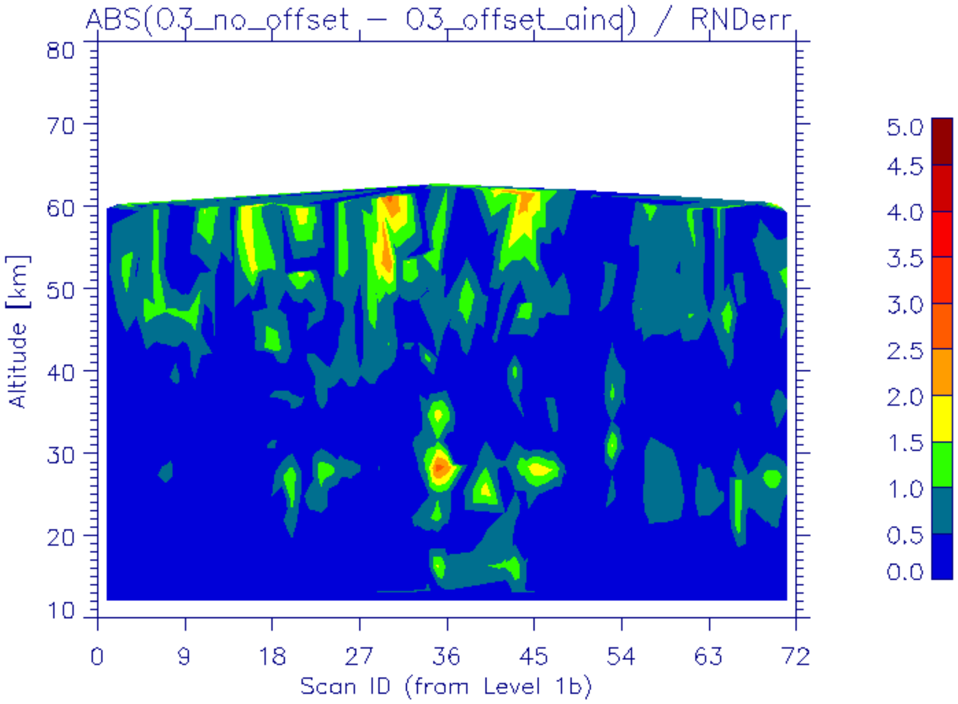
ABS(O3_no_offset − O3_offset_aind) / RNDerr
Altitude [km]
80
70
60
50
40
30
20
10
0
9
18
27
36
45
54
63
72
Scan ID (from Level 1b)
5.0
4.5
4.0
3.5
3.0
2.5
2.0
1.5
1.0
0.5
0.0

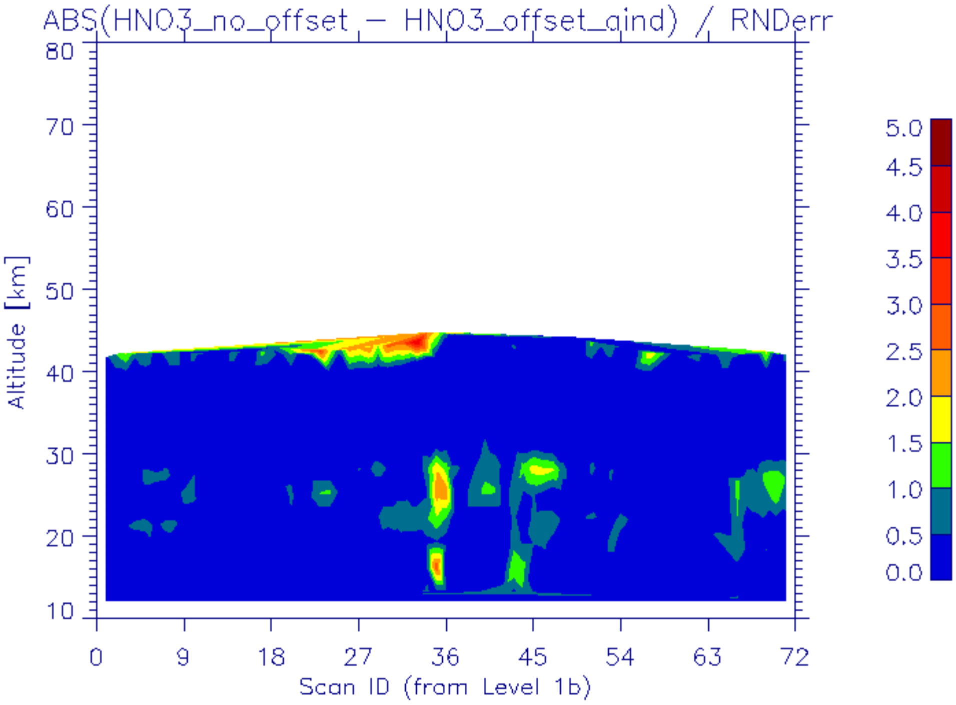
ABS(HNO3_no_offset − HNO3_offset_aind) / RNDerr
Altitude [km]
80
70
60
50
40
30
20
10
0
9
18
27
36
45
54
63
72
Scan ID (from Level 1b)
5.0
4.5
4.0
3.5
3.0
2.5
2.0
1.5
1.0
0.5
0.0

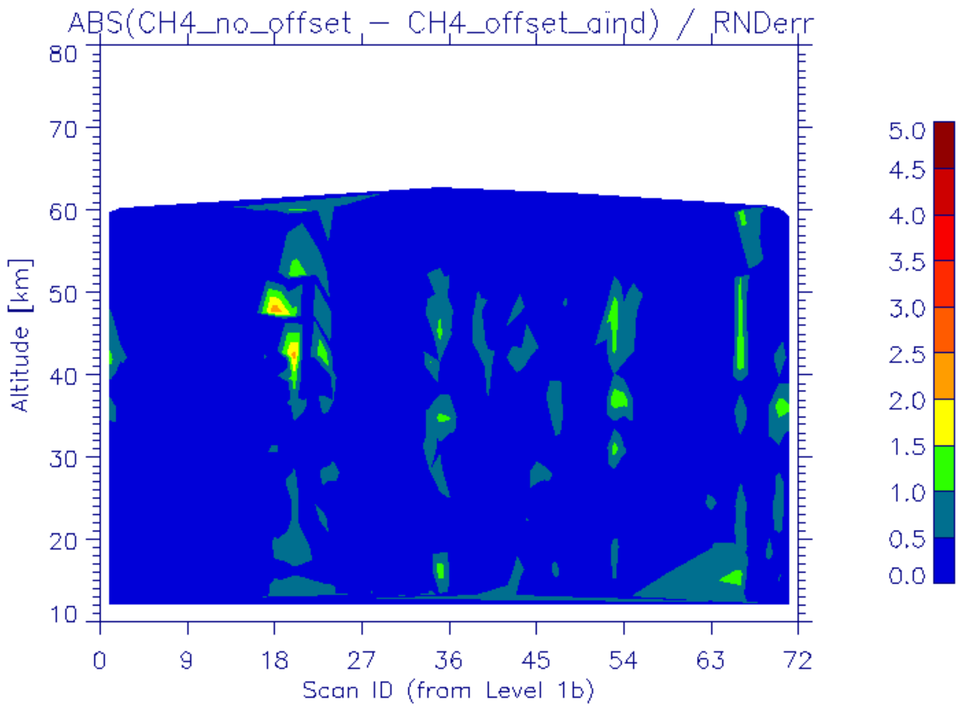
ABS(CH4_no_offset − CH4_offset_aind) / RNDerr
Altitude [km]
Scan ID (from Level 1b)
80
70
60
50
40
30
20
10
0
9
18
27
36
45
54
63
72
5.0
4.5
4.0
3.5
3.0
2.5
2.0
1.5
1.0
0.5
0.0

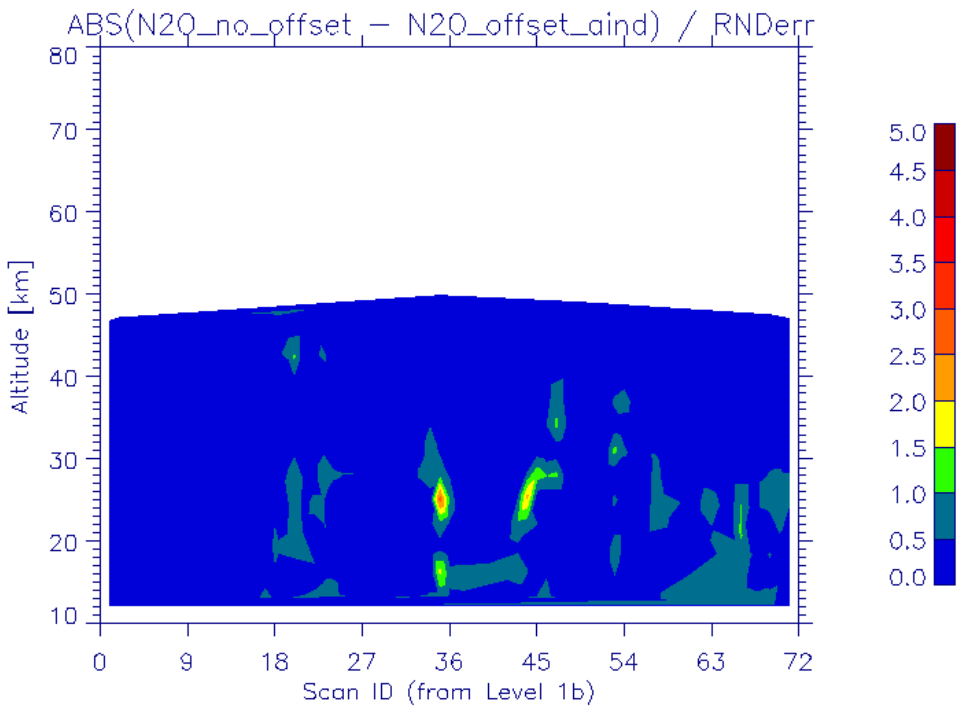
ABS(N2O_no_offset − N2O_offset_aind) / RNDerr
Altitude [km]
Scan ID (from Level 1b)
80
70
60
50
40
30
20
10
0
9
18
27
36
45
54
63
72
5.0
4.5
4.0
3.5
3.0
2.5
2.0
1.5
1.0
0.5
0.0

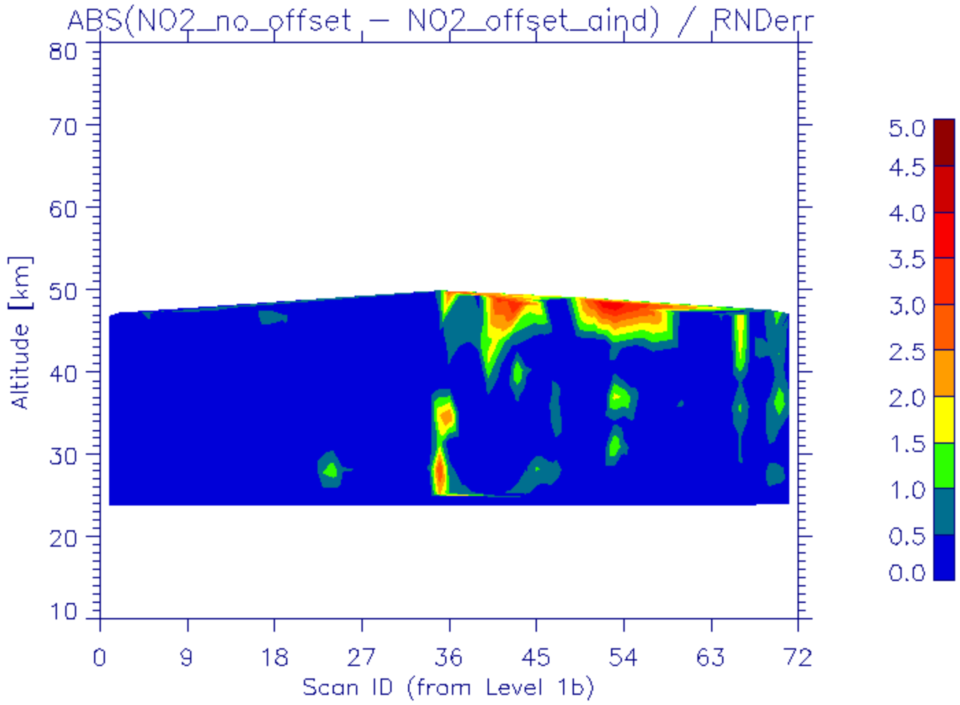

Conclusions

From the analysis reported above we can see that negligible differences in the χ^2 are observed when an offset altitude dependent is fitted or no offset is fitted with respect to the nominal case.
The profiles obtained fitting an altitude dependent offset show significant differences with respect to those obtained with the nominal retrieval. Instead the profiles obtained without fitting the offset are very close to those obtained with the nominal retrieval.
In all the studied cases the retrieved offset is very close to zero when compared with the random error, so it would be possible to avoid to fit the offset, but it is useful to have it as a quality indicator.

5 Other tests: non-linearity correction for forward and reverse sweeps

Ref. [RD9]: Sheet MIP_newtest

Introduction

It was observed that there were oscillations in the retrieved profiles (both in the retrievals from the Oxford processor and in the ESA Level 2 product) for orbit #2081. These oscillations were anti-correlated between scans, indicating a systematic problem with the Level 1 radiances. The problem was traced back to a difference in the treatment of the non-linearity correction for forward and backward sweeps of the interferogram. New Level 1 data for orbit #2081 was supplied in January. In this new data, the difference between forward and backward sweeps is supposed to have been eliminated.

Description of the test and results

For each sweep of each scan of the orbit #2081, the mean value of the radiance over the whole of each band was calculated. Then, a weighted mean for each sweep of each scan was calculated, passing along the orbit, using a weighting of 1/4, 1/2, 1/4 for the previous scan number, the present scan number and the next scan number respectively. A percentage difference between the mean band radiance and the weighted mean taking account of scans on either side was calculated. Figure 1 shows the results for band A. A regular pattern is visible in this plot, and this could indicate a systematic difference between radiances measured during forward and backward interferogram sweeps. Figure 2 shows the results for band AB.

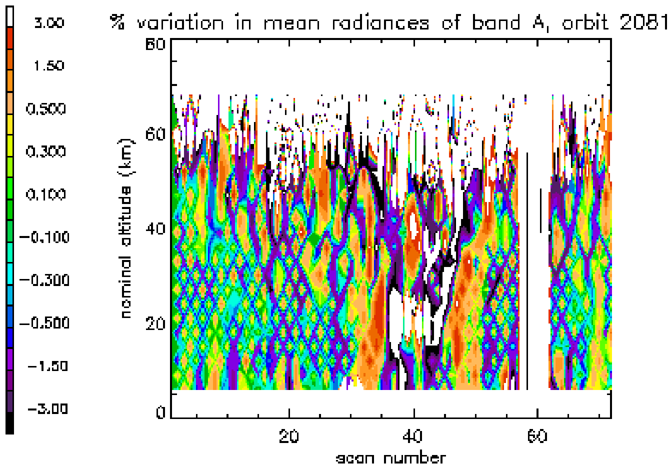

Figure 1 - Percentage difference between the mean band A radiance and the weighted mean band A radiance taking account of scans on either side for orbit #2081 before new non-linearity correction.

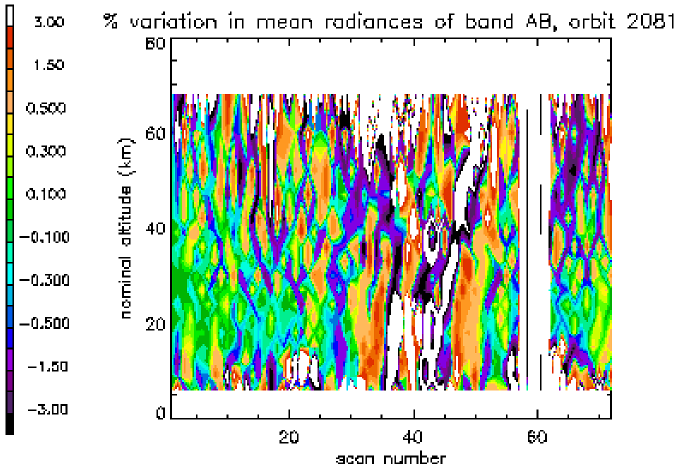

Figure 2 - Percentage difference between the mean band AB radiance and the weighted mean band AB radiance taking account of scans on either side for orbit #2081 before new non-linearity correction.

Figure 3 shows the percentage variation in the new, corrected Level 1 radiances for band A. The regular pattern that was visible before the new non-linearity correction is no longer present, and so the new treatment of the non-linearity correction has provided an improvement.

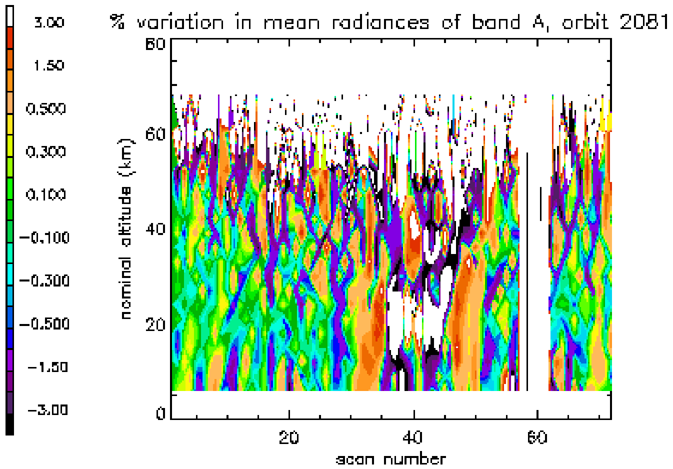

Figure 3 - Percentage difference between the mean band A radiance and the weighted mean taking account of scans on either side for the new, corrected orbit #2081 after new non-linearity correction.

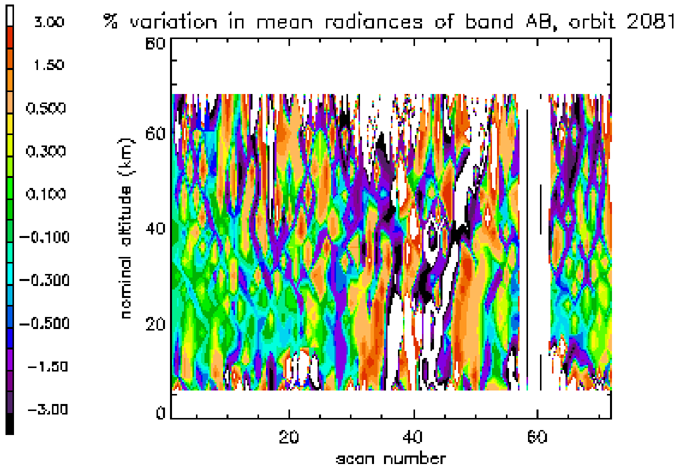

Figure 4 - Percentage difference between the mean band AB radiance and the weighted mean taking account of scans on either side for the new, corrected orbit #2081 after new non-linearity correction.

Results for band AB are shown in Figure 4.
For band AB, the difference between before and after the correction is not as obvious as for band A, but the pattern was not as obvious as in band A in the first place.

Figure 5 and Figure 6 show oscillations in the OPTIMO temperature retrieval, before and after the new non-linearity correction respectively. The retrieved temperature was compared to a running weighted mean, as it was done with the L1 radiances, and although the results are improved, there is still some evidence of a pattern. (The scale is in Kelvin). Results for H2O retrieval before and after the new non-linearity correction are shown in Figure 7 and Figure 8 respectively.

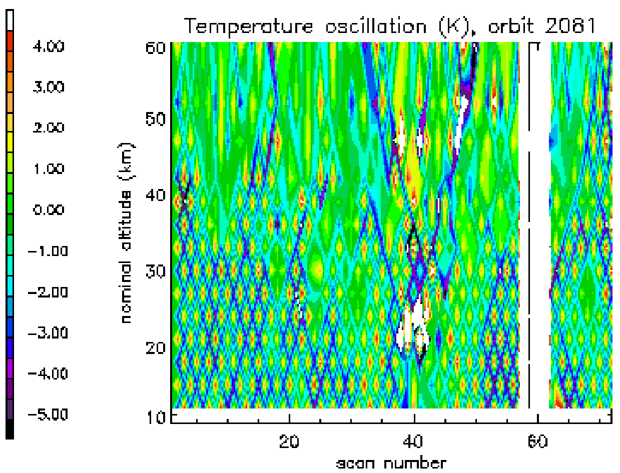

Figure 5 Temperature oscillations before new non-linearity correction.

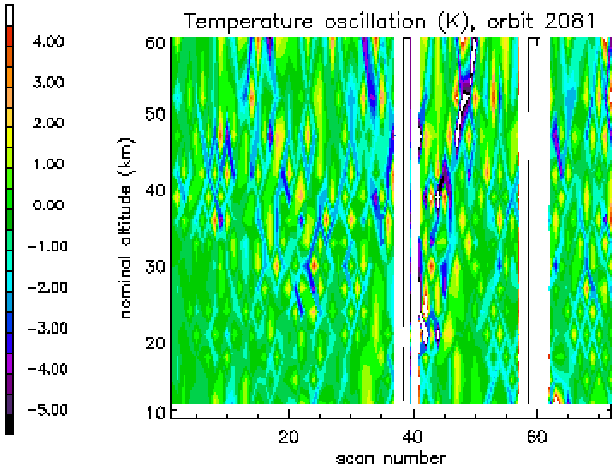

Figure 6 Temperature oscillations after new non-linearity correction.

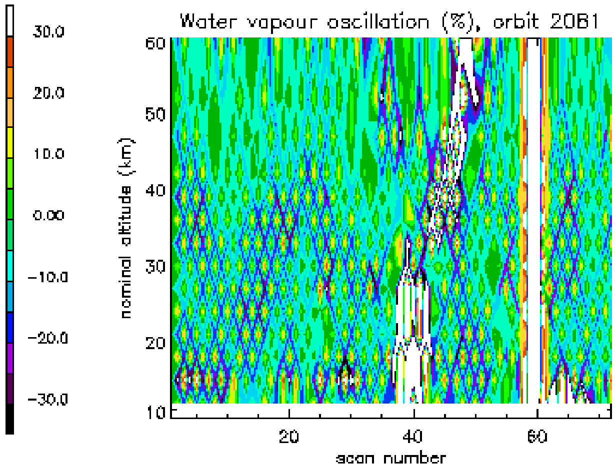

Figure 7 H2O oscillations before new non-linearity correction.

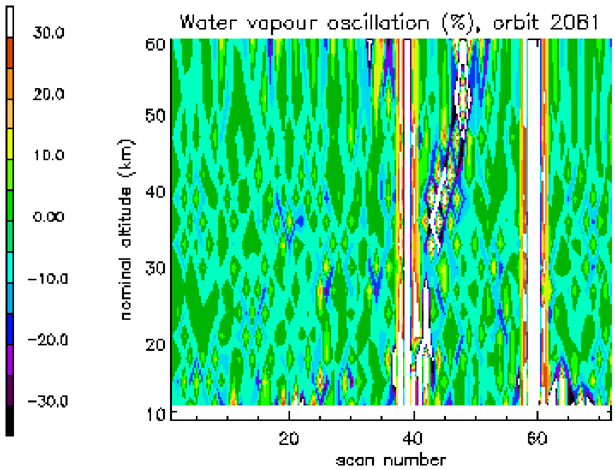

Figure 8 H2O oscillations after new non-linearity correction.

For water vapour, the results after the new non-linearity correction are much improved, but there are still oscillations present of the order of 5-10% of the VMR.

Conclusions

The non-linearity correction used in the new Level1 file seems to be successful in reducing the oscillations in the radiance and, as a consequence, in the retrieved profiles.
However, the problem does not appear to have been entirely eliminated.